

**Development of a novel bioactive glass propelled via
air-abrasion to remove orthodontic bonding materials
and promote remineralisation of white spot lesions**

Ayam Ali Hassoon Taha

Thesis submitted in fulfilment of the requirement for the
Degree of Doctor of Philosophy in The Institute of
Dentistry, Barts and The London School of Medicine and
Dentistry

Queen Mary University of London

2017

Statement of Originality

I, Ayam Taha, confirm that the research included within this thesis is my own work or that where it has been carried out in collaboration with, or supported by others, that this is duly acknowledged below, and my contribution indicated. Previously published material is also acknowledged below.

I attest that I have exercised reasonable care to ensure that the work is original, and it does not to the best of my knowledge break any UK law, infringe any third party's copyright or other Intellectual Property Right, or contain any confidential material.

I accept that the College has the right to use plagiarism detection software to check the electronic version of the thesis.

I confirm that this thesis has not been previously submitted for the award of a degree by this or any other university. The copyright of this thesis rests with the author and no quotation from it or information derived from it may be published without the prior written consent of the author.

Signature: Ayam Taha

Date: 02/11/2017

Abstract

Enamel damage and demineralisation are common complications associated with fixed orthodontic appliances. In particular, the clean-up of adhesive remnants after debonding is a recognised cause of enamel damage. Furthermore, fixed attachments offer retentive areas for accumulation of cariogenic bacteria leading to enamel demineralisation and formation of white spot lesions (WSLs). Bioactive glasses may be used to remove adhesives, preserving the integrity of the enamel surface, while also having the potential to induce enamel remineralisation, although their efficacy in both respects has received little attention.

A systematic review evaluating the remineralisation potential of bioactive glasses was first undertaken. No prospective clinical studies were identified; however, a range of *in vitro* studies with heterogeneous designs were identified, largely providing encouraging results.

A series of glasses was prepared with molar compositions similar to 45S5 (Sylc™; proprietary bioactive glass) but with constant fluoride, reduced silica and increased sodium and phosphate contents. These glasses were characterised in several tests and the most promising selected. This was designed with hardness lower than that of enamel and higher than orthodontic adhesives. Its effectiveness in terms of removal of composite- and glass ionomer- based orthodontic adhesives was evaluated against Sylc™ and a tungsten carbide (TC) bur. This novel glass was subsequently used for remineralisation of artificially-induced orthodontic WSLs on extracted human teeth.

The novel glass propelled *via* the air-abrasion system selectively removed adhesives without inducing tangible physical enamel damage compared to Sylc™ and the conventional TC bur. It also remineralised WSLs with surface roughness and intensity of light backscattering similar to sound enamel. In addition, mineral deposits were detected on remineralised enamel surfaces; these acted as a protective layer on the enamel surface and improved its hardness. This layer was rich in calcium, phosphate, and fluoride; ¹⁹F MAS-NMR, confirmed the formation of fluorapatite. This is particularly beneficial since fluorapatite is more chemically stable than hydroxyapatite and has more resistance to acid attack. Hence, a promising bioactive glass has been developed.

Acknowledgments

First of all, thanks be to Allah almighty for the blessings He bestowed upon me and the strength He has given me when I thought I had no strength left in me.

I am particularly indebted to my first supervisor, Dr. Mangala Patel, for her unconditional support and immense motivation throughout the duration of my study with a thought-provoking reasoning that was a big asset to this thesis. My deepest gratitude and appreciation must also be extended to my second supervisor, Dr. Padhraig Fleming, whose massive contribution was a cornerstone to this study. I owe so much to him for his constant guidance and support. But this study would have never been accomplished without the foresight and expertise of my third supervisor, Professor Robert Hill, whose wisdom was invaluable.

I was honoured and privileged to be given the opportunity of working in the esteemed establishment of Queen Mary University of London and the wonderful staff who accepted me as a member of this big family. I would especially like to thank Dr. Pete Tomlins (Senior lecturer in Dental Biometrics), Dr. Harold Toms (NMR Facility Manager), Dr. Rory Wilson (Experimental Officer in XRD), and Mr. Russell Bailey (Laboratory Technician in Nano Vision Centre). I would also like to extend my gratitude to Professor Sanjukta Deb and Mr. Richard Mallett at Tissue Engineering and Biophotonics Department in King's College London Dental Institute for allowing me to use a Knoop hardness testing machine. Special thanks to my friend Dr. Enas Younis for her priceless friendship and support.

I am also grateful to the Iraqi Ministry of Higher Education and Scientific Research for funding my scholarship.

I would love to dedicate this work to my mother and father; they are my backbone without which I would not stand at all. To my husband, brother and sisters, thank you for your continuous encouragements.

Last and foremost, to my two beautiful daughters, Lial and Lamar, who endured so much with me, thank you for everything; I am blessed by your presence in my life.

List of Contents

1.	INTRODUCTION.....	1
2.	LITERATURE REVIEW	3
2.1.	Orthodontic treatment	3
2.2.	Fixed orthodontic appliances	3
2.3.	Orthodontic attachments	4
2.4.	Bonding mechanisms.....	4
2.5.	Bond strength.....	5
2.6.	Enamel characteristics	6
2.6.1.	Enamel structure	6
2.6.2.	Hydroxyapatite crystals structure	8
2.7.	Enamel surface preparation for bonding.....	8
2.7.1.	Pumice prophylaxis	8
2.7.2.	Acid etching.....	9
2.7.2.1.	Types of acid etching approach	10
2.7.2.2.	Effect of acid etching on enamel surface	12
2.8.	Bracket materials and base morphology	14
2.8.1.	Bracket materials	14
2.8.1.1.	Metal brackets.....	14
2.8.1.2.	Plastic brackets	15
2.8.1.3.	Ceramic brackets	15
2.8.2.	Bracket base design	16
2.9.	Adhesion and adhesives	18
2.9.1.	Resin Based Composites (RBCs).....	18
2.9.2.	Glass Ionomer Cements (GICs).....	19
2.9.3.	Resin Modified Glass Ionomer Cements (RMGICs).....	20
2.9.4.	Compomers.....	22
2.10.	Debonding.....	24
2.10.1.	Bond failure rate.....	24
2.10.2.	Debonding Methods	25
2.10.2.1.	Mechanical methods	25
2.10.2.2.	Electro-thermal debonding methods.....	25
2.10.2.3.	Ultrasonic methods	25
2.10.2.4.	Laser systems	26
2.10.3.	Post debonding clean-up methods	26
2.11.	Enamel demineralisation and remineralisation	29

2.11.1.	White spot lesions (WSLs).....	30
2.11.2.	Timing and location of development of WSLs	31
2.11.3.	Prevalence and incidence	34
2.11.4.	Diagnosis of WSLs.....	40
2.11.4.1.	Macroscopic methods	40
2.11.4.2.	Microscopic methods	43
2.11.5.	Risk factors for developing WSLs.....	43
2.11.6.	Prevention of WSLs	45
2.11.7.	Enamel remineralisation / Treatment of WSLs	48
2.11.8.	Enamel surface tomography after demineralisation/remineralisation: Assessment techniques	54
2.11.8.1.	Profilometer.....	55
2.11.8.2.	Optical Coherence Tomography (OCT).....	56
2.11.8.3.	Surface micro-hardness measurements.....	57
2.11.8.4.	Atomic force microscopy (AFM).....	59
2.11.8.5.	Microradiography	59
2.11.8.6.	X-ray microtomography (XMT).....	59
2.11.8.7.	Chemical analysis	60
2.11.8.8.	Scanning Electron Microscopy (SEM)	60
2.11.8.9.	Energy dispersive X-ray spectroscopy (EDX).....	61
2.11.8.10.	Qualitative Light Fluorescent (QLF)	61
2.11.8.11.	Optical microscopic techniques	61
2.12.	Bioactive glasses	62
2.12.1.	Structure of bioactive glasses	63
2.12.2.	Network connectivity	65
2.12.3.	Bioactivity of bioactive glasses	68
2.12.4.	Glass formation	69
2.12.5.	Glass synthesis	71
2.12.6.	Assessment techniques to investigate glass characteristics	71
2.12.7.	Effect of changing various ions within the glass composition on the glass structure and bioactivity	74
2.12.7.1.	Effect of changing sodium ions	74
2.12.7.2.	Effect of changing phosphate ions.....	75
2.12.7.3.	Effect of changing fluoride ions.....	81
2.12.8.	Application of bioactive glasses	87
2.13.	Air-abrasion.....	88
2.13.1.	Development of air-abrasion.....	88
2.13.2.	Air-abrasion: Theory and Practice	89
2.13.3.	Advantages of air-abrasion	92
2.13.4.	Limitations of air-abrasion.....	94

3.	A SYSTEMATIC REVIEW OF THE EFFECT OF BIOACTIVE GLASSES ON ENAMEL REMINERALISATION (SEE APPENDIX 1)	96
3.1.	Objectives	96
3.2.	Materials and methods.....	96
3.2.1.	Search strategy for identification of studies	96
3.2.2.	Study selection.....	97
3.2.3.	Data extraction	97
3.2.4.	Study quality assessment	97
3.3.	Results	98
3.3.1.	Study selection and characteristics.....	98
3.3.2.	Study quality assessment	98
3.3.3.	Results of individual studies.....	107
3.4.	Discussion.....	111
3.5.	Conclusion	113
4.	AIMS AND OBJECTIVES	114
4.1.	Aims	114
4.2.	Objectives	114
5.	MATERIALS AND METHODS	117
5.1.	Overview of the experiments performed	117
5.2.	Glass development	118
5.2.1.	Glass design	118
5.2.2.	Glass frit synthesis.....	119
5.2.3.	Glass casting.....	120
5.2.4.	Glass powder preparation.....	121
5.3.	Glass characterisation studies	123
5.3.1.	Characterising the amorphous nature of glasses	123
5.3.2.	Glass thermal analysis.....	127
5.3.3.	Glass hardness measurements	128
5.3.4.	Glass bioactivity dissolution <i>in vitro</i> studies.....	129
5.3.5.	Apatite detection using 19F MAS-NMR	132
5.3.6.	Glass particle size distribution analysis	133
5.3.7.	Glass particle shape analysis	134
5.4.	Air- abrasion studies performed using the optimal novel glass, QMAT3.....	135

5.4.1.	Glass cutting efficiency	135
5.4.2.	Glass powder flow rate	136
5.5.	Experiments performed with the optimal novel glass (QMAT3)	138
5.5.1.	Tooth sample preparation	138
5.5.2.	Orthodontic adhesive removal	139
5.5.3.	White spot lesion (WSL) remineralisation	142
5.5.4.	Assessment techniques used in <i>in vitro</i> studies	145
5.5.4.1.	Optical Coherence Tomography (OCT)	145
5.5.4.2.	Profilometer	146
5.5.4.3.	Knoop hardness testing	148
5.5.4.4.	Scanning electron microscopy (SEM)	149
5.5.4.5.	Energy Dispersive X-ray Spectroscopy (EDX)	150
5.6.	Statistical analysis	150
6.	RESULTS.....	151
6.1.	Glass development	151
6.2.	Glass characterisation studies	151
6.2.1.	Characterisation of the amorphous nature of glasses	151
6.2.2.	Glass thermal analysis	156
6.2.3.	Glass hardness measurements	157
6.2.4.	Glass bioactivity dissolution studies.....	158
6.2.4.1.	Tris buffer solution studies at pH 7.3 and 9	158
6.2.4.2.	Acetic acid study	172
6.2.4.3.	Artificial saliva study.....	178
6.2.5.	Apatite type detection using ¹⁹ F MAS-NMR.....	185
6.2.6.	Glass particle size analysis	187
6.2.7.	Glass particle shape analysis	189
6.3.	Air-abrasion studies performed using the selected novel glass: QMAT3	191
6.3.1.	Glass cutting efficiency	191
6.3.2.	Glass powder flow rate	194
6.4.	Experiments performed using the selected novel glass, QMAT3	196
6.4.1.	Orthodontic adhesive removal	196
6.4.1.1.	Profilometer results	196
6.4.1.2.	Scanning electron microscope (SEM) results	199
6.4.1.3.	Time required for adhesive removal	200
6.4.2.	White spot lesions (WSLs) remineralisation	202
6.4.2.1.	Optical coherence tomography (OCT) results	202
6.4.2.2.	Profilometer results	204

6.4.2.3.	Knoop hardness testing	205
6.4.2.4.	Scanning electron microscope (SEM).....	207
6.4.2.5.	Energy dispersive X-ray Spectroscopy (EDX)	210
7.	DISCUSSION.....	212
7.1.	Glass development and characterisation.....	212
7.1.1.	Characterization of amorphous nature of glasses, glass thermal analysis, and hardness measurements.....	212
7.1.2.	Glass bioactivity dissolution studies	214
7.2.	Studies performed with glass particles between 38µm - 90µm in size.....	219
7.2.1.	Glass particle size distribution analysis	219
7.2.2.	Glass particle shape analysis	219
7.3.	Air-abrasion studies performed using the selected novel glass, QMAT3	219
7.4.	EXPERIMENTS PERFORMED USING THE SELECTED NOVEL GLASS, QMAT3.....	221
7.4.1.	Orthodontic adhesive removal	221
7.4.2.	White spot lesion (WSL) remineralisation	223
8.	CONCLUSIONS AND FUTURE WORK	228
8.1.	CONCLUSIONS.....	228
8.2.	FUTURE WORK	229
	REFERENCES.....	231
	APPENDICES	278

List of Figures

Figure 2.1. Scanning electron microscopy of enamel hydroxyapatite crystallites in enamel:..	7
Figure 2.2. Type I enamel etching pattern after 30 seconds of acid etching. The cores of the prism are dissolved (arrow) at 4,500x magnification (Taken from Fava <i>et al.</i> , 1997).....	13
Figure 2.3. Type II enamel etching pattern after 45 seconds of acid etching. The periphery of enamel prisms is dissolved (arrow) at 4,500x magnification (Taken from Fava <i>et al.</i> , 1997). ..	14
Figure 2.4. Techniques to assess enamel surface tomography after demineralisation / remineralisation	55
Figure 2.5. Molecular difference between a) crystalline glass, and b) bioactive glass materials.....	62
Figure 2.6. (a) Silica tetrahedron and (b) Four tetrahedra linked to one central tetrahedron by bridging oxygen (BO) ions (Adapted from Jones and Clare, 2012)	63
Figure 2.7. A schematic structure of a random glass composed of glass formers and glass modifiers (Adapted from Hench and June, 1999)	65
Figure 2.8. Graph illustrating the relationship between network connectivity (NC) and bioactivity (Adapted from Hill, 2009)	68
Figure 2.9. Effect of temperature on the volume of glass forming melts (Adapted from Shelby, 2005)	70
Figure 2.10. Representation of a highly-disrupted glass network after Ca^{2+} is replaced by two Na^+ ions (Adapted from Wallace <i>et al.</i> , 1999)	74
Figure 2.11. A schematic structure of	77
Figure 2.12. Illustration of hypothetical effect of CaF_2 addition on silicate network (Adapted from Brauer <i>et al.</i> 2009)	84
Figure 2.13. Velopex Aquacut Quattro™ air-abrasion system	89
Figure 3.1. Flowchart of article retrieval	99

Figure 5.1. Summary of experiments undertaken.....	117
Figure 5.2. Vibrating machine used for sieving.....	122
Figure 5.3. Rubber balls used during sieving to refine glass particles	122
Figure 5.4. ATR-FTIR spectrometer	124
Figure 5.5. Stick pattern of hydroxyapatite	126
Figure 5.6. Stick pattern of fluorapatite	126
Figure 5.7. A schematic example of a DSC curve demonstrating several common features	127
Figure 5.8. A Stanton Redcroft DSC 1500.....	128
Figure 5.9. Vickers Hardness testing machine (Zwick/Roell, ZHU)	129
Figure 5.10. Malvern Particle Size Analyser (Mastersizer 3000).....	134
Figure 5.11. Malvern Mastersizer/ E	134
Figure 5.12. Velopex Aquacut Quattro™ air-abrasion machine	136
Figure 5.13. Methodology used to test the glass cutting efficiency: a) hand- piece for air-abrasion machine, and b) prepared adhesive disc samples on a microscopic slide.....	136
Figure 5.14. BA Ultimate™ air polisher	137
Figure 5.15. Procedure for assessing the glass powder flow rate	138
Figure 5.16. The prepared tooth sample: a) the tooth is embedded into a plastic mould filled with acrylic resin, and b) a polyvinyl chloride tape is placed on the buccal surface of the tooth sample leaving a window of exposed enamel surface.....	139
Figure 5.17. Flow chart representing the experimental study design to assess enamel surface roughness following orthodontic adhesive removal	141

Figure 5.18. Protocol used to create artificially-induced WSLs	142
Figure 5.19. Experimental study design to assess enamel surface changes under different conditions	144
Figure 5.20. OCT system and the sample	145
Figure 5.21. a) White light profilometer, Proscan®2000, b) Enlarged sample stage	147
Figure 5.22. Knoop hardness testing machine (Struers / Duramin)	148
Figure 5.23. Well-shaped indentations using Knoop hardness testing machine	149
Figure 6.1. ATR-FTIR spectra for untreated 45S5, Syc™ and experimental glasses (QMAT1, QMAT2, QMAT3, QMAT4, QMAT5).....	152
Figure 6.2. XRD data for untreated 45S5, Syc™ and experimental glasses (QMAT1, QMAT2, QMAT3)	153
Figure 6.3. XRD data of QMAT4 and QMAT5	154
Figure 6.4. Stick pattern of Portlandite (Calcium Hydroxide).....	155
Figure 6.5. Stick pattern of Sodium Calcium Silicate (Na ₂ Ca (SiO ₄)	156
Figure 6.6. ATR-FTIR spectra of QMAT1 glass after immersion in Tris buffer solution (pH=7.3)	159
Figure 6.7. ATR-FTIR spectra of QMAT2 glass after immersion in Tris buffer solution (pH=7.3)	159
Figure 6.8. ATR-FTIR spectra of QMAT3 glass after immersion in Tris buffer solution (pH=7.3)	160
Figure 6.9. ATR-FTIR spectra of 45S5 glass after immersion in Tris buffer solution (pH=7.3)	160
Figure 6.10. ATR-FTIR spectra of Syc™ glass after immersion in Tris buffer solution (pH=7.3)	161

Figure 6.11. XRD patterns of QMAT1 glass after immersion in Tris buffer solution (pH=7.3)	162
Figure 6.12. XRD patterns of QMAT2 glass after immersion in Tris buffer solution (pH=7.3)	162
Figure 6.13. XRD patterns of QMAT3 glass after immersion in Tris buffer solution (pH=7.3)	163
Figure 6.14. XRD patterns of 45S5 glass after immersion in Tris buffer solution (pH=7.3).	163
Figure 6.15. XRD patterns of Sylc™ glass after immersion in Tris buffer solution (pH=7.3)	164
Figure 6.16. The pH change of Tris buffer solution (initial pH=7.3) after immersion of 45S5, Sylc™ and experimental glasses (QMAT1, QMAT2, and QMAT3) plotted against the designated immersion time intervals (1, 3, 6, 9 and 24 hours). * Error bars represent the range of pH measured on 2 independent occasions. Where error bars are not shown, the error was smaller than the data point.	165
Figure 6.17. ATR-FTIR spectra of QMAT1 glass after immersion in Tris buffer solution (pH=9)	166
Figure 6.18. ATR-FTIR spectra of QMAT2 glass after immersion in Tris buffer solution (pH=9)	166
Figure 6.19. ATR-FTIR spectra of QMAT3 glass after immersion in Tris buffer solution (pH=9)	167
Figure 6.20. ATR-FTIR spectra of 45S5 glass after immersion in Tris buffer solution (pH=9)	167
Figure 6.21. ATR-FTIR spectra of Sylc™ glass after immersion in Tris buffer solution (pH=9)	168
Figure 6.22. XRD patterns of QMAT1 glass after immersion in Tris buffer solution (pH=9)	169
Figure 6.23. XRD patterns of QMAT2 glass after immersion in Tris buffer solution (pH=9)	169
Figure 6.24. XRD patterns of QMAT3 glass after immersion in Tris buffer solution (pH=9)	170

Figure 6.25. XRD patterns of 45S5 glass after immersion in Tris buffer solution (pH=9)....	170
Figure 6.26. XRD patterns of Sylc™ glass after immersion in Tris buffer solution (pH=9)..	171
Figure 6.27. The pH change of Tris buffer solution (initial pH=9) after immersion of 45S5, Sylc™ and experimental glasses (QMAT1, QMAT2, and QMAT3) plotted against the designated immersion time intervals (1, 3, 6, 9 and 24 hours). * Error bars represent the range of pH measured on 2 independent occasions. Where error bars are not shown, the error was smaller than the data point.....	172
Figure 6.28. ATR-FTIR spectra of QMAT1 glass after immersion in acetic acid (pH=5).....	173
Figure 6.29. ATR-FTIR spectra of QMAT2 glass after immersion in acetic acid (pH=5).....	173
Figure 6.30. ATR-FTIR spectra of QMAT3 glass after immersion in acetic acid (pH=5).....	174
Figure 6.31. ATR-FTIR spectra of 45S5 glass after immersion in acetic acid (pH=5).....	174
Figure 6.32. ATR-FTIR spectra of Sylc™ glass after immersion in acetic acid (pH=5).....	175
Figure 6.33. XRD patterns of QMAT1 glass after immersion in acetic acid (pH=5)	175
Figure 6.34. XRD patterns of QMAT2 glass after immersion in acetic acid (pH=5)	176
Figure 6.35. XRD patterns of QMAT3 glass after immersion in acetic acid (pH=5)	176
Figure 6.36. XRD patterns of 45S5 glass after immersion in acetic acid (pH=5)	177
Figure 6.37. XRD patterns of Sylc™ glass after immersion in acetic acid (pH=5)	177
Figure 6.38. The pH change of acetic acid solution (initial pH=5) after immersion of 45S5, Sylc™ and experimental glasses (QMAT1, QMAT2, and QMAT3) plotted against the designated immersion time intervals (15 minutes, 1, 3, 6, 9 and 24 hours). * Error bars represent the range of pH measured on 2 independent occasions. Where error bars are not shown, the error was smaller than the data point	178
Figure 6.39. ATR-FTIR spectra of QMAT1 glass after immersion in artificial saliva	179
Figure 6.40. ATR-FTIR spectra of QMAT2 glass after immersion in artificial saliva	180

Figure 6.41. ATR-FTIR spectra of QMAT3 glass after immersion in artificial saliva	180
Figure 6.42. ATR-FTIR spectra of 45S5 glass after immersion in artificial saliva	181
Figure 6.43. ATR-FTIR spectra of Sylc™ glass after immersion in artificial saliva.....	181
Figure 6.44. XRD patterns of QMAT1 glass after immersion in artificial saliva	182
Figure 6.45. XRD patterns of QMAT2 glass after immersion in artificial saliva	182
Figure 6.46. XRD patterns of QMAT3 glass after immersion in artificial saliva	183
Figure 6.47. XRD patterns of 45S5 glass after immersion in artificial saliva	183
Figure 6.48. XRD patterns of Sylc™ glass after immersion in artificial saliva	184
Figure 6.49. The pH change of artificial saliva (initial pH=6.5) after immersion of 45S5, Sylc™ and experimental glasses (QMAT1, QMAT2, and QMAT3) plotted against the designated immersion time intervals (15, 30, 45 minutes and 1 hour). * Error bars represent the range of pH measured on 2 independent occasions. Where error bars are not shown, the error was smaller than the data point.....	185
Figure 6.50. ¹⁹ F MAS-NMR spectra of a) QMAT3 immersed in artificial saliva for 1 hour, b) QMAT3 immersed in Tris buffer solution for 24 hours, and c) fluorapatite reference. (*) Asterisk denotes spinning side bands.....	186
Figure 6.51. ¹⁹ F MAS-NMR spectra of enamel blocks under various conditions a) sound enamel, b) demineralised enamel, c) remineralised by only immersed in artificial saliva, d) remineralised by propulsion with Sylc™ glass followed by immersion in artificial saliva, e) remineralised by propulsion with QMAT3 experimental glass followed by immersion in artificial saliva, f) fluorapatite reference. * denotes spinning side bands	187
Figure 6.52. SEM images of 45S5, Sylc™ and experimental glasses.....	190
Figure 6.53. Mean ± SD of the cutting time required to cut a hole within adhesive discs by Sylc™-air-abrasion using various parameters	193
Figure 6.54. Mean ± SD of the cutting time required to cut a hole within adhesive discs by QMAT3-air-abrasion using various parameters	193

Figure 6.55. Amount (in grams) of glass powder propelled via two air-abrasion systems under air pressure 60 psi over one minute. Sig. refers to significant difference, NS refers to non-significant difference, and (^) denotes no significant difference between the two glasses under the same operating parameters	195
Figure 6.56. Bar graph representing means \pm SD of the enamel surface roughness under three different conditions for two bonding adhesives and three post clean-up methods. (Sig.) refers to significant difference, (NS) refers to Non-significant difference, and (^) denotes no significant differences between the two adhesives under the same enamel condition	198
Figure 6.57. Representative SEM images of the enamel surface: a) before bracket bonding; b) after clean-up using the TC bur; c) after clean-up using Sylc™-air-abrasion; d) after clean-up using QMAT3- air-abrasion	200
Figure 6.58. Means \pm SD of the time (seconds) required to remove two residual orthodontic adhesives following bracket debonding by three post-clean-up methods. (*) denotes significant difference in comparison with TC group using the same adhesive. (^) denotes no significant differences between two adhesives using the same clean-up method	202
Figure 6.59. Means \pm SD of the intensity value of light backscattering for each experimental group under four different conditions. (^) denotes no significant difference in comparison with the corresponding baseline.	204
Figure 6.60. Means \pm SD of the enamel surface roughness (Ra) in micrometres for each experimental group under four different conditions. (^) denotes no significant difference in comparison with the corresponding baseline	205
Figure 6.61 Means \pm SD of Knoop hardness number (KHN) for each experimental group under four different conditions. (#) denotes significant increase in enamel hardness compared with Sylc™ and control groups after immersion in artificial saliva.	207
Figure 6.62. SEM images of sound and demineralised enamel surface	208
Figure 6.63. SEM images of remineralised enamel surface after using three remineralisation methods.....	209
Figure 6.64. EDX spectra of sound and demineralised enamel surface	210
Figure 6.65. SEM images of remineralised enamel surface after using three remineralisation methods.....	211

Figure 10.1. The frequency distribution curve for Sylc™batch of particle size ranging between ranging between 38µm-90µm	295
Figure 10.2. The frequency distribution curve for QMAT3 batch of particle size ranging between ranging between 38µm-90µm	296
Figure 10.3. The frequency distribution curve for Sylc™batch of particle size <38µm	297
Figure 10.4. The frequency distribution curve for QMAT3 batch of particle size <38µm	298

List of Tables

Table 2.1. Summary of post debonding clean-up methods	27
Table 2.2. Summary of studies reporting on WSL formation based on observation time and experimental technique	33
Table 2.3. Summary of studies reporting the prevalence of WSLs.....	35
Table 2.4. Summary of studies reporting the incidence of WSLs	36
Table 2.5. Summary of randomised controlled clinical trials of treatment of WSLs.....	50
Table 2.6. Glass compositions (mol%) and network connectivity (NC) assuming phosphate incorporated in the glass network and modified network connectivities (NC') assuming phosphate is orthophosphate species (O'Donnell <i>et al.</i> , 2008a)	76
Table 2.7. Nominal glass composition of Mneimne <i>et al.</i> 's (2011) study in mol% with theoretical network connectivity (NC').....	85
Table 2.8. Glass composition of Mneimne's (2014) study in mol%	86
Table 3.1. Characteristics of the studies included in the review	100
Table 3.2. Methodological quality of the included studies (Sarkis-Onofre <i>et al.</i> , 2014; da Rosa <i>et al.</i> , 2015)	106
Table 3.3. Summary of results from the included studies.....	110
Table 5.1. Design of batch components for each glass (Mol%)	120
Table 5.2. Mass of batch components for each glass (g)	120
Table 5.3. Most characteristic reflections of hydroxyapatite from its JCPD file	125
Table 5.4. Most characteristic reflections of fluorapatite from its JCPD file.....	125
Table 5.5. Summary of all glass dissolution studies	132

Table 6.1. Most characteristic reflections of Portlandite from its JCPD file	154
Table 6.2. Most characteristic reflections of Sodium Calcium Silicate from its JCPD file....	155
Table 6.3. T _g , T _c , and T _m of 45S5, Sylc™ and experimental glasses.	157
Table 6.4. Hardness measurements (VHN and GPa) of 45S5, Sylc™ and experimental glasses.	157
Table 6.5. Mean±SD particle size distribution (in micrometres) of 45S5, Sylc™, and experimental glasses of batches with particle size <38µm using Mastersizer 3000 analyser.	188
Table 6.6. Mean±SD particle size distribution (in micrometres) of 45S5, Sylc™ and experimental glasses of batches with particle size ranging between 38µm-90µm using Mastersizer 3000™ analyser.	188
Table 6.7. Mean±SD particle size distribution (in micrometres) for 45S5, Sylc™ and experimental glasses of batches with particle size ranging between 38µm-90µm using Malvern/ E Mastersizer analyser.	189
Table 6.8. Mean ± SD of the cutting time (in seconds) required to cut a hole within adhesive discs by two propelled glasses using various parameters.	192
Table 6.9. Mean ± SD of the amount (in grams) of glass powder propelled <i>via</i> two air-abrasion systems for one minute.	194
Table 6.10. Mean ± SD of the enamel surface roughness (Ra) in micrometres for each experimental group under three different conditions.	197
Table 6.11. Means ± SD of the time (seconds) required to remove two residual orthodontic adhesives following bracket debonding by three post clean-up methods.	201
Table 6.12. Means ± SD of the intensity value of light backscattering for each experimental group under four different conditions.	203
Table 6.13. Means ± SD of the enamel surface roughness (Ra) in micrometres for each experimental group under four different conditions.	205
Table 6.14. Means ± SD of Knoop hardness number (KHN) for each experimental group under four different conditions.	206

List of Abbreviations

AS: Artificial saliva

AFM: Atomic Force Microscopy

CPP-ACP: Casein Phosphopeptide- Amorphous Calcium Phosphate (CPP-ACP)

°C: Celsius

cm: Centimetre

DW: Deionised water

g: Gram

GPa: Gigapascal

EDX: Energy Dispersive X-ray Spectroscopy

FTIR: Fourier Transform Infrared Spectroscopy

¹⁹F MAS-NMR: Magic Angle Spinning-Nuclear Magnetic Resonance spectroscopy

h: Hour

kg: Kilogram

L: Litre

mg: Milligram

µg: Microgram

min: Minute

ml: Millilitre

mm: Millimetre

µm: Micrometre

mN: Millinewton

Mol: Mole

MPa: Megapascal

N₂: Nitrogen gas

OCT: Optical Coherence Tomography

θ: Theta

ppm: Part per million

psi: Pound per square inch

QLF: Quantitative light Fluorescent
rpm: Round per minute
SEM: Scanning electron microscope
sec: Second
Tc: Crystalline temperature
Tg: Glass transition temperature
Tm: Melting temperature
TM: Trade Mark
vs: Versus
WSLs: White spot lesions
XRD: X-ray Diffraction spectroscopy
XMT: X-ray microtomography

1. INTRODUCTION

Fixed appliances have been used since the early 20th century to predictably produce orthodontic alignment of improperly positioned teeth. These consist of bands and brackets, which are temporarily bonded to the teeth by orthodontic adhesives (Singh, 2008). There are, however, a number of risks associated with treatment with enamel loss and demineralisation being among the more common and significant (Phulari, 2013).

Several factors may predispose to or cause enamel loss during or after fixed orthodontic treatment. The clean-up procedure after removal of attachments is regarded as the most significant cause of enamel loss (Knösel *et al.*, 2010; Pont *et al.*, 2010). Various methods have also been proposed for clean-up of residual orthodontic bonding materials from enamel. However, no technique has yet proven effective in the complete and efficient removal of residual adhesive, without inducing even a minor amount of enamel loss (Bonetti *et al.*, 2011; Janiszewska-Olszowska *et al.*, 2014).

Enamel demineralisation, also known as white spot lesions (WSLs), have been reported in up to 96% of orthodontic patients. Their development during fixed orthodontic treatment relates to impeded ability to clean teeth effectively due to the presence of attachments, resulting in food stagnation and plaque accumulation. Moreover, the roughened surfaces of residual adhesive bonding materials around orthodontic brackets lend themselves to bacterial attachment. This is further aggravated by the fact that most orthodontic patients are adolescents, who are at increased risk due to the susceptibility of newly erupting teeth to acid attack (Mayne *et al.*, 2011; Srivastava *et al.*, 2013). A number of materials and techniques have been used to inhibit and remineralise white spot lesions. However, a material or technique that entirely cures white spot lesions does not exist (Chambers *et al.*, 2013).

In recent years, air-abrasion has shown promise in the removal of residual adhesive bonding materials from sound enamel surfaces. Banerjee *et al.* (2008) reported enamel loss with air-abrasion in an *in vitro* study but highlighted that the bioactive glass powder (45S5) induced less enamel loss than either alumina air-abrasion or tungsten carbide burs. Furthermore, Milly *et al.* (2015) used the same glass powder to enhance remineralisation of artificially-induced WSLs following surface pre-

Introduction

conditioning and application of either a slurry from the same glass powder or a paste involving glass powder and polyacrylic acid for 21 days. This *in vitro* study demonstrated remineralisation of WSLs but there was an increase in the surface roughness of remineralised enamel. Therefore, there remains a need to improve the properties of bioactive glasses to facilitate safe and efficient removal of residual adhesive bonding materials while promoting remineralisation of WSLs.

2. LITERATURE REVIEW

2.1. Orthodontic treatment

Orthodontics has been defined as the branch of dentistry concerned with facial growth, development of the dentition and occlusion, and treatment of occlusal irregularities to improve facial appearance and occlusal function, and to create better dental health and improved aesthetics (Walther, 1994; Phulari, 2013). Orthodontic treatment, like many other interventions, has inherent risks and complications, but the advantages it offers should outweigh any potential risk. The chief risks of treatment include root resorption, loss of periodontal support, white spot lesions (WSLs), and soft tissue damage (Mitchell, 2007).

In general, orthodontic appliances can be classified into four types, which can be used either singly or in combination. These include:

- i) Removable orthodontic appliances
- ii) Fixed orthodontic appliances
- iii) Functional appliances
- iv) Extra-oral appliances

Of these, fixed orthodontic appliances form the mainstay of comprehensive treatment with a proven ability to impart three-dimensional control of orthodontic tooth movement, and to deliver the applied force precisely (Walther, 1994; Phulari, 2013).

2.2. Fixed orthodontic appliances

The “E” arch was the first fixed orthodontic appliance, designed by Edward Angle in the early 1900s, and has since been superseded by the standard edgewise appliance before this was replaced by the pre-adjusted edgewise (or Straight Wire) appliance, developed by Lawrence Andrews in the 1970s. Thereafter, the concept of this appliance has been modified by Roth (1976) without changing the basic principles (Walther, 1994; Phulari, 2013), and it is now widely-used internationally (Keim *et al.*, 2014). Since fixed appliances adhere both mechanically and chemically to the teeth, changes to the enamel surface may be induced during debonding procedures.

2.3. Orthodontic attachments

These appliances consist of passive components (bands, brackets, buccal tubes and lingual attachments), and active components (arch wires, springs and elastics). The passive components are fixed to the teeth using different adhesive bonding materials, whereas active components apply forces *via* the passive components to the teeth (Walther, 1994; Mitchell, 2007; Phulari, 2013).

Before the introduction of acid-etch techniques, bands were used to attach brackets and any auxiliaries to the teeth. These brackets were welded over the bands, which were either custom-made or preformed, from soft stainless steel and cemented around the tooth (Wahl, 2005). As modern bonding techniques have been developed, direct bonding of brackets to the teeth became common, reducing gingival trauma and demineralisation related to bands. However, bands are still preferable in some cases; for example, where both buccal and lingual attachments are required, or when extra-oral devices, such as headgears are to be used. In addition, they may be helpful where moisture control on posterior teeth is difficult and when bonding to gold or porcelain restorations is required (Mitchell, 2007).

2.4. Bonding mechanisms

Bonding as it refers to orthodontics can be defined as a technique of adhering orthodontic brackets, or other attachments, directly to the enamel surface using orthodontic adhesives. This adhesion can be achieved in two ways (Brantley and Eliades, 2001):

- i) Mechanical interlocking: Between the adhesive material and the microscopic irregularities of the etched enamel; for example, bonding between composite resin material (adhesive) and surface micro-irregularities of the etched enamel.
- ii) Chemical bonding: Reliant on the chemical reaction between the adhesive material and the enamel surface; for example, the chemical bond between polyacrylic acid, or phosphate-containing adhesive material, and hydroxyapatite crystals in enamel.

2.5. Bond strength

Direct bonding was introduced in orthodontics in the 1960s (Newman, 1969), following the pioneering work of Buonocore who demonstrated that phosphoric acid could be used to alter the enamel surface (Buonocore, 1955). In general, the feasibility of fixed orthodontic treatment relies on the capability of the adhesive bond (bracket-adhesive-enamel) to resist a combination of shear, tensile and torsional forces, which are usually directed to the brackets through masticatory forces and forces exerted from orthodontic appliances (Marković *et al.*, 2008).

The adhesive bond strength has been evaluated directly in *in vitro* and primarily indirectly in *in vivo* studies. In *in vitro* studies, an Instron® universal testing machine has been used to debond the bracket from the tooth surface, by applying one of the three debonding forces (shear, tension, and torsion), with bond strength measured by dividing the debonding force by the area of the bonded interface (Marković *et al.*, 2008). In *in vivo* studies, the retentive capacity (bond strength) is evaluated by measuring the incidence of bracket failure over a period of time (Gaworski *et al.*, 1999).

Discrepancies in relation to bonding efficacy have been highlighted between *in vivo* and *in vitro* studies. For example, Pickett *et al.* (2001) showed lower *in vivo* shear bond strength values than *in vitro* values. For the *in vivo* part of this study, eight patients were randomly assigned. They had a total of sixty premolars bonded with 3M Unitek Victory Twin brackets, precoated with Transbond XT™ light-cured composite resin, with an average of 23 months of orthodontic treatment. Shear bond strengths were recorded using a debonding device, attached to a digital force gauge. For the *in vitro* part of the study, the same type of bracket was bonded to 60 extracted premolar teeth, which were then divided into two groups of 30 each, and the shear bond strengths were recorded for the first group using the same debonding device, and for the second group with an Instron® universal testing machine. The results were as follows: *in vitro* 12.82MPa using the debonding device, and 11.02MPa using a universal machine, failure occurred *in vivo* at just 5.47MPa. The lower *in vivo* bond strength values may be attributed to the failure of *in vitro* conditions to mimic oral environment in terms of the pH of saliva, type of food and drinks consumed during orthodontic treatment and masticatory forces. Notwithstanding this, *in vitro* studies can give an indication of the appropriate

selection of adhesive for clinical use (Brantley and Eliades, 2001; Marković *et al.*, 2008).

It should be noted that the minimum bond strength threshold to ensure retention of brackets throughout a course of orthodontic treatment, and to allow easy bracket debonding when that is required, varies widely and remains unknown. For example, Reynolds (1975) suggested that the minimum acceptable *in vitro* bond strength value should be between 5.9-7.8MPa for most clinical orthodontic uses, whilst other studies suggested that bond strengths should range from 2.8-10MPa to be sufficient for clinical orthodontic purposes (Buonocore, 1963; Miura *et al.*, 1971; Lopez, 1980; Pus and Way, 1980). These high variations may relate to differences in: i) enamel morphology, ii) enamel preparation, iii) bracket material, iii) morphology of the bracket base, and iv) adhesive type (Marković *et al.*, 2008; Bakhadher *et al.*, 2015). Each of these variables will be discussed below.

2.6. Enamel characteristics

The human tooth has two anatomical parts: the crown, which is the visible part of the tooth, and the root which is embedded in the jaw. It consists of three different dental hard tissues: enamel, dentine and cementum, all of which surround a centrally-located pulp, where nerves and blood vessels supply the tooth with sensation and nutrients (Nanci, 2007). Enamel is the hardest biological tissue known within the human body. It is a highly mineralised structure forming the first protective layer of the crown of the tooth, whereas dentine is the second layer, covered by enamel in the crown portion, and cementum in the root (Stavrianos *et al.*, 2010).

2.6.1. Enamel structure

Enamel has a unique structure and properties appearing macroscopically as yellowish-white, bluish-white or greyish-white because it is semi-translucent and reflects the colour of the underlying dentine (Berkovitz *et al.*, 2005). Microscopically, it is composed of inorganic (mineral) and organic phases with a small amount of water. The mineral component of enamel comprises 95-96% by weight,

characterised by apatitic calcium phosphate (hydroxyapatite) crystallites cemented together by the organic matrix protein polymer (Boyde, 1997).

Microscopically, hydroxyapatite crystallites (Figure 2.1) usually appear as several million fibre-like crystals arranged as long bundles of prisms or rods, with a diameter 5-6 μ m and length 2.5mm, originating from the dentinoenamel junction and extending to the surface. These enamel prisms (rods) intertwine and are almost identical, having a hierarchical structure; the areas between these prisms are known as inter-prismatic (inter-rod) regions (Berkovitz *et al.*, 2005).

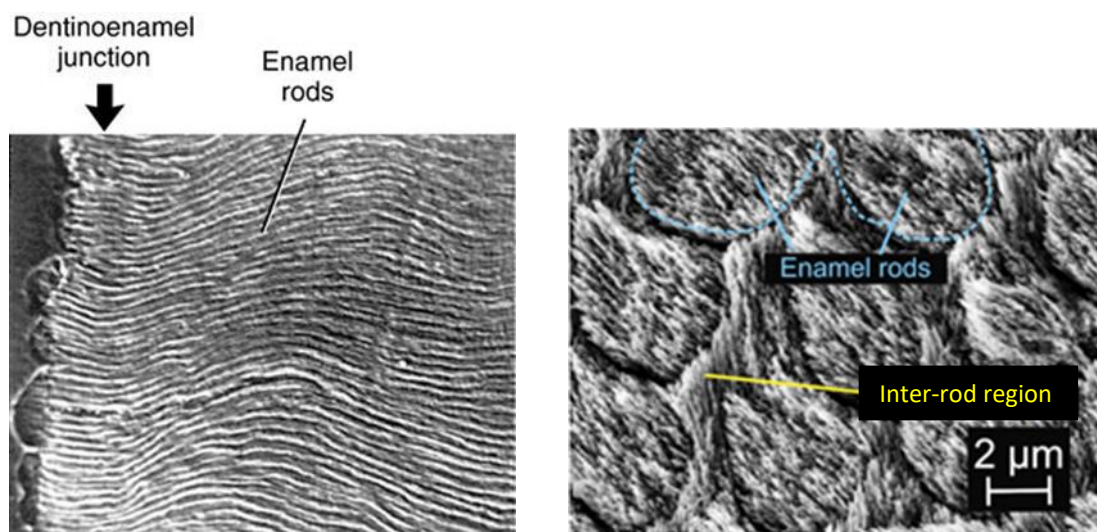


Figure 2.1. Scanning electron microscopy of enamel hydroxyapatite crystallites in enamel:

- a) Enamel rods and dentinoenamel junction (<https://pocketdentistry.com/7-enamel/>)**
- b) Enamel rods and inter-rod regions (Taken from Ang *et al.*, 2012)**

The mineral component of enamel also contains carbonate, magnesium, potassium, sodium and fluoride ions, in varying concentrations depending on their position within the tissue. These elements are incorporated into enamel during embryological development, affecting its susceptibility to demineralisation by bacterial acids, or acid of dietary origin (Laurance-Young *et al.*, 2011). Additionally, mature enamel contains organic matrix proteins, mainly amelogenin and enamelin, and the percentage of this matrix is influenced by the regularity or irregularity of enamel prisms and crystallites. These proteins are secreted during enamel

formation by ameloblasts, which are eventually lost when the tooth erupts. Hence, enamel, unlike bone and dentine, does not have the capability to repair itself, as it is acellular. This unique micro-structural architecture of enamel ensures that it has characteristic physical and chemical properties with the surface being harder, denser and more radio-opaque, compared with underlying layers (Berkovitz *et al.*, 2005). However, it is soluble in acids, this solubility decreases in the presence of fluoride and increases with higher carbonate levels (Robinson *et al.*, 2000).

2.6.2. Hydroxyapatite crystals structure

An appreciation of the apatite structure is central to understanding the behaviour of enamel during acid attack (Robinson *et al.*, 2000). Generally, apatite can be seen naturally as secondary minerals, such as in rocks, with a general formula of $\text{Ca}_{10}(\text{PO}_4)_6\text{X}_2$. If X is fluoride (F), it is fluorapatite, and if X is hydroxyl (OH), it is hydroxyapatite (Elliott, 2013).

Apatite present in enamel is calcium deficient (non-stoichiometric) hydroxyapatite with a formula $\text{Ca}_{10-x}(\text{PO}_4)_6(\text{OH})_{2-x}$ (where x is between 0 and 1). The properties of apatite can alter during ionic exchanges between saliva and enamel. For example, hydroxyl groups can be replaced by carbonate resulting in an increase in the solubility of apatite. In contrast, the solubility of apatite decreases when the hydroxyl groups are replaced by fluoride ions leading to an increase in its resistance to acid dissolution (Robinson *et al.*, 2000). Additionally, calcium can be replaced by magnesium and two sodium ions, and phosphate can be replaced by carbonate resulting in greater apatite solubility (Robinson *et al.*, 2000; Berkovitz *et al.*, 2005). It is apparent; therefore, that these substitutions within the lattice of the hydroxyapatite structure have a considerable effect on the behaviour of apatite, particularly its dissolution at low pH (less than 5.5) (Ten Cate and Featherstone, 1991).

2.7. Enamel surface preparation for bonding

2.7.1. Pumice prophylaxis

The enamel surface may be cleaned of the salivary pellicle layer, plaque, and/or surface debris before acid etching and bonding. The most common includes a prophylactic brush or rubber cup (used in a slow-speed hand-piece), in combination

with pumice or a prophylactic paste (Miura *et al.*, 1973). This procedure facilitates penetration of acid etch into the enamel surface, which may improve the bond strength of the adhesive to the enamel surface as reported in an *in vitro* study based on 200 extracted premolars by Mahajan *et al.*, (2015) using self-etching primer (Transbond™ Plus) and light-cured composite resin (Tranbond XT™).

Conversely, Barry (1995), in a double-blind clinical study, demonstrated that there was no significant difference in the bond strength of 614 brackets when pumice prophylaxis was omitted and conventional acid etch (37% phosphoric acid) was used. In addition, Ireland and Sherriff (2002) reported the results of an *in vivo* study performed, over an 18-month period, in which 60 patients participated in a split-mouth controlled clinical trial. They found that neither the bond strength, nor the enamel surface etch pattern after debonding of the brackets, was affected by pumicing with fluoridated or non-fluoridated pumice. The brackets had been bonded using a conventional acid etching system with resin adhesive (Right-On™) and resin modified glass ionomer cement (Fuji II LC™). The observed differences between the findings of Mahajan *et al.* (2015) and the latter two studies may relate to different acid-etch systems and different bonding adhesives used. Moreover, the previous study was an *in vitro* study with obvious difficulties in reproducing representative oral conditions based on extracted teeth in the *ex vivo* situation, and indeed in mimicking masticatory cycles and forces likely to induce debonding of brackets, with Mahajan *et al.*, (2015), for example, delivering shear forces to the bracket using a universal testing machine with a cross-head speed of 0.5mm per minute.

2.7.2. Acid etching

The concept of etching the enamel surface with phosphoric acid was first suggested by Buonocore in 1955. He used 85% phosphoric acid for 30 seconds and reported that the bond strength and retention were increased between acrylic resin restorations and the etched enamel surface (Swift *et al.*, 2002). Since then, he reduced the concentration of acid to 50% (Buonocore, 1970). Thereafter, separate *in vitro* studies by Silverstone (1974) and Retief (1974), reported that using an acid solution of 20-50% concentration for 1-2 minutes increased the capacity for retention. A range of variables may affect the bond strength of the (enamel-adhesive-bracket) system (Brantely and Eliades, 2001) such as:

- i) Type of acid etchant (phosphoric acid, nitric acid, citric acid, pyruvic acid, polyacrylic acid and ethylene diamine tetra-acetic acid).
- ii) Acid etch concentration
- iii) Duration of etching

Currently, 37% phosphoric acid for approximately 30 seconds is recommended for routine orthodontic bonding, in order to achieve the most suitable enamel etch patterns. This has been reported in an *ex vivo* study, which compared etching enamel with 37% phosphoric acid and 2.5% nitric acid, at three-time intervals (15, 30 and 60 seconds) (Gardner and Hobson, 2001).

2.7.2.1. Types of acid etching approach

a- Total etch approach (etch and rinse)

This technique is still the most widely used, effective approach to enamel bonding. It consists of two steps: removal of calcium phosphate (hydroxyapatite crystals) through etching the enamel surface with 37% phosphoric acid and use of an adhesive resin. Etching results in calcium monophosphate and calcium sulphate by-products on the enamel surface, which are highly soluble in water and can be completely removed by a vigorous water rinse, leaving rough areas, and creating micro-porosities within the enamel surface. The adhesive resin can infiltrate and polymerise within the created micro-porosities, resulting in mechanical interlocking between the enamel surface and adhesive resin (Van Meerbeek *et al.*, 2003; Van Meerbeek, 2008).

b- Self-etch approach

This technique may reduce the clinical etching time and minimise the errors that occur during application, compared with the total etch approach. This self-etch approach can be subdivided into: i) two steps (self-etch primer), which involves using a self-etch primer, followed by a separate bonding adhesive resin, and ii) one step, which contains etch, prime and bond together in one applicator (Yoshida *et al.*, 2004; Van Meerbeek *et al.*, 2008).

Self-etch primers/adhesives contain a high amount of acidic monomers, which are methacrylated phosphoric acid esters originating from the reaction of a diol (divalent alcohol) with methacrylic acid and phosphoric/carboxylic acid derivatives. These phosphate and carboxylic groups can bond ionically with calcium in hydroxyapatites, forming calcium complexes that are not rinsed away but incorporated into the adhesive resin (Van Meerbeek *et al.*, 2003; Yoshida *et al.*, 2004; Van Meerbeek *et al.*, 2008).

In regard to the clinical performance of total and self-etch approaches, conflicting reports have been published. Bishara *et al.* (2001) compared two types of acid etch techniques on 45 extracted human molars, before bonding metal brackets (Victory™), using an adhesive resin (Transbond XT™) in an *in vitro* study. The authors reported that the shear bond strength of orthodontic brackets after using the self-etch approach for 15 seconds (Prompt L-Pop, ESPE™) was significantly lower compared to the conventional etch approach (37% phosphoric acid gel for 30 seconds). These findings were supported by the following *in vitro* studies: Aljoubouri *et al.* (2003), Grubisa *et al.* (2004), and Scougall-Vilchis *et al.* (2009). Furthermore, similar findings were observed in a randomised clinical trial with a split-mouth design (Littlewood *et al.*, 2001). Conventional Transbond™ adhesive primer and hydrophilic primer were compared over a 6-month period after bonding adhesive pre-coated brackets to teeth (all teeth except molars; 33 patients for each acid etch type). The hydrophilic primer had a high bracket failure rate (18.8%) compared to the conventional acid system (6.8%). These findings were mirrored in a further clinical evaluation (Millett *et al.*, 1998). The authors reported that the bond failure of 7,118 brackets was also 6% in 548 patients using conventional Transbond™ adhesive primer.

More recently, Mirzakouchaki *et al.* (2016) evaluated the shear bond strength of metal and ceramic brackets bonded to etched teeth (120 maxillary and mandibular premolar teeth, in 30 orthodontic patients). Conventional acid etching (37% phosphoric acid) and self-etching primer (3M Unitek, USA) were used to etch the enamel surface. All teeth were maintained intra-orally for 30 days prior to extraction using surgical elevators (Aesculap, Tuttlingen, Germany) to prevent dislodgment of the brackets, which were later debonded using Hounsfield testing equipment to measure shear bond strength. The authors found that metal brackets with conventional acid etching had significantly higher shear bond strengths than those brackets bonded with self-etching primer.

Conversely, Aljoubouri *et al.* (2004), in a single blind design, randomised clinical trial, reported that there was no statistically or clinically significant difference between conventional two-stage Transbond adhesive primer and Self Etch Prime (SEP™, 3M) after 6 and 12 months. The study utilised stainless brackets with micro-etched bases that were bonded to 700 teeth (350 for each bonding system with the exception of molars) among 51 patients. Another randomised clinical trial has been performed by Manning *et al.* (2006) also comparing the two aforementioned etching systems. This trial involved robust randomisation procedures and allocation concealment and had a low drop-out rate. The evaluation was also undertaken both over 6 months and the overall duration of orthodontics, thereby accounting for potential deterioration of bond strength over the course of treatment. Bracket failure rate was assessed for 540 adhesive pre-coated brackets in 34 patients and was not statistically different with either etching approach, either over the initial 6-month period or throughout the duration of orthodontic treatment. This finding mirrors Aljoubouri *et al.* (2004), although the overall bracket failure rate reported for each etching system was lower in Manning *et al.* (2006) reflecting the potential confounding effects of operator experience and setting.

Recently, a systematic review and meta-analysis has been carried out to review 11 randomised controlled trials assessing the risk of attachment failure and bonding time of conventional acid etching system and self-etching system in orthodontic patients, over a minimum follow-up period of 12 months (Fleming *et al.*, 2012). The authors found that self-etch bonding systems had slightly higher odds of failure over 12 months but resulted in modest time saving (8 minutes for full bonding) compared with those bonded by the conventional acid etching system.

2.7.2.2. Effect of acid etching on enamel surface

The main iatrogenic effects of acid etching on the enamel surface can be classified into microscopic and macroscopic changes. Microscopically, the acid etching process promotes the formation of micro-porosities of variable depths within the enamel surface (Brantley and Elides, 2001). Based on observations from scanning electron microscopy, three predominant etch patterns are recognised (Silverstone *et al.*, 1975; Fava *et al.*, 1997):

- i) Type I: This is the most common pattern characterised by preferential removal of the prism core material, leaving the prism peripheries relatively intact, and producing a honeycomb pattern (Figure 2.2).
- ii) Type II: The prism periphery regions are removed preferentially, leaving remaining prism cores relatively unaffected, and producing a cobblestone pattern (Figure 2.3).
- iii) Type III: The enamel has a random pattern with areas corresponding both to Types I and II etching patterns.

These enamel etching patterns are affected by a number of variables (Nordenvall *et al.*, 1980; Redford *et al.*, 1986; Garcia-Godoy and Gwinnet, 1991; Fava *et al.*, 1997) such as: i) type of acid etching, ii) method of acid application, iii) duration of etching, iv) tooth morphology, v) surface and type of the tooth.

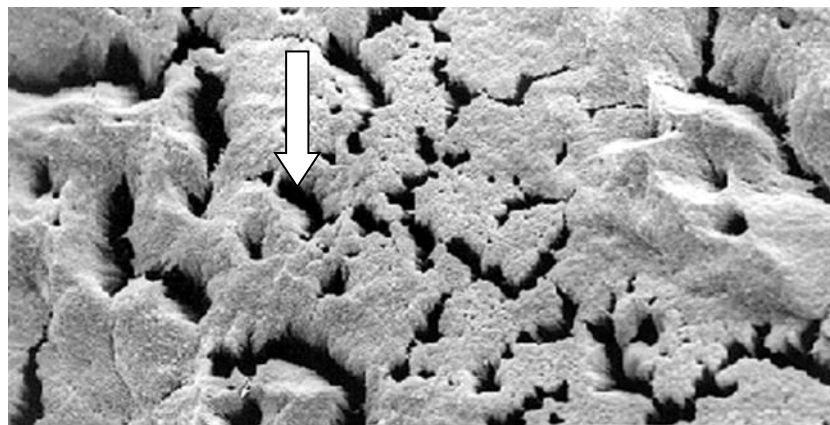


Figure 2.2. Type I enamel etching pattern after 30 seconds of acid etching. The cores of the prism are dissolved (arrow) at 4,500x magnification (Taken from Fava *et al.*, 1997)

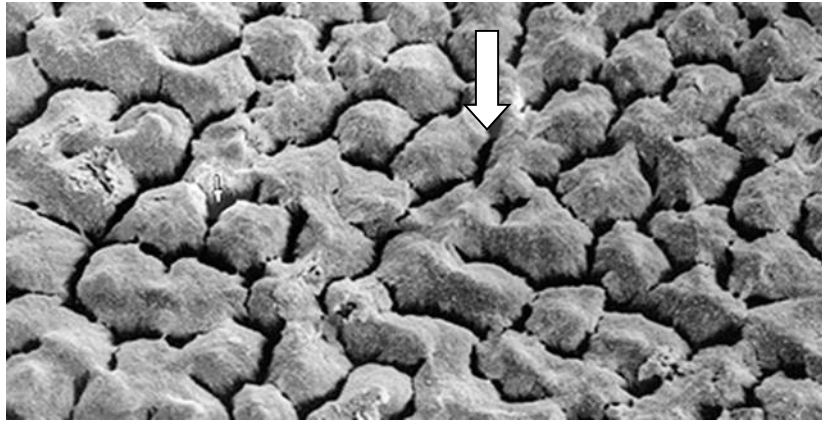


Figure 2.3. Type II enamel etching pattern after 45 seconds of acid etching. The periphery of enamel prisms is dissolved (arrow) at 4,500x magnification (Taken from Fava *et al.*, 1997)

Macroscopic effects of acid etching on the enamel surface following debonding can be divided into: i) enamel demineralisation and development of white spot lesions, ii) enamel discoloration due to retention of stains and precipitation of saliva, food and drinks into the porous etched enamel surface, or because remnants of resin tags were left *in situ* after debonding, which underwent colour change over time, iii) enamel fracture can occur during debonding of ceramic brackets, and iv) enamel loss of about 10-20 μ m due to acid etching, which leads to loss of fluoride found in the outer enamel layer (10 μ m) (Brantley and Eliades, 2001).

2.8. Bracket materials and base morphology

2.8.1. Bracket materials

2.8.1.1. Metal brackets

Initially in the early 20th century, these brackets were made from gold and later after the Second World War from stainless steel. These stainless-steel brackets are the most popular in fixed orthodontic treatment and have been used for decades (Brantley and Eliades, 2001; Phulari, 2013). They usually bond mechanically (micro-mechanical interlock) to the adhesives (see section 2.5), utilising indentations, undercuts, or grooves in the bracket base, which affect the bond strength between brackets and the adhesive (Smith and Reynolds, 1991; Knox *et al.*, 2000).

Metal brackets can withstand fracture and deformation and based on *in vitro* research consistently presents less friction at the bracket-wire interface (Flores *et al.*, 1994). They can be sterilized and recycled, but they are aesthetically unpleasing. In addition, stainless steel brackets contain a significant amount (8-12%) of nickel, which can induce an allergic response in susceptible patients (Huang *et al.*, 2004). Therefore, titanium brackets were introduced in the 1980s, as an alternative to stainless steel, since titanium does not contain nickel. Besides the exceptional biocompatibility of titanium brackets, they exhibit better mechanical properties, bond strength, and corrosion resistance compared with stainless steel brackets (Kusy *et al.*, 1998; Kapur *et al.*, 1999; Kusy *et al.*, 2000).

2.8.1.2. Plastic brackets

These brackets were introduced in the early 1970s and are made from unfilled polycarbonate. They were bonded to adhesives by chemical bonding utilising a plastic bracket primer to cause swelling in the bracket base allowing penetration of the adhesive into the swollen material and improving the bond strength between the plastic bracket and the adhesive. Subsequently, a new generation of brackets with a mechanical interlock base was introduced, to improve their bond strengths without the use of a primer (Brantley and Eliades, 2001; Phulari, 2013); however, the shear bond strengths of plastic brackets are significantly lower than those of metallic brackets (Fernandez and Canut, 1999; Guan, 2000; Liu *et al.*, 2004).

Although plastic brackets were initially introduced to improve aesthetics, they are easily discoloured and distorted in the oral environment due to their poor dimensional stability (Arici, 1998). In addition, they lack rigidity and stiffness, and the friction between the bracket and the arch wire at the bracket-wire interface is high. Thereafter, the use of reinforced polycarbonate brackets with ceramic or metal slots partially alleviated this problem (Feldner *et al.*, 1994; Alkire *et al.*, 1997).

2.8.1.3. Ceramic brackets

Ceramic brackets were introduced in the late 1980s manufactured from high purity aluminium oxide (alumina) or zirconium. These brackets are available as monocrystalline (transparent) and polycrystalline forms (tooth-coloured) (Brantley and Eliade, 2001; Phulari, 2013). They have better aesthetics with colour- and

dimensional-stability, and good resistance to wear and deformation compared with metal and plastic brackets. However, they have low fracture toughness and high frictional resistance (Jena *et al.*, 2007). Ceramic brackets usually bond to the adhesive either mechanically (mechanical interlock bases, utilising indentations or undercuts in bracket bases), or chemically (silane-coated bases), or both providing higher bond strengths. However, the silane-coated ceramic brackets led to an elevated risk of enamel damage at debonding, since the silane coupler (chemical mediator) unites the silica component of the ceramic bracket base and the adhesive resin.

In a comparative *in vitro* study, Wang *et al.* (1997) compared the shear bond strength of two brands of ceramic brackets with a chemically-coated base (Dentaurum™ and Transcend™), two brands of ceramic brackets with a base predisposing to mechanical interlock (Lumina™ and Crystalline™), and one type of metal bracket (Dyna-Lock™). These brackets were bonded to 60 extracted premolars with a resin adhesive (Concise™) and the brackets were debonded using an Instron® universal machine after 24 hours of bonding. The authors found that the bond strengths and the amount of enamel damage with chemically-coated ceramic brackets assessed by scanning electron microscope and energy dispersive x-ray spectroscopy (EDX) were significantly higher than the other bracket types. Similar findings were observed in a number of *in vitro* studies (Gwinnet, 1988; Viazis *et al.*, 1990; Forsberg and Hagberg, 1992; Atsü *et al.*, 2006).

Conversely, Habibi *et al.* (2007), in an *in vitro* study, claimed that the bond strength of metallic brackets was higher compared to ceramic brackets with mechanical interlock bases and chemical coated bases. Enamel cracks were assessed with a stereo-microscope after debonding of ceramic brackets with a plier and were not greater than those observed after debonding of metal brackets. However, this study used different techniques to evaluate the bond strength and to assess the enamel damage than the aforementioned studies.

2.8.2. Bracket base design

The design of the bracket base has a great effect on the longevity and integrity of bonding, and on the amount of enamel surface damage observed at debonding (Brantley and Eliades, 2001). Many conflicting reports have been published

regarding the effect of bracket base design on the bond strength. Knox *et al.* (2000), in an *in vitro* study, evaluated the effect of different types of metal bracket bases on the bond strength after bonding for one hour only and then debonding with a cross-head speed 0.5mm/min. Eighty incisor brackets were selected for each bracket base group, which included (60, 80, and 100) single mesh bases, double mesh bases, Mini Twin basesTM, Master seriesTM, and Dyna-LockTM to be bonded to steel mesh discs. The authors found that (60 and 100) single mesh bases performed better with ConciseTM and Right-OnTM than the 80-mesh bracket, and relatively poorly with TransbondTM. The 60 and 80 mesh bases performed well with Fuji Ortho LCTM but the 100-mesh base performed moderately well. The double mesh base performed well with Right-OnTM, and reasonably well with ConciseTM, TransbondTM, and Fuji Ortho LCTM. The Dyna-LockTM and Mini Twin bases performed well with all adhesives. Certain combinations of bracket base design and bonding adhesive, therefore, appeared to perform optimally complicating the isolation of definite trends in relation to bond strength. Moreover, similar conclusions were made by Smith and Reynolds (1991), in an *in vitro* study which compared three types of metal bracket bases bonded to plastic cylinders with a composite resin (ConciseTM). The authors reported that fine-mesh bases (A CompanyTM) produced the highest tensile strength using an Instron universal testing machine, followed by coarse-mesh bases (DentaurumTM) and finally undercut bases (Dyna-LockTM). In addition, Olsen *et al.* (1993) compared two types of ceramic brackets in an *in vitro* study on 40 extracted human premolars. They found that Ceramaflex brackets (TP Orthodontics) had significantly higher shear bond strength compared with traditional ceramic brackets (Unitek Corp, Monrovia, Calif) attached using the same bonding system (Right-OnTM).

The effect of bracket base design has also been reported by Sorel *et al.* (2002) in an *in vitro* study. They found that metal brackets with a laser-etched base had higher bond strength compared to metal brackets with a foil mesh base. Similar findings were observed by Sharma-Sayal *et al.* (2003) in a comparison of shear bond strength with 6 different bracket base designs, and Cozza *et al.* (2006) in a study comparing the shear bond strength of 5 different brands of metal brackets. On the basis of the available evidence, it therefore appears that bracket base designs with highly complex arrangements of undercuts may lead to improved bond strength by increasing the depth, size, and distribution of the adhesive within the bracket-adhesive interface, promoting a sufficiently large stress distribution area.

Conversely, Bishara *et al.* (2004), in a further *in vitro* study, reported no significant differences between the shear bond strengths of two metallic brackets with different bracket bases: Victory™ (single-mesh bracket base), and Ovation™ (a double-mesh bracket base). The authors compared between 20 upper left central incisor brackets for each bracket base group bonded to 40 extracted human molars (20 per group) using Transbond XT™ adhesive. The testing of shear bond strength was accomplished using the flattened end of a steel rod attached to the cross-head of a Zwick test machine. In addition, Cuco *et al.* (2002) found no significant difference in the shear bond strength between brackets of the same surface area with a different gauge mesh size using the same approach to testing. The authors tested metal brackets (80- and 100- gauge mesh bases) with mini and standard size bases, which were bonded to 80 extracted human premolars. The observed variations between the results of Bishara *et al.* (2004) and Cuco *et al.* (2002) with other studies can be attributed to differences in research protocol and the technique sensitivity of the materials, reflecting inconsistencies in experimental design. Further clinical studies in this area are therefore required to obtain reliable and more generalisable findings.

2.9. Adhesion and adhesives

2.9.1. Resin Based Composites (RBCs)

These are the most frequently used adhesives in orthodontic bonding as they adhere to the enamel surface by mechanical interlocking retention with a sufficient bonding strength (Brantley and Eliades, 2001). It has been reported that RBCs have shown the greatest bond strength among the other orthodontic adhesives (Rock and Abdullah, 1997; Summers *et al.*, 2004).

In general, resin-based composites contain an organic polymeric matrix, inorganic reinforcing fillers, and a silane coupling agent. The conventional organic matrix, (also known as Bowen's resin), is bisphenol A-glycidyl methacrylate (BisGMA), which is highly viscous, and may also contain urethane dimethacrylate (UDMA), which is less viscous than BisGMA. This matrix further requires the addition of low viscosity dimethacrylate monomers (diluent) to improve their handling for clinical use. Examples of diluents are triethyleneglycol dimethacrylate (TEGDMA) or diethyleneglycol dimethacrylate (DEGDMA) (Lutz and Philips, 1983; Ferracane, 2011). RBCs are cured by a free radical addition polymerisation reaction of the

methacrylate monomer resin matrix, by using different polymerisation promoting systems (Brantley and Eliades, 2001).

The inorganic filler particles consist of glass beads or rods of either aluminium silicate, barium, strontium or silicate glasses; they encompass between 50-80% by mass of the contents of resin-based composites. Incorporation of fillers reduces the polymerisation shrinkage and the coefficient of thermal expansion of RBCs, and improves their wear resistance, and tensile and compressive strengths. Consequently, the components and amount and size of fillers influence the mechanical, physical and optical properties of RBCs (Ferracane *et al.*, 2014). With regard to coupling agents, the most commonly used is 3-methacryloxypropyl trimethoxysilane. These agents are used to chemically bond the hydrophilic inorganic fillers to the hydrophobic organic resin matrix and to increase the filler loading by enhancing the particle wetting improving the mechanical properties and the clinical performance of RBCs (Cramer *et al.*, 2011).

2.9.2. Glass Ionomer Cements (GICs)

The first glass ionomer cements were designed by Wilson and Kent in the early 1970s as restorations, cavity liners, and luting cements for crowns and inlays. Over the years (late 1980s), these cements became popular for use as adhesives for orthodontic bands and brackets (Brantley and Eliades, 2001). GICs are composed of an ion-leachable glass powder (calcium fluoroaluminosilicate) that reacts with the water-soluble polyalkenoic acid to form a cement by an acid-base reaction. Their advantages have caught the attention of many researchers, since they bond chemically to the enamel surface. The carboxyl groups of polyalkenoic acid form chemical ionic bonds with the calcium ions in hydroxyapatite of enamel (Yoshida *et al.*, 2000; Brantley and Eliades, 2001). In addition, they release fluoride ions since these cements contain high concentrations of fluoride (10-23% by weight) (Brantley and Eliades, 2001).

Despite the distinct advantages of GICs, they have some limitations chiefly poor bond strength compared to RBCs (Rekha and Varma, 2012). In a three-year clinical trial on 17 patients, Miller *et al.* (1996) compared the bracket failure of GIC (Ketac-fil™) and a composite resin (Rely-a-bond™), at 6, 18, 30 and 36 months. Bracket failure rates in the GIC group were 13%, 28%, 31% and 33%, respectively. In the

composite resin group, the corresponding values were 11%, 13%, 14% and 15%. These findings revealed that bracket failure was more common in the GIC group, thus suggesting that GIC has lower bond strength compared with composite resin. Similar conclusions were also reported in other *in vivo* studies (Voss *et al.*, 1993; Norevall *et al.*, 1996).

2.9.3. Resin Modified Glass Ionomer Cements (RMGICs)

Glass ionomer cements have been modified with the addition of a small amount of water-soluble resin monomer, hydroxyethyl methacrylate (HEMA; up to 10%) to form Resin-Modified Glass Ionomer cements (RMGICs). These materials are suitable for orthodontic bonding as they combine the favourable properties of both GICs (chemical bond to enamel in a moist environment and fluoride release), and resin-based cements (quick set and superior bonding strength) (Movahhed *et al.*, 2005). RMGICs undergo two reactions: an acid-base reaction between the polyacrylic acid and the glass of the conventional GICs, and polymerisation of the resin component (HEMA) by free radicals, to harden the cement (Brantley and Eliades, 2001).

With regard to the bond strength of RMGICs, a plethora of studies have been undertaken. In an *in vitro* study, Owens and Miller (2000) bonded 75 twin premolar brackets coated with Optimesh XRT™ (Ormco, Calif) to extracted teeth, with two resin adhesives: (Transbond XT™ and Enlight™), and RMGIC (Fuji Ortho LC™). The shear bond strength of RMGIC was significantly lower than the two resin adhesives. Similar findings were also reported in an *in vitro* study by Meehan *et al.* (1999).

Interestingly, Lippitz *et al.* (1998), in an *in vitro* study, found that etching the enamel surface with 10% phosphoric acid led to no significant difference between the shear bond strengths of resin adhesive and those of three RMGICs (Advance™, Fuji Duet™ and Fuji Ortho LC™), after 24 hours and 30 days of bonding 100 mesh backed stainless steel brackets to 100 extracted human premolars. The shear bond strength of these RMGICs, with unetched enamel was lower than with etched enamel. These findings are supported by other *in vitro* studies (Chung *et al.*, 1999; Sfondrini *et al.*, 2001). In addition, in an *in vitro* and *in vivo* study, Summer *et al.* (2004) compared resin adhesive (Light Bond™) and RMGIC (Fuji Ortho LC™), after

using them to bond 50 GAC micro-arch universal orthodontic brackets to extracted human premolars. For the resin group, 37% phosphoric acid was used to etch the enamel surface, whereas for the RMGIC group, 10% polyacrylic acid was used. The authors reported no significant difference between resin adhesive and RMGIC, with bracket failure rates at 5% and 6.5%, respectively, over 1.3 years. Furthermore, the *in vitro* findings of Summer *et al.* (2004) showed that resin adhesive had higher shear bond strengths than those obtained with RMGIC, after bonding for 30 minutes and 24 hours, respectively. However, Chitnis *et al.*, (2006), in an *in vitro* study demonstrated that there was no significant difference in the shear bond strength between resin adhesive bonded to etched enamel with 37% phosphoric acid, and RMGIC bonded enamel etched with 10% polyacrylic acid, after bonding for 1 hour and 7 days, respectively. More recently, Cheng *et al.* (2011), in an *in vitro* study also supported these findings in an investigation on the shear bond strength between resin adhesive (Transbond™) and RMGIC (Fuji Ortho™). After 24 hours bonding of 100 mini Dyna-Lock™ brackets to extracted human premolars, with etched or non-etched enamel surfaces, they found no significant difference in the shear bond strength between resin and RMGIC. In addition, a systematic review of 11 clinical trials has concluded that RMGIC may be associated with the same clinical debonding (failure) rate as RBCs after 12 months (Mickenautsch *et al.*, 2012). This review also recommended further high quality randomised controlled trials to confirm this finding.

It has been suggested that etching the enamel surface with 37% phosphoric acid can significantly increase the bond strength of RMGIC, instead of etching with 10% or 20% polyacrylic acid (Bishara *et al.*, 2000). In addition, Cacciafesta *et al.* (2003), in an *in vitro* study using bovine teeth, reported that RMGIC (Fuji Ortho™) with a self-etching primer, produced the highest shear bond strength under different enamel surface conditions (dry enamel, water-moistened enamel, and saliva-moistened enamel); these values were significantly higher than those etched with conventional 37% phosphoric acid and 10% polyacrylic acid, except when RMGIC was used in combination with 37% phosphoric acid on dry enamel. In addition, the shear bond strength of RMGIC in combination with 10% polyacrylic acid was lower than RMGIC with 37% phosphoric acid, except when both conditioners were used on water-moistened enamel. Furthermore, the shear bond strength of RMGIC on unetched enamel gave the lowest values.

In summary, RMGICs have lower bond strengths than RBCs. This bond strength can be improved by etching the enamel surface either with self-etching primer under various conditions (dry, water-moistened and saliva-moistened enamel), or 37% phosphoric acid on dry enamel and 10% polyacrylic acid on moistened enamel.

2.9.4. Compomers

Compomers are polyacid modified resin composites formed by combining composite resin and fluoro-silicate glass into a single component composite resin. They differ from RMGICs in that the resin component comprises 30-50% of the total components (Eberhard *et al.*, 1997; Gladys *et al.*, 1997).

Millett *et al.* (2000) carried out a split-mouth comparative clinical trial using 426 brackets, with half bonded with compomer (Dyract Ortho™) and the other half with chemical cured resin adhesive (Right-On™) on 45 randomly selected patients. Compomer produced bond strengths comparable to resin adhesive over the entire duration of fixed orthodontic treatment, with bracket failure rates of 17% and 20% recorded for compomer and resin adhesive, respectively. The authors reported that neither patient gender nor malocclusion had any effect on the time to failure of the first bracket (526 days for each bonding material), but patient age was considered to be a predictor. In addition, the split-mouth design of this study was useful in evaluating the clinical performance of both bonding materials under the same environmental conditions.

Interestingly, similar conclusions were made in a comparative *in vitro* study, which used 75 stainless pre-adjusted edgewise brackets with micro-etched bases. Five bonding materials (15 brackets for each) were used: compomer (Dyract Ortho™), chemical cured resin adhesive (Right-On™), light-cured resin adhesive (Transbond™), RMGIC (Fuji Ortho LC™), and conventional GIC (Ketac-Cem™) (Millet *et al.*, 1999b). The authors found no significant differences in shear bond strengths among the first four bonding materials after bonding for 24 hours, but the shear bond strength of the latter was significantly less than the others. Furthermore, the bracket failure rate was similar for Dyract Ortho™, Right-On™, and Fuji Ortho LC™ but less than those for Transbond™ and Ketac-Cem™.

There is, however, an *ex vivo* study, which used two types of brackets: 'A' Company Straight-Wire® twin brackets backed with foil mesh and Unitek brackets with Dyna-Lock™ bases incorporating machined undercuts and serrated ridges. The authors reported that light-cured resin adhesive (Transbond™) produced significantly higher shear bond strengths than compomer (Dyract Ortho™) after 15 minutes and 24 hours, respectively, for both bracket types (Rock and Abdulla, 1997). The observed difference between *in vitro* and *ex vivo* studies may stem from environmental differences, and the use of different bracket-base design.

Additionally, Millett *et al.* (2000) also highlighted that enamel demineralisation was reduced significantly with compomer (Dyract Ortho™) compared to adhesive resin (Right-On™). The percentage of teeth affected was 20% for compomer and 26% for adhesive resin. This indicates the potential efficacy of compomer in preventing enamel demineralisation, since it has the capability of releasing fluoride. These results support the findings from another split-mouth design study, which confirmed that compomer (Dyract Ortho™) significantly reduced the rate of recurrent caries when used as a restoration for primary molars compared to amalgam restoration (Tytin™) over a 3-year period (Marks *et al.*, 1999).

Rekha and Varma (2012), in an *in vitro* study using 96 primary molars, reported that compomer (Compoglass™) produced the highest tensile bond strengths, and microleakage level compared to RMGIC (Fuji II LC) and conventional GIC (Fuji IX GP). This was attributed to the presence of resin in a larger fraction by weight compared to RMGIC and conventional GIC facilitating bonding to the etched tooth surface by micromechanical interlock, whilst the high microleakage level of compomer was due to the polymerisation shrinkage of the light-cured resin component of compomer causing the material to shrink away from the tooth surface, creating a gap resulting in microleakage. These results were supported by an *in vitro* study comparing the microleakage of compomer (Dyract Ortho™) and RMGIC (Fuji Ortho LC™) (Toledano *et al.*, 1999). However, Brackett *et al.* (1998) found that there was no significant difference in microleakage between RMGIC (light-cured) and compomer, which might be due to the differences in the sample preparation procedure and the use of bovine teeth instead of human teeth; the latter were used by Toledano *et al.* (1999) and Rekha and Varma (2012).

2.10. Debonding

The term “debonding” refers to removal of attachments (bands and brackets) from the surfaces of teeth after fixed appliance-based orthodontic treatment, followed by clean-up methods to remove remnants of adhesives from the enamel surface (Ahrari *et al.*, 2013). Ideally debonding and post clean-up techniques should leave the enamel surface intact and with the same degree of smoothness as the pre-treated tooth. However, this is not always possible; these procedures may result in mechanical removal of enamel (Bonetti *et al.*, 2011). If remnants of the adhesive are not completely removed or enamel fracture occurs, staining and plaque formation on the tooth surface are likely, resulting in compromised aesthetics. Furthermore, the enamel becomes less resistant to organic acids, which may predispose to enamel demineralisation and dental caries. Therefore, preservation of enamel surfaces after orthodontic treatment is extremely important for orthodontists (Pont *et al.*, 2010).

Several factors may affect the integrity of the enamel surface during or after fixed orthodontic treatment. These include: i) enamel etching before bonding, ii) the adhesive bonding material itself, iii) the brackets used (metal or ceramic brackets), iv) debonding and adhesive clean-up technique. The latter is considered to be the most significant cause of enamel loss (Azzeh and Feldon, 2003; Arhun and Arman, 2007; Knösel *et al.*, 2010; Pont *et al.*, 2010).

2.10.1. Bond failure rate

At debonding, three types of bond failure can occur (Pont *et al.*, 2010; Sumali *et al.*, 2012):

- i) Adhesive failure: Adhesion fails at the adhesive-enamel interface or the bracket-adhesive interface and all the remnants of the adhesive would remain either on the bracket base, or on the enamel surface.
- ii) Cohesive failure: The bond fails within the adhesive layer. This type of bond failure is preferable as the remnants of the adhesive would be spread between the enamel surface and the bracket base.

iii) Combination of adhesive and cohesive failure: The remnants of the adhesive are unequal but present both on the enamel surface and the bracket base.

The amount of the adhesive remaining on the enamel surface after debonding can be inspected visually using the Adhesive Remnant Index (ARI) (Artun and Bergland, 1984), by assigning a score from zero to 3. The highest ARI score implies that the adhesive material remained on the enamel surface in its entirety after debonding (Oztoprak *et al.*, 2010; Tehranchi *et al.*, 2011).

2.10.2. Debonding Methods

2.10.2.1. Mechanical methods

These involve the use of special instruments including tailored bracket removal pliers (Pignatta *et al.*, 2012). The force required to mechanically debond is high, resulting in either deformation of the bracket itself, or adhesive bond failure at the adhesive-enamel interface, which may potentially damage the enamel surface (Bishara and Fehr, 1993; Jena *et al.*, 2007).

2.10.2.2. Electro-thermal debonding methods

This method is based on heating the bracket with a rechargeable, cordless heating gun to soften the adhesive materials resulting in bond failure between the bracket base and the adhesive material (Sheridan *et al.*, 1986). It is a relatively quick, effective method and it causes less enamel damage or bracket fracture compared with mechanical debonding (Bishara and Trulove, 1990). In addition, the heating temperature during electro-thermal debonding was reported to be too low for pulpal damage (Jost-Brinkmann *et al.*, 1992; Brouns *et al.*, 1993), in spite of the earlier investigation by Rueggeberg and Lockwood (1990), who reported that electro-thermal debonding has the potential to cause pulp necrosis.

2.10.2.3. Ultrasonic methods

These methods are used to apply high-frequency vibration using specially designed tips at a point between the bracket base and the adhesive. The resulting force magnitudes are significantly lower than those required for mechanical debonding.

This approach may serve to reduce the likelihood of enamel damage while simultaneously removing the adhesive remnants (Bishara and Trulove, 1990). However, this approach is time-consuming and may induce discomfort in sensitive teeth (Krell *et al.*, 1993; Boyer and Bishara, 1995).

2.10.2.4. Laser systems

These methods have been used in several studies. A low risk of enamel damage has been reported using laser systems compared with other debonding methods (Azzeh and Feldon, 2003). Ahrari *et al.* (2013) in an *in vitro* study measured the adhesive remnant index (ARI) and length, number and direction of enamel cracks. They found that debonding of ceramic brackets using a carbon dioxide (CO₂) laser resulted in minimal damage to the enamel surface and no bracket fracture was identified. This may relate to the thermal softening of the adhesive bonding material with laser systems, creating a bond failure site closer to the (bracket-adhesive) interface, as reported by Tehranchi *et al.* (2011). In their *in vitro* study, they observed that ARI scores were high on the tooth surface compared to those obtained using the conventional methods, where the debonding sites were closer to the enamel-adhesive interface, thus increasing the probability of enamel damage.

The other advantage of using a laser system is that the amount of force required for debonding is significantly lower compared to other methods; pain is therefore considered minimal during removal of ceramic brackets (Azzeh and Feldon, 2003; Oztoprak, 2010). Additionally, Sarp *et al.* (2011) using an Ytterbium laser and Saito *et al.* (2015) using CO₂ laser reported that laser debonding consumes less time (6 seconds) and provides more precise control of the heat applied to soften the adhesive bonding materials, compared to other electro-thermal debonding methods. However, the surface temperature of the brackets could reach ~150°C, which is extremely high for the oral cavity, and therefore expertise is required to remove the brackets (Hayakawa, 2005).

2.10.3. Post debonding clean-up methods

The search for an efficient and safe protocol for clean-up of enamel after debonding has led to various methods being tried (Table 2.1; Janiszewska-Olszwska *et al.*, 2014).

Table 2.1. Summary of post debonding clean-up methods

Clean-up methods	Examples
I) Hand instruments	Adhesive removing pliers, Debonding pliers
II) Dental stones	Arkansas stone, Green stone
III) Wheels and discs	Green rubber wheel, Soflex discs
IV) Scalers	Hand scaler, Ultrasound scaler
V) Dental burs	Fibre-reinforced composite, Tungsten carbide, Diamond finishing, Ultra-fine diamond, Finishing carbide
VI) Lasers	CO ₂ (Carbon dioxide) Nd:YAG (Neodymium-doped Yttrium Aluminium Garnet) Er:YAG (Erbium-doped Yttrium Aluminium Garnet) Diode
VII) Pumice or zirconium paste	

These various clean-up methods have been undertaken in a range of settings. Moreover, the lack of standardisation of the volume of adhesive remnants may also influence these findings (Uluosoy, 2009; Karan *et al.*, 2010; Ozer *et al.*, 2010). Therefore, it is apparent that an accepted protocol for removal of adhesive remnants is not yet established. However, the most common and efficient method for adhesive removal is by using tungsten carbide burs in a slow-speed, water-cooled rotary hand-piece. Janiszewska-Olszwska *et al.* (2014) reported that this method resulted in minimal damage to the enamel surface compared to other alternatives.

Ireland *et al.* (2005) found in an *in vitro* study on eighty human premolars that enamel loss arose to varying depths following four post clean-up methods (slow-speed tungsten carbide bur, high-speed tungsten carbide bur, debonding plier, and ultrasonic scaler) following removal of two orthodontic adhesives (Transbond XT™ and Fuji Ortho LC™). The lowest enamel loss depth (0.75µm) was observed in the Fuji Ortho LC™ group with a slow-speed tungsten carbide bur. The depth of enamel loss was measured by Planer Surfometer. Similarly, Pus and Way (1980) observed enamel loss after adhesive removal using high speed bur, green rubber wheel, and slow-speed tungsten carbide bur of 19.2µm, 18.4µm and 11.3µm, respectively. This enamel loss was measured by a Nikon profile projector fitted with a microstage calibrated in micrometres for 100 human premolars. This between study variations may stem from differences in the technique utilised to remove orthodontic adhesives, the type of orthodontic adhesive, and the methodology used to assess enamel loss. Bollen *et al.* (1997) suggested that enamel surface roughness of 0.2µm is a threshold for bacterial adhesion and caries formation highlighting the importance of preserving a smooth enamel surface following orthodontic debond.

Banerjee and co-workers (2008) have pioneered the use of air-abrasion *in vitro* to selectively remove residual adhesive bonding materials. They bonded metal brackets to the buccal surfaces of thirty human extracted premolars using an adhesive bonding material (Unite™, 3M Unitek). Thereafter, these brackets were debonded using debonding pliers with the adhesive remnants removed using three methods: a slow-speed, eight bladed tungsten carbide bur; alumina air-abrasion; and bioactive glass air-abrasion (45S5). The air-abrasion unit (Abradent™, Crystalmark, CA, USA) was used with an air pressure of 60 psi (pound per square inch) and a powder flow rate of 2.2g/min. Bioactive glass powder (45S5) propelled *via* air-abrasion produced the least enamel loss (0.135mm³) compared with alumina air-abrasion (0.386mm³) and tungsten carbide burs (0.285mm³). Enamel loss was

assessed by volumetric analysis involving stereo-lithic files after propelling this glass. This was attributed to its hardness value which slightly exceeded that of sound enamel (~3.5GPa; O'Donnell, 2011). Various hardness values for 45S5 have been reported in the literature, for example, 4.5GPa (Cook *et al.*, 2008) and 5.75GPa (Lopez-Esteban *et al.*, 2003). Therefore, there is still a need to design a bioactive glass with hardness similar to, or lower than that of enamel in order to facilitate safe but efficient removal of residual adhesive bonding materials after bracket debonding.

2.11. Enamel demineralisation and remineralisation

Enamel demineralisation can be defined as a process of partial or complete dissolution of minerals (calcium-deficient hydroxyapatite crystallites) resulting in the release of calcium and phosphate ions and leading to changes in the microstructure of enamel and loss of hydroxyapatite. This dissolution of minerals exposes the organic matrix to microbially-determined deterioration, followed by microbial attachment and dental caries (Ehrlich *et al.*, 2008). A white spot lesion is also considered as the first clinical sign of enamel caries prior to the carious lesion reaching the dentine (Sangamesh *et al.*, 2011).

Enamel demineralisation has been attributed to four main factors: bacteria, fermentable carbohydrate, a susceptible tooth surface and time. The acidogenic bacteria (*Streptococcus mutans*, and *Lactobacillus* spp.) attach to the tooth surface *via* the plaque biofilm. They ferment carbohydrate producing organic acids (lactic, formic, acetic and propionic acid), thus decreasing the pH of plaque below the critical value of 5.5. This process occurs within 1 to 3 minutes and results in dissolution (demineralisation) of the enamel surface minerals (hydroxyapatites) (Kidd and Fejerskov, 2003). On the contrary, the process of deposition of calcium, phosphate and other biomineral ions within or on partially demineralised enamel surface is called remineralisation. These biomineral ions originate either from dissolved dental tissues, an external source, or a combination of these sources (Cochrane *et al.*, 2010).

A variety of demineralising solutions and gels containing either lactic acid or acetic acid undersaturated with respect to hydroxyapatite have been used to induce artificial enamel demineralisation within *in vitro* research (Gray, 1966; van Dijk *et al.*, 1979; Ingram and Silverstone, 1981; ten Cate and Duijsters, 1982; White, 1987; ten

Cate *et al.*, 1996; Kielbassa *et al.*, 2005; Vieira *et al.*, 2005; Ten Cate *et al.*, 2006; Lynch *et al.*, 2007; Magalhaes *et al.*, 2009). Variations in these solutions and gels including their nature and the viscosity of the acid used, fluoride concentration, and the degree of saturations of some minerals can lead to differences in the chemical composition (Lynch and ten Cate, 2006) and the hardness values (Magalhaes *et al.*, 2009) of the artificial demineralised enamel surfaces. The mineral distribution within the enamel surfaces can also be affected (Arends *et al.*, 1987; Lynch *et al.*, 2007).

2.11.1. White spot lesions (WSLs)

White spot lesions are one of the most prevalent iatrogenic effects of orthodontic fixed appliance treatment. These lesions are the initial clinical manifestation of enamel demineralisation with the potential to develop into overt caries, thus requiring restorative treatment (Sangamesh *et al.*, 2011). Therefore, WSLs can be defined as subsurface enamel porosities, due to carious demineralisation. Clinically, these lesions can be identified as opaque, white areas on smooth surfaces as the degree of enamel mineralisation influences their translucency (Bishara and Ostby, 2008; Sundararaj *et al.*, 2015). They may also be apparent under bright white light to the naked eye after air-drying the enamel surface as the air, which has a refractive index of 1.0, fills the pores of the lesion instead of water (refractive index: 1.33) and both have a refractive index below that of enamel (1.63; Kidd and Fejerskov, 2004).

Orthodontic patients are often teenagers, who have a higher risk of enamel demineralisation than adults due to differences in the level of oral hygiene, and as newly erupted teeth are more susceptible to acid attack (Dirks, 1966; Garcia-Godoy and Hicks, 2008; Mayne *et al.*, 2011). A plethora of studies have reported the association between fixed appliance-based orthodontic treatment and WSL formation (Gorelick *et al.*, 1982; Mizrahi, 1983; O'Reilly and Featherstone, 1987; Mitchell, 1992b; Banks *et al.*, 2000; Boersma *et al.*, 2005). Gwinnett and Ceen (1979), in a clinical study involving 10 patients, found a rapid increase in plaque accumulation related to the fixed orthodontic attachments, which act as plaque stagnation areas since they impede regular oral hygiene procedures. Plaque in orthodontic patients may have a lower pH compared with individuals with no orthodontic appliances (Chatterjee and Kleinberg, 1979). Hence, plaque induces the enamel demineralisation process and hinders remineralisation.

There may also be a significant increase in the level of cariogenic bacteria, such as *Streptococcus mutans* (*S. mutans*) and *Lactobacilli* spp. in the saliva and plaque of orthodontic patients, leading to enamel demineralisation stemming from the production of organic acids. Scheie *et al.* (1984), in a clinical study, observed a significant increase in the level of *S. mutans* in the saliva and plaque of 14 patients after insertion of orthodontic appliances. Øgaard *et al.* (2001) in a longitudinal study of 220 patients also found that the best predictor for WSLs at debonding was the presence and preponderance of *S. mutans*. However, Boersma *et al.* (2005), in a clinical study involving 62 patients, reported that there was a positive correlation between orthodontic appliance and *Lactobacilli* counts, but not to *S. mutans* counts, since the reduction in bacterial counts was more pronounced for *Lactobacilli* spp. after 6 weeks of debonding. This may indicate that *S. mutans* levels need more time to return to the normal levels in the mouth, or that the natural balance between these acid-forming bacteria is shifted during orthodontic treatment.

More recently, Lombardo *et al.* (2013), in a prospective clinical study on 20 patients aged between 19 and 23 years, confirmed that there were changes in the oral environment after placement of orthodontic appliances. They found that there was more plaque retention within 4 to 8 weeks of bonding and higher *S. mutans* counts after 8 weeks in patients wearing appliances.

2.11.2. Timing and location of development of WSLs

Based on an *in vivo* study involving 20 participants, WSLs can be detected around orthodontic brackets as early as four weeks after starting fixed orthodontic treatment (O'Reilly and Featherstone, 1987). In a combined clinical and *in vitro* evaluation, teeth were extracted after 4 weeks of orthodontic treatment and their mineral profiles determined after sectioning (O'Reilly and Featherstone, 1987). The authors found that these lesions could be inhibited and/or reversed by the use of commercially available fluoride products, such as fluoride-containing toothpaste (1,100 ppm sodium fluoride), sodium fluoride (0.05%) mouth-rinse, and acidulated phosphate fluoride treatment (1.2% fluoride).

Similar findings were reported in an *ex vivo* study by Gordon and Featherstone (2003), where 21 teeth were extracted for orthodontic purposes after 4 weeks of treatment. These teeth were sectioned and evaluated quantitatively with

microhardness testing. The authors found that fluoride-releasing glass ionomer cement for bonding orthodontic brackets successfully inhibited enamel demineralisation, which was located around the brackets bonded with non-fluoridated composite resin after four weeks of orthodontic treatment. In addition, Holman *et al.* (1988), in an *in vivo* study involving 14 patients, found that weekly professional removal of the bands and plaque over a five-week period, prevented lesion formation, while leaving both intact resulted in visible WSLs. Furthermore, in an *ex vivo* study, WSLs were noticed on 22 extracted premolars after 6 to 13 weeks of orthodontic treatment following evaluation using a stereo-microscope (Twetman *et al.*, 1996). These differences in the timing of development of enamel demineralisation might be due to the study design and the methods used to assess enamel demineralisation, but in general all these studies reveal the correlation between the introduction of fixed orthodontic treatment and enamel demineralisation (Table 2.2).

Table 2.2. Summary of studies reporting on WSL formation based on observation time and experimental technique

Study	Study type	Duration of orthodontics prior to extraction	Preventive measure	Clinical findings
O'Reilly and Featherstone (1987)	Combined <i>in vivo</i> and <i>in vitro</i>	4 weeks	Fluoride-containing toothpaste (1,100 ppm sodium fluoride), sodium fluoride (0.05%) mouth-rinse, and acidulated phosphate fluoride treatment (1.2% fluoride)	WSLs developed in the untreated group but inhibited in treated groups with commercially-available fluoride products
Gordon and Featherstone (2003)	<i>Ex vivo</i>	4 weeks	Fluoride-releasing glass ionomer cement	WSLs developed on teeth bonded with non-fluoridated composite, whilst successfully inhibited with fluoride-releasing cement
Holman <i>et al.</i> (1988)	<i>In vivo</i>	5 weeks	Professional removal of the bands and plaque weekly	WSLs prevented in the treated group and arose in untreated (without intervention)
Twetman <i>et al.</i> (1996)	<i>Ex vivo</i>	6-13 weeks	Fluoride-releasing glass ionomer cement	WSLs developed on teeth bonded with conventional composite and inhibited with the fluoride-releasing cement

With regard to the location of WSLs, they often develop under loose bands and around the bracket base, especially on the buccal surfaces of the teeth in the gingival areas predisposed to plaque accumulation (Gorelick *et al.*, 1982; Willmot, 2008). It has also been reported that the most frequently affected teeth are maxillary lateral incisors, followed by maxillary canines, and mandibular premolars, with no significant differences between the right and left sides (Sangamesh *et al.*, 2011). The susceptibility of the maxillary lateral incisor may be due to its palatal position at the outset in certain malocclusion types, as well as manual difficulty in cleansing gingival to the attachment, thereby predisposing to plaque accumulation (Stecksén-Blicks *et al.*, 2007).

2.11.3. Prevalence and incidence

In a cross-sectional study, Gorelick *et al.* (1982) reported that 50% of individuals who underwent fixed orthodontic treatment had WSLs compared with 25% of untreated controls. The cross-sectional nature of this study may have led to an overestimate of WSL prevalence due to the inability to differentiate between these lesions and other developmental enamel lesions. Richter *et al.* (2011) also reported in a clinical study that among 350 individuals, 72.9% of individuals developed WSLs during fixed appliance treatment.

More recently, Sundararaj *et al.* (2015) in a meta-analysis included data from 14 studies regarding the incidence and prevalence of WSLs. The analysis indicated that a total of 935 patients out of 2041 patients (45.8%) developed new WSLs during 12 months of orthodontic treatment. A total of 1,242 patients were studied for prevalence, with 850 found to have WSLs, suggesting that 68.4% of those undergoing orthodontic treatment had WSLs.

It should be mentioned that significant variations in terms of both the prevalence and incidence of WSLs were observed (Tables 2.3 and 2.4). The prevalence of WSLs ranged from 13% to 88% of patients, with 7.4% to 31% of teeth affected. Similarly, the incidence of WSLs also showed a wide range from 0.1% to 78.7% for teeth and from 10% to 73% for individuals. These high variations are attributable to the variety of methods used to assess and record the size of the lesion, the difficulty in standardising clinical examinations, and the problems in differentiating between WSLs and other idiopathic lesions.

Table 2.3. Summary of studies reporting the prevalence of WSLs

Study	Study design	No. of subjects Control / Experimental	No. of teeth		Detection method	% of teeth with WSLs		% of subjects with WSLs	
			Control group	Experimental group		Control group	Experimental group	Control group	Experimental group
Bank and Richmond (1994)	Randomised controlled trial (split-mouth design)	40per group	282 untreated 305 untreated	289 Maximum Cure 306 Transbond™	Clinical examination*	31 25	19 23	73 75	n/a n/a
Banks <i>et al.</i> (1997)	Randomised controlled trial (split-mouth design)	50	371 untreated	366 Rely-a-bond™	Clinical examination	14.5	12.5	50	n/a
Øgaard <i>et al.</i> (2001)	Randomised controlled trial	100 / 220 (110 each with fluoride varnish or antimicrobial varnish and fluoride varnish)			Clinical examination	n/a	n/a	88	(61, 58)
Fornell <i>et al.</i> (2002)	Randomised controlled trial (split-mouth design)	39	216 untreated	218 polymer enamel coating	Clinical examination	7.4	n/a	13	n/a
Boersma <i>et al.</i> (2005)	Prospective cohort study	62			QLF images on PC	30		n/a	n/a
Heinig and Hartmann (2008)	Randomised controlled trial	40 / 38 using light bond™ sealant			Clinical examination and photograph	n/a	n/a	85	68

QLF= Quantitative Light Fluorescence, * Clinical examination (see section 2.11.4.1)

Table 2.4. Summary of studies reporting the incidence of WSLs

Study	Study design	No. of subjects Control / Experimental (Mean age)	No. of teeth		Detection method	Duration (Mean±SD) months	% of teeth with WSLs		% of subjects with WSLs	
			Control group	Experimental group			Control group	Experimental group	Control group	Experimental group
Trimpenees and Dermaut (1996)	Randomised controlled trial (cross-over design)	50	383 Orthon™	379 Lee InstaBond™	Photographic slides	21	12.7	10	n/a	n/a
Millett <i>et al.</i> (1999c)	Randomised controlled trial (split-mouth design)	20 / 20 (13.4years)	120 Ketac- Cem™	120 Right- on™	Photographic slides	15.3 ± 3.2	n/a	n/a	n/a	n/a
Gaworski <i>et al.</i> (1999)	Prospective cohort study	16	149 Reliance Light bond™	149 Fuji Ortho™	Clinical examination	12-14	75	77.1	n/a	n/a
Millett <i>et al.</i> (2000)	Randomised controlled study (split-mouth design)	45	213 Dyract Ortho™	213 Right-on™	Photographic slides	21.3 ±6.6	20	26	n/a	n/a

Table 2.4. Summary of studies reporting the incidence of WSLs (continued)

Study	Study design	No. of subjects Control / Experimental (Mean age)	No. of teeth		Detection method	Duration (Mean±SD) months	% of teeth with WSLs		% of subjects with WSLs	
			Control group	Experimental group			Control group	Experimental group	Control group	Experimental group
Alexander and Ripa (2000)	Randomised controlled trial	22//25 and 29 (14.5 years)	Phosflur™ rinse	Prevident™ gel, Prevident 5000Plus™ dentifrice	Clinical examination	27	0.2	(0.2 / 0.1)	n/a	n/a
Banks <i>et al.</i> (2000)	Randomised controlled trial	45 / 49	740 non- fluoridated elastomerics	782 fluoride- releasing elastomerics	Clinical examination	18	26	16	73	63
Mattick <i>et al.</i> (2001)	Randomised controlled trial (split-mouth design)	21	63 non- fluoridated elastomerics	63 fluoride- releasing elastomerics	Photographic slides	11-34	n/a	n/a	n/a	n/a
Le <i>et al.</i> (2003)	Randomised controlled trial (split-mouth design)	18 (14-18 years)	47 cyano- acrylate adhesive	47 composite (Reliance™)	Photographic slides	12-14	78.7	76.8	n/a	n/a

Table 2.4. Summary of studies reporting the incidence of WSLs (continued)

Study	Study design	No. of subjects Control / Experimental (Mean age)	No. of teeth		Detection method	Duration (Mean±SD) months	% of teeth with WSLs		% of subjects with WSLs	
			Control group	Experimental group			Control group	Experimental group	Control group	Experimental group
Elaut and Wehrbei (2004)	Randomised controlled trial (split-mouth design)	45 (12-18 years)	106 conventional light curing methods	106 argon laser curing method	Photographic slides	14	54.7	58.5	n/a	n/a
Øgaard et al. (2006)	Randomised controlled trial	50 / 47 (14.5 years)	297(AmF/ SnF ₂) toothpaste	282 (NaF mouth-rinse)	Clinical examination	18	4.3	7.2	n/a	n/a
Bowman and Ramos (2005)	Randomised controlled trial (cross-over design)	10 (10-14 years)	100 untreated	100 fluoride varnish (Duraflor™)	Photographs	12	50.83	31.19	n/a	n/a
Stecksen-Blicks et al. (2007)	Randomised controlled trial with two parallel arms	125 / 132 (12-15 years)	placebo varnish	fluoride varnish (Fluor protector™)	Photographic slides	18	25.7	7.4	n/a	n/a

Table 2.4. Summary of studies reporting the incidence of WSLs (continued)

Study	Study design	No. of subjects Control / Experimental (Mean age)	No. of teeth		Detection method	Duration (Mean±SD) months	% of teeth with WSLs		% of subjects with WSLs	
			Control group	Experimental group			Control group	Experimental group	Control group	Experimental group
Kronenberg <i>et al.</i> (2009)	Randomised controlled trial (split-mouth design)	20 (15 years)	200 untreated	200 (100 ozone treated, 100 Cervitec™ and fluor protector™)	Clinical, DIAGNO- dent and QLF images on PC	26	1.9	2.7, 0.2	n/a	n/a
Benham <i>et al.</i> (2009)	Randomised controlled trial (split-mouth design)	60 (11-16 years)	untreated	Ultraseal XT Plus™ clear sealant	Clinical, photographic slides and DIAGNO- dent	15-18	n/a	n/a	10	n/a
Chapman <i>et al.</i> (2010)	Retrospective study	332	n/a	n/a	Digital photographs	36	36		n/a	n/a
Shungin <i>et al.</i> (2010)	Prospective cohort study	59	n/a	n/a	Digital photographs	18	Sum areas		n/a	n/a

2.11.4. Diagnosis of WSLs

Variation may exist in the depth of the lesion, the amount of mineral loss, and the extent or surface of the tooth affected. The methods of diagnosing and quantifying WSLs can be classified into macroscopic and microscopic (Benson *et al.*, 2003; Benson, 2008).

2.11.4.1. Macroscopic methods

These approaches rely principally on the light backscattering from demineralised enamel. The white appearance of WSLs is attributed to the light travelling a distance through enamel before being backscattered. This distance is shorter in sound enamel compared with demineralised enamel, since the loss of minerals leads to pores in the enamel resulting in significant light backscattering (Angmar-Mansson *et al.*, 1996). The degree of whiteness depends on whether the enamel pores are filled with air or water because of differences in their refractive indices. Macroscopic methods can be subdivided into four types: clinical examination (indices), photographic examination, optical non-fluorescent methods, and optical fluorescent methods (Benson, 2008). These are described below:

- Clinical examination (Indices)

This method relies on direct visual examination to identify the location and extent of WSLs on the tooth surface. It requires clinicians who have the experience to differentiate between WSLs and other opacities, such as dental fluorosis; this may be challenging in some cases. For example, according to Russell's criteria, dental fluorosis manifests as white/yellowish lesions with undefined borders distributed symmetrically in the mouth, while WSLs have well-defined borders and are usually distributed randomly (Russell, 1961; Bishara and Ostby, 2008). Several clinical studies have used this method to assess WSLs before, during, or after orthodontic treatment (Gaworski *et al.*, 1999; Alexander and Ripa, 2000; Banks *et al.*, 2000; Gillgrass *et al.*, 2001; Øgaard *et al.*, 2001). The main advantages of using indices are that they are relatively simple to apply and inexpensive with minimal training required. However, this approach is subjective, inaccurate and it may be open to bias (Anderson *et al.*, 2004; Anderson *et al.*, 2007; Benson, 2008).

- Photographic examination

Many clinical studies have used photographs (digital or slides) and computer-based image analysis to assess the prevalence of WSLs (Mitchell, 1992a; Turner, 1993; Trimpeneers *et al.*, 1996; Marcusson *et al.*, 1997; Millett *et al.*, 1999c; Wenderroth, 1999; Mattick *et al.*, 2001). This technique is simple, accessible, and efficient requiring minimal training. It provides a permanent record using inexpensive equipment. In a research setting this approach can be standardised by masking the lesion details and measuring in a random order (Benson, 2008).

The potential disadvantages of this technique are the overestimation of lesions due to flash reflection from the tooth surface, which can be reduced by using a ring flash with cross-polarised filters (Robertson and Toumba, 1999), or slanting of the camera (Cochran *et al.*, 2004). Moreover, standardisation is difficult because of inconsistency in lighting, reflection, angulations, film types and processing methods (Benson *et al.*, 2005).

- Optical non-fluorescent methods (Optical caries monitor)

This method was first used by Ten Bosch *et al.*, (1980) utilising a 100W white light as a light source and measuring the backscattering of light with a densitometer. It is a useful, non-destructive method of studying enamel demineralisation and can be applied in the clinical environment but is affected by the degree of moisture within the tooth (Benson, 2008). This method has been applied in one clinical study (Øgaard and Ten Bosch, 1994).

- Optical fluorescence methods

The basic concept of these methods relies on the amount of light absorbed by a material, which influences the level of fluorescence. Since the demineralised enamel leads to more light backscattering than light absorption, it appears as a dark area using different fluorescent methods which include: fluorescent dye uptake, ultraviolet, laser and quantitative light-induced fluorescence (Angmar-Mansson and Ten Bosch, 1987).

Fluorescent dye uptake: This method is mainly used to detect demineralised areas on the enamel by applying different fluorescent dyes, which are subsequently examined using a suitable light source (Rawls and Owen, 1978). The main disadvantage of this method is that any variation in the preparation process can lead to different degrees of dye uptake (Hosoya *et al.*, 2007).

Ultraviolet Radiation: Ultraviolet radiation was used in previous studies to detect early lesions on the enamel, but requires some precautions because this radiation, which has a shorter wavelength than visible light (<400nm), can cause damage to the eyes and skin of the operator and patient (Shrestha, 1980).

Laser: Quantitative laser fluorescence was developed by De Josselin de Jong and co-workers (1995). This method utilises an argon laser, with a wavelength 440-570nm, to measure the difference in fluorescence between demineralised and intact areas of enamel by quantifying the lesion size and mineral loss through collecting and analysing fluorescent images of carious teeth after illumination with diffuse laser light. The major problem with this technique is the large laser source, which limits its use. In addition, special precautions, as with ultraviolet radiation, are required (De Josselin de Jong *et al.*, 1995; Benson, 2008). A portable instrument (DIAGNOdent™) utilises the same principle of laser fluorescence by emitting a light of wavelength 655nm to provide readings based on bacterial metabolites rather than mineral loss (Lussi *et al.*, 2004). Caution is required during interpretation of these readings as they can be affected by the presence of stains, plaque and calculus (Pretty, 2003).

Quantitative light-induced fluorescence (QLF): Nowadays this technique is the preferred fluorescent method, for *in vivo* and *in vitro* tests, to detect WSLs and to quantify the mineral loss over time. It measures the intensity of the fluorescence, resulting from an interaction between near ultraviolet radiation light and the enamel surface (Al-Khateeb *et al.*, 2000; Angmar-Mansson and Bosch, 2001; Benson *et al.*, 2003; Pretty *et al.*, 2003; Aljehani *et al.*, 2004). This fluorescent light is scattered rather than absorbed when WSLs are assessed due to the presence of pores in the lesions, resulting in a reduction in the degree of fluorescence compared to natural enamel surface. However, QLF measurements can be affected by the presence of dentine beneath the enamel surface as well as by staining and curvature of the enamel surface (Adeyemi *et al.*, 2006).

2.11.4.2. Microscopic methods

These methods include caries models, which involve placing a band or a bracket on a tooth that will be extracted in the future (O'Reilly and Featherstone, 1987; Melrose *et al.*, 1996), and *in situ* caries models. The latter involves placing a piece of enamel in a custom-made holder, worn by a volunteer by attaching it to an orthodontic arch wire or other auxiliary for a specified time period (Benson *et al.*, 1999). The main advantage of *in situ* models over caries models is that they can be used during the entire period of orthodontic treatment, allowing an accurate assessment of the changes arising during demineralisation and further remineralisation on the same specimen that is subjected to the same oral environment (Zero, 1995).

2.11.5. Risk factors for developing WSLs

A plethora of potential risk factors are associated with the development of WSLs. In particular, pre-existing WSLs predispose to further development of WSLs (Zimmer and Rottwinkel, 2004; Lovrov *et al.*, 2007). However, Stecksen-Blicks *et al.* (2007), in a randomised controlled trial with two parallel groups involving 273 patients contradicted these findings. This discrepancy might be related to the method used to assess WSLs, as Zimmer and Rottwinkel (2004) and Lovrov *et al.* (2007) relied on the clinical examination (indices), while Stecksen-Blicks *et al.* (2007) used photographs.

Interestingly, a prospective cohort study reported a correlation between age and WSL development (Kukleva *et al.*, 2001). This study comprised 42 participants in two age cohorts (22 aged between 11-15 years and 20 aged 19-24 years). The authors found that teenagers had a higher risk of enamel demineralisation than adults, which may be attributable to either variation in oral hygiene levels, or to the fact that erupting teeth are more susceptible to acid attack. Kim (2015) also reported a similar relationship in a clinical study of 115 patients aged between 12 and 20 years. However, Boersma *et al.* (2005) in a clinical study of 62 participants (aged 12 years or older) did not find any relationship. This discrepancy may be related to the age distribution as Boersma *et al.* (2005) involved 11% of participants over 30 years of age.

With regard to gender, some studies have found that WSLs were more prevalent among boys than girls; for example, Khalaf (2014) in a cross-sectional study of 45

patients (19 males and 26 females, with a mean age of 15.81) reported that males had a higher incidence of WSLs (almost 3-fold) than females. Boersma *et al.* (2005) also reported 40% of the buccal surfaces in males were affected by WSLs compared with 22% in females in a clinical study of 62 participants. Julian *et al.* (2013), however, found little difference between genders in an analysis of 885 patients (378 males and 507 females) with 25% of males and 22% of females developing WSLs. Other studies have found a higher prevalence of WSLs in females (Mattousch *et al.*, 2007) or did not find a trend related to gender (Millett *et al.*, 1999a; Lovrov *et al.*, 2007; Karadas *et al.*, 2011; Kim, 2015).

Additionally, Mitchell (1992b) reported in a review article that patient selection and education is key to the prevention of WSLs. This finding is in accordance with Zimmer and Rottwinkel (2004), who used two regimes for preventing WSLs in a longitudinal prospective study involving a high- and low- risk group of patients. The rigorous regime undertaken by a dental hygienist and involving scaling, mechanical tooth cleaning, chlorhexidine rinsing and fluoride application significantly outperformed a less stringent regime incorporating motivation sessions and nutritional counselling.

The relationship between fixed appliance-based orthodontic treatment and WSL development is clear-cut since these appliances are associated with a rapid increase in plaque accumulation and high levels of cariogenic bacteria, which is in turn positively correlated with the presence of WSLs (see section 2.11). In addition, some studies found an increase in WSL development as the length of orthodontic treatment increased, for example, after 12 months (Lucchese and Gherlone, 2013), 17 months (Marcusson *et al.*, 1997), 24 months or 36 months (Geiger *et al.*, 1988; Khalaf, 2014) of orthodontic treatment, while other studies reported no relationship between the length of orthodontic treatment and the formation of WSLs (Zaghrisson and Zachrisson, 1971; Boersma *et al.*, 2005; Karadas *et al.*, 2011). Moreover, a large number of studies have linked poor oral hygiene prior to orthodontic treatment to the development of WSLs (Gorelick *et al.*, 1982; O'Reilly and Featherstone, 1987; Øgarrrd, 1989; Boyd, 1991; Geiger *et al.*, 1992; Gorton and Featherstone, 2003; Chapman *et al.*, 2010; Khalaf, 2014) emphasising the need for optimal baseline hygiene levels before proceeding with orthodontics.

2.11.6. Prevention of WSLs

Undoubtedly, fluoride plays an important role in the prevention of WSLs during orthodontic treatment. The frequency of fluoride application and the exact area where fluoride is required are considered to be the most important factors in preventing WSL formation (Chambers *et al.*, 2013; Khalaf, 2014). Different methods of delivering fluoride have been used. These include:

- i) Topical fluoride from for example toothpastes, mouth-rinses, gels and varnishes,
- ii) Fluoride releasing materials such as bonding materials (sealants, primers, and adhesives) and elastics, and
- iii) Fluoride releasing devices attached to fixed appliances.

Additionally, there are alternative fluoride delivery methods to prevent WSLs such as the use of chewing gum containing xylitol, and products containing Casein Phosphopeptide- Amorphous Calcium Phosphate (CPP-ACP) (Bishara and Ostby, 2008; Srivastava *et al.*, 2013).

With regard to the fluoride concentration in toothpastes (which usually contain either sodium fluoride, monofluorophosphate, amine fluoride, stannous fluoride or a combination), a minimum level of 0.1% is recommended for those at high risk of developing WSLs (Øgaard *et al.*, 2004). In addition, the use of fluoridated antiplaque toothpastes, such as stannous fluoride toothpastes, reduced demineralisation of enamel more than fluoridated toothpaste alone by inhibiting plaque adsorption to the enamel surface and preventing acid production by blocking sucrose passage to the acid-forming bacteria (Øgaard *et al.*, 1980; Boyde and Chun, 1994).

Recently, two Cochrane systematic reviews have concluded that using fluoridated mouth-rinses containing 0.05% sodium fluoride daily, with or without fluoridated toothpastes, significantly reduced lesion formation (Marinho *et al.*, 2004; Benson *et al.*, 2004a). These mouth-rinses are usually combined with anti-bacterial agents such as chlorhexidine, triclosan, and zinc to enhance their anti-caries activity (O'Reilly and Featherstone, 1987; Øgaard, 2001). Moreover, irregular use of a sodium fluoride mouth-rinse was associated with more WSLs than those with regular mouth-rinsing (Geiger *et al.*, 1988). The method of fluoride delivery is therefore important, especially as it depends on patient compliance.

The application of fluoridated varnishes may be more effective for less compliant patients than mouth-rinses, because varnish application relies on the clinician rather than patient cooperation. Bowman and Ramos (2005), in a prospective clinical study of 10 patients and 200 teeth reported a 44.3% reduction in WSL formation in orthodontic patients after tri-monthly fluoride varnish application, over a period of 12 months compared to the controls. Similar conclusions were reported by Todd *et al.* (1999) and Petersson *et al.* (2000). More recently, in a Cochrane review, Benson *et al.*, (2013) concluded that fluoride varnish applied every six weeks during orthodontic treatment was effective in preventing of WSLs, although this conclusion was based on a single randomised study. The authors therefore concluded that further double-blind randomised controlled trials are required to confirm this. It should be mentioned that this in-office varnish application is usually done in the dental clinic, which limits the frequency of varnish application and increases chair time, raising the costs of treatment. In addition, using varnishes may induce temporary discoloration of teeth and gingival tissues (Bishara and Ostby, 2008).

Since orthodontic treatment requires a prolonged period, the introduction of fluoride-releasing adhesive bonding materials with sustained release, such as resin composites and glass ionomer cements, are of great interest because these materials do not rely on patient compliance. Wilson and Donly (2000) reported in an *in vitro* study involving 45 teeth that RMGIC (Fuji Ortho™) and fluoridated composite (Light Bond™) exhibited significant inhibition of demineralisation compared to non-fluoridated composite (Concise™). However, it has also been reported that the amount of fluoride released initially is high and then drops rapidly to levels that may be insufficient to prevent WSL development during the course of orthodontic treatment. Regalla *et al.* (2014) evaluated fluoride release from three different orthodontic adhesives in an *in vitro* study. Adhesives assessed included RMGIC (Fuji Ortho LC™), a fluoride-releasing composite resin material (Excel™) and conventional composite (Rely-a-bond™). These adhesives were applied to 78 freshly-extracted premolars (26 per group). Fluoride levels were assessed at 24 hours, 10 days, 17 days, 24 days and 31 days after bonding. The authors found that fluoride release significantly decreased after 24 hours and continued to decrease until 31 days after placement of the attachments.

The findings of the aforementioned study are consistent with Basdra *et al.* (1996), who conducted an *in vitro* study on 15 extracted premolars using two different fluoride-releasing orthodontic bonding adhesives (Fluoride bond/Concise™ and

Rely-a-bond™). The authors showed that maximum fluoride release occurred within the first 24 hours, with Fluoride bond/Concise™ releasing more fluoride than Rely-a-bond™. Thereafter, fluoride release decreased significantly after 48 hours for both materials and continued to decrease over 2 to 3 months. Therefore, the clinical effectiveness of these fluoride-releasing materials in preventing WSL formation may be questionable since the amount of fluoride required to prevent caries is still unknown (Benson *et al.*, 2004a; Bishara and Ostby, 2008; Pseiner, 2010).

Recently, fluoride-releasing antibacterial bonding agents including sealants and primers have been developed, combining the antibacterial activity of 12-methacryloyloxydodecyl-pyridinium bromide (MDPB) and the physical advantage of adhesive systems (Imazato *et al.*, 2003; Pithon *et al.*, 2015). The preventive effect of fluoride released from these agents is influenced by its concentration and the duration of release, as well as their rechargeability with fluoride ions, for example, with a foaming solution of acidulated phosphate fluoride (Soliman *et al.*, 2006).

Some studies have shown that using other fluoride-releasing mechanisms, such as fluoride-releasing elastomeric chain and elastic ligatures, reduced plaque accumulation and WSL formation (Whitshire, 1999; Banks *et al.*, 2000; Mattick *et al.*, 2001). However, Benson *et al.* (2004b) reported that fluoride releasing elastic ligatures did not reduce the amount of plaque. Furthermore, at the time of fixed orthodontic appliance placement, it was also shown that applying an argon laser for 60 seconds reduced the WSL area by 94.6% and lesion depth by 91.4% compared with untreated teeth (Anderson *et al.*, 2002).

Xylitol, which is a type of carbohydrate that does not act as a metabolising substrate for *S. mutans*, has also been used in chewing gums to prevent WSLs. It has anti-caries properties since it is metabolised by bacteria, resulting in inhibition of glycolysis and reduced acid production. In addition, it increases the production of stimulated saliva, which contains more calcium and phosphate compared with non-stimulated saliva (Sengun *et al.*, 2004; Stecksén-Blicks *et al.*, 2004). Additionally, Casein Phosphopeptide- Amorphous Calcium Phosphate (CPP-ACP), which is derived from milk casein, is considered the most potent remineralising agent among the calcium phosphate-based remineralising agents in the prevention of WSLs. CPP-ACP allows movement of the free calcium and phosphate ions from CPP-ACP to the enamel surface to attach to apatite crystals (Willmot, 2008; Reema *et al.*, 2014).

Most recently, a double-blind, randomised clinical study on 63 patients was conducted to assess the effect of slow-release fluoride glass devices threaded onto the orthodontic wire in the prevention of enamel demineralisation during fixed appliance orthodontics (Tatsi, 2014). The author assessed cross-polarised digital photographs for the presence and severity of WSLs. Use of this device decreased the severity of these lesions by preventing demineralisation in 2.88 times more teeth compared to use of 225 ppm fluoride mouth-rinse once daily and 1,450 ppm fluoride toothpaste twice daily.

2.11.7. Enamel remineralisation / Treatment of WSLs

Generally, it is believed that remineralisation of WSLs is a natural phenomenon in saliva because it is supersaturated with calcium-phosphate salts, which are identical to enamel hydroxyapatite (Garcia-Gordy and Hicks, 2008). However, several studies have reported that this phenomenon induces little improvement in the appearance of WSLs and results in partial repair of WSLs located superficially, while deeper lesions may require intervention to arrest and prevent development into dental caries (Dirks, 1966; Karlinsey *et al.*, 2009; Cochrane *et al.*, 2010).

This partial repair has been linked to salivary phosphoproteins rich in proline, which have been found on the enamel pellicle inhibiting spontaneous precipitation of minerals by masking the enamel surface and preventing hydroxyapatite crystal growth (Hay *et al.*, 1984; Carpenter *et al.*, 2014). In addition, the amount of mineral deposition is sometimes so small that it cannot overcome demineralisation, particularly as the extent of the lesions varies significantly from individual to individual and from site to site in the mouth. This finding was confirmed by Dirks (1966) who reported that half of the recorded lesions had disappeared after 6 years without any interventions. Another *in vivo* study also reported that complete remineralisation occurred in 2.7% of teeth with WSLs 2 years after removal of fixed orthodontic treatment (Mattousch, 2007).

Common interventions used to arrest WSLs include application of fluoride and calcium phosphate based remineralising agents but the concentration and the ideal method of delivery for fluoride are still unclear (Benson *et al.*, 2005). Some authors believe that high concentrations of fluoride lead to increased remineralisation of the superficial layer of enamel and a significant reduction of demineralisation in the

deeper layers (Castellano and Donly, 2004; Bishara and Ostby, 2008; Ten Cate *et al.*, 2008; Trairtvorakul *et al.*, 2008). It has also been postulated, however, that high concentrations of fluoride may reduce the penetration of calcium and phosphate to the deeper layers because the well-mineralised superficial layer might act as a barrier. Consequently, remineralisation of the deeper layers of WSLs may be inhibited maintaining the white appearance of the lesions (Phantumvanit *et al.*, 1977; Linton, 1996; Øgaard, 1998; Garcia-Godoy and Hicks, 2008; Willmot, 2008).

In general, treatment of WSLs should start with the most conservative method by using toothpastes, mouth-rinses, varnishes, topical creams, chewing gum, or sugar free lozenges, which contain fluoride or CPP-ACP as reported in a number of randomised controlled clinical trials (Table 2.5).

Table 25. Summary of randomised controlled clinical trials of treatment of WSLs

Authors	Participants Test/control	Follow-up after debonding	Intervention vs control	Assessment methods	Significant differences
Willmot (2004)	15/11	12 and 26 weeks	50ppm NaF rinse vs control rinse	Photographs	No
Bailey <i>et al.</i> (2009)	23/22	4, 8 and 12 weeks	CPP-ACP (tooth mousse) vs control cream	Clinical scores	Yes
Beerens (2010)	35/30	6 and 12 weeks	CPP-ACFP (MI-Paste) vs control paste	QLF	No
Baeshen <i>et al.</i> (2011)	19/18	2, 4 and 6 weeks	0.5% NaF Miswaks vs control Miswaks	DIAGNOdent, clinical scores	Yes
Bröchner <i>et al.</i> (2011)	30/30	4 weeks	CPP-ACP (tooth mousse) vs fluoride toothpaste (Colgate1,100 ppm F)	Clinical scores, QLF	No
Du <i>et al.</i> (2012)	55/55	3 and 6 months	5% NaF varnish vs saline solution	DIAGNOdent	Yes

The inconsistent findings from these clinical trials might be due to insufficient sample sizes, unclear selection criteria, and the use of different methods to assess WSLs. Additionally, Aljehani *et al.* (2006) in a longitudinal *in vivo* study over a period of 1 year reported that there were no significant differences between normal home care and professional tooth cleaning among 12 patients, with 127 test teeth exhibiting white spot lesions on the buccal surfaces after completion of orthodontic treatment. This finding is in accordance with a parallel-group randomised controlled trial on 150 patients by Huang *et al.* (2013), who also showed that there were no significant differences between the professional application of MI Paste Plus™ and PreviDent™ fluoride varnishes and normal home care for improving WSL appearance.

If the application of fluoride does not predictably improve the appearance of WSLs, whitening the surrounding enamel surfaces may be appropriate by using either in-office or at home external bleaching techniques, which may result in camouflage of WSLs and more uniform appearance of the enamel surface as reported by Knösel *et al.* (2007). The authors applied a 30% H₂O₂ bleaching gel (Illumine office™, Dentsply, Germany) in a tray for 60 minutes on the anterior maxillary teeth of 19 patients with inactive WSLs followed by daily home bleaching for 1 hour with a 15% H₂O₂ gel (Illumine home™, Dentsply, Germany) for 14 days.

Micro-abrasion may also be considered to remove the superficial layer of WSLs. This involves the use of 18% hydrochloric acid and pumice and has been shown to produce a significant size reduction in WSLs by up to 83% (Murphy *et al.*, 2007). This *in vivo* study involved a small sample (8 patients) with multiple demineralised enamel lesions after fixed orthodontic therapy. Similar conclusions were made by Welbury and Carter (1993) and Croll and Bullock (1994). However, Jahanbin *et al.* (2015) reported in an *in vitro* study on 60 extracted premolar teeth that micro-abrasion using 18% hydrochloric acid makes the enamel susceptible to staining.

In addition, acid etching of WSLs has also been suggested to enhance remineralisation of WSLs (Al-Khateeb *et al.*, 2000). The authors used 35% phosphoric acid for 30 seconds on enamel blocks with induced WSLs. Meireles *et al.* (2009), in an *in vitro* study on 20 extracted bovine teeth compared two micro-abrasion methods: 18% hydrochloric acid and 37% phosphoric acid. They evaluated the surface roughness and

enamel loss using a digital profilometer and stereoscope finding that the use of phosphoric acid was safer and less aggressive than hydrochloric acid.

Argon laser has also been used to arrest WSLs by creating micro-spaces that stabilise ions in the enamel surface during an acid attack rather than being lost. Hence, the surface characteristics of the crystalline structure of enamel are altered making it more acid resistant (Mattousch *et al.*, 2007). In addition, Oho and Morioka (1990) in an *in vitro* study found that the lasered enamel surface showed a high positive birefringence compared with the untreated enamel. They also noticed gradual changes in birefringence of the enamel surface during treatment with acid solutions; these were attributed to mineralisation of the micro-spaces as the ions released after acid demineralisation became trapped in the micro-spaces of lasered enamel, whereas such ions diffuse to the surrounding solution of the untreated surface.

This has been corroborated within clinical research with a 51% reduction in WSL area reported after using Nd-YAG laser combined with acidulated phosphate fluoride solution in 10 patients, who had WSLs on upper six anterior teeth, compared to 10 untreated controls (Harazaki *et al.*, 2001). Moreover, Anderson *et al.* (2002) showed significantly less depth and surface area of induced WSLs, after using argon laser for 60 seconds with or without pumice/etching on 36 extracted premolar teeth. They induced lesions 5 weeks before extraction by fitting and cementing an oversized orthodontic band on each premolar to create a pocket for demineralisation; these teeth were then sectioned and examined under polarised light. These findings are consistent with Hicks *et al.* (2004) who demonstrated that the lesion depth had significantly reduced compared to controls (without treatment), by either using an argon laser for 10 seconds (reduced by 44%), or by application of a topical fluoride (0.5% fluoride ion, Thera-Flur-N™) followed by argon laser (reduced by 62%). The addition of topical fluoride treatment prior to argon lasing resulted in a 32% reduction in lesion depth compared to argon laser treatment alone. Those lesions were induced by cementing of orthodontic bands with plaque-retentive slots on the buccal surfaces of 14 teeth for 5 weeks prior to extraction, which were then sectioned and examined under a polarised light microscope.

Additionally, a resin infiltration technique was also used, and a significant reduction of WSL size was reported by Kim *et al.* (2011). The authors selected 20 teeth with a developmental defect of enamel and 80 with post-orthodontic demineralisation. They treated the teeth with resin infiltration finding that 5 and 11 teeth, respectively, were classified as completely masked after 1 week of treatment, whereas 8 and 1 remained unchanged, respectively. In addition, it has also been reported in a split-mouth randomised clinical trial on 21 patients involving 231 WSLs that resin infiltration significantly improved the clinical appearance of those lesions over a period of 6 months (Knösel *et al.*, 2013).

If all aforementioned treatments are unsuccessful, then composite restorations or porcelain veneers may be required to address discoloration (Mattousch *et al.*, 2007). However, the refinement of bioactive glass treatment may facilitate a less invasive approach to improving the appearance of WSLs. Mehta *et al.* (2014) in an *in vitro* study found that the bioactive glass 45S5, in the form of dentifrice (toothpaste), significantly remineralised WSLs assessed by Vickers hardness testing compared with a CPP-ACP dentifrice in 30 extracted human premolars. In addition, Bakry *et al.* (2014b), in an *in vitro* study on 60 extracted human molars, demonstrated that using a gel composed of 45S5 glass powder and phosphoric acid covered by a layer of bonding agent (Clearfil SE Bond), significantly enhanced enamel remineralisation after immersion in remineralising solution for 24 hours. This remineralisation was identified by the formation of a layer of brushite crystals ($\text{CaHPO}_4 \cdot 2\text{H}_2\text{O}$) on the enamel surface using scanning electron microscope (SEM), energy dispersive X-ray spectroscopy (EDX), and X-ray diffraction (XRD) techniques. This layer was resistant to brushing and became converted to hydroxyapatite crystals after 14 days of immersion in the same remineralising solution.

Furthermore, Milly *et al.* (2015) have shown in an *in vitro* study that surface pre-conditioning of artificially-induced WSLs on 90 extracted molar teeth, by propelling a 45S5 glass powder *via* air-abrasion followed by application of a slurry or paste enhanced remineralisation of WSLs. The propelled powder was composed of 60% by weight bioactive glass powder (45S5) and 40% polyacrylic acid powder. The operating parameters of the air-abrasion machine (Aquacut™, Velopex, Harlesden, UK) were air pressure, 20psi; flow rate of powder 1g/min; nozzle tip angle, 90°; nozzle-lesion

distance of 5mm; nozzle tip diameter, 90µm, and application time of 10 seconds. Following the use of the air-abrasion machine, a slurry composed of bioactive glass (45S5) powder (100% by weight) and deionised water, or a paste (containing 36% by weight bioactive glass, chalk, glycerine, and stabilisers), were applied on the lesions (10 teeth for each application), twice a day (5 minutes per application) for 21 days to promote remineralisation of WSLs. This *in vitro* study reported that the use of bioactive glass (45S5) slurry had a superior remineralisation effect compared with bioactive glass (45S5) paste and two control groups (WSLs treated with acid etching and deionised water, respectively). Changes were assessed by changes in light backscattering and increase in the mineral contents and surface hardness of the remineralised lesions. However, an increase in the surface roughness of the remineralised WSLs was found. Further studies on the treatment of WSLs using 45S5 glass are described in Chapter 3. There is a need for further development of bioactive glasses to promote remineralisation of WSLs without inducing an increase in the enamel surface roughness. This can be achieved by designing a glass with hardness lower than that of enamel, and with a composition enhancing enamel remineralisation.

In summary, different methods have been used to treat WSLs. These include: i) toothpastes, mouth-rinses, gels, varnishes, topical creams, chewing gum, or sugar-free lozenges, containing either fluoride, 45S5 glass powder or CPP-ACP, ii) whitening with H₂O₂ bleaching gel, iii) micro-abrasion by using 18% hydrochloric acid and pumice, iv) acid etching by phosphoric acid, v) use of composite restoration, vi) use of laser, vii) use of resin infiltration technique, and viii) use of 45S5 glass in the form of a paste or slurry to remineralise WSLs with or without pre-conditioning.

2.11.8. Enamel surface tomography after demineralisation/remineralisation: Assessment techniques

A number of assessment methods have been used to evaluate surface enamel tomography changes during demineralisation and remineralisation of enamel (Figure 2.4) (Barber and Rees, 2004; Schlüter *et al.*, 2011; Janiszewska-Olszowska *et al.*, 2014).

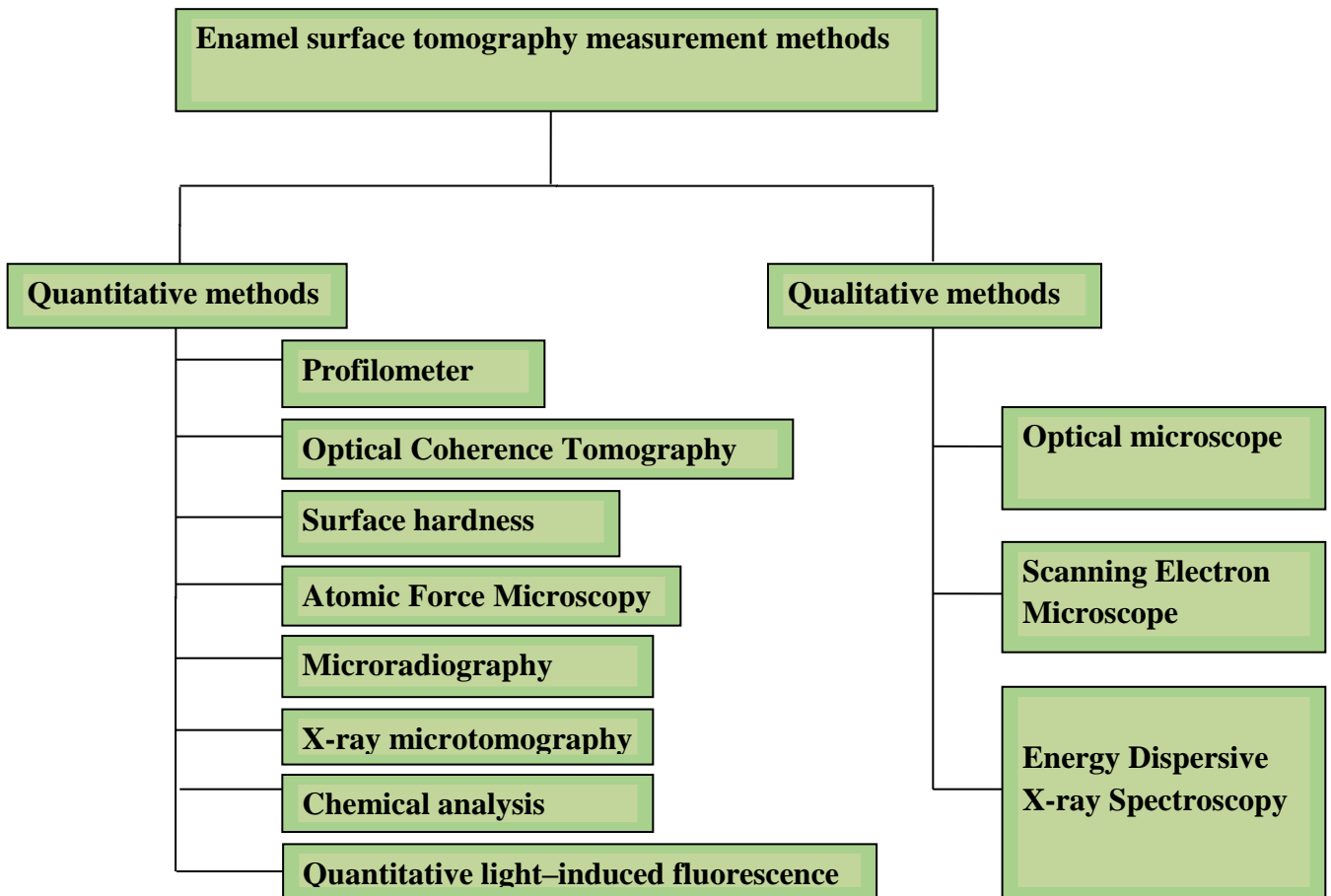


Figure 2.4. Techniques to assess enamel surface tomography after demineralisation/remineralisation

2.11.8.1. Profilometer

This relies upon measuring the time taken for the light beam to return to its source, after emission from the instrument to the sample surface, in order to determine enamel surface tomographical changes. This allows assessment of enamel roughness and evaluation of the quantity of enamel surface loss by providing a digital map of the surface with 3D coordinates X, Y, and Z planes (Ireland *et al.*, 2008; Field *et al.*, 2010). This technique can be classified into:

- i) Contact profilometer: It was the first type of profilometer and is still in use in spite of its limitation as it utilises a stylus with a tip (made of diamond, steel, or tungsten

carbide), which scans the sample surface. It cannot penetrate narrow grooves and may cause surface deformation. Although the scanning process is very accurate, it is relatively slow when compared to non-contact optical systems (Ireland *et al.*, 2008).

ii) Non-contact profilometer: This approach employs a laser light probe (blue or white light), which scans the sample surface without any physical contact. It is faster and easier than the contact profilometer (Ireland *et al.*, 2008; Theocharopoulos *et al.*, 2010).

Enamel surface roughness has been shown to increase after demineralisation compared with corresponding sound surfaces. Cross *et al.* (2009) evaluating sound and demineralised bovine enamel induced enamel demineralisation either by exposure to *Streptococcus mutans* biofilm for 72 hours at 37°C, or 30% chemical synthetic lactic acid of pH 5 over varying time intervals (45, 90, 225 minutes). Kielbassa *et al.* (2005) also found the enamel roughness of sound bovine enamel surfaces was 50% less than those of demineralised surfaces. Enamel demineralisation was induced by a demineralised solution of pH 5.1 containing calcium chloride, potassium dihydrogen phosphate, lactic acid, potassium hydroxide, methyl hydroxy-diphosphonate, and traces of thymol at 37°C for 10 days. This increase has been characterised in SEM-based studies (Holman *et al.*, 1985; Hannig and Hannig, 2010). Specifically, Hannig and Hannig (2010) found changes in the histological and compositional structure of the enamel surface including reduction in prism size relative to sound enamel. This was attributed to the mineral loss during acidic attacks resulting in an increase in the inter-prismatic spaces between the enamel prisms, producing a more porous (pitted) and roughened surface.

2.11.8.2. Optical Coherence Tomography (OCT)

This is a non-invasive, cross-sectional imaging technique that can give information about the internal tooth structures non-destructively. It utilises near-infrared light which is inversely related to the mineral content of the sample surface and proportionally correlated with the number and size of pores in the enamel surface (Jones *et al.*, 2006; Hariri *et al.*, 2012; Kang *et al.*, 2012). Backscattering of light usually increases with demineralised enamel surfaces due to the presence of pores that affects the OCT signal generated by the light which travels into deeper layers within the complex

structure of demineralised enamel surfaces. Hence, the backscattered light is a combination of two types of light-pore interactions: i) back reflection of light from abrupt changes in the optical refractive index at the pore/enamel interfaces, and ii) the passage of light through the space inside the pores without deviation. Each of these leads to an increase in the intensity of the light being transferred to the OCT detection system. Conversely, the light associated with both sound and remineralised enamel surfaces is scattered from well-ordered prisms (rod) structures resulting in little penetration of light within the enamel structure of extracted human teeth leading to low intensity values (Jones and Fried, 2006; Milly *et al.*, 2014b; Milly *et al.*, 2015). The cross-sectional images generated from multiple axial measurements of echo time delay can be displayed in a false colour or grey scale to visualise tissue changes (Hariri *et al.*, 2012; Kang *et al.*, 2012; Mandurah *et al.*, 2013). However, the OCT signal intensity is affected by the dehydration of the enamel surface, which limits this technology as reported in an *in vitro* longitudinal study (Nazari *et al.*, 2013). The authors reported that there were significant differences between the depth-integrated OCT signals, under dry and hydrated enamel conditions, after evaluating the subsurface lesion progression at 3, 9 and 15 days.

2.11.8.3. Surface micro-hardness measurements

Hardness can be defined as the resistance of a material to the penetration of an indenter. Interestingly, there are two common techniques available to measure the hardness of enamel: micro-indentation hardness and nano-indentation hardness. The basic concept of micro-indentation hardness relies on an indenter, a diamond tip of known geometrical dimensions, such as Knoop and Vickers indenters, which penetrate the enamel surface. The Knoop or Vickers hardness numbers are calculated from the depth of the indentation and the applied load (Sirdeshmukh *et al.*, 2006; Schlüter *et al.*, 2011).

The use of microhardness indentation (with loads not exceeding 1kg) is a preferred method, particularly the Knoop diamond indenter, since it is reported to be more sensitive to the superficial changes in the enamel surface than the Vickers diamond indenter (Meredith *et al.* 1996; He *et al.*, 2010, Milly *et al.*, 2015). This sensitivity is attributed to its shallow indentation depth on the tested surface with the Knoop indenter

penetrating about half as deep as Vickers. Alternatively, nano-indentation hardness uses the same concept of microhardness indentation but at a smaller scale (i.e. penetration does not exceed 1µm [150–500nm] in depth under loads of 0.25–50mN) using a trigonal pyramidal Berkovich diamond indenter. The indenter applies an increasing load first to measure the hardness of the tested surface and then the load is decreased until partial or complete relaxation of the tested surface occurs, allowing calculation of Young's (elastic) modulus and fracture toughness (Mahoney *et al.*, 2003; Schlüter *et al.*, 2011).

It has been reported in the dental literature that surface hardness testing provides information on mineral loss and gain in the enamel surface during demineralisation and remineralisation, respectively (Amaechi *et al.*, 2013; Lippert and Lynch, 2014). Featherstone *et al.* (1983) in an *in vitro* study, reported a linear relationship between the hardness and the mineral content of WSLs assessed by comparing the micro-hardness data (represented as square root of Knoop Hardness Number (KHN) obtained from the Knoop hardness tester machine) with that of microradiography in the mineral range of 40–90 volume percent. Also, Kielbassa *et al.* (1999) found a strong relationship between the mineral volume percent of an *in situ*-induced WSL in irradiated and non-irradiated human enamel and the square root of KHN, assessed also by comparing micro-hardness data with transversal microradiographical (TMR) data. These examples support the concept of using a hardness tester machine as a reliable method for the indirect measurement of WSL mineral content *in vitro* and *in situ* (Kielbassa *et al.*, 1999). However, the data obtained from hardness testing might vary according to the sample's condition and the area and depth of indentation (Margalhaes *et al.*, 2009). The latter study used five different demineralisation protocols to artificially induce carious enamel lesions comparing Cross-Sectional Hardness (CSH) and Transverse Microradiography (TMR), finding that CSH as an alternative to TMR does not estimate mineral content accurately but gives information on the surface properties of those lesions. These findings are consistent with those of Lippert and Lynch (2014), who compared between Knoop and Vickers surface micro-hardness data and transverse microradiography to evaluate the hardness of early caries lesion formation in human and bovine enamel.

2.11.8.4. Atomic force microscopy (AFM)

This microscopy technique was first introduced in the 1980s using a scanning probe. The probe has a sharp tip attached to a flexible cantilever that scans the sample surface recording the sample features when a diode laser beam hits the sample surface (Finke *et al.*, 2000). The main advantages of AFM over other techniques are: firstly, both conductive and insulating surfaces can be scanned by AFM, unlike SEM, as it does not require harsh sample preparation, such as coating and dehydration, which leads to damage of the sample surfaces. Secondly, AFM, unlike SEM, can be performed in a vacuum as well as under ambient conditions (liquid or air). Thirdly, AFM images have a resolution greater than those obtained by profilometer. However, AFM is restricted to limited areas (less than 0.5 x 0.5 mm²) and each scan requires an hour to complete (Barber and Rees, 2004).

2.11.8.5. Microradiography

This technique is used to assess the enamel surface by measuring the attenuation of monochromatic x-rays that are transmitted and absorbed by the enamel surface in comparison with a reference aluminium step wedge, to obtain a map of the mineral contents of enamel. The intensity of the emergent beam is recorded on a photographic plate or a photon counter. Three types of microradiography are available: transverse microradiography (which is more commonly used), longitudinal microradiography, and wavelength-independent microradiography (Barber and Rees, 2004; Lo *et al.*, 2010; Schlüter *et al.*, 2011). However, this technique is a destructive method (the sample cannot be used again), time consuming, and the sample has to be prepared by sectioning into thin slices of 100µm, which is difficult if the structure is brittle demineralised enamel (Fontana *et al.*, 1996; Can *et al.*, 2008).

2.11.8.6. X-ray microtomography (XMT)

This is a non-destructive 3D analytical technique, which provides images of the mineral density of the hard tissue samples based on changes in X-ray attenuation coefficients. This technique can be classified based on X-ray source into: monochromatic and polychromatic (Park *et al.*, 2011). It has many advantages over the other destructive

methods as there is no need to do any physical sectioning, which leads to loss of information. In addition, it is accurate in detecting the demineralisation characteristics of caries lesions with automated software to analyse the data. Furthermore, repeated scans can be performed on the same sample before and after different experimental procedures are carried out on it. However, this technique requires several hours to scan the sample, which is the only disadvantage of using this technique (Dowker *et al.*, 2003; Hahn *et al.*, 2004; Taylor *et al.*, 2010).

2.11.8.7. Chemical analysis

Chemical analysis has been undertaken using immersion solutions to study the dissolution of enamel (hydroxyapatite crystals) by measuring the concentration of different ions, such as calcium, phosphate, and fluoride that are released within them. The pH of these solutions has also been recorded before and after immersion of the sample (Barber and Rees, 2004).

2.11.8.8. Scanning Electron Microscopy (SEM)

It is a well-established analytical technique in which electrons are accelerated towards the enamel surface, where they interact and produce signals, as secondary or backscattered electrons, to obtain three dimensional images at high resolutions. A wide range of magnifications can be used to observe the ultrastructural changes and chemical composition of the enamel surface for greater accuracy (Städlander, 2007). SEM technique can be used to study teeth surfaces without polishing the surface (Barbour and Rees, 2004). However, these teeth cannot be used again since they are pre-prepared by coating with a conductive surface coat, such as gold or carbon, prior to SEM imaging. In addition, SEM is incapable of providing three-dimensional measurements (Zhang *et al.*, 2000; Lyman, 2012). Based on SEM studies it has been reported that the surface characteristics of sound enamel surfaces are homogenous, smooth and dense (Dong *et al.*, 2011; Ferrazzano *et al.*, 2011), while demineralised enamel surfaces exhibited a more porous, rough and looser structure (Jayarajan, 2011; Gjorgieyska *et al.*, 2013; Milly *et al.*, 2015).

2.11.8.9. Energy dispersive X-ray spectroscopy (EDX)

EDX is an analytical technique incorporated into SEM, which gives information on the chemical composition (elemental distribution) of the sample surface (biological or synthetic materials) after interaction with an electrical beam. This results in emission of a characteristic X-ray pattern by the atoms and ions located within the top few micrometres of the sample surface (Barbour and Rees, 2004; Schlüter *et al.*, 2011).

EDX has the ability to measure the concentration of calcium, phosphorous and fluoride in sound, demineralised, and remineralised enamel surfaces, as well as the concentrations of new mineral depositions from therapeutic treatments (Naumova *et al.*, 2012; Amaechi *et al.*, 2013; Gjorgievska *et al.*, 2013). However, Canli (2010) reported that the accuracy of quantitative information obtained from EDX is questionable as there are many factors affecting the intensity of the peaks in its spectrum, such as the beam voltage changes, and the overlapping of some peaks that might interrupt the findings. Moreover, it has insufficient resolution in detecting some elements, since the density of the tested material affects the degree of electron beam penetration within the sample. Hence, when EDX is used as a qualitative method, it will give valuable and accurate information to determine the chemical composition of the material.

2.11.8.10. Qualitative Light Fluorescent (QLF)

QLF is non-destructive and thus is a suitable method for quantitative measurements of one and the same lesion at different times. The first image of this series is made of the sound tooth, which serves as the baseline for all later images. QLF utilises fluorescent light that is not induced by X-rays or other ionising radiation but by visible or near ultraviolet radiation (Angmar-Masson and Bosch, 2001).

2.11.8.11. Optical microscopic techniques

Polarised light microscopy has been used to obtain information about the mineral content of enamel surface *in vitro* by illuminating a bi-refrigent sample (enamel) with a polarised light that interacts strongly with the sample generating a contrast with the background by using different media such as water and quinoline (Hicks and

Silverstone, 1984). As it is unclear whether the liquid fully fills the pores of demineralised enamel or not, this technique has been used to provide only qualitative information, such as the histological examination of enamel (Lo *et al.*, 2010).

2.12. Bioactive glasses

Bioactive glasses are amorphous materials that lack long-range structural order, unlike crystalline materials that have long-range order with atomic positions repeated in space in a regular array (Figure 2.5) (Jones and Clare, 2012); these glasses also vary in composition. The first bioactive glass, Bioglass® 45S5, was discovered by Professor Larry Hench in the late 1960s. This glass is composed of SiO₂ (46.1mol%), CaO (26.9mol%), Na₂O (24.4mol%), and P₂O₅ (2.6mol%) and has been in clinical use within both medicine and dentistry since 1985 (Hench *et al.*, 1971; Elagayer *et al.*, 2003; Hench, 2006). Bioactive glasses have varying mechanical, physical, thermal, and chemical properties, depending on their composition. However, compared with bone, they cannot be used in load bearing areas because they have: lower tensile strength (42MPa) and lower fracture toughness (0.6MPa.m^{1/2}) than that of cortical bone (50-150MPa and 2-12MPa.m^{1/2}, respectively), and higher compressive strength (500MPa) and higher elastic modulus (35GPa) than that of cortical bone (100-230MPa and 7-30GPa, respectively) (Amaral *et al.*, 2002; Kokubo *et al.*, 2003; Chen *et al.*, 2012).

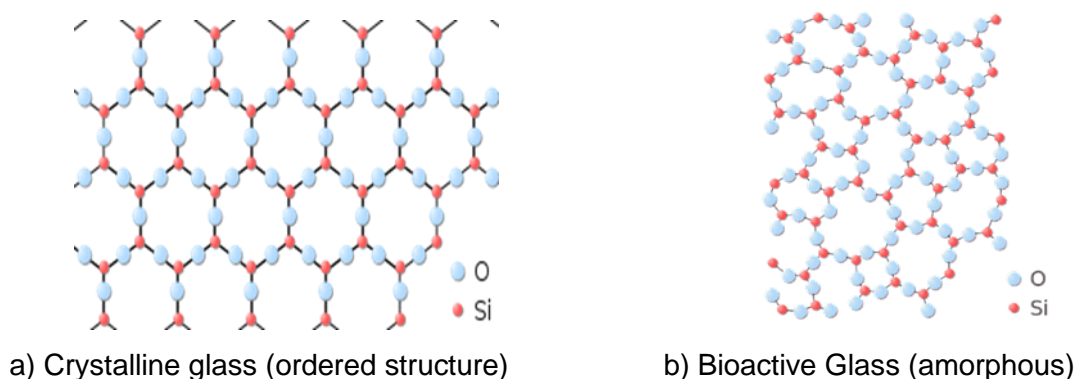


Figure 2.5. Molecular difference between a) crystalline glass (https://commons.wikimedia.org/wiki/File:SiO%C2%B2_Quartz.svg) and b) bioactive glass materials (<https://en.wikipedia.org/wiki/Glass>)

2.12.1. Structure of bioactive glasses

Numerous attempts have been made to explain the structure of bioactive glasses but Zachariasen's random network theory is the most widely accepted proposing that a glass is composed of a random three-dimensional network made from irregular units (Jones and Clare, 2012). By applying this concept, silicate glasses are composed of a three-dimensional network based on a SiO_4 tetrahedron, where the silicon ion is positioned at the centre of the tetrahedron, and four oxygen ions are at the four corners. Each oxygen ion is shared either between two silicons forming silicon oxide, or one silicon and another cation ion (e.g. Na^+ , Ca^{2+} , Al^{3+} ,...), and form various oxides. When the oxygen connects two silicons, it is termed a bridging oxygen (BO), while sharing oxygen between one silicon and another ion is defined as a non-bridging oxygen (NBO) (Figure 2.6) (Jones and Clare, 2012).

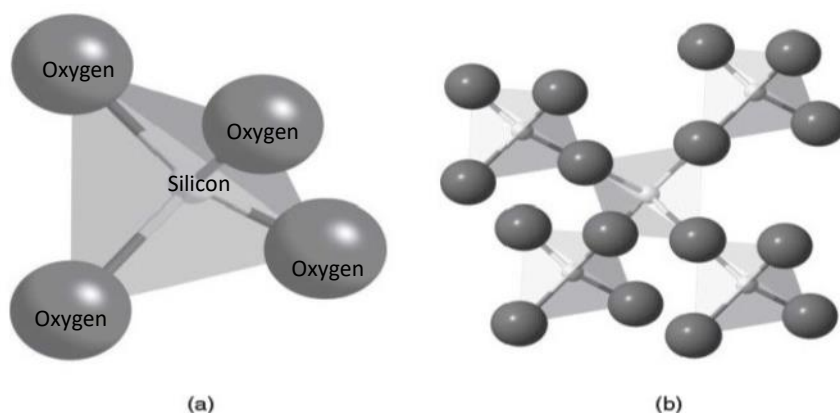


Figure 2.6. (a) Silica tetrahedron and (b) Four tetrahedra linked to one central tetrahedron by bridging oxygen (BO) ions (Adapted from Jones and Clare, 2012)

The oxides of the glass network structure can be classified according to the electronegativity of cations into (Shelby, 2005):

- (i) Glass formers: These oxides (for example, silicon oxides and phosphorus oxide) are considered to be the backbone of the glass network structure. They have high electronegativity and can form a glass network on their own when melted.
- (ii) Glass modifiers: These oxides (for example, calcium oxides, sodium oxides and strontium oxides) are not able to form a glass network when they melt alone or with

glass formers, since they have low electronegativity and can disrupt or modify a glass network.

(iii) Glass intermediates: These oxides (magnesium oxides, aluminium oxides and zinc oxides) are not able to form a glass network on their own but can either reinforce or loosen the glass network when they are melted with glass formers because they have slightly lower electronegativity than glass formers.

The role of these metal oxides can be determined by their field strength measurement index, based on the Dietzel's theory of glass (Scholze, 2012), which can be defined as follows (Equation 1.1):

$$\text{Field Strength} = \frac{Z}{a^2} \quad (1.1)$$

Where **Z** is the charge of the metal cation (M^+) and **a** is the M-O bond distance (nanometers) in the metal oxide. The oxides that tend to behave as modifiers should have field strength index of between 0.1 and 0.4, whereas those that behave as intermediates should have field strength index in a range of 1.3 to 2.0.

With regard to the bonds in the glass network structure, there are two types: i) bridging oxygen bonds (BO bonds), which link together two network forming silicon atoms (Si^{4+}) with an oxygen atom (Si-O-Si), leading to the formation of the backbone of the glass network, and ii) non-bridging oxygen bonds (NBO bonds). The latter bond glass modifier atoms (Na^+ and Ca^{2+}) with oxygen atoms after replacing a glass former atom (Si^{4+}), resulting in disruption of the glass network. Generally, when glass modifiers are increased, the number of non-bridging oxygens is also increased. This weakens and disrupts the glass network because the non-bridging oxygens break the strong bridging oxygen bonds (A-O-A; where A= a glass former atom) forming weak ionic bonds. The latter bond is between an oxygen ion that carries a partial negative charge and connects to a glass network former ion at one end only, whilst the other end is connected to a glass network modifier ion, resulting in decreased connectivity of the glass network structure (Figure 2.7) (Hench and June, 1999).

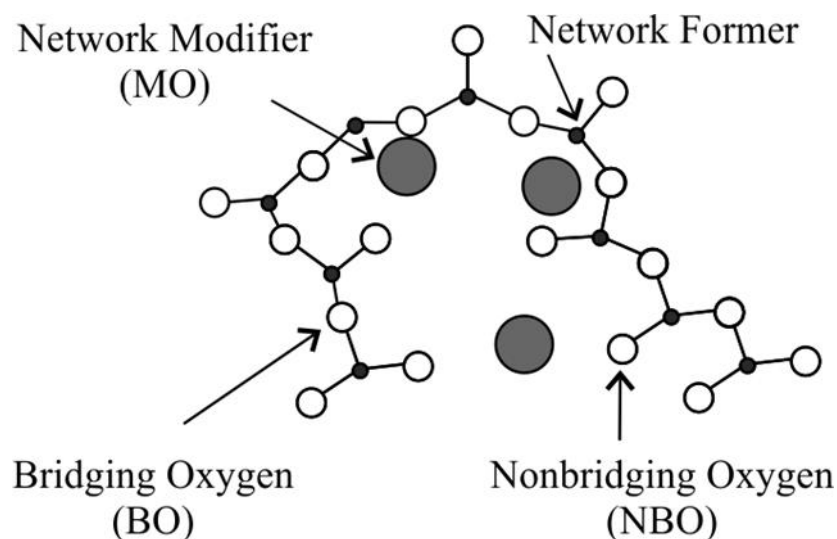


Figure 2.7. A schematic structure of a random glass composed of glass formers and glass modifiers (Adapted from Hench and June, 1999)

2.12.2. Network connectivity

The average number of bridging oxygen atoms per network forming element is known as the network connectivity (NC) of that glass. It is a useful tool in designing new bioactive glasses because the number of bridging oxygens determines the characteristic features of the glass network structure (Hill, 1996). For example, a glass with a network connectivity of two would have an average of two bridging oxygen atoms per silicon atom. A glass of network connectivity of three would have an average of three bridging oxygen atoms per silicon atom, and so on. In addition, the Q^n structure of glasses, which determines the shape of the glass network, has a strong relationship with network connectivity values since (n) also represents the number of bridging oxygens per silicon atom. From this, NC of 4 corresponds to Q^4 structures, representing four bridging oxygen atoms per silicon atom, such as pure silica glass. NC of 3 corresponds to Q^3 structures denoting a silicon atom connected to three bridging oxygen atoms (SiO_3^{2-}). Q^3 structures are presented mostly in three dimensions. NC of 2 corresponds to Q^2 structures where the silicon atom has two bridging oxygen atoms (SiO_2), presented as linear silicate chains. NC of 1 corresponds to Q^1 structures representing as a silicon atom has one bridging oxygen atoms. They are presented as a single unit (SiO). In terms of how to calculate the network connectivity of bioactive glasses, O'Donnell *et al.* (2008a) used the following equation (1.2):

$$NC = 2 + \frac{BO - NBO}{G} \quad (1.2)$$

Where BO is the total number of bridging oxygens per network-forming silicon ion, NBO is the total number of non-bridging oxygens per network modifier ions and G is the total number of glass-forming units. To calculate the network connectivity for a bioactive glass of $\text{SiO}_2\text{-Na}_2\text{O-CaO-P}_2\text{O}_5$ structure, O'Donnell *et al.* (2008a) suggested two different equations depending on two assumptions (see section 2.12.6.2 for further details). In the first assumption, phosphate (P) incorporates into the silicate glass network structure forming Si-O-P bonds. Therefore, the network connectivity is calculated following equation (1.3):

$$NC = 2 + \frac{[(2 \times \text{SiO}_2) + (2 \times \text{P}_2\text{O}_5)] - [(2 \times \text{CaO}) + (2 \times \text{Na}_2\text{O})]}{\text{SiO}_2 + (2 \times \text{P}_2\text{O}_5)} \quad (1.3)$$

Conversely, the second assumption was based on presuming that the phosphate is present as orthophosphate species $(\text{PO}_4)^{3-}$ rather than being a part of the silicate glass network structure. This orthophosphate species $(\text{PO}_4)^{3-}$ has three negative charges that require three positive charges from modifier cations (e.g. Na_2^+ , Ca^{2+}) to charge-balance itself. Thus, the network connectivity can be calculated according to equation (1.4):

$$NC = 2 + \frac{[2 \times \text{SiO}_2] - [(2 \times \text{CaO}) + (2 \times \text{Na}_2\text{O}) + (2 \times \text{P}_2\text{O}_5 \times 3)]}{\text{SiO}_2} \quad (1.4)$$

Interestingly, by applying these two equations on the bioactive glass (45S5) composition, the network connectivity values equal 1.9 and 2.1, respectively. FitzGerald *et al.* (2007) and Pedone *et al.* (2010) derived a network connectivity of 2.1, confirming the second assumption of O'Donnell *et al.* (2008a). This agreement clearly reveals that the phosphate content of bioactive glass 45S5 presents as an orthophosphate species $(\text{PO}_4)^{3-}$ and suggests that the concept of calculating network connectivity may be theoretically used as a tool in designing new bioactive glasses. Furthermore, Eden (2011) developed the split network model to assess the average glass network polymerisation (r_f) and the mean number of bridging oxygen atoms per network former, which is virtually equal to the network connectivity value. Eden (2011) designed glasses

with different network connectivities and different r_f values finding that these differences resulted in alteration of the glass properties. Similar conclusions were made by Hill (1996) and Hill and Brauer (2011), who reported a correlation between glass bioactivity and their NC, while studying glasses with different network connectivities.

Eden's (2011) split network model demonstrated that optimum bioactivity existed when the network connectivity of a glass ranged between 2.0 and 2.6, while a NC below 1.8 and above 2.7 was considered as unfavourable for the glass bioactivity. These findings are in agreement with Hill (1996) who suggested in his NC model that glass has an optimum bioactivity when its NC was close to 2.0 and less than 2.4 (Figure 2.8). To explain this, the glass bioactivity, as proposed by Hench (1991), depends on the dissolution process that occurs at the surface of the glass in a physiological solution allowing for apatite formation. Consequently, glasses of two dimensional chains (NC=2) would be more effective for glass dissolution (glass bioactivity) than three-dimensional silicate glasses (NC=3), since the former glasses would have a larger surface area compared to volume ratios, and a greater number of glass sites that would react with the surrounding solution. The glasses with a NC above two begin to change their structure to three dimensional networks decreasing their bioactivity.

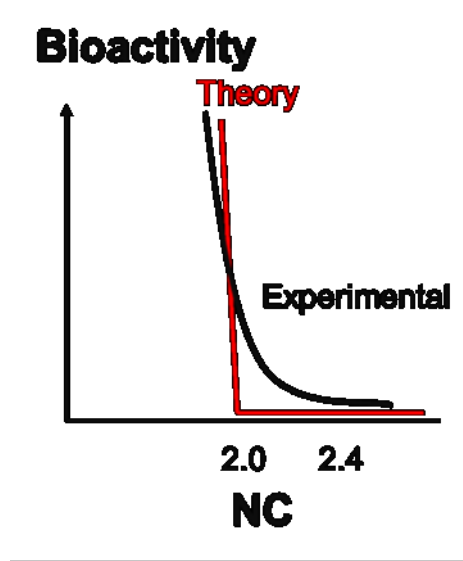


Figure 2.8. Graph illustrating the relationship between network connectivity (NC) and bioactivity (Adapted from Hill, 2009)

2.12.3. Bioactivity of bioactive glasses

Bioactivity can be defined as the ability of a material to induce a specific biological activity, forming a bond between the tissue and the material. Bioactive glasses are surface reactive substances because their surface undergoes structural and chemical changes, resulting in degradation of the glass. The dissolved products change the pH and composition of the physiological solution, leading to an increase in pH and formation of a unique chemical bond between the glass surface and ions in the physiological solution. A hydroxyapatite layer is formed on the applied glass surface. The mechanism of apatite formation proposed by Hench is as follows (Hench, 1991; Jones and Clare, 2012):

- i) Rapid ion exchange of alkali-metal cations (Na^+) with H^+ from physiological solution.
- ii) Loss of soluble silica, leaving behind Silanol groups (Si-OH bonds) on the glass surface.
- iii) Condensation and re-polymerisation of the Si-OH bonds to create a silica-rich layer on the glass surface.

iv) Migration of Ca^{2+} and PO_4^{3-} groups from inside the glass and from the body fluid, forming an amorphous calcium phosphate layer that grows on the silica-rich layer at the glass surface.

v) Crystallisation of the amorphous layer by incorporation of OH^- from the solution leading to hydroxyapatite formation.

Although Hench clearly explained apatite formation, he did not provide any information about the bioactive behaviour of a glass, nor its structure. Thus, the introduction of the concept of network connectivity to predict the bioactive behaviour of glasses containing particular elements in any composition has gained attention (Hill, 1996; Hill and Brauer, 2011). There are, however, still some limitations in designing new glasses and predicting their bioactivity relying on only NC values since the concentration of modifier ions could also affect the glass bioactivity and other glass characteristics, while the NC is kept constant.

2.12.4. Glass formation

Generally, the classical way to form a glass is by super-cooling a highly viscous molten liquid very rapidly to a temperature below its melting temperature (T_m), to form a viscoelastic solid state (glass formation), without crystallisation (crystal formation) taking place. The atomic arrangement of the molten liquid will be changed gradually during cooling to form either a periodic, long-range ordered atomic structure (crystal), or a random, short-range ordered atomic structure (glass)(Shelby,2005).

The volume/temperature diagram (Figure 2.9) shows the changes in the volume of the molten liquid as it is cooled to form either a glass or a crystal, depending on the cooling rate. If the cooling rate of the molten liquid is slow below its melting temperature, crystallisation (crystal formation) would occur accompanied by a sharp decrease in the volume. Conversely, if the cooling rate is fast, a glass will be formed from the super-cooled liquid with no abrupt decrease in the volume, since the atomic structure of the liquid has no time to rearrange into a periodic, long-range ordered arrangement. Thus, crystallisation does not take place as the temperature decreases (Paul, 1989; Shelby,

2005). If crystallisation occurs, there will be a decrease in the glass dissolution rate and bioactivity due to a limited exchange of ions (Ducheyne *et al.*, 1997; Brauer *et al.*, 2010; Mneimne *et al.*, 2011).

The transition from a viscous liquid state to a glassy solid state occurs over a temperature range with no definite temperature (Paul, 1989; Shelby, 2005). However, it is beneficial to use a single temperature as an indication of the onset of the transformation from one state to another during cooling or heating. This temperature is called the glass transformation temperature or glass transition temperature (T_g ; Shelby, 2005). Furthermore, the difference in the thermal history between the glassy solid state and viscous liquid state of the same material intersects at a temperature called fictive temperature (T_f) where equilibrium occurs between the liquid and solid states of the material (Paul, 1989).

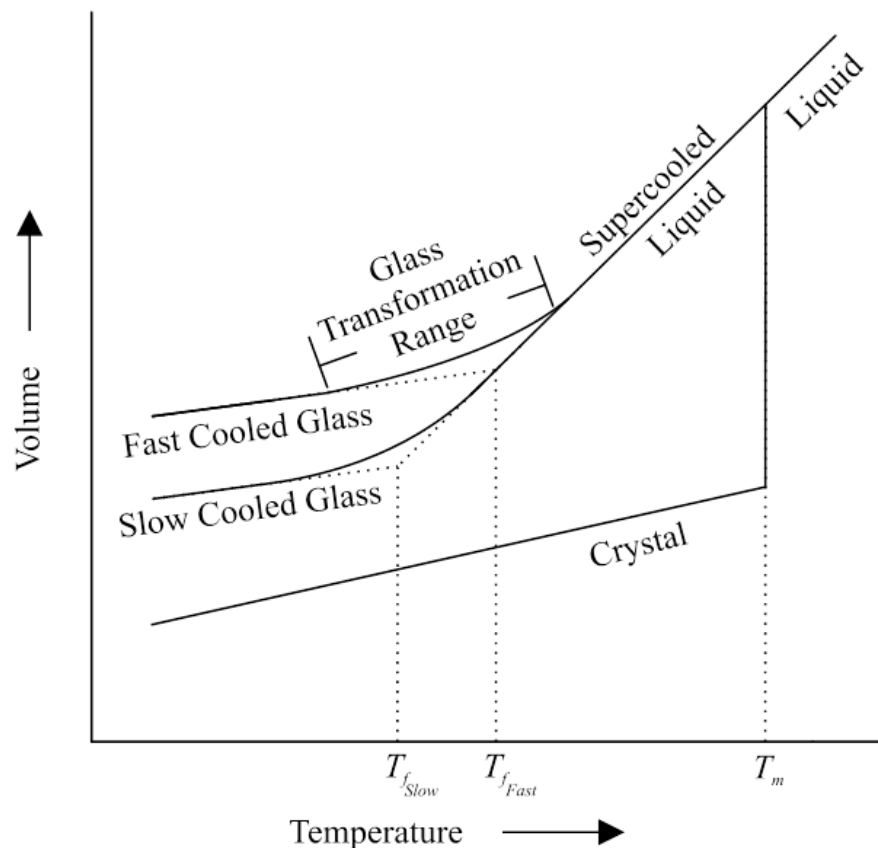


Figure 2.9. Effect of temperature on the volume of glass forming melts (Adapted from Shelby, 2005)

2.12.5. Glass synthesis

Bioactive glasses can be produced using two processing methods. These include: i) the traditional melt–quench route, which utilises high temperatures (above 1300°C) to melt the oxides together in a crucible. The molten mixture is quenched in a graphite mould or in water; ii) the sol-gel route, with temperatures of 600-700°C to form a gel from a glass solution after undergoing polymerisation at room temperature. This gel, which is a wet inorganic polymer, similar to a highly cross-linked short chain inorganic polymer, is dried and heated to 600°C to produce a pure, homogenous glass (Jones and Clare, 2012). Therefore, the temperature required to form a glass using the sol-gel route is lower than that required by the melt–quench route. However, the use of the sol-gel route is limited as it takes considerably longer than the melt-quench route (Shelby, 2005).

2.12.6. Assessment techniques to investigate glass characteristics

Different techniques are used to investigate the glass characteristics including:

a. Fourier-transform infrared spectroscopy (FTIR)

FTIR is a technique used to obtain an infrared absorption or emission spectrum of a solid, liquid or gas with infrared radiation is passed through a sample. Some of the infrared radiation is absorbed by the sample and some of it is passed through (transmitted). The FTIR spectrometer simultaneously collects high-spectral-resolution data over a wide spectral range. The resulting spectrum represents the molecular absorption and transmission, creating a molecular fingerprint of the sample with absorption peaks which correspond to the frequencies of vibrations between the bonds of the atoms making up the material. Since each different material is a unique combination of atoms, no two compounds produce the exact same infrared spectra (Kazarian and Chan, 2006).

Generally, there are three types of FTIR namely: Transmission, attenuated total reflectance (ATR) and specular reflectance. ATR is commonly used to probe the surface properties of materials rather than their bulk properties. The penetration depth of this technique, or the depth from which the infrared signal is generated varies as a

function of the crystal, angle of incidence, and wavenumber but it is in the range of microns. This limited path length into the sample avoids the problem of strong attenuation of the infrared signal in highly absorbing media, such as aqueous solutions. In the ATR technique, the samples are examined directly in the solid or liquid state without further preparation, while the transmission technique requires preparation of the sample into a pellet before the transmission measurement can be made. This requires expertise and can be time consuming (Kazarian and Chan, 2013).

b. X-ray diffraction (XRD)

XRD is one of the most important non-destructive tools to analyze all kinds of matter ranging from fluids, to powders and crystals. This technique is used for the identification of crystalline phases of various materials and the quantitative phase analysis subsequent to identification. X-ray diffraction is superior in elucidating the three-dimensional atomic structure of crystalline solids. The properties and functions of materials largely depend on the crystal structures (Moore and Reynolds, 1989).

The Bragg equation, $n\lambda = 2d\sin\theta$ is central to understanding X-ray diffraction. In this equation, n is an integer, λ is the characteristic wavelength of the X-rays impinging on the crystallize sample, d is the interplanar spacing between rows of atoms, and θ is the angle of the X-ray beam with respect to these planes. When this equation is satisfied, X-rays scattered by the atoms in the plane of a periodic structure are in phase and diffraction occurs in the direction defined by the angle θ . In the simplest instance, an X-ray diffraction experiment consists of a set of diffracted intensities and the angles at which they are observed. This diffraction pattern can be thought of as a chemical fingerprint, and chemical identification can be performed by comparing this diffraction pattern to a database of known patterns (Baron, 2015).

c. Magic angle spinning- Nuclear Magnetic resonance (MAS-NMR)

Magic-angle spinning (MAS) is a technique often used to perform experiments in solid-state NMR spectroscopy and, more recently, liquid proton nuclear magnetic resonance (McDermott and Polenova, 2012).

Solid-state magic angle spinning (MAS) NMR provides a versatile method for the determination of structure for ordered systems without translation symmetry, such as proteins, macromolecular complexes, aggregates, or membrane systems. Two directionally dependent interactions commonly found in solid-state NMR are the chemical shift anisotropy (CSA) and the internuclear dipolar coupling. Anisotropic interactions modify the nuclear spin energy levels (and hence the resonance frequency) of all sites in a molecule, and often contribute to a line-broadening effect in NMR spectra. This technique is used to obtain high resolution NMR data from solids when the solid sample is placed in a rotor and mechanically rotated (spinning) at a high frequency (1 to 130 kHz) about an axis oriented at the magic angle θ_m (54.74°) with respect to the direction of the static magnetic field. By spinning the sample, the normally broad lines become narrower, increasing the resolution for better identification and analysis of the spectrum. The physical spinning of the sample is achieved via an air turbine mechanism. These turbines (or rotors) come in a variety of diameters (outside diameter), from 0.70–15 mm, and are usually spun on air or nitrogen gas. The rotors are made from a number of different materials such as ceramics e.g. zirconia, silicon nitride or polymers such as poly (methyl methacrylate) (PMMA), polyoxymethylene (POM). The cylindrical rotors are axially symmetric about the axis of rotation. Samples are packed into the rotors and these are then sealed with a single or double end cap. These caps are made from a number of different materials e.g. Kel-F, Vespel, zirconia or boron nitride depending on the application required (Polenova *et al.*, 2015).

2.12.7. Effect of changing various ions within the glass composition on the glass structure and bioactivity

2.12.7.1. Effect of changing sodium ions

The content of sodium oxide (Na_2O) within the glass composition can influence the properties of a bioactive glass. Wallace *et al.*, (1999) studied the effect of adding one mol of Na_2O for every one mol of CaO removed to maintain the same value of network connectivity. The authors reported that increasing the sodium content in a series of glasses (from zero mol% to 26.5mol%), with a constant network connectivity value close to 2 resulted in a linear decrease in the glass transition temperature (T_g) (from 750°C to 500°C). This was attributed to the substitution of CaO for Na_2O that led to a disrupted silicate glass network, since one Ca^{2+} was replaced by two Na^+ ions (Figure 2.10). This resulted in the loss of the ionic bridges that Ca^{2+} ions provided between two adjacent non-bridging oxygens contributing to a decrease in the packing density of the glass. Therefore, less rigid glasses were formed that required a lower glass transition temperature (T_g) to transform them from a molten liquid to a glassy state.

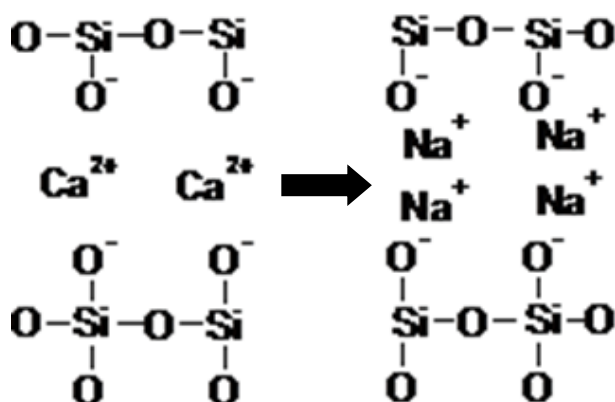


Figure 2.10. Representation of a highly-disrupted glass network after Ca^{2+} is replaced by two Na^+ ions (Adapted from Wallace *et al.*, 1999)

Conversely, it has also been demonstrated that decreasing the sodium content from 24.4mol% to zero mol%, across a series of glasses with a constant network connectivity value close to 2 ($\text{NC}=2.08$) resulted in a linear increase in the T_g (from 530°C to 730°C) and hardness (from 5.54GPa to 6.66GPa) (Farooq *et al.*, 2013). The authors reported that this could relate to an increase in Ca^{2+} ions (in exchange for Na^+) that can form stronger ionic bridges between two adjacent non-bridging oxygens. This

leads to the formation of a highly cross-linked glass (rigid glass) that requires a higher T_g to transform it from the liquid state to the glassy state.

2.12.7.2. Effect of changing phosphate ions

a- Glass structure

The effect of increasing phosphate content on the structural properties of bioactive glasses was studied by O'Donnell *et al.* (2008a). They designed two different series of bioactive glasses based on a similar composition to 45S5. The amount of phosphate in the first series was increased from 1.07mol% to 9.25mol% (substituting for reduced content silica from 49.46mol% to 37.28mol%; Table 2.6), whilst the ratio between modifier oxides (sodium oxide and calcium oxide) was kept constant (1:0.87), and was associated with inconstant network connectivities. The authors assumed that the phosphate ion acts as a glass former and incorporates itself in the silicate glass network forming Si-O-P bonds.

In contrast, in the second series (Table 2.6) both modifier oxides (sodium oxide and calcium oxide) were increased to provide a sufficient number of cations (Na^+ and Ca^{2+}). The charge of these two cations balanced the negatively charged orthophosphate species $(\text{PO}_4)^{3-}$, which the authors assumed were present as the phosphate content was increased from zero to 6.33mol% (substituting for reduced content silica from 51.06mol% to 38.14mol%, while the network connectivity value was kept constant (2.08). This aided in studying the effect of adding phosphate on its own without changing the network connectivity values of the glasses.

Table 2.6. Glass compositions (mol%) and network connectivity (NC) assuming phosphate incorporated in the glass network and modified network connectivities (NC') assuming phosphate is orthophosphate species (O'Donnell *et al.*, 2008a)

Bioactive glasses	Mol%				NC	NC'
Series I	SiO ₂	Na ₂ O	CaO	P ₂ O ₅		
ICIE1	49.46	26.38	23.8	1.07	2.04	2.13
ICSW2	47.84	26.67	23.33	2.16	2.00	2.18
ICSW3	44.47	27.26	23.85	4.42	1.92	2.30
ICSW5	40.96	27.87	24.39	6.78	1.83	2.44
ICSW4	37.28	28.52	24.95	9.25	1.75	2.62
Series II						
ICSW1	51.06	26.10	22.84	0.00	2.08	2.08
ICSW6	48.98	26.67	23.33	1.02	2.00	2.08
ICSW7	47.07	27.19	23.78	1.95	1.92	2.08
ICSW8	43.66	28.12	24.60	3.62	1.79	2.08
ICSW10	40.71	28.91	25.31	5.07	1.67	2.08
ICSW9	38.14	29.62	25.91	6.33	1.56	2.08

Based on the findings of Magic-Angle-Spinning Nuclear Magnetic Resonance (MAS-NMR) Spectroscopy, O'Donnell *et al.* (2008a) demonstrated that phosphate was present as orthophosphate species (see Figure 2.11a) for almost all of the first glass series, with the exception of the glass with the highest phosphate content (=9.25mol%); this glass also had the highest network connectivity (2.62). In addition, another X-ray diffraction (XRD) study by the aforementioned authors (O'Donnell *et al.*, 2008b) revealed that the latter glass was partially crystalline, and its phosphate content existed as pyrophosphate (see Figure 2.11b). These findings were in agreement with the results of Grussaute *et al.* (2000), who also confirmed the presence of phosphate in the form of pyrophosphate in glasses of network connectivities above 2.5. The authors attributed the presence of pyrophosphate either to the partial crystallinity of this glass or to its high network connectivity value.

In the second glass series with a constant network connectivity value of 2.08 (O'Donnell *et al.*, 2008a), the authors noted that the pyrophosphate species were absent and orthophosphate species were present, using (MAS-NMR) spectroscopy (O'Donnell *et al.*, 2008a) and XRD analysis (O'Donnell *et al.*, 2008b). These findings are in accordance with those reported by FitzGerald *et al.* (2007) and Pedone *et al.* (2010), who confirmed the presence of phosphate in 45S5 (NC=2.1) as orthophosphate species. There was no pyrophosphate, nor Si-O-P bonds, in the composition of glasses with network connectivity less than 2.5.

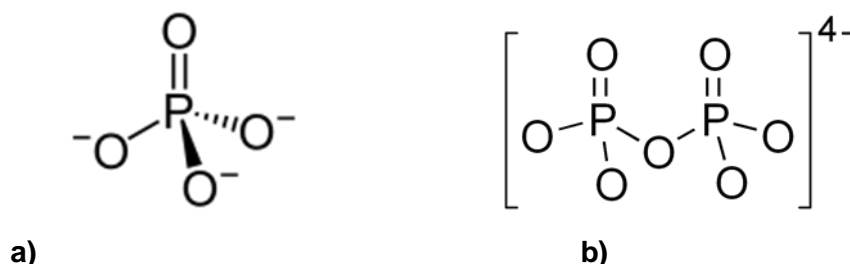


Figure 2.11. A schematic structure of

a) Orthophosphate (<http://eternawiki.org/wiki/index.php5/File:Phosphat-Ion.png>)

b) Pyrophosphate (https://commons.wikimedia.org/wiki/File:Pyrophosphate_anion.png)

The effect of increasing the phosphate content on the glass structure was also studied by Tilocca *et al.* (2007a, 2007b), who used a modern computational technique called molecular dynamic (MD) simulations. They designed three glasses with high silica (46.1mol%, 56.5mol%, and 66.9mol%, respectively) and phosphate content (2.75mol%, 2.63mol%, and 2.63mol%, respectively) (Tilocca *et al.*, 2007a). This design resulted in an increase in the network connectivity values (2.07, 2.7 and 3.24, respectively). In a subsequent study (Tilocca *et al.*, 2007b), the phosphate content was increased (from zero mol% to 12.17mol%) by substituting silica content (i.e. decreasing silica) from 48.87mol% to 36.30mol%, similarly to the first series described by O'Donnell *et al.* (2008a). This substitution led to an increase in the network connectivity values from

1.91 to 2.77. Both of Tilocca *et al.*'s studies confirmed the presence of phosphate in the form of orthophosphate species, by the presence of two dissolution processes - dissolution of the silica glass phase and dissolution of the orthophosphate glass phase. However, the authors also observed the presence of phosphate in the form of pyrophosphate species in some glasses, which had network connectivities above 2.5. This finding supported O'Donnell *et al.* (2008a) showing that pyrophosphate species exist in glasses with network connectivity above 2.5. This may explain why the bioactivity of these glasses is less than that of 45S5, which has network connectivity of between 2.08 and 2.1 and has only orthophosphate species as reported previously (Lockyer *et al.*, 1995; Elgayar *et al.*, 2005; O'Donnell *et al.*, 2008a; O'Donnell *et al.*, 2008b; Brauer *et al.*, 2009). This NC range of 2.08 to 2.1 seems to favour the formation of orthophosphate species that promote glass bioactivity.

Mathew *et al.* (2013) has also elucidated the relationship between the presence of phosphate in the form of orthophosphate species in glasses and their network connectivities. The authors demonstrated that by keeping the phosphate content at approximately $\leq 6\text{mol}\%$ in glasses of network connectivity between 2 and 2.5, the orthophosphate species were present and indiscriminately distributed in the silicate network glasses. These species occupy interstitial positions in the silicate glass network together with the calcium and sodium cations. These findings are in accordance with the aforementioned findings of O'Donnell *et al.* (2008a) and Tilocca *et al.* (2007a, 2007b) in glasses with approximately $\leq 6\text{mol}\%$ phosphate content and network connectivity of between 2 and 2.5. Conversely, in glasses with high network connectivity (above 2.5) and high phosphate content (above $6\text{mol}\%$), the silicate network structure is highly cross-linked with insufficient spaces to accommodate orthophosphate species. Hence, the silica and orthophosphate tend to be phase separated at high network connectivity (above 2.5). This phase separation may result in the presence of phosphate content as pyrophosphate species in these glasses, which is unfavorable for apatite formation.

b- Glass physical properties

O'Donnell *et al.* (2008b) have also assessed the physical properties of their two glass series (Table 2.6) by using Differential Thermal Analysis to determine their T_gs. They observed that T_g decreased when the phosphate content was increased in both glass series. This behaviour was unexpected and it contradicted the authors' assumption. In the first glass series, they assumed that the addition of phosphate would simply reduce modifier cations (Na⁺ and Ca⁺²) from their modifying oxide states (sodium oxide and calcium oxide) available in the silicate glass network, to charge balance the added phosphate ions (orthophosphate species; (PO₄)³⁻). Therefore, this would result in glass network polymerisation due to reducing non-bridging oxygens (modifier oxides) that will lead to an increase in T_g. In the second glass series, the added phosphate was assumed to be compensated by charge balancing from the added modifier cations (Na⁺ and Ca⁺²). This means that the silicate glass network would remain unchanged leading to no change in T_g.

To explain this contradiction between the expected behaviour, which was relying on the hypothesis that T_g correlates with the degree of disruption of silicate glass network phase, and the real behaviour (a decrease in T_g), O'Donnell *et al.* (2008b) attributed this to phase separation into two phases, the silicate phase and the phosphate phase. They believed this separation was likely to occur in association with the addition of phosphate, and that the T_g was affected by both phases. Hence, they hypothesized that a 'composite T_g' appeared when this two-phase separation had occurred and this T_g did not depend only on the silicate phase, as expected. However, this explanation is doubtful and cannot be applied for glasses that have network connectivity below 2.5 because this phase separation is unlikely to occur at this network connectivity value (Mathew *et al.*, 2013).

O'Donnell *et al.* (2008b) used X-ray Diffraction (XRD) to confirm that both first and second glass series (up to 6mol% phosphate content) were amorphous, with the exception of the glass (in the first glass series) that had 9.25mol% of phosphate and a network connectivity of 2.6, which was partially crystallised. The XRD results showed three crystalline phases in this glass: 68mol% NaCaPO₄ (sodium calcium orthophosphate), 28mol% Na₂O.2CaO.3SiO₂ (combeite), and 4mol% Na₄P₂O₇ (sodium

pyrophosphate). Thus, these crystalline phases support the assumption of pyrophosphate formation, and phase-separated glass phenomena that occurs in glasses with network connectivity above 2.5. These findings implied that the phosphate content should be no more than 6mol% and the glass network connectivity should be below 2.5 to avoid glass crystallisation which impairs the bioactivity of glass. These findings were in agreement with the results of O'Donnell *et al.* (2008a) using MAS-NMR and Mathew *et al.* (2013).

c- Glass bioactivity

In regard to the glass bioactivity and its relation to phosphate content, O'Donnell *et al.* (2009) immersed their two glass series (Table 2.6) in simulated body fluid (SBF), for different time intervals (up to 21 days). Fourier Transform Infrared Spectroscopy (FTIR) and XRD were used to assess the bioactivity of these glasses by detecting their capability to form apatite, in a similar manner to Kokubo *et al.* (1990). In the first glass series, the glass with 6.78mol% phosphate content, which had a network connectivity value of 2.4, formed apatite after 16 hours' immersion in SBF. These apatites were characterised by the presence of a distinct P-O splitting band at 550cm^{-1} (ATR-FTIR), and by the appearance of apatitic diffraction peak at $26^{\circ} 2 \text{ Theta}$ using XRD. In contrast, 45S5 of 2.6mol% phosphate content did not show these peaks during the same period. This suggests that increasing phosphate content of a glass will improve its bioactivity by forming apatite faster than 45S5. However, a glass with a much higher phosphate content ($\approx 9.25\text{mol}\%$) and higher network connectivity value (≈ 2.6), from their first glass series, formed apatite more slowly (within one day) than glasses with approximately 6mol% phosphate content and network connectivity ~ 2 or less than 2.5 (within 16 hours) in both glass series (Table 2.6). This may relate to the phosphate content glass (9.25mol%) being partially crystallised and forming pyrophosphate species that affected its bioactivity (apatite formation) (O'Donnell *et al.*, 2008a; 2008b). This means that there are some constraints to increasing the phosphate content to enhance the bioactivity of glasses. Specifically, the network connectivity should be kept around 2 or less than 2.5, and the added phosphate should be no more than 6mol%, which will then be presented as the orthophosphate species. A proportional increase in the glass bioactivity is observed with these species. These findings were confirmed by

Eden (2011), who reported that the phosphate content of glasses plays a significant role in enhancing glass bioactivity by forming apatite when the network connectivity is favorable (around 2 or less than 2.5). Otherwise, the added phosphate will lead to polymerisation of the glass network of high network connectivity (above 2.5). This would affect glass degradation and bioactivity because glasses with high network connectivity (above 2.5) have phosphate in the form of pyrophosphate rather than orthophosphate species (O'Donnell *et al.*, 2008a; 2008b and Tilocca *et al.*, 2007a; 2007b).

In a follow-on study to O'Donnell *et al.* (2009), Mneimne *et al.* (2011) reported that increasing the phosphate content of fluoride-containing bioactive glasses led to a significant increase in the glass bioactivity and fluorapatite formation. This apatite formation occurred more rapidly (within 6 hours) in glasses of high phosphate content compared to those with low phosphate content (within 3 days). These researchers also found that increasing the phosphate content in fluoride-containing bioactive glasses resulted in the formation of fluorapatite rather than calcium fluoride (fluorite) using MAS-NMR analysis.

In summary, it could be concluded that the presence of phosphate in the form of orthophosphate is the most important factor for increasing bioactivity. Orthophosphate is highly degradable and extremely soluble in physiological solutions; this will lead to an increase in the degradation of the glass (glass solubility) and consequently its bioactivity (apatite formation). However, this is reliant on the network connectivity of these glasses being kept below 2.5 with the phosphate content being approximately 6mol%.

2.12.7.3. Effect of changing fluoride ions

a- Glass structure

The incorporation of fluoride in bioactive glasses has gained interest since it has the capability to i) inhibit enamel demineralisation as it forms fluorapatite, which is more chemically stable than hydroxyapatite, and would therefore less readily dissolve when the mouth is exposed to acidic conditions (Featherstone, 2000), ii) treat dentine

hypersensitivity by precipitating apatite on to the tooth surface and subsequently occluding exposed dentinal tubules (Lynch *et al.*, 2012), and iii) enhance bone mineralisation by promoting bone cell activity to proliferate and regenerate new bone tissue (Caverzasio *et al.*, 1998; Gentleman *et al.*, 2013). All these advantages led to investigation on fluoride incorporation into the glass network and its effect on the glass structure and bioactivity.

A number of studies have evaluated the effects of adding fluoride to the glass network structure by substituting a glass-modifying oxide, such as sodium oxide or calcium oxide with calcium fluoride (Stebbins and Zeng, 2000; Lusvardi *et al.*, 2008; Christie, 2011). This reduced the non-bridging oxygen content in the glass network structure resulting in the formation of highly cross-linked glasses with high bridging oxygens content. Consequently, both glass dissolution rate and glass bioactivity decreased. However, the outcome of these studies was difficult to interpret accurately as different glasses were designed with inconsistent ratios, and different methods were used to incorporate fluoride into these glasses. For example, Stebbins and Zeng (2000) investigated glasses with predominantly Q3 structure and demonstrated that fluoride was bonded only to high field strength modifier cations, whilst Lusvardi *et al.* (2008) designed glasses with mostly Q2 structure and observed that the addition of fluoride increased the polymerisation of the silicate glass network structure by reducing the modifier cations.

Conversely, Brauer *et al.* (2009) also studied the effect of adding calcium fluoride on the glass network structure, whilst keeping the ratio between the glass components constant. These findings were beneficial in understanding the effect of adding fluoride on the glass properties, since the glass network structure was maintained (fixed network connectivity) without being disturbed by the addition of fluoride, confirmed by the absence of non-bridging fluorines (Si-F). There were no detectable amounts of Si-F by using MAS-NMR (Brauer *et al.*, 2009). This means that calcium fluoride did not bond to the silicate network structure. In addition, the MAS-NMR peaks were identical for all glasses with increasing calcium fluoride content from 4.53mol% to 32.71mol%, thus confirming a constant theoretical network connectivity value (2.13) for all experimental glasses, since calcium fluoride was not added at the expense of glass network modifiers, and it charge balanced itself without affecting the network connectivity.

Furthermore, the authors also observed that fluoride formed complex structures with calcium. This outcome was in agreement with Hayashi *et al.* (2004) and Watanbe *et al.* (2004). The latter studies demonstrated that there was no change in the network connectivity values across a series of sodium-free glasses, with only calcium present as a modifier, confirming the formation of fluoride complexes with calcium.

In summary, the addition of fluoride to the glass network structure promotes the formation of complexes between fluoride ions and calcium with no Si-F bonds. This can be achieved in glasses that have network connectivities close to two, and a constant ratio between the glass components. Conversely, substitution of fluoride by a glass modifier oxide, such as calcium oxide or sodium oxide may increase the network connectivity value. Therefore, highly cross-linked glass may be formed due to a reduction in glass modifiers (non-bridging oxygen content). This in turn affects the glass bioactivity.

b- Glass physical properties

With regard to the effect of adding calcium fluoride on the physical properties of glass, Brauer *et al.* (2009) used Differential Scanning Calorimetry (DSC) to assess the changes in the thermal behaviour. The authors found that increasing calcium fluoride content led to a decrease in the glass transition temperature (T_g), the onset of crystallisation and crystallisation peak temperatures. This may be attributed to fluoride-free glasses having divalent calcium ions (Ca^{2+}) that form ionic bridges (electrostatic forces) between two adjacent non-bridging oxygens (silicate anions, SiO^{1-}). In contrast, in fluoride-containing glasses, the fluoride ions form complexes with calcium ions (hypothetical CaF^+ species) resulting in a reduced positive charge of the calcium ion from two to one, allowing the complex to bond only to one non-bridging oxygen instead of two (Figure 2.12). Thus, this would weaken the glass durability and impair the thermal properties of the glass.

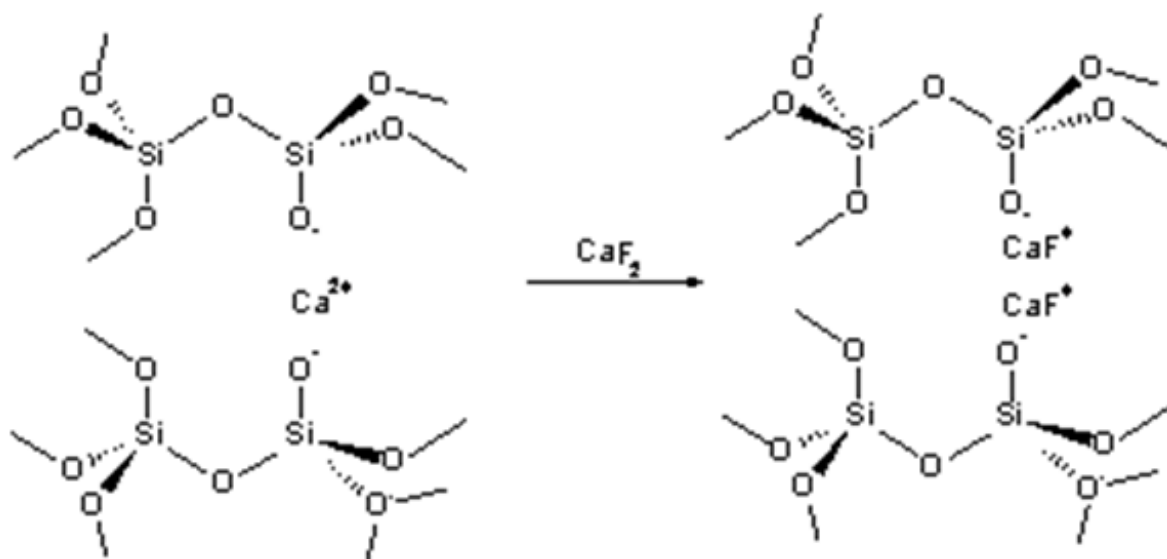


Figure 2.12. Illustration of hypothetical effect of CaF_2 addition on silicate network (Adapted from Brauer *et al.* 2009)

c- Glass bioactivity

Brauer *et al.* (2010) designed a series of glasses that had a similar composition to 45S5 but with a lower phosphate content (between 0.97mol% to 1.07mol%) compared to that of 45S5 (2.6mol%). The fluoride was also added to this glass series in the form of calcium fluoride, ranging between zero to 9.28mol%, whilst the ratio of glass modifiers to glass formers and the network connectivity across the glass series was kept constant. The authors immersed these glasses in simulated body fluid (SBF) for three different immersion periods to study their bioactivity. They reported that apatite formation was retarded in the lowest fluoride content (4.75mol%) glass compared to their respective fluoride-free glasses after 1-week immersion in SBF. The formation of fluorapatite was characterised by ATR-FTIR, X-ray diffraction and MAS-NMR analysis. In addition, the other fluoride-containing glasses across Brauer *et al.*'s (2010) glass series showed fluorapatite and some crystal phases represented by calcium fluoride (fluorite) during the same period.

A follow-up study to Brauer *et al.*'s (2010) study was performed by Mneimne *et al.*'s (2011). They designed two fluoride-containing glass series which were immersed in Tris buffer solution for different periods. The first glass series was similar to that of Brauer *et al.*'s (2010) glass series, while the second comprised fluoride-containing

glasses with high phosphate content (Table 2.7). They reported that the glass with the lowest fluoride content (4.75mol% and 4.53mol%) in the first and second glass series formed apatite faster than their respective fluoride-free glasses and other glasses within the glass series. This finding contradicted Brauer *et al.*'s (2010) results, although the type of immersion solution (Tris buffer or simulated body fluid) varied between the experiments. In addition, the glass with 4.53mol% fluoride content in the second-high phosphate glass series formed apatite faster (after 6 hours of immersion) than the glass with 4.75mol% fluoride content in the first low phosphate series (after 3 days). This finding agrees with O'Donnell *et al.*'s (2009) study by showing the importance of increasing phosphate content on the rate of apatite formation. Furthermore, the other fluoride-containing glasses of both Mneimne *et al.*'s (2011) glass series revealed apatite formation with some crystal phase (calcium fluoride) after 1-week immersion in Tris buffer solution. These apatites were characterised by using MAS-NMR, ATR-FTIR, and X-ray diffraction (XRD).

Table 2.7. Nominal glass composition of Mneimne *et al.*'s (2011) study in mol% with theoretical network connectivity (NC')

Bioactive glasses	Mol%					NC'
Series I	SiO ₂	Na ₂ O	CaO	P ₂ O ₅	CaF ₂	
A	49.46	26.38	23.08	1.07	-	2.13
B	47.12	25.13	21.98	1.02	4.75	2.13
C	44.88	23.93	20.94	0.97	9.28	2.13
D	42.73	22.79	19.94	0.92	13.62	2.13
E	40.68	21.69	18.98	0.88	17.76	2.13
F	36.83	19.64	17.18	0.80	25.54	2.13
H	44.88	-	44.87	0.97	9.28	2.13
Series II						
A2	38.14	29.62	25.91	6.33	-	2.08
B2	36.41	28.28	24.74	6.04	4.53	2.08
C2	34.60	26.87	23.51	5.74	9.28	2.08
D2	32.95	25.59	22.38	5.47	13.62	2.08
E2	31.37	24.36	21.31	5.21	17.76	2.08
F2	28.40	22.06	19.29	4.71	25.54	2.08
H2	34.60	-	50.38	5.74	9.28	2.08

In summary, both Brauer *et al.* (2010) and Mneimne *et al.* (2011) agreed on the presence of some crystal phases (fluorite) over apatite when the amounts of fluoride content exceeded 5mol% in fluoride-containing bioactive glasses with low and high phosphate content. However, both studies contradicted each other in terms of the effect of fluoride within the glass composition on the rate of apatite formation.

Mneimne (2014) studied the effect of immersing two glasses (G1 and G2) with high phosphate content, and high phosphate and fluoride contents, respectively (Table 2.8), into three different solutions (Tris buffer, simulated body fluid, and artificial saliva) at different time intervals and pH. Both glasses (G1 and G2) formed apatite faster (6 hours in Tris buffer, 24 hours in simulated body fluid, and 30 minutes in artificial saliva) than 45S5 glass (24 hours in Tris buffer, 72 hours in simulated body fluid, and 45 minutes in artificial saliva). The difference in the observed apatite formation time between these solutions was attributed to the difference of the chemical composition of each solution, in particular to the addition of phosphate.

Table 2.8. Glass composition of Mneimne's (2014) study in mol%

Bioactive glasses	SiO ₂	Na ₂ O	CaO	P ₂ O ₅	CaF ₂
45S5	46.13	24.35	26.91	2.6	0.0
G1	38.5	26.2	29.0	6.3	0.0
G2	35.9	25.1	27.7	6.3	5.0

Additionally, Bingel *et al.* (2015) studied the effect of immersion 45S5 (Bioglass®) glass in three solutions of varying pH: Tris buffer (pH 7.3), a basic Tris buffer solution (pH 9), and acetic acid (pH 5) over different immersion times. 45S5 glass promoted apatite formation after 3 hours of immersion in acetic acid, after 24 hours in Tris buffer solution (pH 7.3), and after 72 hours in Tris buffer solution (pH 9). Both of these studies (Mneimne, 2014; Bingel *et al.*, 2015) clearly demonstrate the influence of different dissolution solutions and pH of the same solution both on the degradation of glasses (glass dissolution rate) and on the bioactivity of these glasses (apatite formation).

2.12.8. Application of bioactive glasses

It has been reported that the first clinical use of bioactive glass was in the reconstruction of the bony ossicular chain of the middle ear for the treatment of conductive hearing loss (Greenspan, 1999). Nowadays, these glasses have a wide range of applications. These include:

i) Medical applications: Bioactive glasses have been used as bone grafts and bone cements, for bone replacement and regeneration in orthopaedic applications. Ilharreborde *et al.* (2008) suggested in a comparative retrospective study that Bioglass® was effective as an iliac crest graft to achieve fusion and maintain correction in thoracic adolescent idiopathic scoliosis. Peltola *et al.* (2006) reported that bioactive glass has the capability to be a reliable frontal sinus obliteration material, providing favourable conditions for total bony sinus obliteration in patients who suffered from chronic suppurative frontal sinusitis based on a longitudinal evaluation of 42 patients.

ii) Dental applications: Several studies have confirmed that bioactive glasses are safe for dental use (Erol-Taygun *et al.*, 2013). For example, bioactive glasses (NovaBone™ and Perioglas™) have been used to fill defects in the jaw, following the extraction of teeth, to reduce the resorption of lingual and buccal alveolar plates (Hench and Wilson, 1993) and as a bone graft in alveolar ridge augmentation (Hench *et al.*, 2013). In addition, Robinson (2013) suggested that bioactive glass (perioglas™) can be used as a regenerative material to treat osseous periodontal disease without any biological complications since the ionic dissolution of this glass enhanced bone regeneration. Furthermore, Tai *et al.* (2006), in a randomised, double-blinded, controlled clinical trial, found that use of a dentifrice containing bioactive glass (NovaMin™) significantly reduced gingival bleeding and decreased supragingival plaque compared with a use of a placebo dentifrice for 6 weeks. Du Min *et al.* (2008), in a 6-week, randomised, parallel-arm, double-blind clinical study, also reported that NovaMin™ dentifrice was more effective at reducing dentine sensitivity compared with a commercial dentifrice and placebo control.

Furthermore, Sauro *et al.* (2012) in an *in vitro* study suggested that resin bonding systems containing bioactive fillers may have a therapeutic effect on the nano-mechanical properties and sealing ability of the dentine surface. This may reduce the

micro-permeability between the dentine surface and the resin layer and minimise the risk of demineralisation within the dentine surface.

Bioactive glass propelled *via* air-abrasion devices have also been used in a number of *in vitro* studies as i) a surface modification material of titanium implants to enhance the process of implantation in osseous tissue (Koller *et al.*, 2007), ii) a surface pre-conditioning of WSLs to promote remineralisation of these lesions (Milly *et al.*, 2015), iii) a stain removal material by polishing teeth surfaces (Banerjee *et al.*, 2010), and iv) an abrasive material to selectively remove carious tooth structure (Paolinelis *et al.*, 2008; Banerjee *et al.*, 2011).

2.13. Air-abrasion

2.13.1. Development of air-abrasion

The basic concept of air-abrasion was first introduced by Robert Black in the early 1940s for use in dentistry, as a less traumatic and more conservative operative method for removing dental caries and preparing cavities compared to conventional drilling methods. However, this technique did not gain popularity as it lacked the ability to prepare a cavity with well-defined margins and walls for metallic fillings, such as amalgam and gold, the most popular fillings at that time. Furthermore, the invention of the air turbine hand-piece in the 1950s simplified and expedited cavity preparations. It was also difficult to suck up generated dust particles because there was no sucking system at the time (White and Eakle, 2002; Hedge and Khataavkar, 2010).

Many improvements were made to the air-abrasion system in the 1950's by Rainey, including: i) reduced noise, heat and vibration compared with the conventional drilling methods, and ii) less dust production by using a water shroud in the air-abrasion system and utilising the development of high-velocity suction. These improvements allied to the development of modern adhesive restorative materials, which reduced the onus on mechanical retention for cavity tooth preparation, has prompted a re-emergence of air-abrasion in dentistry (Hedge and Khataavkar, 2010; Sambashiva *et al.*, 2011; Arora *et al.*, 2012). Thus, air-abrasion technology has been harnessed as part of

a drive towards more conservative cavity tooth preparation in recent years (Sambashiva *et al.*, 2011; Arora *et al.*, 2012).

2.13.2. Air-abrasion: Theory and Practice

Generally, air-abrasion devices are usually composed of a cart, table top and handheld models. Some of these devices have built-in additional features, such as a compressor, water spray and evacuation system. Operators can control these devices either mechanically or digitally (Sambashiva *et al.*, 2011; Arora *et al.*, 2012). In the current study, the Velopex Aquacut Quattro™ air-abrasion system is being used (Figure 2.13). The table top part of this machine consists of twin chambers and keys to manually control air pressure, powder flow rate and water supply.

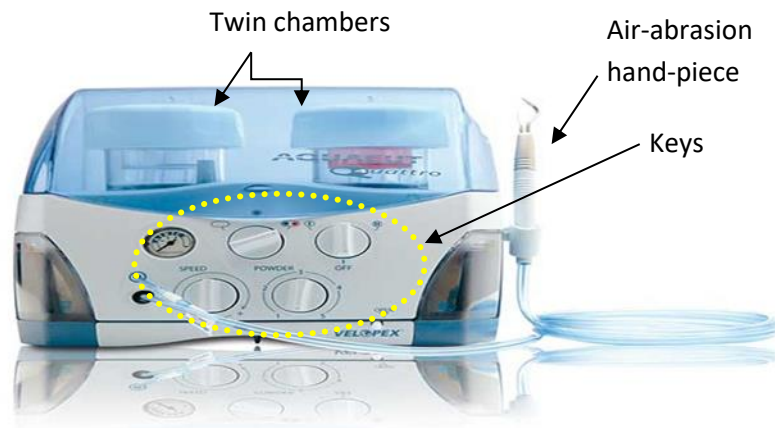


Figure 2.13. Velopex Aquacut Quattro™ air-abrasion system

Air-abrasion utilises kinetic energy allowing the dental operator to propel a stream of abrasive powder particles using either compressed air or gas at high pressure and velocity on a specific area of the tooth. The particles are either sodium bicarbonate, aluminium oxide or bioactive glass powder 45S5 (Sylc™) (Hedge and Khatavkar, 2010).

Bioactive glass powder (45S5) propelled from this device has been shown to have a sustained desensitising and whitening effect (Banerjee *et al.*, 2010). It was tolerated better and had improved handling properties for professional dental stain removal

compared with sodium bicarbonate powders (Banerjee *et al.*, 2010) based on 25 patients using a double-blind, split-mouth model and a Dentsply Cavitron Jet air-polishing device (Dentsply, USA). In addition, this glass powder has the potential to selectively remove more carious enamel tooth surface than intact enamel tooth surface because of its lower hardness (458 VHN= 4.49GPa) compared to that of aluminium oxide powder (2300VHN=22.56GPa), minimising its abrasive effect on the intact enamel surface (hardness 3.5GPa) (Banerjee *et al.*, 2008; 2011). Furthermore, bioactive glass powder (45S5) has the potential to remineralise WSLs as reported by Milly *et al.* (2014b). Consequently, compared to propulsion of aluminium oxide, bioactive glass powder (45S5) propelled *via* air-abrasion machine (Aquacut™, Velopex, Harlesden, UK) is a more conservative cutting method.

The mode of action of the air-abrasion system depends on the kinetic energy (E) of the abrasive powder particles, calculated using equation 1.5:

$$E = \frac{1}{2} MV^2 \quad (1.5)$$

Where M represents the mass of abrasive powder particles and V represents their velocity.

This equation emphasises the fact that the cutting ability of air-abrasion relies on the energy of mass in motion rather than on the friction as in conventional drilling methods. When the abrasive powder particles strike a surface rapidly, most of their energy will transfer to that surface and if the latter is hard it will result in the removal of small amounts of that surface. Conversely, if the surface is soft, the energy is mostly absorbed and the abrasive particles bounce off (Sambashiva *et al.*, 2011; Arora *et al.*, 2012). A range of variables may affect cutting efficiency with air-abrasion systems. These include (Hedge and Khatavkar, 2010; Sambashiva *et al.*, 2011; Arora *et al.*, 2012):

- i) Hardness of the tissue or material being exposed to a stream of abrasive powder particles
- ii) Hardness of the propelled powder particles
- iii) Air pressure level
- iv) Shape and size of powder particles
- v) Powder particle flow rate

- vi) Diameter and angle of nozzle tip
- vii) Operating distance from the tooth surface

In an *in vitro* study, Santos-Pinto *et al.* (2001) found that propelling 27 μ m aluminium oxide particles by an air-abrasion machine (PrepStar, Danville Eng, San Ramon, CA, USA) with an 80° angle nozzle tip produced narrow, deep cuts and a 45° angle nozzle tip produced shallow cavities, while using 0.38 or 0.48 mm inner tip diameters. In addition, in an *in vitro* study, Paolinelis *et al.* (2009) examined the cutting rate of the air-abrasion technique using aluminium oxide (particle size 27 μ m) and Abradent™ air-abrasion machine (Crystalmark, CA, USA). The authors found the following: i) increasing the propellant pressure (20, 40, 60, 80, and 100 (psi) pounds per square inch) caused an almost linear increase in the cutting rate, ii) increasing the powder flow rate (0.5, 1, 1.5, 2, 2.5, and 3 g/minute) caused an increase in the cutting rate but with different patterns for different propellant pressures, iii) the 60° and 75° nozzle angles produced the highest cutting rates for static and dynamic cutting, respectively, whilst 45° and 90° nozzle angles produced lower cutting rates using different operating distances (1, 2, 3, 4, 5 and 6 mm). The authors suggested that using 60 psi at 5mm from the enamel surface at a flow rate of 2.5g/minute produced the highest cutting efficiency. Furthermore, in an *in vitro* study Farooq *et al.* (2013) reported that using a bioactive glass powder with a specific formulation with decreased sodium content (in exchange for calcium) resulted in an increase in the hardness of the glass powder, which significantly decreased the cutting time of the glass powder propelled *via* Velopex™ air-abrasion machine.

To maximise the cutting efficiency, it was demonstrated that using air-abrasive powder particles harder than the target surface lead to abrasion (Horiguchi *et al.*, 1998). The latter study, for example, demonstrated the possibility of selective caries removal using air-abrasion. Four types of air-abrasive (alumina powder, glass beads, crashed glass powder and crushed polycarbonate resin) were propelled *via* an air-abrasion machine (Heraeus, Hanau, Germany) on intact human enamel, dentine, and demineralised dentine (caries-model dentine). Alumina was shown to remove more intact enamel and dentine rather than just carious dentine than was found with alternatives because of its high hardness (2300VHN) compared to the other powders (550VHN) and polycarbonate resin (50VHN). In addition, the angular crashed glass powder removed

more intact enamel and dentine surface without having better efficiency in terms of caries removal compared with the spherical glass beads in spite of similar hardness. As such, angular particles can penetrate deeper in the caries tissues, where some of their kinetic energy may be lost by the cushioning effect between angular particles and soft carious dentine. Increasing the particle size of both alumina and crushed glass powders increased the amount of intact enamel and dentine removed due to a commensurate increase in kinetic energy, which is proportional with the mass of these particles. Conversely, the spherical glass particles removed more carious dentine than intact enamel and dentine. These particles cannot penetrate deep into carious dentine because of its smooth surface; hence, their energy leads preferentially to deformation and destruction of carious dentine. Furthermore, crushed polycarbonate resin was the only air-abrasive powder that selectively removed the carious dentine without damaging intact enamel and dentine due its lower hardness, which was similar to that of intact enamel and dentine.

Another interesting previous observation reported by Milly *et al.* (2014a) was that propelling the glass powder *via* air-abrasion machine (Aquacut™, Velopex, Harlesden, UK) with a curtain of water did not affect either the cutting efficiency or the cutting pattern, since no significant differences were observed between the wet and dry air-abrasion systems. In addition, increasing the operating distance between the nozzle tip and the target surface resulted in an increase the cutting surface area and *vice versa* (Peruchi *et al.*, 2002). It therefore appears that the hardness, size and shape of propelled abrasives, allied to operating parameters may have a bearing on the efficiency and safety of removal of dental materials and other substrates.

2.13.3. Advantages of air-abrasion

Air-abrasion is regarded as a minimally invasive procedure preserving tooth structure without any apparent damage such as cracking, chipping and micro fractures, which are evident with conventional drilling methods. Laurell *et al.* (1995), in an *in vitro* study, used scanning electron microscopy to compare the effects of two techniques in preparing Class V buccal cavities on 28 extracted teeth. The authors revealed that high-speed carbide burs at 400,000 rpm (round per minute) showed sharp line angles,

chipping of the cavosurface margin, and striated internal surfaces, whereas air-abrasion (using aluminium oxide particles) had rounded cavosurface margins and internal line angles.

The aforementioned findings have been confirmed by Mhatre *et al.* (2015), in an *in vitro* study. They reported that the enamel surface roughness, after removal of orthodontic composite remnants (Transbond™ and Heliosit™), by the intraoral sandblasting technique was less (2.14µm and 2.63µm, respectively) than with the carbide bur technique (3.54µm and 3.81µm, respectively), based on data recorded using three-dimensional surface profilometer and SEM. However, Kim *et al.* (2007) found that there were no significant differences in the overall average roughness arising with sandblasting and carbide bur technique based on profilometer data. This might be due to the differences in the type of adhesive material, the remnant removal procedures, and the forces used for debonding the bracket in each study. Consequently, further standardisation of debonding procedure is required to achieve reliable results with respect to the amount of remnants for each composite resin.

Interestingly, air-abrasion is typically used without the need for local anaesthesia and does not involve any noise or vibrations, which can be disconcerting for children and anxious patients. Rafique *et al.* (2003) reported on their clinical trial with 22 patients that 75% participants were happy with Carisolv™ gel and all aspects of the air-abrasion technique including dust, pain/discomfort and vibrations produced, compared with local anaesthesia and conventional rotary methods. Also, 91% of participants expressed some level of anxiety with conventional rotary methods. In addition, air-abrasion can be applied to more than one tooth during a single visit and this could save serviceable time in the dental clinic (Sambashiva *et al.*, 2011; Arora *et al.*, 2012). Moreover, in an *in vitro* study, Cook *et al.* (2001) referred to Black's (1950) study, which demonstrated that low (around 2°C) temperature changes occurred while using air-abrasion. Lloyd *et al.* (1976) reported that very high (around 300°C-400°C) temperature changes occurred with conventional drilling, thus posing a risk of damage to the surrounding tissues. These findings are consistent with a recent *in vitro* study (Kim *et al.* 2007), who used 20 extracted human premolar teeth. They bonded composite resin to the buccal surfaces dividing the teeth into two groups, one for removal of resin with sandblasting and low speed hand-piece (100-40.000rpm) and the other with tungsten carbide burs,

respectively. The pulpal temperature was more elevated with tungsten carbide burs compared with sandblasting.

2.13.4. Limitations of air-abrasion

Air-abrasion cannot be used to prepare the tooth prior to placement of metallic restorations or for their removal (OSHA regulation, 2007; Hedge and Khatavkar, 2010). There is loss of tactile sensation in comparison to a conventional rotary bur. This may be problematic, risking either over-preparation of the cavity or insufficient caries removal (Sambashiva *et al.*, 2011; Arora *et al.*, 2012).

Cook *et al.* (2001), in an *in vitro* study using real-time confocal imaging reported that air-abrasion with aluminium oxide (27 μ m) cut the deeper sound dentine layer faster than the carious dentine. However, Motisuki *et al.*, (2006) who used three different aluminium oxide particle sizes (27, 50 and 125 μ m) demonstrated that 27 μ m and 50 μ m particle sizes removed less sound dentine than the 125 μ m particles. This finding was confirmed by another *in vitro* study (Horiguchi *et al.* 1998) where increasing the particle size of aluminium oxide produced an increase in the cutting rates. These variations may be attributed to the differences in the operating distance and air pressure used, which influence the kinetic energy of the particles. The use of a different model of artificial caries might also affect the cutting rate.

Furthermore, air-abrasion cannot remove soft carious dentine, in spite of its efficiency in cutting hard tissues with aluminium oxide and glass powder (45S5) removing more intact dentine than carious model dentine (Horiguchi *et al.*, 1998). These results were confirmed by Paolinelis *et al.* (2008), who demonstrated in an *in vitro* study that Bioglass, 45S5 removed healthy dentine at a higher rate than carious dentine. This cutting inefficiency might be due to loss of kinetic energy of the abrasive particles during their penetration into the carious surface because of the cushioning effect between the particles and carious surface.

Air-abrasion method using bioactive glass 45S5 shows promise for removing residual adhesives after bracket debonding and potentially in the treatment of WSLs. However,

some of its properties need to be improved by designing a bioactive glass with hardness lower than that of enamel but harder than that of orthodontic adhesives. Consequently, this novel glass material would selectively remove residual adhesives without damaging the enamel surface. Moreover, it might have the potential to promote WSL remineralisation without inducing enamel roughness. These two areas will be explored further in the present research.

3. A SYSTEMATIC REVIEW OF THE EFFECT OF BIOACTIVE GLASSES ON ENAMEL REMINERALISATION (See Appendix 1)

3.1. Objectives

The purpose of this systematic review is to evaluate the effectiveness of bioactive glasses in promoting enamel remineralisation based on *in vivo* and *in vitro* research.

3.2. Materials and methods

3.2.1. Search strategy for identification of studies

This systematic review was conducted in accordance with the PRISMA guidelines (Moher *et al.*, 2009) based on a pre-defined, unpublished protocol. The research question was: How effective are bioactive glasses in inducing enamel remineralisation in comparison to placebo or other topical treatments. The following selection criteria were applied:

Participants: Prospective clinical studies including randomised and non-randomised designs. *In vitro* studies involving assessment of enamel demineralisation utilising human teeth were also to be included.

Interventions: Use of bioactive glasses in any formulation.

Comparators: Untreated control or alternative intervention to address enamel demineralisation including fluoride and casein phosphopeptide-amorphous calcium phosphate (CPP-ACP).

Outcomes: Clinical and *in vitro* measures of enamel remineralisation.

A comprehensive literature search was performed without language or date restrictions. The following databases were screened: PubMed/Medline (PubMed, www.ncbi.nlm.nih.gov), EMBASE via OVID, the Cochrane Oral Health Group's Trials Register (February, 2017), the Cochrane Central Register of Controlled Trials (CENTRAL The Cochrane Library Issue 1, 2017), Literature in the Health Sciences in Latin America and

Systematic Review

the Caribbean (LILACS, February 2017). Unpublished literatures were searched using ClinicalTrials.gov (www.clinicaltrials.gov) and the National Research Register (www.controlled-trials.com) using the terms 'dental' and 'dentistry'. After identifying the potential eligible studies in the above databases, these studies were imported into Endnote X7 software (Thompson Reuters, Philadelphia, PA, USA) to remove duplicates. In addition, the reference lists of included studies were assessed to identify further potentially eligible studies.

3.2.2. Study selection

The titles and abstracts of all articles identified by the electronic search were read and assessed by two authors (AT, PSF). The full text article was retrieved if the title and abstract were deemed ambiguous or when no abstract was available. All studies, which unrelated to bioactive glasses or enamel remineralisation, were excluded initially on the basis of the titles and abstracts of these studies.

3.2.3. Data extraction

One author (AT) extracted the data using a pre-piloted data collection form, and a second author (PSF) verified data extraction independently for completeness and accuracy. Data obtained included number of teeth used, tooth type, demineralisation protocol, remineralisation procedures and control conditions; and approach to outcome analysis. Any potential conflict was resolved by joint discussion between the two authors.

3.2.4. Study quality assessment

The methodological quality of each included study was assessed independently by two authors (AT, PSF). If randomised studies were identified, the risk of bias was to be assessed using the Cochrane risk of bias tool with ROBINS-I used for non-randomised interventional designs. The methodological quality of the *in vitro* studies was to be evaluated using an accepted quality assessment tool for dental *in vitro* studies (Sarkis-Onofre *et al.*, 2014; da Rosa *et al.*, 2015). Specifically, studies were evaluated according to the description of randomisation of teeth, presence of caries, blinding of

Systematic Review

the examiner, statistical analysis, the presence of a control group, sample preparation, outcome measures used and sample size calculation. Where the parameter was reported clearly the domain was scored as “Yes”. If it was not possible to find the information, it was graded as “No”. Studies that reported one to three items were classified as having a low methodological quality, four or five items as medium methodological quality and six to eight items as having high methodological quality.

Meta-analysis was to be considered if sufficient studies of high or moderate methodological quality with clinical homogeneity existed. Statistical heterogeneity was to be assessed using a chi-squared test and quantified on the basis of an I-squared statistic. The existence of publication bias was to be assessed if sufficient (>10) clinical studies were included within a meta-analysis.

3.3. Results

3.3.1. Study selection and characteristics

A total of 116 potentially relevant records were identified from the database search (Figure 3.1). After the removal of duplicates, 86 records were examined; 72 studies were excluded because they did not meet the eligibility criteria and 14 full-texts were assessed. Of the 14 studies retained for detailed full-text review, 3 were excluded- one review article and two *in vitro* studies involved bovine tooth samples. A total of 11 studies were included in this review. No clinical studies were identified; therefore, all included studies were laboratory-based. The characteristics of the included studies are summarised in Table 3.1.

3.3.2. Study quality assessment

Of the 11 *in vitro* studies included, four were deemed to have high and seven medium methodological qualities (Table 3.2). In particular, blinding of the examiner was rarely reported potentially introducing a level of bias within these. In view of the lack of overlapping clinical studies, meta-analysis was not considered appropriate.

Systematic Review

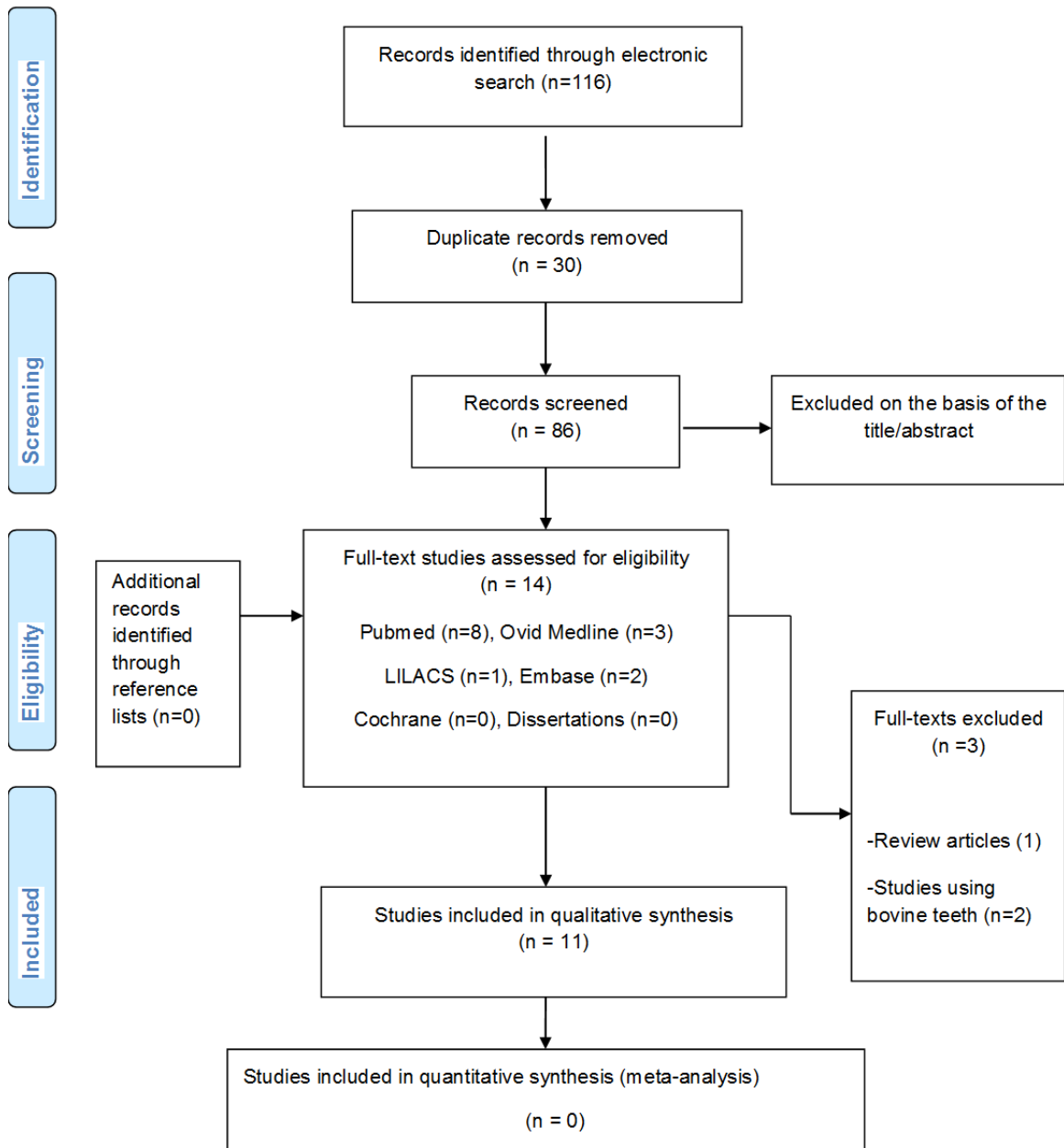


Figure 3.1. Flowchart of article retrieval

Systematic Review

Table 3.1. Characteristics of the studies included in the review

Authors	Total number of samples	Human tooth type	Sample type	Demineralisation protocol	Remineralisation protocol/Control conditions	Storage	Outcome/Analysis technique
Bakry <i>et al.</i> (2014a)	100	Third molars	Flat enamel discs	Orange juice (pH 3.85) for 1 hour at 20°C	<ul style="list-style-type: none"> - Fluoride gel (20mg/g, 9000ppmF, Brand Medico Dental™) applied for 5 minutes then washed with deionised water. - Fluoride gel (20mg/g, 9000ppmF, Brand Medico Dental™) applied for 24 hours then left without washing. - Bioactive glass (Novamin™)- phosphoric acid gel. - Control (untreated). 	Immersed in remineralisation solution (1.5mM CaCl ₂ , 0.9mM NaH ₂ PO ₄ , 0.13M KCl, 5 mM NaN ₃ ; pH 7 using HEPES buffer) for 24 hours	Vickers hardness number (VHN), SEM images, EDX elemental composition
Bakry <i>et al.</i> (2014b)	60	Third molars	Flat enamel blocks	2.2mM/L CaCl ₂ , 2.2mM/L NaH ₂ PO ₄ , 50mM/L acetic acid, pH 4.5) for 4 days	<ul style="list-style-type: none"> - Bioglass (Novamin™) - phosphoric acid gel with no brushing-abrasion - Brushing-abrasion after immersion in remineralising solution for 24 hours with no gel - Both bioglass (Novamin™)-phosphoric-acid gel + brushing-abrasion after immersion in remineralising solution for 24 hours. - Control: Neither gel nor brushing-abrasion was applied 	-Remineralising solution (1.0mM CaCl ₂ , 3.0mM KH ₂ PO ₄ , 100mM acetate, 100mM NaCl, 0.02%, NaN ₃ ; pH 6.3) for 24 hours, 7 days and 14 days	SEM images, XRD

Systematic Review

Table 3.1. Characteristics of the studies included in the review (continued)

Authors	Total number of samples	Human tooth type	Sample type	Demineralisation protocol	Remineralisation protocol/Control conditions	Storage	Outcome/Analysis technique
Gjorgievska <i>et al.</i> (2013)	Not specified	Molars	Enamel tooth surface	6% hydroxyl-ethyl cellulose, 0.1mol/L lactic acid, and 1.0mol/L NaOH (pH 4.5) for 24 hours	<ul style="list-style-type: none"> - Mirasensitive hap+ tooth paste (containing hydroxyapatite) applied for 1 minute and then cleaned with a toothbrush for 5 minutes under copious water spray. - Mirawhite® tc toothpaste (containing bioglass 45S5) applied for 1 minute and then cleaned with a tooth brush for 5 minutes under copious water spray. - Sensodyne® toothpaste applied for 1 minute and then cleaned with a toothbrush for 5 minutes under copious water spray. 	-	SEM images, EDX elemental composition, 3D Stereo-Photograph images
Kohda <i>et al.</i> (2015)	120	Premolars	Enamel tooth surface after bracket bonding with 4-methacryloxyethyl trimellitic anhydride/methyl methacrylate-tri-n-butyl borane (4META/MMA-TBB)-based resin containing various amounts (0–50%) of bioactive glass.	2 ml of demineralising solution (2mM calcium chloride and 2mM sodium dihydrogen phosphate, with 50mM acetic acid added to pH 4.55) for 4 hours at 37°C followed by remineralisation. This cycle was repeated daily for 14 days.	2ml of remineralising solution (2mM CaCl ₂ and 2mM NaH ₂ PO ₄ with 0.1M of NaOH added to pH 6.8) for 20 hours at 37°C	-	Berkovich hardness measurements

Systematic Review

Table 3.1. Characteristics of the studies included in the review (continued)

Authors	Total number of samples	Human tooth type	Sample type	Demineralisation protocol	Remineralisation protocol/Control conditions	Storage	Outcome/Analysis technique
Manfred <i>et al.</i> (2013)	50	Third molars	Enamel surface with brackets bonded with orthodontic adhesive	pH cycling protocol for 14 days: 40mL of artificial saliva at pH 7.0 [1.5 mmol/L Ca, 0.9 mmol/L PO ₄ , 0.1 5 mol/L KCl, and 20 mmol/L cacodylate buffer) for 18 hours, followed by 6 hours in 40mL of buffered artificial caries challenge solution at pH 4.4 (2.0 mmol/L Ca, 2.0 mmol/L PO ₄ , 0.075 mol/L acetate]. The cycle was repeated 5 days a week, with teeth remaining in artificial saliva at weekends	Four BAG-Bonds (62BAG-Bond, 65BAG-Bond, 81BAG-Bond, and 85BAG-Bond) and Transbond-XT used to bond orthodontic brackets	-	Knoop hardness number (KNH)
Mehta <i>et al.</i> (2014)	30	Premolars	Flat enamel surface	2.2mM calcium chloride, 2.2mM sodium phosphate and 0.05M acetic acid; pH adjusted with 1M potassium hydroxide to 4.4. Demineralisation was performed twice for 3 hours of a day with 2-hour immersion in a remineralising solution in between.	- BAG containing dentifrice (SHY-NM; Group Pharmaceuticals; India) - CPP-ACP(GC tooth mousse Recaldent; GCcorp; Japan) containing dentifrice	-	Vickers hardness number (VHN)

Systematic Review

Table 3.1. Characteristics of the studies included in the review (continued)

Authors	Total number of samples	Human tooth type	Sample type	Demineralisation protocol	Remineralisation protocol/Control conditions	Storage	Outcome/Analysis technique
Milly <i>et al.</i> (2014)	52	Molars	Flat enamel slabs	8% methylcellulose gel buffered with a lactic acid layer (0.1 mol/L, pH 4.6) for 14 days at 37°C	<ul style="list-style-type: none"> -Bioactive glass (Sylc™) slurry prepared with deionised water (L/P ratio of 1 g/m) for 7 days at 37°C. -Polyacrylic acid-modified bioactive glass paste prepared with deionised for 7 days at 37°C. water (L/P ratio of 1 g/m) - Remineralisation solution 20 mM Hepes, 130mMKCl, 1.5mM CaCl₂ and 0.9mM KH₂PO₄ (adjusted to pH 7.0 with KOH). - Deionised water. 	-	SEM images, Knoop hardness Number (KHN), Micro-Raman spectroscopy grey-scale images, surface roughness using non-contact profilometer
Milly <i>et al.</i> (2015)	90	Molars	Flat enamel slabs	8% methylcellulose gel buffered with a lactic acid layer (0.1 mol/L, pH 4.6) for 14 days at 37°C, followed by surface conditioning via propelling polyacrylic acid-bioactive glass (45S5) powder using air-abrasion for 10 seconds	<ul style="list-style-type: none"> - Bioactive glass (45S5) slurry prepared with de-ionised water (L/P ratio of 1 g/m) twice daily for 5 minutes for 21 days at 37°C. -Polyacrylic acid-modified bioactive glass (BAG-PAA) paste prepared with deionised applied twice daily for 5 minutes for 21 days at 37°C. 	-	Surface roughness using non-contact profilometer, Knoop hardness number (KHN), intensity of light backscattering using OCT, Raman spectroscopy grey-scale images, SEM images, EDX elemental composition

Systematic Review

Table 3.1. Characteristics of the studies included in the review (continued)

Authors	Total number of samples	Human tooth type	Sample type	Demineralisation protocol	Remineralisation protocol/Control conditions	Storage	Outcome/Analysis technique
Narayana <i>et al.</i> (2014)	20	Molars	Enamel tooth surface	- pH cycling for 7 days involving immersion in demineralisation solution [2mM $\text{Ca}(\text{NO}_3)_2 \cdot 4\text{H}_2\text{O}$, 2mM $\text{NaH}_2\text{PO}_4 \cdot 2\text{H}_2\text{O}$, 0.075mM acetate buffer for 5 days, followed by 0.02ppm F (pH 4.7) for 6hours and in remineralised solution (1.5mM $\text{Ca}(\text{NO}_3)_2 \cdot 4\text{H}_2\text{O}$, 0.9mM $\text{NaH}_2\text{PO}_4 \cdot 2\text{H}_2\text{O}$, 150mM KCl, 0.1 mol/l Tris buffer, 0.03 ppm F pH 7] for 18 hours. Samples were maintained only in the remineralised solution for the last 2 days.	- Bioactive glass (Novamin™) for 10 minutes - Fluoride toothpaste (Amflor) for 10 minutes - CPP-ACP (Tooth mousse) for 10 minutes - CPP-ACPF (Tooth mousse plus) for 10 minutes - Control (untreated)	Artificial saliva at 37°C for 10 days	SEM images, EDX elemental composition
Palaniswamy <i>et al.</i> (2016)	20	Premolars	Enamel tooth surface	37% phosphoric acid for 20 minutes	- ACP-CPP (GC Tooth Mousse, Recaldent; GC Corp.; Japan) for 3 minutes - BAG (Novamin, Sensodyne Repair and Protect; GlaxoSmithKline; UK) for 1 minute - 37% phosphoric acid; Ivoclar Vivadent, - Natural saliva, - Deionised water.	Artificial saliva for 10 days, and then 15 days	Vickers hardness number (VHN)

Systematic Review

Table 3.1. Characteristics of the studies included in the review (continued)

Authors	Total number of samples	Human tooth type	Sample type	Demineralisation protocol	Remineralisation protocol/Control conditions	Storage	Outcome/Analysis technique
Pulido <i>et al.</i> (2012)	10	Molars	Enamel tooth surface	8% methylcellulose aqueous solution (1500cP, 63 kDa) with an equal volume of 0.1 mol/L of lactic acid, with an adjusted pH with KOH at 4.6 a 37°C for a 5-day period	<ul style="list-style-type: none"> - Bioactive glass (VBio): Biogran® (Biomet 3i™) at a 5 weight% concentration twice daily 2 for 15 days - Stannous fluoride Gel Kam (Colgate Palmolive®) 0.4% twice daily for 15 days 		SEM images, EDX elemental composition

Systematic Review

Table 3.2. Methodological quality of the included studies (Sarkis-Onofre *et al.*, 2014; da Rosa *et al.*, 2015)

Study	Teeth randomisation	Free of caries	Control group	Blinding of the examiner	Statistical analysis carried out	Presence of outcomes	Sample preparation	Sample size calculation	Methodological quality
Bakry <i>et al.</i> (2014a)	Yes	Yes	Yes	No	Yes	Yes	Yes	Yes	High
Bakry <i>et al.</i> (2014b)	Yes	Yes	Yes	No	Yes	Yes	Yes	Yes	High
Gjorgievska <i>et al.</i> (2013)	Yes	Yes	No	No	Yes	Yes	Yes	No	Medium
Kohda <i>et al.</i> (2015)	No	Yes	Yes	No	Yes	Yes	Yes	Yes	Medium
Manfred <i>et al.</i> (2013)	No	Yes	No	No	Yes	Yes	Yes	Yes	Medium
Mehta <i>et al.</i> (2014)	Yes	Yes	No	No	Yes	Yes	Yes	Yes	Medium
Milly <i>et al.</i> (2014)	Yes	Yes	Yes	No	Yes	Yes	Yes	Yes	High
Milly <i>et al.</i> (2015)	Yes	Yes	Yes	No	Yes	Yes	Yes	Yes	High
Narayana <i>et al.</i> (2014)	No	Yes	Yes	No	Yes	Yes	Yes	Yes	Medium
Palaniswamy <i>et al.</i> (2016)	No	Yes	Yes	No	Yes	Yes	Yes	Yes	Medium
Pulido <i>et al.</i> (2012)	No	Yes	Yes	No	Yes	Yes	Yes	Yes	Medium

3.3.3. Results of individual studies

Considerable methodological variation existed in the included studies with different demineralisation protocols followed including use of orange juice (Bakry *et al.*, 2014a), phosphoric acid (Palaniswamy *et al.*, 2016), acetic acid (Bakry *et al.*, 2014b; Mehta *et al.*, 2014; Koda *et al.*, 2015), methylcellulose gel (Pulido *et al.*, 2012; Milly *et al.*, 2014b; Milly *et al.*, 2015), and hydroxyethyl cellulose gel protocols (Gjorgievska *et al.*, 2013; Manfred *et al.*, 2013; Narayana *et al.*, 2014;). In addition, various types of bioactive glass were used e.g. Novamin™ and Sylc™ using different modes of application such as pastes, gels, slurries, and orthodontic adhesives. Bioactive glass as a gel mixed with phosphoric acid was used in 2 studies (Bakry *et al.*, 2014a ; Bakry *et al.*, 2014b), while bioactive glass-impregnated toothpaste was used in 6 studies: Mirawhite® TC toothpaste (Gjorgievska *et al.*, 2013), SHY-NM d (Mehta *et al.*, 2014), Polyacrylic acid-modified bioactive glass paste (Milly *et al.*, 2014b), or the latter after enamel pre-conditioning with air-abrasion (Milly *et al.*, 2015), Novamin™ toothpaste (Narayana *et al.*, 2014), Novamin™, Sensodyne Repair and Protect (Palaniswamy *et al.*, 2016), VBio (Biomet 3i™) (Pulido *et al.*, 2012). The glass was used as a slurry after enamel pre-conditioning with air-abrasion in one *in vitro* study (Milly *et al.*, 2015), and incorporated within orthodontic adhesives in two studies (Manfred *et al.*, 2013; Koda *et al.*, 2015).

Furthermore, bioactive glasses were applied for very variable lengths of time and held in different solutions to induce its potential remineralisation within these experimental models. Two studies involved topical application of bioactive glass (Novamin™)-phosphoric acid gel on enamel discs/blocks for 24 hours (Bakry *et al.*, 2014a; Bakry *et al.*, 2014b). These discs were immersed in remineralising solution during the application time, while Novamin™ tooth paste was applied to the enamel surface for 10 minutes followed by immersion in artificial saliva for 10 days in one study (Narayana *et al.*, 2014). Immersion in artificial saliva was also performed for 10 days followed by 5 more days in another study after application of Novamin™, Sensodyne Repair and Protect toothpaste on the enamel for just 1 minute (Palaniswamy *et al.*, 2016). However, the other included studies did not use any storage solution (Pulido *et al.*, 2012; Gjorgievska *et al.*, 2013; Manfred *et al.*, 2013; Mehta *et al.*, 2014; Milly *et al.*, 2014b; Koda *et al.*, 2015; Milly *et al.*, 2015).

Systematic Review

Different assessment techniques were also used. Scanning electron microscopy (SEM) was used to examine the morphological changes of the enamel surface by imaging (Pulido *et al.*, 2012; Gjorgievska *et al.*, 2013; Bakry *et al.*, 2014a; Bakry *et al.*, 2014b; Milly *et al.*, 2014b; Narayana *et al.*, 2014; Milly *et al.*, 2015). Energy dispersive x-ray spectroscopy (EDX) was undertaken to obtain information on the elemental composition of the enamel in 4 studies (Pulido *et al.*, 2012; Gjorgievska *et al.*, 2013; Bakry *et al.*, 2014a; Narayana *et al.*, 2014; Milly *et al.*, 2015). X-ray diffraction (XRD) was also used to detect the formation of apatite crystals (Bakry *et al.*, 2014b). 3D stereo-photograph (anaglyphs) was used in a single study to evaluate topographical changes in detail. Hardness testing involving a Berkovich hardness tester to measure Berkovich hardness was used in a single study (Koda *et al.*, 2015), while Knoop hardness was assessed more commonly (Manfred *et al.*, 2013; Milly *et al.*, 2014b; Milly *et al.*, 2015) as was Vickers hardness (Bakry *et al.*, 2014b; Mehta *et al.*, 2014; Palaniswamy *et al.*, 2016). Raman spectroscopy to evaluate phosphate peak intensity, coupled with non-contact profilometer to assess the enamel surface roughness and optical coherence tomography (OCT) to measure intensity of light backscattering from the enamel were undertaken in 2 studies (Milly *et al.*, 2014b; Milly *et al.*, 2015).

The findings from these studies are summarised in Table 3.3. All studies demonstrated the potential efficacy of bioactive glasses in inducing enamel remineralisation, irrespective of the mode of delivery, when comparing with control conditions and other topical remineralising treatments. Specifically, improved mechanical properties (hardness) of the enamel (Manfred *et al.*, 2013; Bakry *et al.*, 2014a; Mehta *et al.*, 2014; Milly *et al.*, 2014b; Koda *et al.*, 2015; Milly *et al.*, 2015; Palaniswamy *et al.*, 2016) and formation of mineral deposits acting as a protective layer on the enamel surface were repeatedly shown (Pulido *et al.*, 2012; Gjorgievska *et al.*, 2013; Bakry *et al.*, 2014a ; Bakry *et al.*, 2014b; Milly *et al.*, 2014b; Narayana *et al.*, 2014; Milly *et al.*, 2015). This protective layer was rich in calcium and phosphate content (Pulido *et al.*, 2012; Gjorgievska *et al.*, 2013; Bakry *et al.*, 2014a; Narayana *et al.*, 2014; Milly *et al.*, 2015), and was shown to have the same crystalline pattern as the natural enamel hydroxyapatites (Bakry *et al.*, 2014b). Furthermore, the phosphate content of the newly-formed protective layer was high compared to the demineralised enamel (Milly *et al.*, 2014b; Milly *et al.*, 2015). Reduction in the intensity of the light backscattering from the remineralised enamel surface was also observed compared to demineralised enamel

Systematic Review

(Milly *et al.*, 2014b; Milly *et al.*, 2015). However, one study reported an increase in the enamel surface roughness after use of a bioactive glass. This involved treatment of the demineralised enamel with a dual approach, which included the propulsion of a mixed powder comprising of polyacrylic acid and bioactive glass (Sylc™) *via* air-abrasion before applying the glass in the form of slurry and paste (Milly *et al.*, 2015).

Table 3.3. Summary of results from the included studies

Study	Summary of results
Bakry <i>et al.</i> (2014a)	Bioactive glass application significantly improved the enamel lesions when compared to fluoride gel and control samples. This was observed by the formation of a mineral layer on the enamel, rich with calcium, phosphate, and silica, associated with an increase in its enamel hardness.
Bakry <i>et al.</i> (2014b)	The applied bioactive glass gel was able to form a brushite layer within 24 hours. This layer showed resistance to abrasion and transformed to hydroxyapatite crystals after 14 days of storage
Gjorgievska <i>et al.</i> (2013)	The bioactive glass-containing toothpaste was highly efficient in promoting enamel remineralisation by formation of deposits and a protective layer on the demineralised surface in comparison with other approaches
Kohda <i>et al.</i> (2015)	Bioactive glass containing 4META/MMA-TBB-based resin showed potential enamel remineralisation inferred from improved mechanical properties (hardness) of the enamel surface surrounding brackets.
Manfred <i>et al.</i> (2013)	All tested bioactive glass-containing orthodontic adhesives outperformed the traditional adhesive Transbond XT by maintaining enamel hardness surrounding the brackets
Mehta <i>et al.</i> (2014)	Bioactive glass-containing dentifrice was more effective in remineralising enamel lesions relative to CPP-ACP based on enamel hardness.
Milly <i>et al.</i> (2014b)	Both bioactive glass slurry and polyacrylic acid-modified bioactive glass paste enhanced enamel remineralisation, based on hardness results, with higher phosphate content and mineral deposits within the artificial lesions.
Milly <i>et al.</i> (2015)	Pre-conditioning of the lesion surface using BAG-PAA air abrasion enhanced the remineralising potential of slurry and paste, manifesting as increased enamel mineral content and improved mechanical (hardness) properties. However, this was associated with increased enamel surface roughness.
Narayana <i>et al.</i> (2014)	Bioactive glass was considered as an effective remineralising agent.
Palaniswamy <i>et al.</i> (2016)	Bioactive glass toothpaste showed better results than CPP-ACP based on enamel hardness results.
Pulido <i>et al.</i> (2012)	Significant differences observed between fluoride gel (Colgate Palmolive®) and bioactive glass (Biomet 3i™) based on the elemental analysis.

3.4. Discussion

The aim of the current systematic review was to investigate the effect of bioactive glasses on enamel remineralisation. Only eleven studies satisfied the inclusion criteria. In particular, it was disappointing that clinical studies evaluating the relative benefits of these approaches were unavailable. Consequently, only *in vitro* studies were identified highlighting the need for further research and moderating the level of evidence obtained. Notwithstanding this, a plethora of the techniques to assess enamel changes are impossible to undertake clinically and therefore rely on an *ex vivo* setting. As such, while further clinical research is undoubtedly required, the findings from the individual studies indicate that these materials have promise in inducing enamel remineralisation.

Within the identified studies bioactive glasses, regardless of formulation or mode of application technique, were found to be more effective in enamel remineralisation compared to other topical agents such as fluoride and CPP-ACP. This finding was based on a battery of tests including enamel hardness measurements using different hardness testing machines such as Vickers hardness tester, Knoop hardness tester, and Berkovich hardness tester. In addition, routine formation of a protective layer rich in calcium and phosphate content was detected by EDX elemental analysis (Pulido *et al.*, 2012; Gjorgievska *et al.*, 2013; Bakry *et al.*, 2014a; Narayana *et al.*, 2014; Milly *et al.*, 2015), XRD analysis (Bakry *et al.*, 2014b) and Raman-spectroscopy (Milly *et al.*, 2014b; Milly *et al.*, 2015). The consistency of these overall findings lends further evidence to the potential benefit of these approaches.

A reduction in the intensity of the light backscattering from the enamel surface was observed with OCT relative to the demineralised surfaces following use of bioactive glasses (Milly *et al.*, 2014b; Milly *et al.*, 2015). This observation hinges on the inverse relationship between the intensity value of light backscattering and the mineral content within the enamel surface (Jones *et al.*, 2006; Hariri *et al.*, 2012; Kang *et al.*, 2012). Typically, beneficial changes of this nature were not associated with enamel damage. Notwithstanding this, in one study, increased enamel surface roughness was observed. However, the treatment protocol incorporated both propulsion of a mixed powder supplemented with polyacrylic acid and subsequent application of a slurry and paste (Milly *et al.*, 2015). Moreover, this finding may relate to the higher hardness of the

Systematic Review

experimental glass than that of sound enamel (~3.5GPa) (O'Donnell, 2011) with reported values varying between 4.5GPa (Cook *et al.*, 2008) and 5.75GPa (Lopez-Esteban *et al.*, 2003). Formulations with lower hardness levels have since been developed; these are likely to be more compatible with enamel integrity.

In view of the inclusion of *in vitro* studies, it is important to highlight that the demineralisation evaluated was invariably artificially-induced with a range of different demineralisation protocols used. It is unclear how well this approach mimics the *in vivo* situation. In addition, bioactive glass, which is made up of amorphous sodium-calcium-phosphosilicate, is a highly reactive material in an aqueous environment such as saliva in the oral cavity. In saliva, sodium ions from the bioactive glass particles readily react with hydrogen cations (in the form of H_3O^+) from saliva inducing the release of calcium and phosphate (PO_4^-) ions from the glass. A localised, transient increase in pH occurs during the initial exposure of the material to saliva due to the release of sodium. This increase in pH helps to precipitate the extra calcium and phosphate ions provided by the bioactive glass material to form a calcium phosphate layer. As these reactions continue, this layer crystallises into hydroxyapatites (Hench, 2006; Jones and Clare, 2012). This means that the composition of the remineralising solution used in *in vitro* studies might affect the bioactivity (the remineralisation potential) of the bioactive glass. As such, salivary substitutes were used in the identified studies in an effort to mimic this effect *in vitro*. Nevertheless, the longer-term effects of bioactive glasses and indeed other demineralisation agents are difficult to assess in the *in vitro* situation. This is an important shortcoming of the *in vitro* studies identified, particularly as demineralisation and white spot lesions, in particular, commonly arise during orthodontic treatment- a process known to take close to 2 years on average (Tsichlaki *et al.*, 2016). However, the clinical relevance of the *ex vivo* data was enhanced by restricting the review to analysis of human teeth only. In particular, studies using bovine teeth were excluded due to the structural difference between human and bovine teeth, such as thicker crystallites, lower fluoride concentration and increased porosities of enamel in bovine teeth. Moreover, the latter are not subjected to the same genetics, as well as environmental and dietary factors as human material and, as such, will behave in a different physical and chemical manner (Mellberg, 1992; Laurance-Young *et al.*, 2011). Notwithstanding, bovine enamel does provide a more similar substrate to human enamel than either ovine or porcine enamel (de Dios Teruel *et al.*, 2015).

Systematic Review

In common with many systematic reviews within dentistry, the present review was hampered by a lack of clinical research studies. Moreover, it was not possible to include any prospective clinical studies. Clearly, further research investigating whether the promise of bioactive glasses highlighted in numerous *in vitro* studies would be reproduced clinically is warranted. It is important that subsequent well-designed parallel-design randomised controlled trials investigate the relative merits of bioactive glasses in various formulations in relation to existing gold standards including both fluoride and CPP-ACP.

3.5. Conclusion

Based on *in vitro* findings in isolation, bioactive glasses appeared capable of enhancing enamel remineralisation more effectively than other topical remineralising materials including fluoride, and CPP-ACP. However, clinical research to investigate their effectiveness is now overdue.

4. AIMS AND OBJECTIVES

4.1. Aims

To design a novel fluoride-containing bioactive glass powder propelled *via* an air-abrasion hand-piece with:

- i) hardness lower than that of enamel but higher than orthodontic adhesives to safely and effectively remove the adhesive without inducing damage to the enamel surface.
- ii) the ability to form fluorapatite instead of hydroxyapatite in order to remineralise artificially-induced white spot lesions leaving the enamel surface more resistant to demineralisation.

4.2. Objectives

- Prepare 45S5 glass as a laboratory analogue to the commercially-available glass (Sylc™) using the melt quench route.
- Prepare and characterise a series of novel glasses with i) molar compositions similar to 45S5/Sylc™ but with constant addition of fluoride, reduced silica, increased sodium and phosphate contents, and ii) lower hardness values in order to have i) enhanced solubility/apatite formation capabilities to facilitate remineralisation, and ii) equivalent adhesive removal characteristics inducing less damage to underlying enamel, to alternative glasses or other methods used in contemporary dental practice.
- Measure the glass transition temperature (T_g) of Sylc™, 45S5 and experimental glasses using Differential Scanning Calorimetry (DSC) in order to subsequently facilitate glass casting by preheating the furnace at the determined T_g for each glass.

Aims & Objectives

- Measure the hardness of 45S5, SylcTM and experimental glass castings using Vickers Hardness testing to select a glass with hardness lower than that of enamel in order to remove the adhesive safely without inducing enamel damage.
- Analyse the particle size distribution within two batches (<38µm and 38-90µm) for all glasses (45S5, SylcTM and experimental glasses) using the Particle Size Distribution Analyser, to manage the production of glass particles with correct size distributions for use in air-abrasion experiments.
- Observe the particle shape of each glass within the 38-90µm batch using Scanning Electron Microscopy (SEM) to ensure the production of glass particles with correct morphology for use in air-abrasion experiments aiding in adhesive removal.
- Calculate the time required to cut a hole within prepared orthodontic adhesive (Transbond XTTM) discs utilising the Velopex Aquacut QuattroTM air-abrasion machine to propel two glasses (the most promising novel experimental glass and the commercially-available SylcTM glass) in order to evaluate their cutting efficiency against each other at various air pressures, powder flow rates and nozzle-tip angles.
- Calculate the amount of the glass propelled per minute with the preferred novel experimental glass and SylcTM using two air-abrasion systems (Velopex Aquacut QuattroTM air-abrasion machine and BA UltimateTM air polisher) in order to detect any difference in the glass powder flow rate between these two air-abrasion systems.
- Compare between three post clean-up methods (tungsten-carbide bur with low speed hand-piece, SylcTM-air-abrasion and the novel experimental glass-air-abrasion) in the removal of two orthodontic adhesives (Transbond XTTM and Fuji Ortho LCTM) in respect of the enamel surface roughness structural changes assessed using non-contact profilometer and SEM, in addition to the time required to remove remnants adhesives.

Aims & Objectives

- Measure the hardness of prepared discs from two orthodontic adhesives (Transbond XT™ and Fuji Ortho LC™) using Vickers Hardness testing machine in order to ensure that the selected novel glass has hardness higher than orthodontic adhesives for facilitating complete adhesive removal.
- Immerse all glasses (45S5, Sylc™ and experimental glasses) in different solutions with pH levels ranging from 5 to 9 in order to observe the dissolution behaviour and the bioactivity of all glasses (their capability to form apatite) utilising Attenuated Total Reflectance-Fourier Transform Infrared Spectrometry (ATR-FTIR), X-Ray Diffraction (XRD) and pH meter.
- Confirm the presence of fluorapatite following the interaction between the glass and the immersion solution using Magic Angle Spinning Nuclear Magnetic Resonance (MAS-NMR) spectroscopy.
- Artificially induce WSLs on extracted human teeth to assess the capability of the most promising experimental glass and commercially-available Sylc™ in remineralising these lesions following glass propulsion *via* the air-abrasion technique. This potential remineralisation would be assessed in respect of: enamel surface roughness using non-contact profilometer, enamel optical changes using Optical Coherence Tomography (OCT), structural changes of the enamel (SEM and Energy Dispersive Spectroscopy) and hardness (Knoop hardness testing machine).

5. MATERIALS AND METHODS

5.1. Overview of the experiments performed

A summary of all experiments undertaken within this research project is given below (Figure 5.1). These experiments were divided into five main parts: i) glass development and characterisation, ii) air-abrasion studies, iii) *in vitro* studies performed with the selected novel glass, iv) Assessment techniques used in *in vitro* studies and v) statistical analysis.

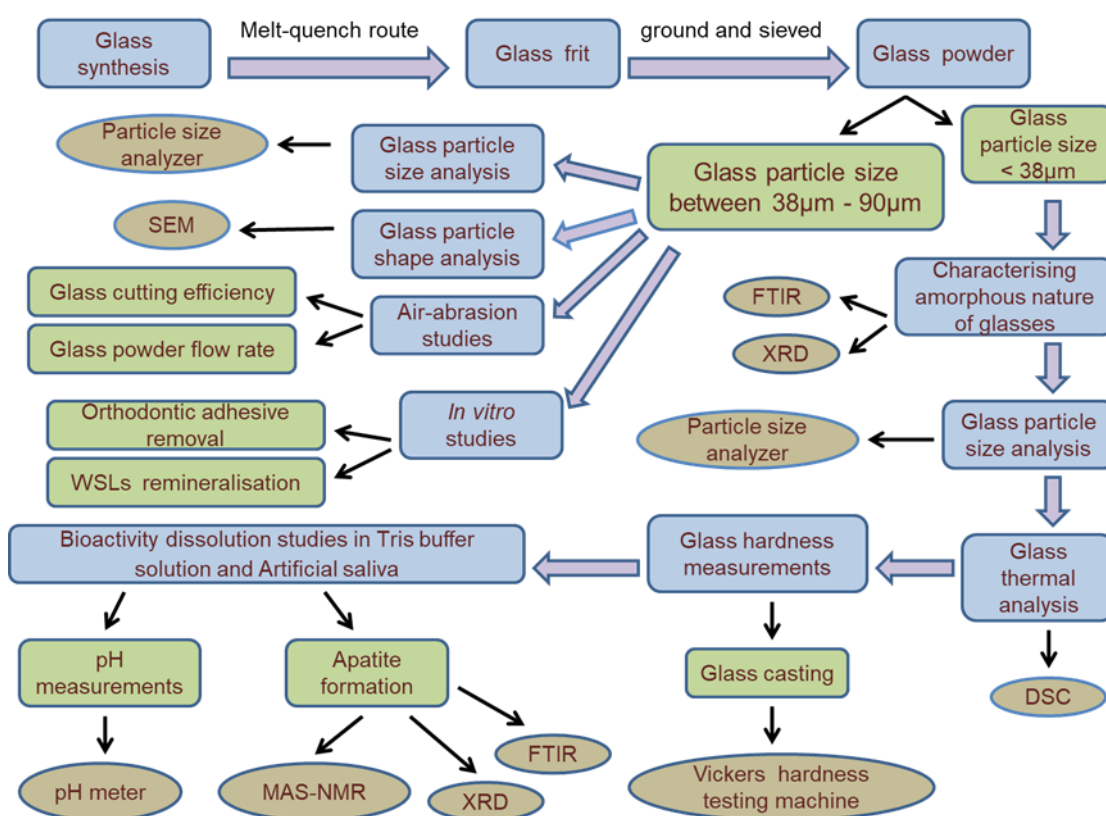


Figure 5.1. Summary of experiments undertaken

5.2. Glass development

5.2.1. Glass design

A bioactive glass (45S5) mirroring the formula of commercially-available 45S5 (Sylc™; Denfotex Research Ltd., London, UK) was prepared by the melt quench route (Table 5.1). Thereafter, a series of novel experimental glasses incorporating $\text{SiO}_2\text{-P}_2\text{O}_5\text{-CaO-Na}_2\text{O-CaF}_2$ was prepared with constant network connectivity (NC~2). Na_2O and CaO were obtained from Na_2CO_3 and CaCO_3 , respectively. The compositions of these experimental glasses were based on the molar composition of the laboratory-prepared 45S5 glass mirroring the commercial one (Sylc™). As such, the laboratory-prepared 45S5 glass was used as a reference in this research. Both the mole percentage (mol%) and the mass (in grams) of laboratory-prepared 45S5 and experimental glasses are shown in Table 5.1 and Table 5.2, respectively. The batch mass was calculated for each glass using equation 1:

$$\text{Batch mass (z)} = (\text{mol\% (z)} \times \text{molecular weight (z)} \times 200) / \text{Total molecular weight of all chemical components of a glass} \dots\dots\dots 1$$

Where z refers to each chemical component (e.g. SiO_2 , P_2O_5 , CaO , Na_2O , CaF_2) incorporated within each glass.

Three design strategies were used to develop a novel glass with improved properties in comparison to those of Sylc™ glass, in order to satisfy the aims of this research. These strategies were derived from the studies of O'Donnell *et al.* (2009), Brauer *et al.* (2010), Mneimne *et al.* (2011), and Farooq *et al.* (2013). They included:

- i) Increasing the sodium oxide (Na_2O) content for the experimental glasses within a range from 20mol% to 40mol% instead of 24.4mol% in 45S5 glass. Therefore, 5mol% of Na_2O was added for every 5%mol of CaO removed, to maintain the same value of network connectivity. This strategy would produce a more disrupted glass network, which requires a lower glass transition temperature (T_g) to form a less rigid glass (of lower hardness) compared to 45S5 and Sylc™, since it was reported that increasing the sodium content in a series of glasses, with a constant network connectivity value close to two, resulted in a linear decrease in the transition temperature (Wallace *et al.*, 1999). In addition, a strong correlation between T_g and

hardness of bioactive glasses has been observed (Farooq *et al.*, 2013). This means that decreasing the T_g of a glass leads to a decrease in its hardness and *vice versa*.

- ii) Increasing the phosphate content in the form of phosphorus pentoxide (P₂O₅) from 2.6mol% in 45S5 to 6.1mol% in the experimental glasses. This was also accompanied by a decrease in silica (SiO₂) content from 46.1mol% in 45S5 to 37mol% for all experimental glasses. This strategy has been used in two studies showing a decrease in the T_gs of bioactive glasses (O'Donnell *et al.*, 2008b), and a decrease in their hardness (Farooq *et al.*, 2013). In addition, an increase in the ability of glass to form apatite was observed when the phosphate content was only increased to approximately 6mol%, combined with a decrease in the silica content at a constant network connectivity (NC~2) (O'Donnell *et al.*, 2009; Mneimne *et al.*, 2011). A further increase in phosphate content inhibited apatite formation as the glass crystallised resulting in retardation of glass dissolution and apatite formation (O'Donnell *et al.*, 2008a).
- iii) Adding a constant ratio of calcium fluoride (3mol% CaF₂) following the same strategy used by Farooq *et al.* (2013) to enhance fluorapatite formation and prevent fluorite development that affects glass dissolution and subsequently apatite formation (Lusvardi *et al.*, 2009; Brauer *et al.*, 2010; Mneimne *et al.*, 2011). In addition, it has been shown that the T_g significantly reduced when fluoride is incorporated in the glass network structure (Hill *et al.*, 1999; Brauer *et al.*, 2009) resulting in a decrease in the hardness of bioactive glasses (Farooq *et al.*, 2013).

5.2.2. Glass frit synthesis

Five novel experimental glasses were synthesised using a melt quench route. Each glass (batch size 200g) was prepared by melting SiO₂ (analytical grade; Prince Minerals Ltd, Stoke-on-Trent, UK), Na₂CO₃, CaCO₃, P₂O₅, and CaF₂ (Sigma-Aldrich, Gillingham, UK) in a platinum-rhodium crucible, in an electric furnace (EHF 17/3, Lenton, UK) for 60 minutes between 1400°C to 1450°C based on the glass composition. A platinum/rhodium crucible was used because it is made from inert materials, thus avoiding its interaction with the final glass product, and it is capable

of withstanding the high furnace temperatures. The resulting molten glass was rapidly quenched in deionised water (DW) to obtain glass frits (~100g), which were collected into a sieve and kept in a vacuum oven (Harvard LTE, UK) to dry at 80°C overnight.

Table 5.1. Design of batch components for each glass (Mol%)

Bioactive glasses	Mol%				
	SiO ₂	Na ₂ CO ₃	CaCO ₃	P ₂ O ₅	CaF ₂
45S5	46.1	24.4	26.9	2.6	—
QMAT1	37	20	33.9	6.1	3
QMAT2	37	25	28.9	6.1	3
QMAT3	37	30	23.9	6.1	3
QMAT4	37	35	18.9	6.1	3
QMAT5	37	40	13.9	6.1	3

Table 5.2. Mass of batch components for each glass (g)

Bioactive glasses	Mass (g)					
	SiO ₂	Na ₂ CO ₃	CaCO ₃	P ₂ O ₅	CaF ₂	Total (g)
45S5	65.81	61.44	63.96	8.77	—	200
QMAT1	50.31	47.98	76.79	19.60	5.30	200
QMAT2	50.14	59.77	65.24	19.53	5.28	200
QMAT3	49.98	71.49	53.78	19.47	5.26	200
QMAT4	49.81	83.13	42.38	19.41	5.24	200
QMAT5	49.65	94.69	31.07	19.34	5.23	200

5.2.3. Glass casting

A glass rod (20mm in diameter) was prepared from each glass batch (45S5, SycTM and all experimental glasses) by re-melting approximately 100g of glass frit, pouring into a graphite mould, and annealing for 1 hour in a preheated furnace at the T_g

determined in section 5.3.2 to ensure slow cooling of the glass during casting. Thereafter, the casted glass was slowly cooled to room temperature overnight in the furnace, which was switched off. The rod from each glass batch was sectioned into approximately 1mm thick discs using a diamond cutting machine (Accutom-5, Struers A/S, Ballerup, Denmark). These discs were subsequently polished with silica carbide grit paper (P1000 in roughness) and wet with acetone (instead of water) to avoid reaction of the glass with water during polishing.

5.2.4. Glass powder preparation

After drying, 100 grams of each glass frit was ground using a vibratory mill (Gy-Ro mill, Glen Creston, London, UK) for one minute to form glass powder, which was then sieved using a vibrating machine (Retsch VS 1000; Figure 5.2) for 10 minutes at an amplitude of 60. The ground powder was vibrated between two stainless steel sieves of mesh sizes 38 μ m and 90 μ m, respectively (Endecotts, Ltd, London, UK). Four rubber balls of 1cm in diameter (Figure 5.3) were placed in each of the two sieves to discourage adherence of glass particles to one another and to encourage more particles to pass through the sieve. After sieving, the glass particles of size fractions between ~38 μ m and 90 μ m in the 38 μ m mesh sieve, and those of a size fraction <38 μ m in the base, were collected and stored in dry re-sealable plastic bags, which were kept in a dry desiccator at room temperature until further use.

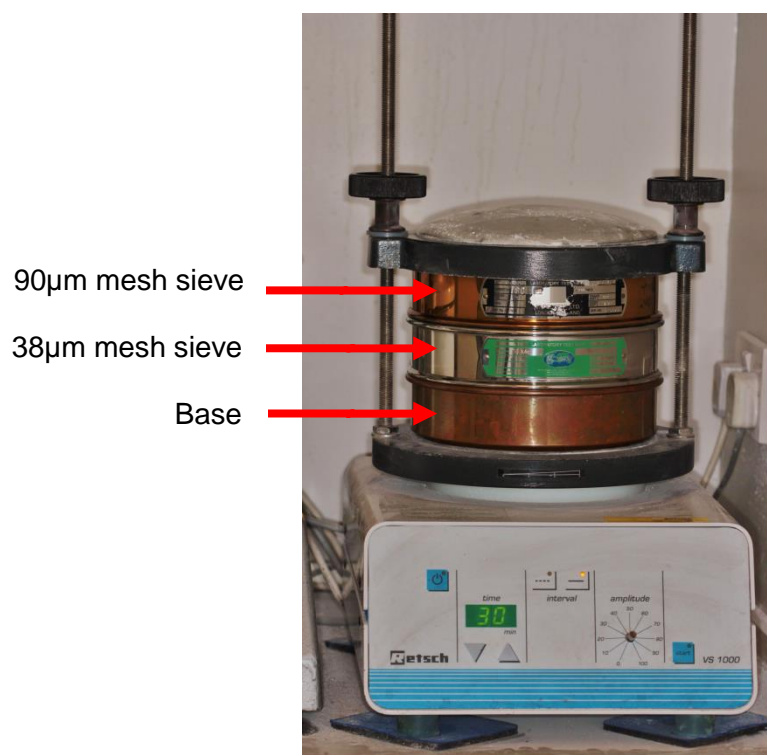


Figure 5.2. Vibrating machine used for sieving



Figure 5.3. Rubber balls used during sieving to refine glass particles

5.3. Glass characterisation studies

The glass particles of $<38\mu\text{m}$ in size were used for the subsequent glass characterisation studies. The rationale for the use of this glass particles size was to maximise efficiency, and to allow comparison with other published work. Moreover, propulsion of larger glass particles ($38\text{--}90\mu\text{m}$) onto the enamel surface would result in them fracturing into smaller particles, many $<38\mu\text{m}$ in size.

5.3.1. Characterising the amorphous nature of glasses

a. Attenuated Total Reflectance-Fourier Transform Infrared Spectroscopy (ATR-FTIR)

ATR-FTIR (Perkin-Elmer, Waltham, USA; Figure 5.4) was used, in the attenuation total reflection mode (described earlier in section 2.12.6), to identify the molecular components and structure for each glass by obtaining information on the vibrational absorbance of the Si-O bond. A preliminary background scan was performed before assessment of the glass powder samples to ensure the accuracy of the device. The data were collected from $1800\text{--}500\text{cm}^{-1}$ in absorbance mode and 10 scans were taken for each glass powder sample (45S5, SylcTM and all experimental glasses; approximately 5mg) to eliminate any noise. The ATR-FTIR spectra were taken prior to commencing biological dissolution studies (untreated glasses) and then after to monitor glass degradation and apatite formation.

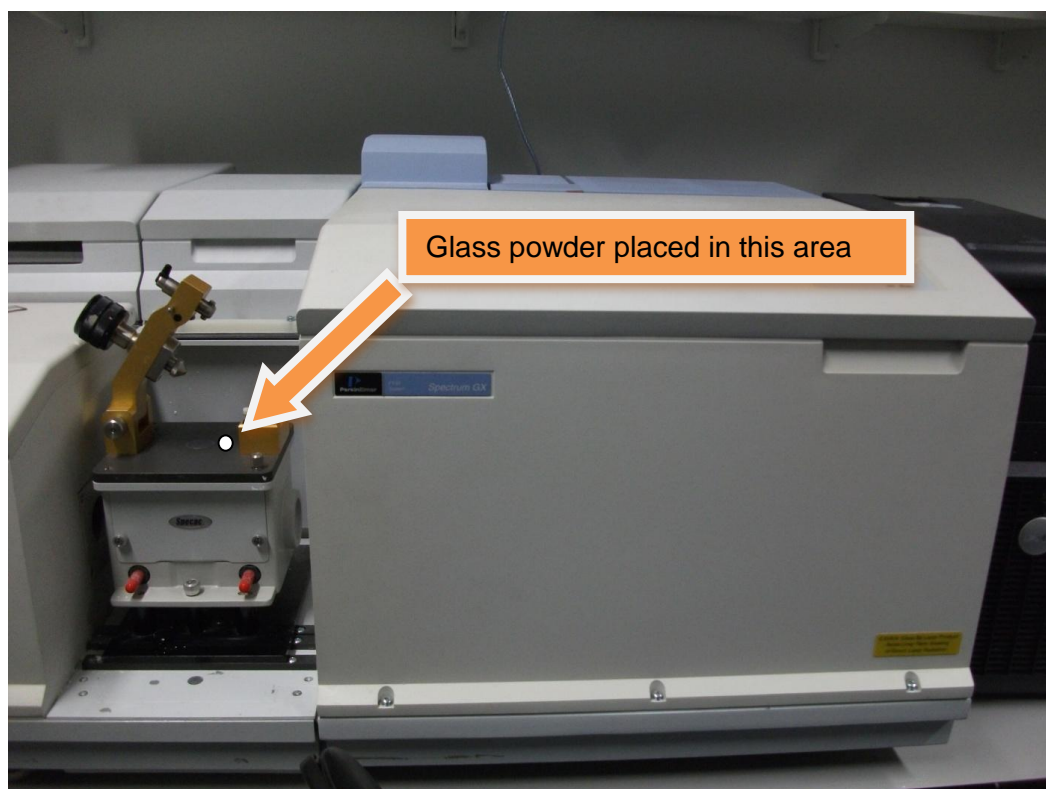


Figure 5.4. ATR-FTIR spectrometer

b- X-ray diffraction (XRD)

An X-ray diffractometer (XRD; X'Pert PRO MPD, PANalytical, Cambridge, UK; 40kV/40mA, Cu K α), which is a powerful and rapid analytical technique used in crystalline phase identification as well as confirming the amorphous nature of glasses produced. The data were collected at room temperature in the 2 Theta (2θ) range of 10° to 70° degrees, with a step size of 0.03° and a step time of 200 seconds, for one sample of each glass powder ranging from 1 to 20mg with a particle size <38 μ m. These data were then correlated with the ATR-FTIR data to confirm the results obtained for each glass powder sample (45S5, Sylc™ and all experimental glasses) before starting biological dissolution studies (untreated glasses) and then after. The 2 Theta and intensity (%) of the most characteristic reflections of the phases of interest for both hydroxyapatite and fluorapatite used in standard reference XRD (which is called JCPD file) for each apatite are presented in Tables 5.3 and 5.4, respectively. Two main peaks are observed for each apatite at approximately 25.8° and 31.8° 2 Theta. The stick patterns for both apatites are also given in Figures 5.5 and 5.6, respectively.

Table 5.3. Most characteristic reflections of hydroxyapatite from its JCPD file

Reference pattern: Hydroxyapatite, syn (NR), 04-0106315	
2 Theta (degree)	Intensity (%)
10.831	15.3
25.858	34.5
31.760	100.0
32.174	48.2
32.895	60.0
34.043	22.3
35.449	4.0

Table 5.4. Most characteristic reflections of fluorapatite from its JCPD file

Reference pattern: Fluorapatite, syn (NR), 00-060-0667	
2 Theta (degree)	Intensity (%)
10.884	6.2
25.846	35.4
29.066	19.0
31.891	100.0
32.222	36.5
33.062	54.2
34.106	24.2
35.603	4.1
38.362	0.3

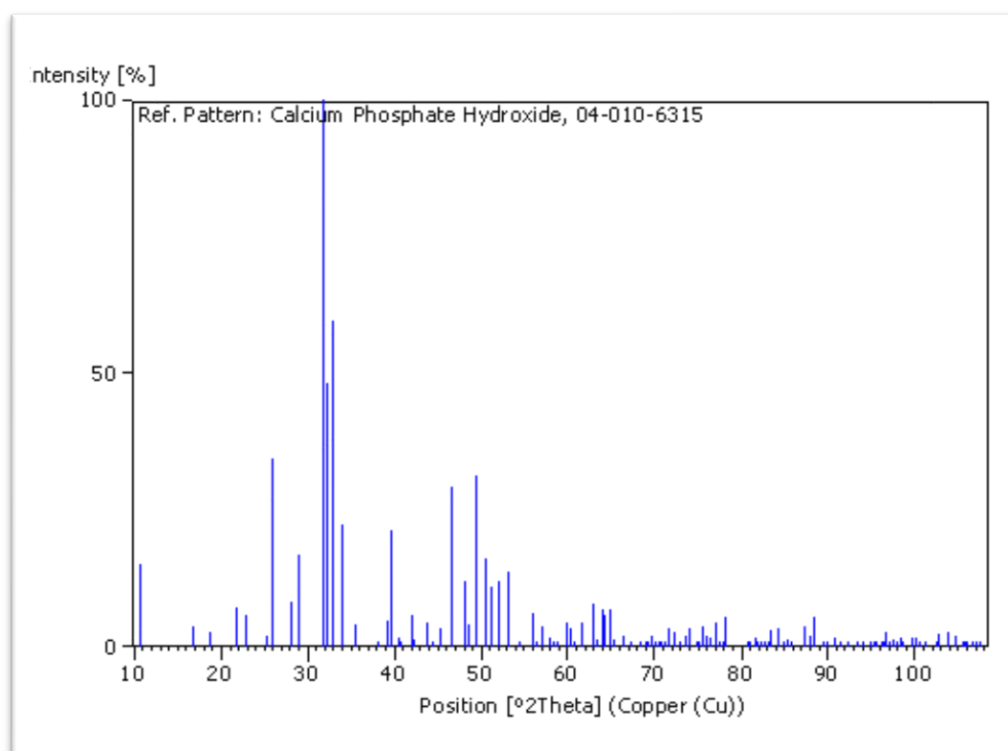


Figure 5.5. Stick pattern of hydroxyapatite

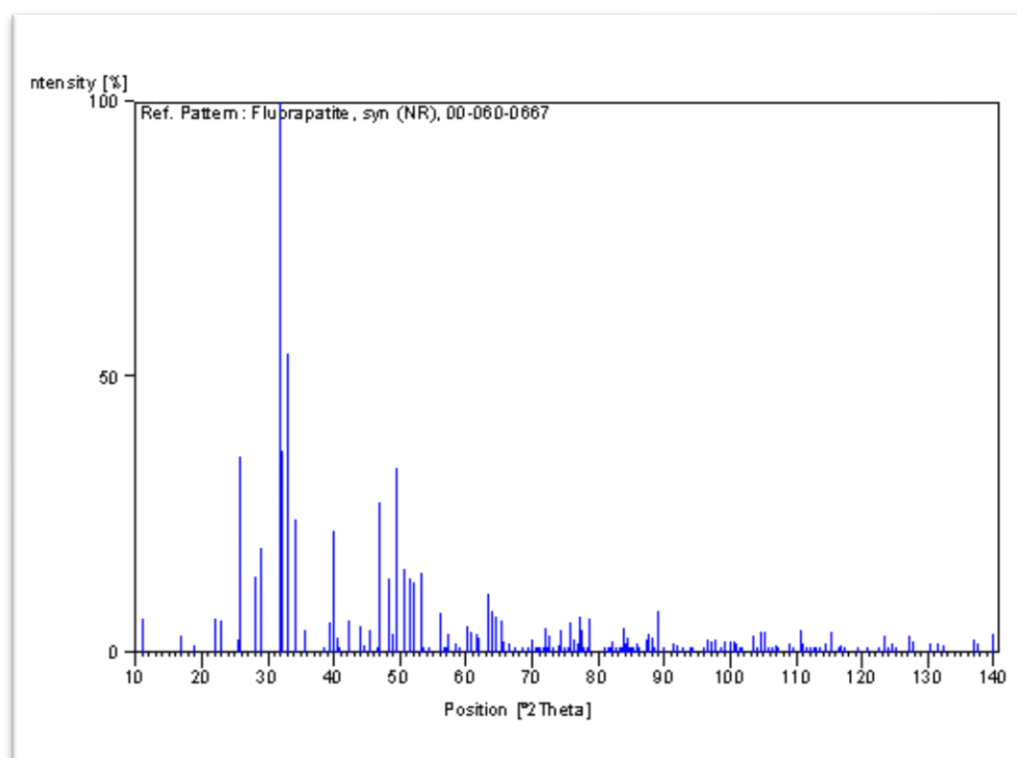


Figure 5.6. Stick pattern of fluorapatite

5.3.2. Glass thermal analysis

Differential Scanning Calorimetry (DSC) is a thermal analysis technique used for measuring the uptake of heat energy by a sample during controlled increase or decrease in temperature (Gill *et al.*, 2010). It is used to determine the glass transition temperature (T_g) of bioactive glasses, which is the onset of change from a viscous liquid state to a glassy solid state. Each glass has its unique T_g , which is utilised in casting each glass for measuring its hardness. This temperature is represented in DSC analysis as shown in Figure 5.7, as a first step change in the baseline when the heat capacity of a molten material is increased. This step is usually followed by an exothermic peak, which represents the crystalline temperature (T_c) and an endothermic peak indicative of the melting temperature (T_m) (Figure 5.7).

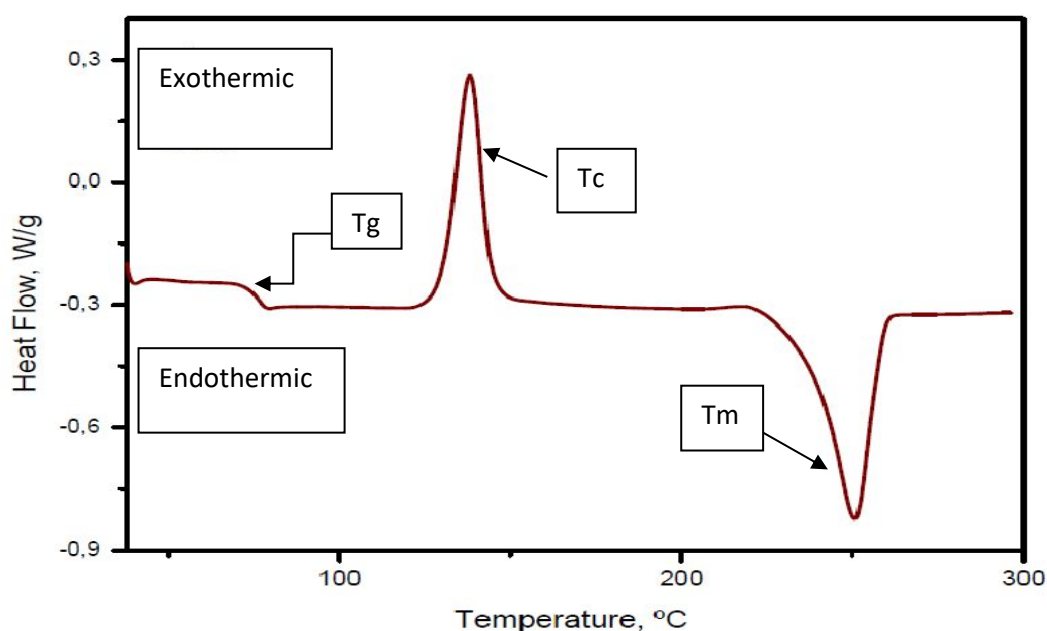


Figure 5.7. A schematic example of a DSC curve demonstrating several common features

A Stanton Redcroft DSC 1500 (Rheometric Scientific, Epsom, UK) was utilised to obtain the T_g of all glass powders (Figure 5.8). 50mg (± 0.1 mg) of each glass powder ($< 38\mu\text{m}$) was placed into a DSC platinum crucible and run against analytical grade alumina powder as a reference. The temperature was increased from 25°C to 1000°C, at a heating rate of 20°C per minute, in flowing Nitrogen gas, with a flow rate of 60ml/min. This setting is common when dealing with bioactive glasses.

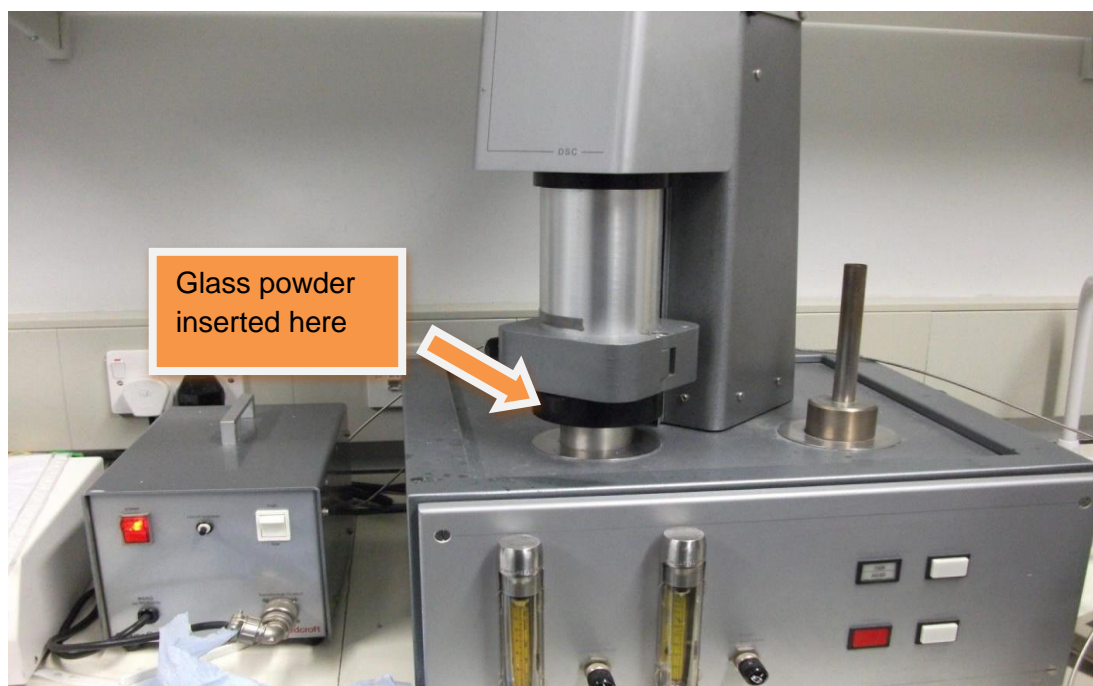


Figure 5.8. A Stanton Redcroft DSC 1500

5.3.3. Glass hardness measurements

The hardness of the discs (10 per glass) was measured using a Vickers diamond pyramid indenter (Zwick/Roell, ZHU 187.5; Figure 5.9) with an applied load of 29.4N for 10 seconds. The Vickers Hardness Number (VHN) of each glass composition (45S5, Sylc™ and all experimental glasses) was recorded (per disc) for each glass (n=10). The VHN values (displayed on the LCD) were averaged and presented as mean \pm standard error of mean (SE). Subsequently, QMAT3 glass was selected for air-abrasion studies due to its lower hardness compared to that of enamel, Sylc™ and other experimental glasses.

A similar methodology was also utilised to measure the hardness of 20 prepared discs of two orthodontic adhesives (Transbond XT™ and Fuji Ortho LC™; 10 discs each) for further use in section 5.4.1. These were prepared by placing the adhesive material in bespoke cavities formed in a Perspex® sheet (of diameter 1cm and 1mm thickness). These were light-cured using an LED curing light unit (3M ESPE, Elipar™, 3M Dental Products, Germany) following the manufacturer's instructions used during bonding of orthodontic brackets (10 seconds for Transbond XT™ and 40 seconds for Fuji Ortho LC™ at a distance of 2-3mm). The adhesive discs were

subsequently stored in a polyethylene container at room temperature for two days before use.



Figure 5.9. Vickers Hardness testing machine (Zwick/Roell, ZHU)

5.3.4. Glass bioactivity dissolution *in vitro* studies

a. Tris buffer solution study

Tris buffer solution is a simple physiological solution that does not contain calcium or phosphate ions and can be accurately used to characterise the released ions from the dissolved bioactive glasses (45S5, SycTM and all experimental glasses). This is useful in clarifying the bioactivity of the glasses by observing their potential to form apatite. Tris buffer solution was prepared as reported by Mneimne (2014), by slowly adding 15.09g Tris (hydroxyl methyl) aminomethane powder to 800ml of DW with stirring using a magnetic stirrer to encourage the powder to dissolve. After adding 44.2ml of 1M hydrochloric acid (Sigma Aldrich) with a pipette, the solution was placed into an orbital shaker (IKA® KS 4000i Control, Germany) and was shaken at $37 \pm 0.1^\circ\text{C}$ overnight.

After this period, the solution was removed from the shaker and left to reach room temperature (~30 minutes). The pH of the solution was then measured using a pH meter (Oakton Instruments), which was calibrated before use. Standard solutions of different pH, such as 4.01, 7.00 and 10.01 were used to calibrate the pH electrode, which was rinsed with DW after immersion in each solution. Once the pH of Tris buffer solution reached ~7.25-7.4 (mimicking the oral environment), by adding small amounts of 1M hydrochloric acid, this solution was then filled with DW until the total volume of the solution reached two litres. It was then placed in a polyethylene bottle and stored in an incubator at $37\pm0.1^{\circ}\text{C}$ (oral/body environment temperature) until further use. Its pH was checked prior to each experiment. The same methodology was used to prepare a Tris buffer solution with pH=9.

In order to observe the potential apatite formation of each glass in Tris buffer with two different pHs, a test was performed by dispersing 75mg of each glass powder ($< 38\mu\text{m}$) into 50ml of Tris buffer solution in a polyethylene bottle (150ml). These bottles were then kept in a shaking incubator at $37\pm0.1^{\circ}\text{C}$, with a rotation rate of 60 rpm (rounds per minute) for the following immersion time intervals: 1, 3, 6, 9 and 24 hours. These immersion time intervals were sufficient to observe the glass bioactivity (its potential to form apatite) in Tris buffer solution as reported by Mneimne (2014). After the designated time intervals, the samples were removed from the shaking incubator and filtered through filter paper (Fisher brand® qualitative filter paper; 150mm) to collect the powder from each glass sample. The glass powder within the filter paper was then placed in an oven (Camlab™) at $37\pm0.1^{\circ}\text{C}$ for 24 hours to dry. The dried powders were then analysed using ATR-FTIR and XRD. The pH of Tris buffer solution was also recorded for each glass after the designated time intervals.

b. Acetic acid study

A 0.1 M acetic acid solution was prepared by diluting 6.005g of 100% acetic acid solution (Analar Normapur, VWR International, France) in 800ml of DW. The pH of the acid solution was then buffered to 5.0 by slowly adding a 0.5 M solution of KOH, which was prepared from KOH flakes (Sigma Aldrich). The volume of the acid solution was then adjusted to 1 litre by adding DW.

To observe the potential apatite formation of each glass (45S5, SylcTM and all experimental glasses) in an acidic medium, a test was carried out by dispersing 75mg of each glass powder (<38µm) into 50ml of acetic acid solution in a polyethylene bottle (150ml). These bottles were kept in a shaking incubator at 37±0.1°C, with a rotation rate of 60 rpm (rounds per minute) for the following immersion time intervals: 15 minutes, and (1, 3, 6, 9 and 24) hours. These immersion time intervals were sufficient to observe the glass bioactivity (its potential to form apatite) in acetic acid as reported by Bingel *et al.* (2015). After the designated time periods, each glass powder was then collected following the methodology described in the Tris buffer study. Thereafter, the dried powders were analysed using ATR-FTIR and XRD. The pH of acetic acid solution was also recorded for each glass after the designated time intervals.

c. Artificial saliva study

Artificial saliva was prepared by dissolving the following reagents: potassium chloride (KCl, 2.24g); potassium dihydrogen phosphate (KH₂PO₄ 1.36g); sodium chloride (NaCl, 0.76g); calcium chloride dihydrate (CaCl₂·2H₂O, 0.44g) dissolved in 15ml DW to prevent precipitation of calcium, and Mucin from porcine stomach (2.2g) (all from Sigma Aldrich, UK) in 800ml DW. The pH of AS was then adjusted to 6.5 by slowly adding a 0.5M solution of potassium hydroxide (KOH), which was prepared from KOH flakes (Sigma Aldrich, UK). Finally, the artificial saliva was topped up with DW until the total volume of the solution reached one litre. It was then placed into a polyethylene bottle in a fridge at 4±0.1°C before further use and was used within a week in order to avoid precipitation of calcium phosphate. The protocol for preparing the artificial saliva used in this research was developed by Modus Laboratories (Reading, UK), and it has been used by Earl *et al.* (2010) and Mneimne (2014) to study the glass dissolution behaviour and bioactivity. 75mg of each glass powder (<38µm) was dispensed into 50ml of artificial saliva in a polyethylene bottle (150ml). These bottles were kept in a shaking incubator at 37±0.1°C, with a rotation rate of 60 rpm (rounds per minute) for the following immersion time intervals: 15, 30, and 45 minutes and 1 hour. These immersion time intervals were sufficient to observe the glass bioactivity (its potential to form apatite) in artificial saliva as reported by Mneimne (2014). After the designated time periods, each glass powder was then collected following the methodology described in the Tris buffer study. The collected, dried powders from 45S5, SylcTM and all

experimental glasses were then analysed using ATR-FTIR and XRD. The pH of artificial saliva was also recorded for each glass after the designated time intervals. Table 5.5. summarises all glass dissolution studies.

Table 5.5. Summary of all glass dissolution studies

Solution	Initial pH	Time points	Glass mass/solution volume
Tris buffer	7.3	(1, 3, 6, 9, and 24) hours	75mg/50ml
Tris buffer	9	(1, 3, 6, 9, and 24) hours	75mg/50ml
Acetic acid	5	15 minutes and (1, 3, 6, 9, and 24) hours	75mg/50ml
Artificail saliva	6.5	(15, 30, 45) minutes, and 1 hour	75mg/50ml

5.3.5. Apatite detection using ^{19}F MAS-NMR

Magic Angle Spinning - Nuclear Magnetic Resonance (MAS-NMR) spectroscopy is a powerful technique that gives information on the type of apatite formed. ^{19}F MAS-NMR was carried out using a 600MHz (14.1T) spectrometer (Bruker, Germany) at a Larmor frequency of 564.5MHz, under spinning conditions of 22kHz in a 2.5mm rotor. The spectra were acquired using a low-fluorine background probe in a single-pulse experiment of 30 seconds recycle duration. The ^{19}F chemical shift scale was referenced using the -120ppm peak of 1M NaF solution. The spectra were acquired for overnight based on 256 scans. One novel, most promising experimental glass (QMAT3, further details are shown in results chapter) was assessed using the ^{19}F MAS-NMR technique to identify the type of apatite formed after immersion in Tris buffer solution and artificial saliva for 24 hours and 1 hour, respectively. In addition, the ^{19}F MAS-NMR was also used to confirm the presence of fluorapatite on the enamel surface, after propelling the novel glass (QMAT3) *via* the air-abrasion hand-piece (BA UltimateTM air polisher). Five enamel blocks (~4x4mm) were harvested with a maximum thickness of ~1mm using a diamond cutting machine (Accutom-5, Struers A/S, Ballerup, Denmark). The immersion time was standardised at 24 hours in 50ml artificial saliva at $37^{\circ}\text{C} \pm 1^{\circ}\text{C}$ in an orbital shaker (IKA® KS 4000i Control, Germany). One of the blocks was kept as a sound enamel surface for ^{19}F MAS-NMR analysis, whereas the others were demineralised. After demineralisation (see

section 5.5.3), one enamel block was kept as a demineralised enamel surface for ^{19}F MAS-NMR analysis, another was immersed in artificial saliva (AS) alone, whilst the others underwent air-abrasion with either the novel glass (QMAT3) or SylcTM (further details described in section 5.5.3). Each enamel block was dried and ground to a fine powder before ^{19}F MAS-NMR analysis.

5.3.6. Glass particle size distribution analysis

Glass particle size distribution analysis was performed on 45S5, SylcTM and all experimental glass powders of particle size $<38\mu\text{m}$ in size and between $38\text{--}90\mu\text{m}$ using a Malvern particle size analyser (Mastersizer 3000, Malvern instruments, UK; Figure 5.10). Approximately 30mg of each glass powder ($<38\mu\text{m}$ in size) was weighed using a digital balance (Mettler instrument, Switzerland; used for all experiments of the present study) and dispersed in 700ml of DW until the ideal laser absorbance level was achieved. Five measurements were recorded per glass and then averaged to produce a more reliable value.

A Malvern/ E Mastersizer (Malvern instruments, UK; Figure 5.11) was also used to analyse the particle size distribution of all glass powders with a size ranging between $38\mu\text{m}$ and $90\mu\text{m}$. The reason behind using two analysers was due to the latter analyser being replaced by the former during this research project. Approximately 30mg of each glass powder was dispersed in 500ml of DW until the ideal laser absorbance level was achieved. The laser is scattered through a dispersed particulate sample. Large particles scatter light at small angles relative to the laser beam and small particles scatter light at large angles. Subsequently, the angular scattering intensity data was analysed to calculate the particle size responsible for creating the scattering pattern. Two measurements were recorded for each glass and the average of these measurements was taken to produce a more reliable value.

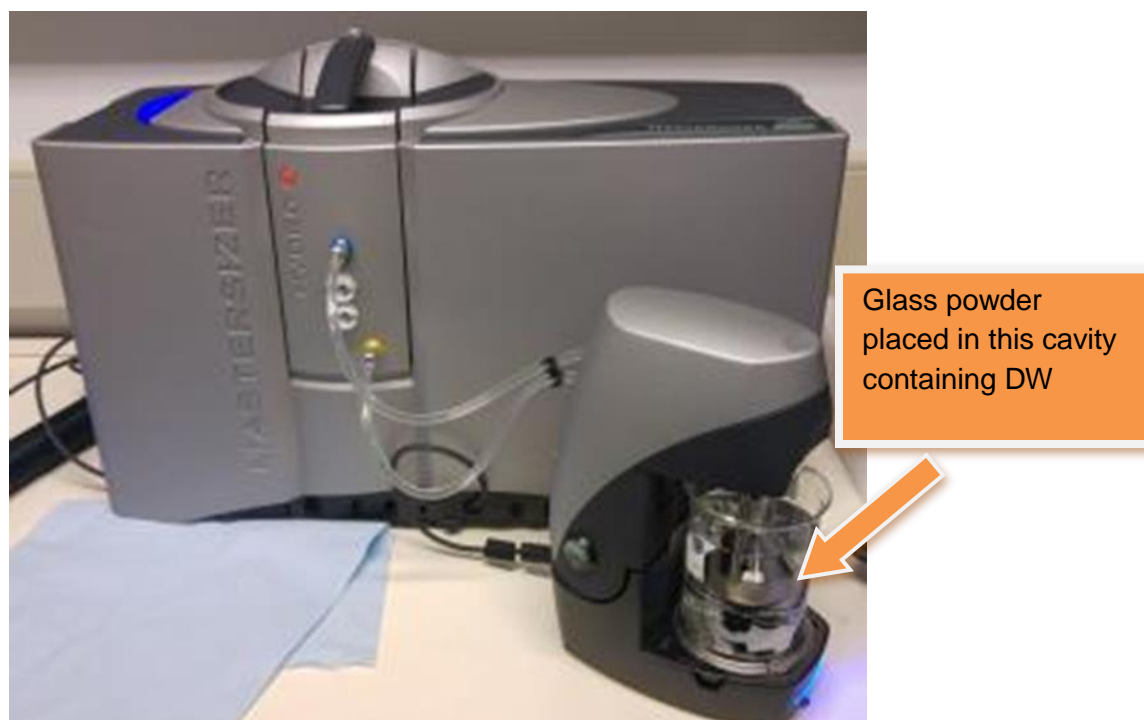


Figure 5.10. Malvern Particle Size Analyser (Mastersizer 3000)

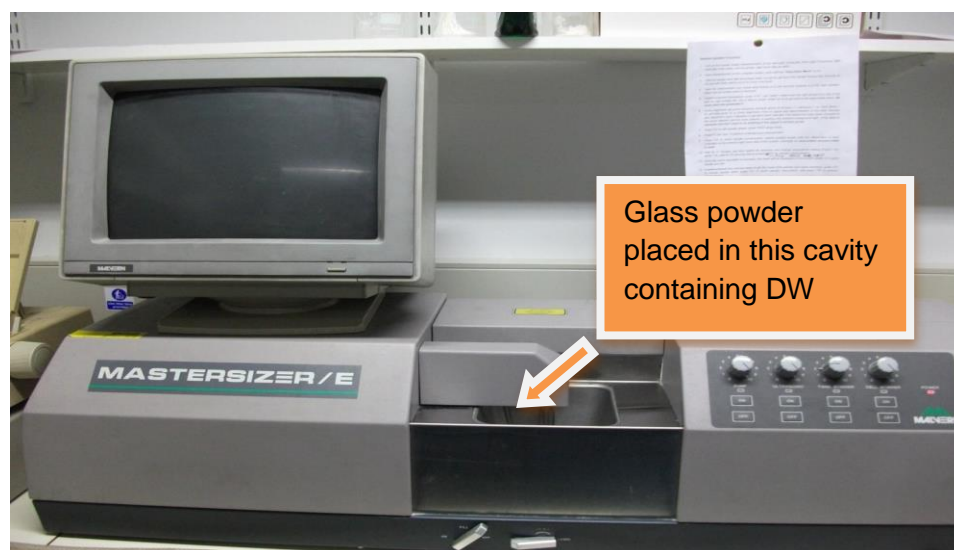


Figure 5.11. Malvern Mastersizer/ E

5.3.7. Glass particle shape analysis

A scanning electron microscope (SEM-FEI Inspect F, Oxford instruments, UK) with an accelerating voltage of 20kV and a working distance of 10mm was used to scan

and analyse the shape of the glass particles, which were later used in air-abrasion studies, orthodontic adhesive removal studies and WSLs remineralisation studies. Prior to SEM scanning, the glass particles of each glass (45S5, Sylc™ and all experimental glasses) of particle size ranging between 38-90µm were mounted on stubs and sputter-coated with gold using an automatic sputter coater (SC7620, Quorum Technologies, UK). The reason behind analyse the shape of glass particle ranging between 38-90µm was due to this range of particle size allowed escape of the glass powder through the hand-piece nozzle tip without agglomeration, therefore, it has been decided to use in this research for subsequent air-abrasion studies and experiments using the novel most promising experimental glass.

5.4 Air- abrasion studies performed using the optimal novel glass, QMAT3

5.4.1. Glass cutting efficiency

The cutting efficiency of the novel most promising experimental glass (QMAT3; its properties are shown in the results chapter) was tested against the commercially-used Sylc™ (each glass has a particle size ranging between 38-90µm). A Velopex Aquacut Quattro™ air-abrasion machine (Figure 5.12) was used to propel these two glasses using a hand-piece (0.8mm internal nozzle tip diameter; Figure 5.13a). The stream of glass particles was surrounded by a water shroud. The test involved recording the time required to cut a hole within 60 pre-prepared disc samples (Figure 5.13b) of an orthodontic light-cured adhesive (Transbond XT™). These adhesive discs were prepared by placing the adhesive material in prepared cavities in a Perspex® sheet (of diameter 1cm and a thickness of 1mm) and light-cured using an LED curing light unit (3M ESPE, Elipar™, 3M Dental Products, Germany) following the manufacturer's instructions (10 seconds on one side at a distance 2-3 mm from the light gun tip to the adhesive surface). These adhesive discs were subsequently stored in a polyethylene container at room temperature for two days. Thereafter, they were made to adhere to a microscopic slide using double-sided adhesive tape. A red tape was placed on the opposite side of the microscopic slide to allow better visual perception when the hole had reached its base. Thirty adhesive discs were used per glass powder, which were further subdivided into 6 groups (n=5) based on different air pressures (40 and 60 psi; per square inch) and different powder flow setting rates using the dials on the machine (1, 3, and 5). Two nozzle tip angulations (90° and 45°) were tested while the operating distance from the nozzle tip to the disc surface remained constant at 5mm. The effects of varying

these parameters on the cutting efficiency of each glass were observed and recorded.

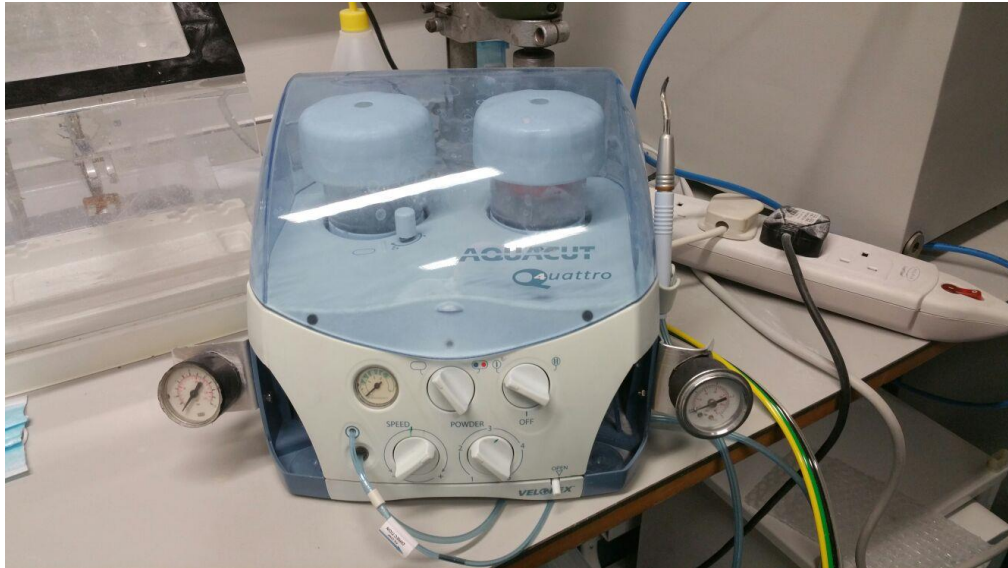


Figure 5.12. Velopex Aquacut Quattro™ air-abrasion machine

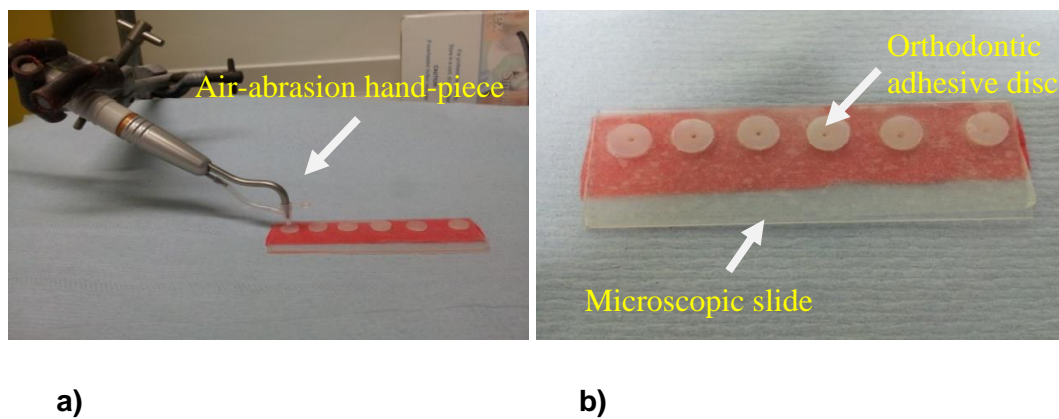


Figure 5.13. Methodology used to test the glass cutting efficiency: a) hand-piece for air-abrasion machine, and b) prepared adhesive disc samples on a microscopic slide

5.4.2. Glass powder flow rate

The glass powder flow rate of a Velopex Aquacut Quattro™ air-abrasion machine was compared with that of BA Ultimate™ air polisher (Figure 5.14), which was

connected to a dental chair unit. Both air-abrasion systems were used without a water shroud, since the latter might affect the recorded weight data. Two glasses (QMAT3) and the commercially-used Sylc™ glass were propelled (each glass has a particle size ranging between 38-90µm) inside polyethylene containers (as shown in Figure 5.15) *via* these two air-abrasion systems. Forty-two containers were weighed before and then after glass propulsion. The nozzle tip of the hand piece of each air-abrasion system was fitted into a hole at the top of the container. This hole was surrounded by condensation silicone laboratory putty (polyvinyl siloxane, Coltene) in order to avoid escape of the glass powder from the container *via* the back flow. Each glass powder was propelled into the container for one minute, respectively. During that time, a black paper was placed at the bottom of the container to monitor any escape of the white powder. The operating parameters of the Velopex Aquacut Quattro™ air-abrasion machine were varied from 40 and 60 psi, while the powder flow setting rate dial on the machine varied from 1, 3 and 5 per glass. Three readings were carried out per air pressure and powder flow rate setting dial with either QMAT3 or Sylc™, which were then averaged. Three readings for each glass were recorded and then averaged when BA Ultimate™ air polisher was used at an air pressure of 60 psi, which was built into the setting of the dental chair unit.

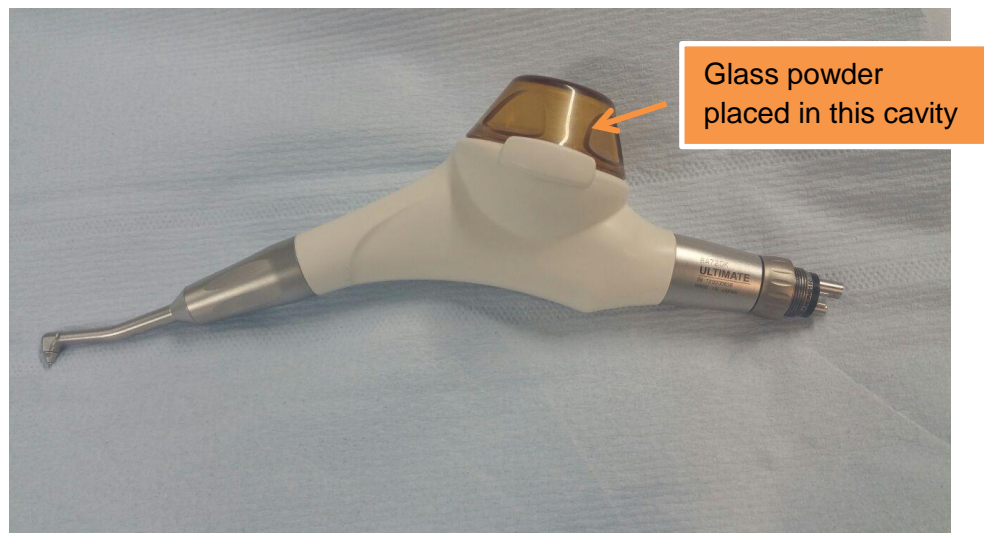


Figure 5.14. BA Ultimate™ air polisher

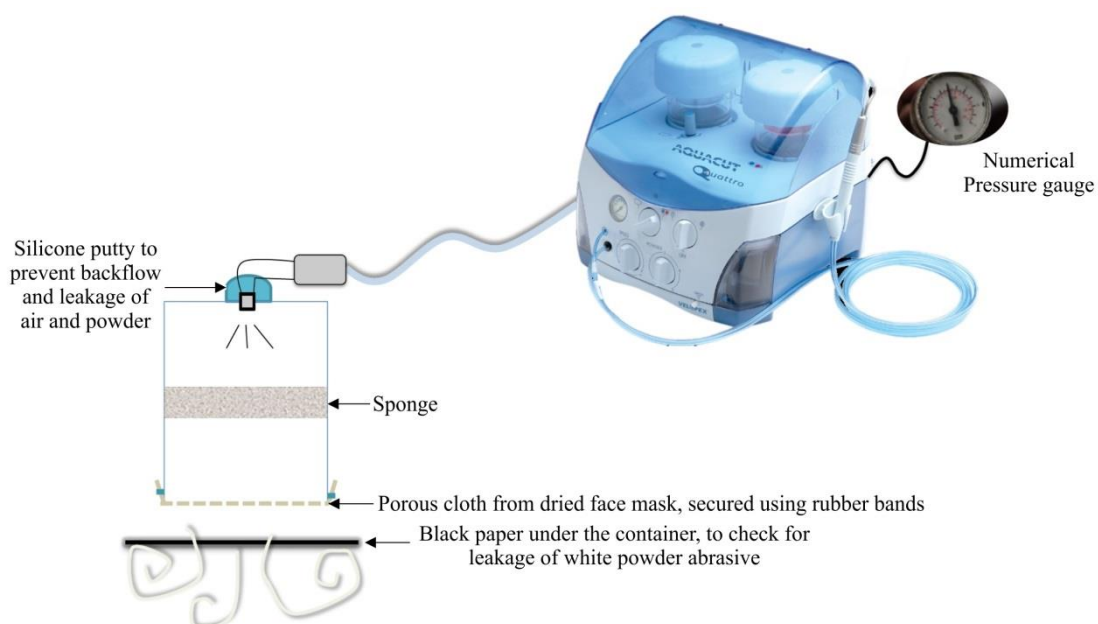


Figure 5.15. Procedure for assessing the glass powder flow rate

5.5. Experiments performed with the optimal novel glass (QMAT3)

Two experiments have been performed on human extracted teeth samples (see section 5.5.1) utilising the novel most promising glass (QMAT3) to investigate its functionality as i) orthodontic adhesive removal against Sylec glass and a slow-speed tungsten carbide bur (further details in section 5.5.2.), and ii) WSL remineralisation in comparison with Sylec™ glass and artificial saliva (further details in section 5.5.3). The particle size for each glass was ranging between 38-90µm.

5.5.1. Tooth sample preparation

Human premolar teeth (n =120), extracted for orthodontic purposes, were used (with approval from Queen Mary Research Ethics Committee QMREC 2011/99). These teeth were selected on the basis of visual observation using an optical stereo-microscope at 4.5x magnification (VWR International Microscope). The inclusion criteria were: no carious lesions, cracks or any other defects on their buccal surfaces. The selected teeth samples were cleaned and stored in DW in a refrigerator at $4 \pm 0.1^\circ\text{C}$ until required. Prior to the start of the experiment, the teeth were washed with DW, air-dried and embedded into plastic moulds filled with cold-

cure acrylic resin (Orthocryl™, UK) leaving the buccal surfaces exposed (Figure 5.16a). The buccal surface of each tooth sample was then polished with non-fluoridated pumice paste for 20 seconds, rinsed with water and air-dried. Thereafter, a polyvinyl chloride tape was placed on the buccal surface of each tooth sample, excluding a window (4mm x 4mm) at the centre (Figure 5.16b). The covered area was used as a reference for later visual comparison between the treated and untreated surfaces. Finally, these prepared teeth samples were stored in an incubator at $37\pm0.1^{\circ}\text{C}$ until use.

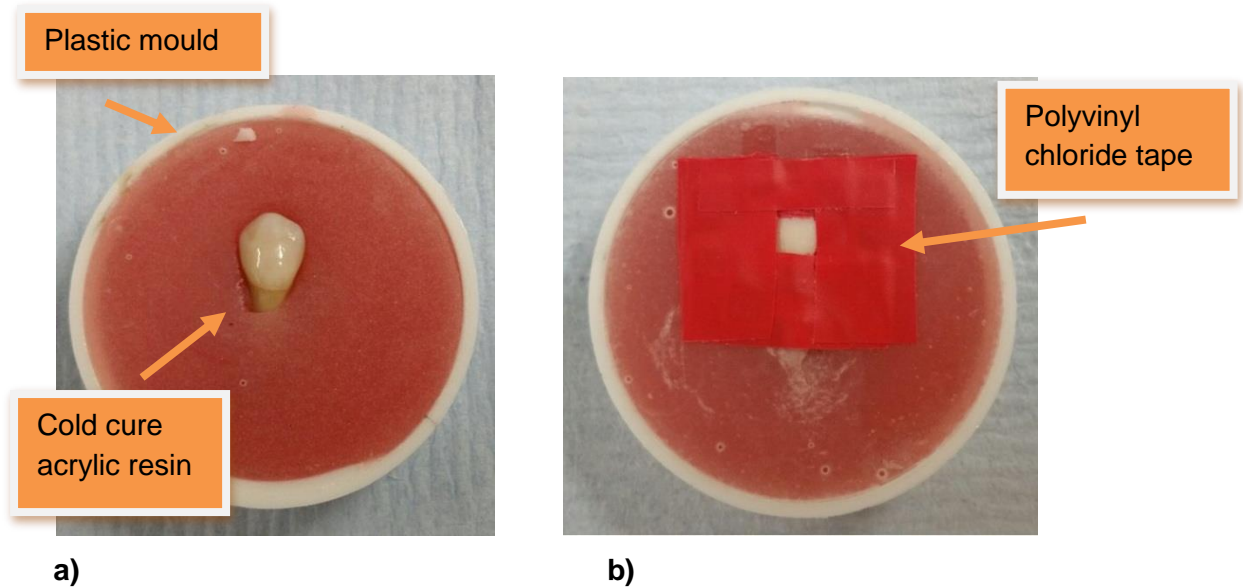


Figure 5.16. The prepared tooth sample: a) the tooth is embedded into a plastic mould filled with acrylic resin, and b) a polyvinyl chloride tape is placed on the buccal surface of the tooth sample leaving a window of exposed enamel surface

5.5.2. Orthodontic adhesive removal

Following the manufacturer's instructions, two light-cured orthodontic adhesive systems: resin composite, Transbond XT™ (3M Unitek, Monrovia, CA, USA) and resin modified glass ionomer cement, Fuji Ortho LC™ (GC corporation, Tokyo, Japan) were used to bond 60 premolar metal brackets (MiniSprint®, Forestadent, Pforzheim, Germany) to the prepared teeth samples (30 premolar teeth per adhesive system group). Enamel etching with 37% phosphoric acid was undertaken for 30 seconds prior to application of Transbond XT™, while the enamel surface was left unetched prior to application of Fuji Ortho LC™. Each bracket was subjected to a 300g compressive force during placement using a force gauge

(Correx Co, Berne, Switzerland) for 5 seconds, to ensure a uniform thickness of the adhesive (Eliades and Brantley, 2000). The teeth with the attached brackets were then stored in DW for one week at 37°C. Thereafter, the plastic moulds (with the extracted teeth mounted) were held in a mounting jig (Instron®, UK) to allow removal of the brackets using a debonding plier (Ixon™, DB Orthodontics) by one operator. Three different clean-up methods were used for removal of the residual orthodontic adhesive: slow-speed tungsten carbide bur (TC), commercially-available Sylc™-air-abrasion, and novel experimental glass (QMAT3)-air-abrasion. The teeth samples within each orthodontic adhesive group were randomly assigned to three groups (10 teeth per clean-up method). Both Sylc™ and QMAT3 glass were propelled *via* an air-abrasion hand-piece (BA Ultimate™ air polisher) connected to a dental chair unit with a water shroud. This air-abrasion system was chosen in view of its clinical applicability and relevance. The operating parameters were: air-pressure 60 psi, nozzle angle 75° and nozzle tip-enamel surface distance of 5mm. Complete removal of the adhesive remnants was assessed by visual inspection under a dental operating light, and later verified by an optical stereo-microscope at 4.5x magnification (VWR International Microscope).

A non-contact white light profilometer (Proscan®2000, Scantron, Taunton, UK; see section 5.5.4.2) was used to measure the enamel surface roughness for all prepared teeth samples under different conditions before bracket bonding, after post clean-up and after polishing (using rubber cup and non-fluoridated pumice for 20 seconds). The study design is summarised in Figure 5.17. Additionally, two prepared teeth samples, which represented the enamel surface under different conditions (before bracket bonding, after clean-up using the TC bur, after clean-up using Sylc™-air-abrasion, and after clean-up using QMAT3-air-abrasion) were examined using scanning electron microscopy (SEM-FEI Inspect F, Oxford instruments, UK) to assess the enamel surface damage. Furthermore, the time required to remove the remnants of the two adhesives was also assessed for each post clean-up method.

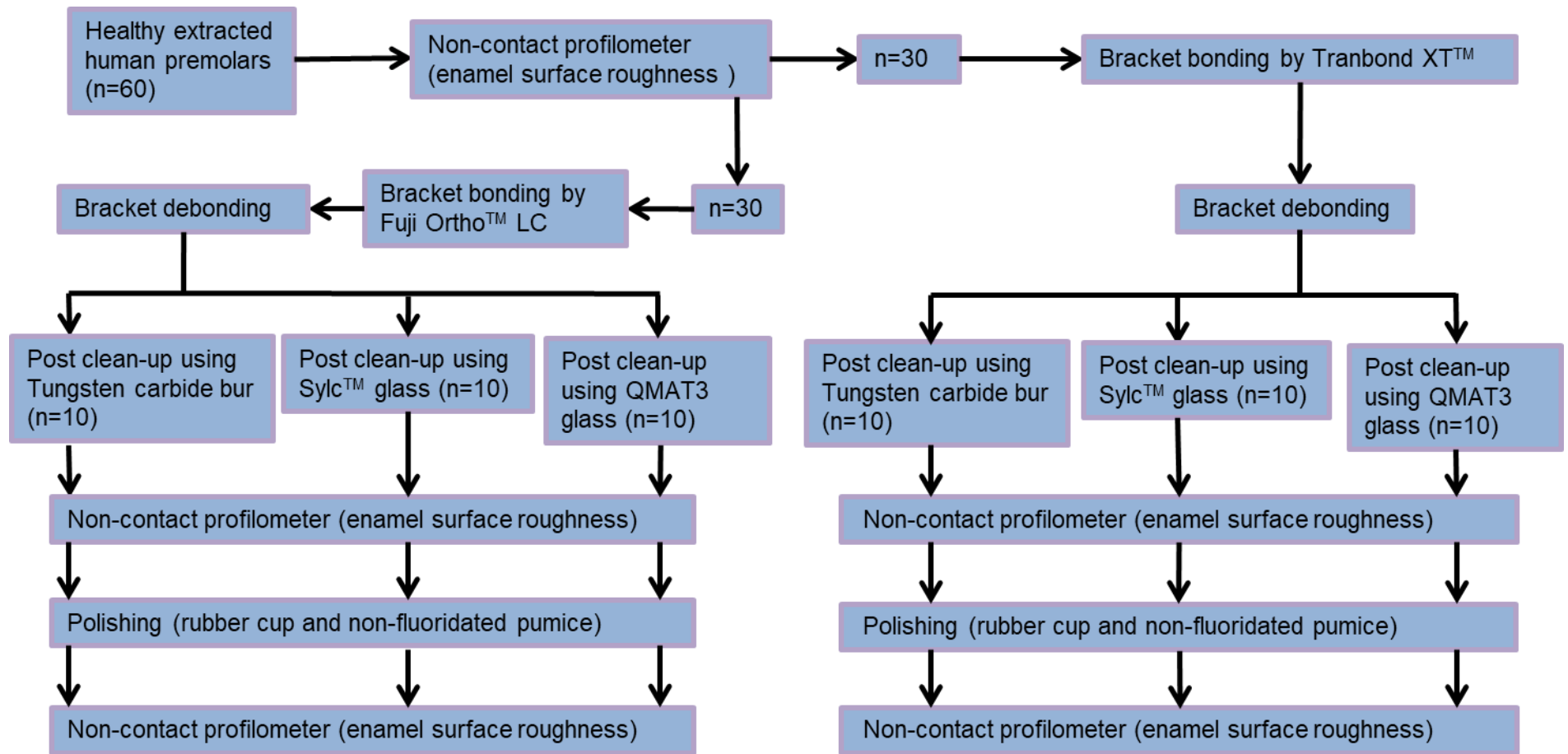


Figure 5.17. Flow chart representing the experimental study design to assess enamel surface roughness following orthodontic adhesive removal

5.5.3. White spot lesion (WSL) remineralisation

Thirty prepared human premolar teeth samples (described earlier in 5.5.1 section) were used to compare the enamel surface changes under different conditions (sound, demineralised, after glass propulsion and after immersion in artificial saliva to induce remineralisation). A bi-layer demineralisation protocol (Figure 5.18) involving 8% methylcellulose gel (50ml) buffered with a layer of lactic acid solution (50ml, 0.1 mol/L, pH 4.6) for 14 days at 37°C was used to induce artificial subsurface lesions (WSLs) with an average depth of 70–100µm (ten Cate *et al.*, 2006; Milly *et al.*, 2015). The methylcellulose gel covered the enamel surface of the prepared tooth sample, followed by filter paper and then by a layer of lactic acid solution where the methylcellulose gel buffered the effect of the acid during induction of an artificial WSL on the buccal surface of each tooth. Thereafter, the average lesion depth (70-100µm) was confirmed by the data obtained from optical coherence tomography (OCT; see later), which was analysed by an Image J software programme (Fiji™).

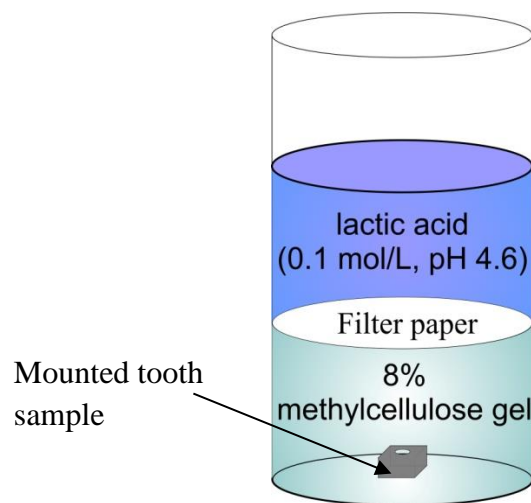


Figure 5.18. Protocol used to create artificially-induced WSLs

After demineralisation, the thirty teeth samples were randomly assigned into three experimental groups (n=10) based on the remineralisation treatment. These are: Sylc™-air-abrasion group, QMAT3-air-abrasion group, and the control group. An air-abrasion hand-piece (BA Ultimate air polisher) connected to a dental chair unit, was used to propel bioactive glasses on the artificially-induced WSLs. A commercially-available glass (Sylc™: Sylc™-air-abrasion group) and the novel experimental glass

(QMAT3: QMAT3-air-abrasion group) were used to remineralise the demineralised teeth samples. A third group (control) was left untreated and only immersed in DW. The hand-piece (BA Ultimate™ air polisher) was used with the following operating parameters: air-pressure 60psi, nozzle angle 90°, and nozzle tip-enamel surface distance of 5mm. This procedure was followed by immersing the teeth samples from all three groups individually into separate plastic containers containing artificial saliva for 24 hours (50ml of artificial saliva for each tooth sample). These containers were placed in an orbital shaker (IKA® KS 4000i Control, Germany) to keep the temperature constant at $37\pm0.1^{\circ}\text{C}$, mimicking the oral environment. The prepared teeth samples from each group were scanned using optical coherence tomography (OCT), non-contact profilometer, and Knoop hardness testing machine, respectively, after each enamel condition (Figure 5.19). Moreover, for further investigations, twenty prepared teeth samples (described earlier in 5.5.1 section) were randomly selected to be examined by scanning electron microscope (SEM) and energy dispersive x-ray spectroscopy (EDX). Two prepared teeth samples were scanned per technique representing the enamel surface under specific conditions: i) sound enamel, ii) demineralised enamel using the aforementioned demineralisation protocol, iii) remineralised enamel using only artificial saliva, iv) remineralised enamel following Syc™-air-abrasion and immersion in artificial saliva, and v) remineralised enamel following QMAT3-air-abrasion and immersion in artificial saliva.

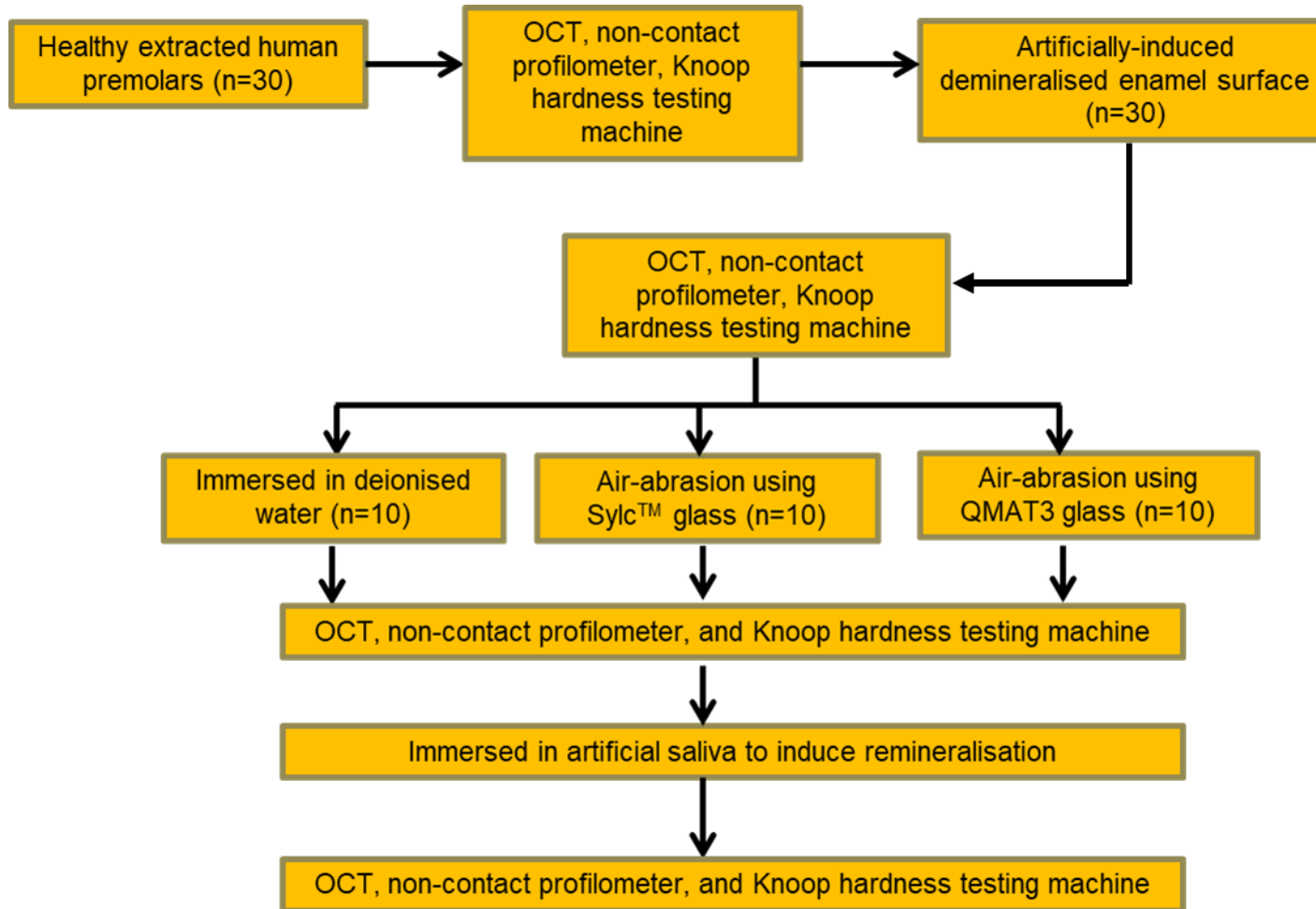


Figure 5.19. Experimental study design to assess enamel surface changes under different conditions

5.5.4. Assessment techniques used in *in vitro* studies

Since no single technique has been proven to be superior in evaluating enamel changes, a combination of different techniques were used based on the study design, the technique availability, the technique sensitivity and accuracy, the cost and the time required.

5.5.4.1. Optical Coherence Tomography (OCT)

The prepared teeth samples (10 teeth per experimental group) were scanned using the OCT system (laboratory custom built) to assess the intensity of the light backscattering from the enamel surface prior to demineralisation (sound), after demineralisation, after glass propulsion and after immersion in artificial saliva. All teeth samples were hydrated for OCT scanning; they were assessed in a dry state (left at room temperature for at least 2days) prior to assessment by other techniques (e.g. profilometer, Knoop hardness, SEM and EDX). OCT system (Figure 5.20) was operated at 1325nm central wave-length, 10 kHz frequency rate and 15 mW energy power. The axial and transverse resolutions were 8 μ m and 10 μ m in air, respectively. The scanning beam of OCT was oriented perpendicular to the enamel surface of each sample covering an area of 3mm x 3mm, with approximately 3mm scans in depth. Five hundred B-scans, grey-scale images were performed by the OCT system and analysed using image processing Fiji software image JTM.

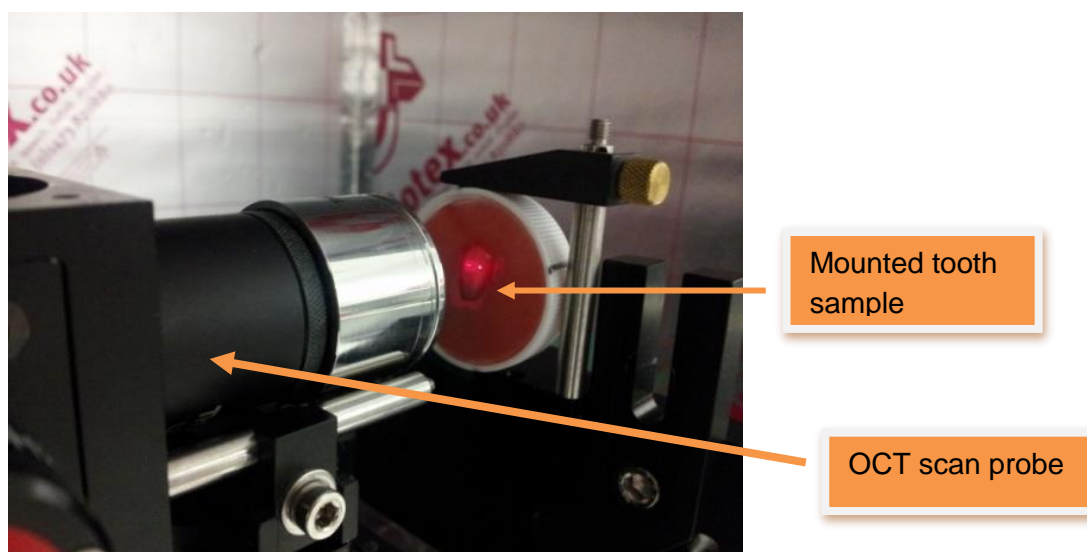


Figure 5.20. OCT system and the sample

5.5.4.2. Profilometer

A non-contact 3D white light profilometer (Proscan®2000, Scantron, Taunton, UK; Figure 5.21a) was used to measure the surface roughness of the enamel under different conditions in the two *in vitro* studies performed in this research. A standard scan area (1mm x 1mm) within the exposed window (4mm x 4mm) of the enamel surface was scanned within each tooth. Prior to scanning, the plastic mould (where the extracted tooth was mounted) was placed into a pre-prepared cavity made of Virtual® Putty Regular (Ivoclar Vivadent) polyvinylsiloxane impression material on the upper surface of the circular aluminium plate of 8.5cm in diameter (Figure 5.21b). This impression material was imprinted with four lines corresponding to those drawn on the border of each plastic mould to ensure consistent positioning of the mould during repeated scans for 10 teeth per experimental group.

The operating parameters of profilometer were: sample rate (frequency rate): 100Hz; step size: 0.01mm; and number of steps: 10, to optimise the measuring performance based on the Proscan 2000 manual instructions. Prior to each scan, the same operating parameters were applied, and the samples were accurately repositioned in the same X and Y position, which was verified by the software. The most common profilometer parameter for measuring the surface roughness is Ra, which is defined as the arithmetic mean of the absolute values of profile deviations from the mean line. Therefore, Ra values were recorded in this study.

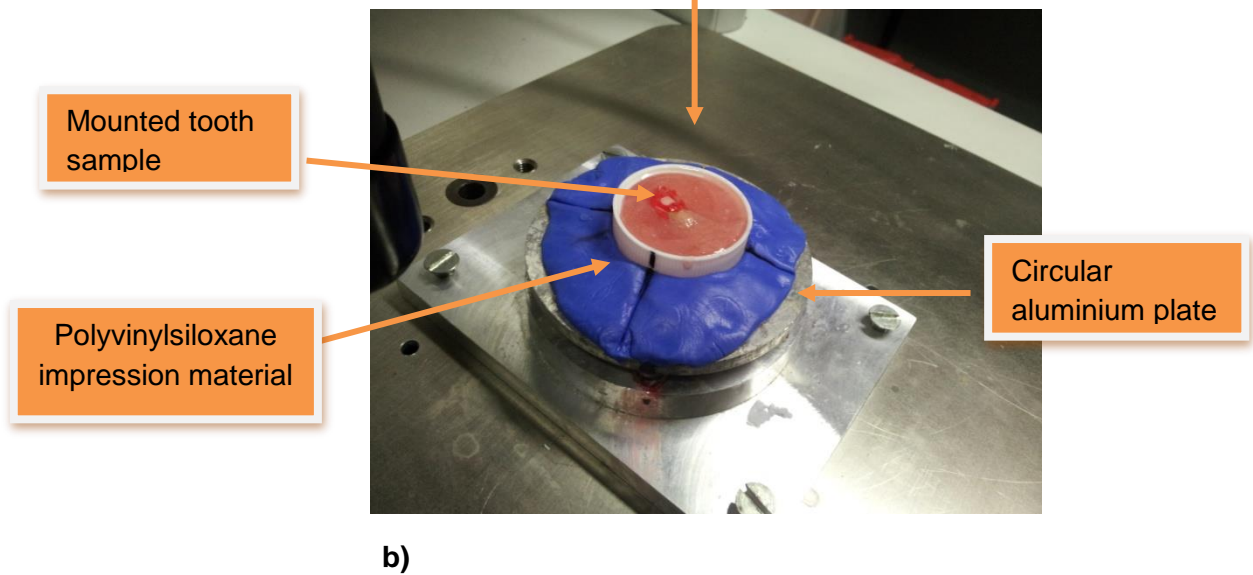


Figure 5.21. a) White light profilometer, Proscan®2000, b) Enlarged sample stage

5.5.4.3. Knoop hardness testing

For testing the enamel surface hardness, a Struers Duramin microhardness tester with a Knoop elongated pyramid-shaped diamond indenter (Struers Ltd., Denmark; Figure 5.22) was used at a predetermined load and dwelling time (50g for 10 seconds). This work has been performed at King's College London. An elongated pyramid-shaped indentation with long and short diagonals was produced after the elongated Knoop indenter was perpendicularly located at the centre of the exposed enamel surface of each sample and then imaged with a 40x air objective lens. The indentation was assessed based on the sharpness of indentation edges, uniformity and symmetry of indentation shape (geometry) and absence of irregularities in the testing area. The Knoop hardness number (KHN) was calculated by measuring the length of long-axis indentation (long diagonal) using the manufacturer's software. Since the enamel has a convex surface, three well-shaped indentations (Figure 5.23), 200µm apart, were made to minimise any discrepancy, and to avoid the risk of interferences and crack propagation between indentations. These indentations were recorded and then averaged to obtain the KHN of each sample (10 teeth per experimental group) in varying states (sound, demineralised, after glass propulsion, and after immersion in artificial saliva).

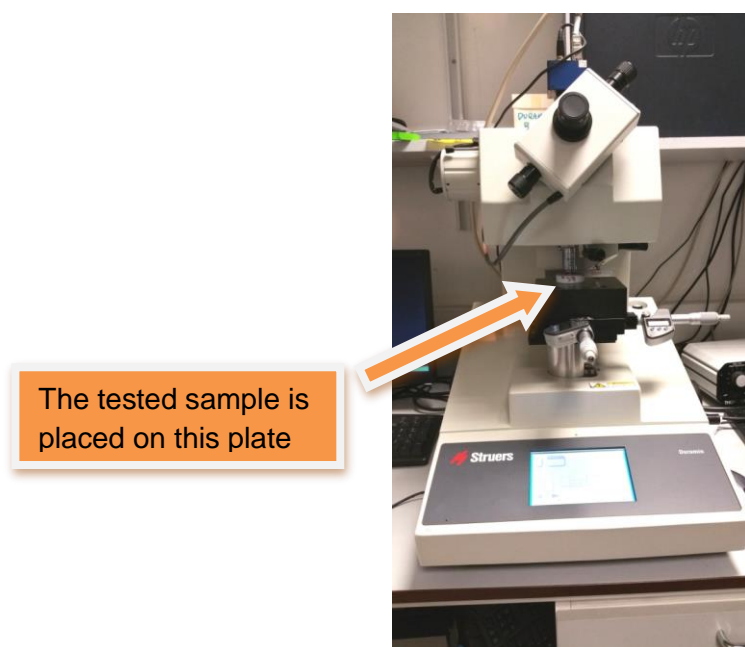


Figure 5.22. Knoop hardness testing machine (Struers / Duramin)

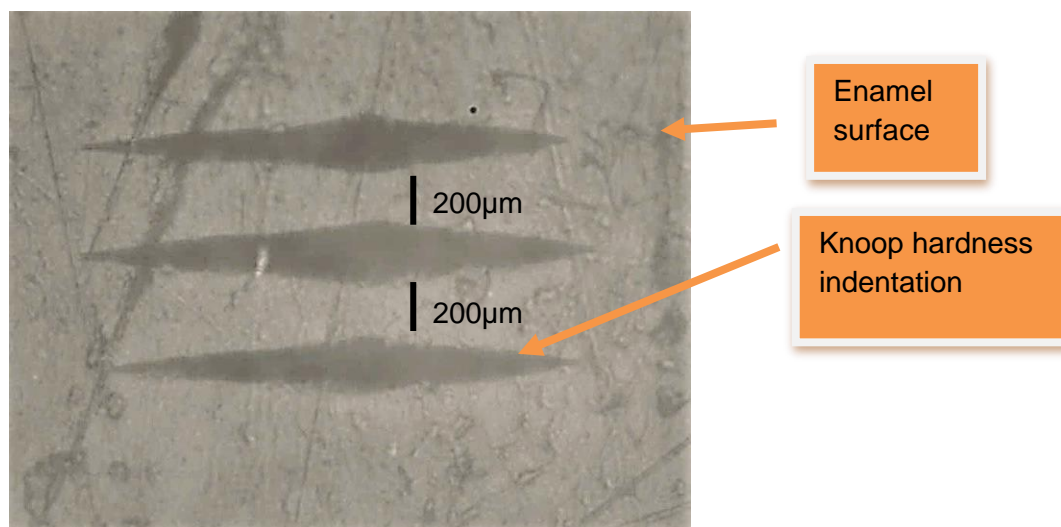


Figure 5.23. Well-shaped indentations using Knoop hardness testing machine

5.5.4.4. Scanning electron microscopy (SEM)

A scanning electron microscope (SEM-FEI Inspect F, Oxford instruments, UK) with an accelerated voltage of 20kV and a working distance of 10mm was used to obtain information on the morphology of the prepared enamel tooth sample from each experimental group under different conditions: sound, demineralised, after glass propulsion and immersion in artificial saliva to induce remineralisation (2 teeth per state). The SEM images were produced by an interaction between accelerated electrons and the enamel surface. This interaction caused signals in the form of secondary electrons, backscattered electrons and heat. Each signal was detected by a specific detector. Before SEM imaging, the tooth sample was rinsed thoroughly with deionised water, dried at room temperature for 48 hours, and then coated with a conductive coating (gold) using an automatic sputter coater (SC7620, Quorum Technologies, UK). This gold layer cannot be removed without inducing enamel damage. Consequently, the teeth samples could not be further used after SEM imaging.

5.5.4.5. Energy Dispersive X-ray Spectroscopy (EDX)

The elemental compositions of the prepared enamel samples under different conditions from each experimental group (2 teeth per state) were identified using energy dispersive X-ray spectroscopy (EDX; Oxford instruments, UK) operating at accelerated voltage of 20kV and a working distance of 10mm. Prior to EDX mapping, each tooth sample was dried at room temperature for 48 hours and coated with carbon using a carbon sputter-coated machine (Balzers/CED 030, Baltec) to detect the emission lines of elements such as calcium (Ca), sodium (Na), phosphorus (P), fluoride (F), carbon (C), oxygen (O) and silicon (Si).

5.6. Statistical analysis

Descriptive statistics were calculated with data entered into Microsoft Excel for analysis. Inferential statistical analysis was performed with the SPSS software package (Version 24; SPSS Inc., New York, NY, USA). One-way analysis of variance (ANOVA) was used to compare mean differences between groups with Tukey's HSD *post hoc* test at a pre-specified significant level ($p=0.05$).

6. RESULTS

6.1. Glass development

A bioactive glass (45S5) mirroring the formula of commercially-available 45S5 (Sylc™) was prepared and the subsequent results confirmed that both behaved in a similar manner. Five novel experimental glasses (QMAT1-5) incorporating SiO₂, P₂O₅, CaO, Na₂O, CaF₂ with a constant network connectivity (NC) of 2.08 were also developed. The compositions of these experimental glasses were based on changing the molar composition of the laboratory-prepared 45S5 to better approximate the required clinical properties of the most promising novel glass. In particular, a hardness lower than that of the enamel surface and the commercially-used glass (Sylc™), but higher than that of orthodontic adhesives to permit safe and effective removal of adhesive following fixed orthodontic treatment was required. In addition, a glass powder with potential remineralising characteristics was considered important.

The characteristics of each glass were studied using two different particle sizes: <38µm and between 38µm-90µm. Thereafter, the most promising novel glass, as well as the commercially-available glass (Sylc™), were used in two air-abrasion studies to test the cutting efficiency of each glass powder and its flow rate, respectively. These air-abrasion studies were followed by two *in vitro* studies which included orthodontic adhesive removal and remineralisation of WSLs on extracted human teeth.

6.2. Glass characterisation studies

6.2.1. Characterisation of the amorphous nature of glasses

a. ATR-FTIR

Prior to commencing the glass bioactivity dissolution studies, the ATR-FTIR spectra of untreated (not immersed) Sylc™, 45S5 and experimental glasses (QMAT1-5) were obtained. Figure 6.1 displays two main bands at 920cm⁻¹ and 1030cm⁻¹ wavenumbers related to non-bridging oxygens (Si-O⁻-M⁺, where M⁺ is an alkali metal modifier element) and vibrational stretching of Si-O-Si, respectively (Jones *et al.*, 2001; Cerruti *et al.*, 2005; Aina *et al.*, 2009) for Sylc™, 45S5 and QMAT1-3. These spectra indicate that the

Results

experimental glasses have the characteristic features of being amorphous, similar to 45S5 and Sylc™ glasses. However, there was a broad band at approximately 580cm^{-1} for all experimental glasses, which may be related to PO_4 vibrations, as they contained a higher phosphate content than both 45S5 and Sylc™ (Mniemne, 2014). Conversely, both QMAT4 and QMAT5 showed the presence of two bands at 568 cm^{-1} and 613 cm^{-1} .

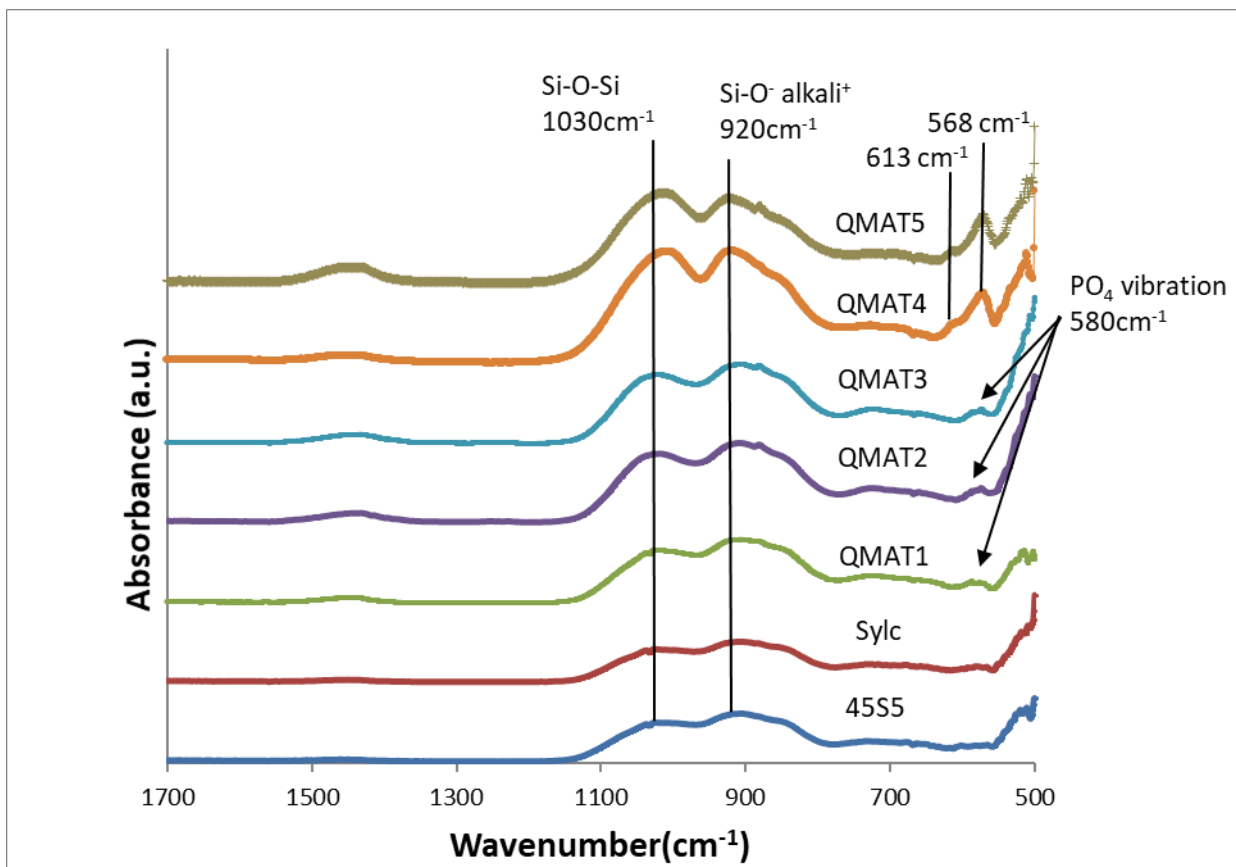


Figure 6.1. ATR-FTIR spectra for untreated 45S5, Sylc™ and experimental glasses (QMAT1, QMAT2, QMAT3, QMAT4, QMAT5)

Results

b. XRD

The XRD patterns of the three untreated experimental glasses (QMAT1, QMAT2, and QMAT3), 45S5 and Sylc™ were obtained (Figure 6.2) before commencing the glass bioactivity dissolution studies. The spectra confirmed that these glasses were amorphous in structure based on the presence of the main characteristic peaks centred at 32° 2θ (broad halo) and 22° 2θ (secondary halo) (Mneimne *et al.*, 2011).

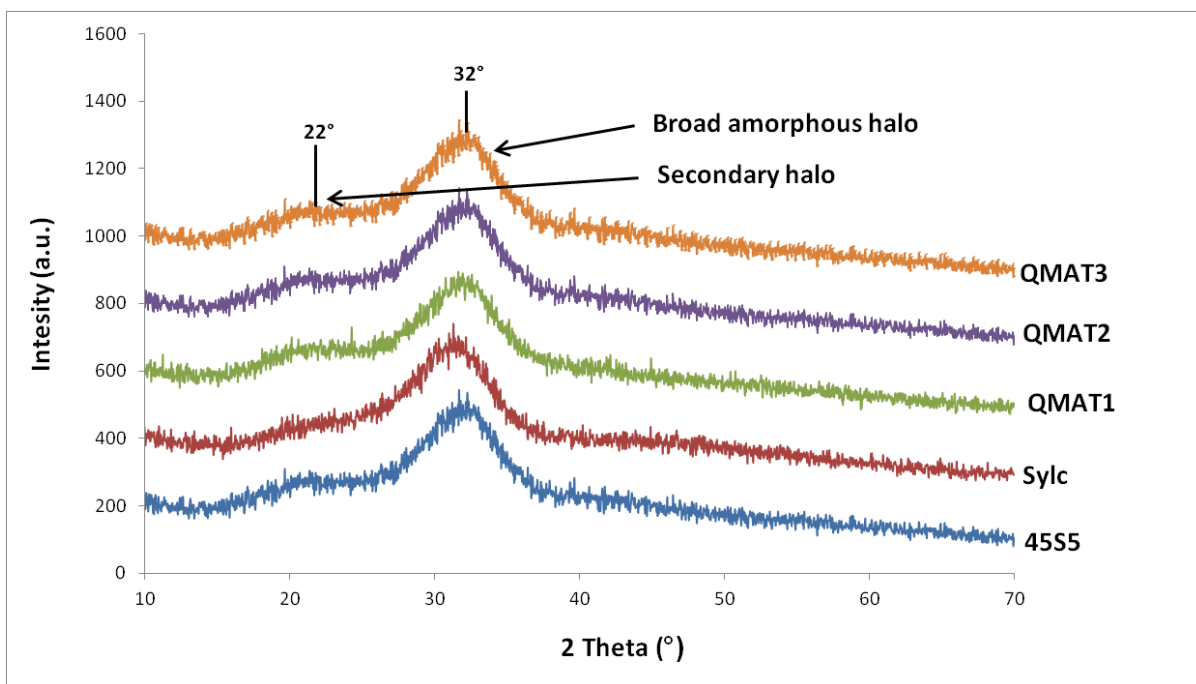


Figure 6.2. XRD data for untreated 45S5, Sylc™ and experimental glasses (QMAT1, QMAT2, QMAT3)

Conversely, the XRD patterns of both QMAT4 and QMAT5 (Figure 6.3) confirmed that they contained crystalline phases, due to the presence of distinct diffraction peaks between 20° 2θ and 70° 2θ instead of the smooth, broad halos that were observed with the amorphous glasses (Mneimne *et al.*, 2011).

Results

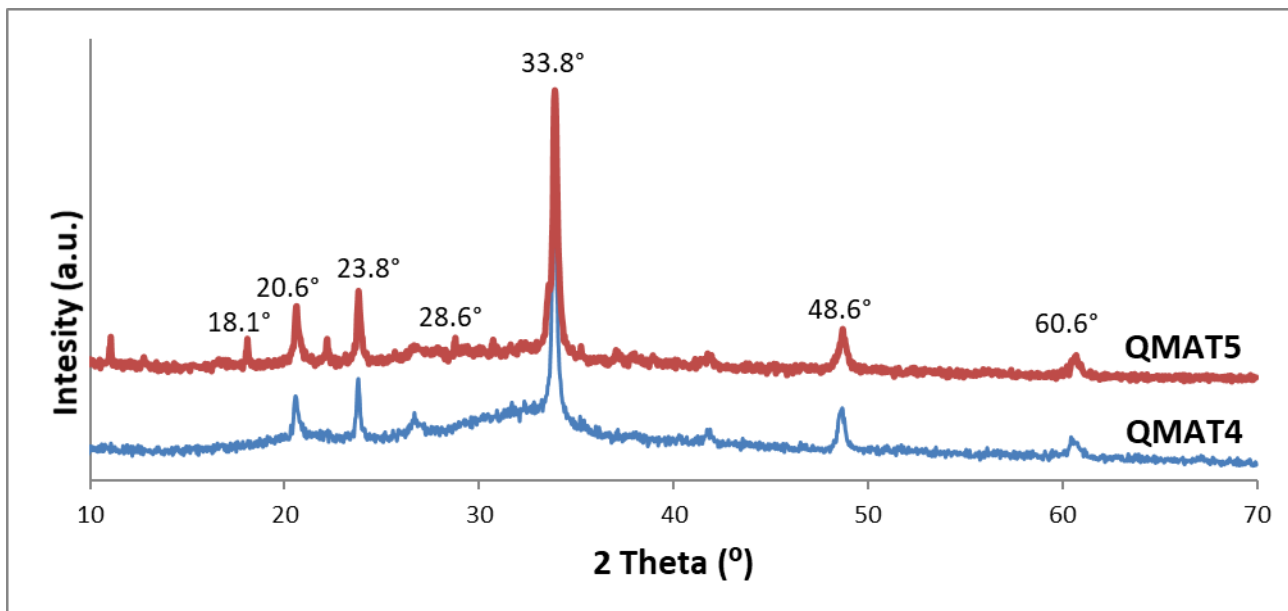


Figure 6.3. XRD data of QMAT4 and QMAT5

These crystalline phases were Portlandite (Calcium Hydroxide; reference code 01-078-0315) and Sodium Calcium Silicate ($\text{Na}_2\text{Ca}(\text{SiO}_4)$; reference code 04-012-6691). The 2 Theta and intensity (%) of the most characteristic reflections of the phases of interest for both crystalline phases from their JCPD files are shown in Tables 6.1 and 6.2, respectively. In addition, the stick pattern for both crystalline phases are also represented in Figure 6.4 and 6.5, respectively.

Table 6.1. Most characteristic reflections of Portlandite from its JCPD file

Reference pattern: Portlandite (Calcium hydroxide), 01-078-0315	
2 Theta (degree)	Intensity (%)
18.1	74.1
28.6	18.9
34.1	100.0
47.2	39.3

Results

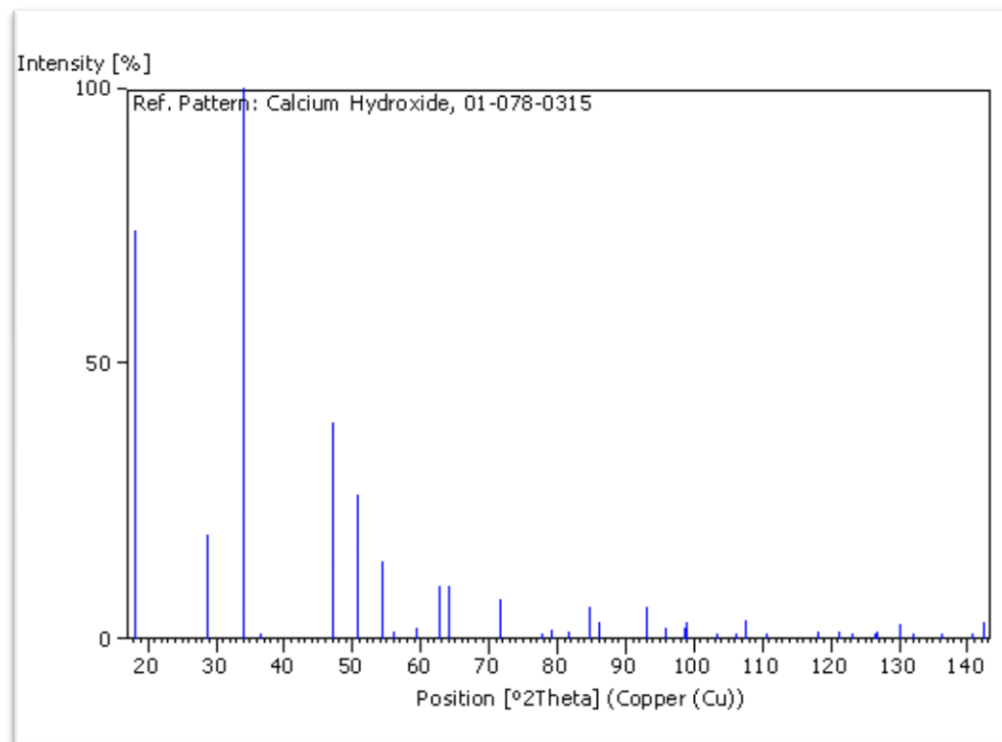


Figure 6.4. Stick pattern of Portlandite (Calcium Hydroxide)

Table 6.2. Most characteristic reflections of Sodium Calcium Silicate from its JCPD file

Reference pattern: Sodium Calcium Silicate, 04-012-6691	
2 Theta (degree)	Intensity (%)
20.5	36.1
33.8	100.0
48.6	15.3
60.5	31.0

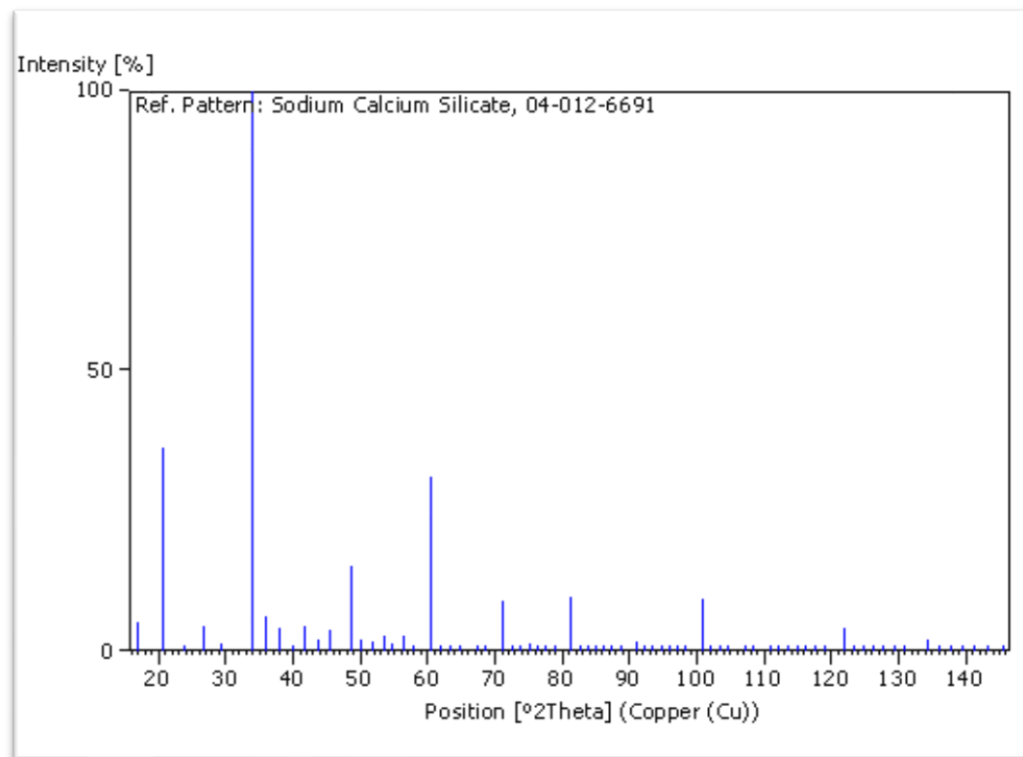


Figure 6.5. Stick pattern of Sodium Calcium Silicate ($\text{Na}_2\text{Ca} (\text{SiO}_4)$)

The XRD patterns for all seven glasses were in agreement with the findings observed from the ATR-FTIR spectra. Further experiments with both QMAT4 and QMAT5 experimental glasses were discontinued at this stage because their crystalline structure will have affected their dissolution rates and bioactivity (apatite formation).

6.2.2. Glass thermal analysis

The glass transition temperature (T_g), crystalline peak temperature (T_c) and melting temperature (T_m) of 45S5, SylcTM and experimental glasses are shown in Table 6.3. The T_g was 530°C for 45S5 with sodium and phosphate and silica contents of 24.4mol% 2.6mol% and 46.1mol%, respectively. A similar T_g was recorded for SylcTM, while the T_g of experimental glasses decreased as the sodium and phosphate content increased in each formulation. For example, the T_g of QMAT3 reduced to 355°C as the

Results

sodium and phosphate content increased to 30mol% and 6.1mol%, respectively, with a constant ratio of fluoride (3mol%) and a reduction in silica to 37mol%.

Table 6.3. T_g, T_c, and T_m of 45S5, Sylc™ and experimental glasses.

Bioactive Glasses	T _g (°C)	T _c (°C)	T _m (°C)
45S5	530	741	1450
Sylc™	530	741	1450
QMAT1	524	689	1440
QMAT2	450	647	1430
QMAT3	355	555	1420

6.2.3. Glass hardness measurements

The Vickers hardness number (VHN) decreased dramatically (Table 6.4) from 472.8±2.28VHN (~4.63GPa) and 475.7±2.07VHN (~4.66GPa) for Sylc™ and 45S5, respectively, to 350.4±1.14VHN (~3.43GPa) for QMAT3. The experimentally-determined VHN were converted to GPa units using the following equation:

$$\text{GPa} = \text{VHN} \times 0.009807.$$

Table 6.4. Hardness measurements (VHN and GPa) of 45S5, Sylc™ and experimental glasses.

Bioactive Glasses	Vickers Hardness Number (VHN) Mean ± SD	Hardness (GPa) (Mean± SD)
45S5	475.7 ± 2.07	4.66 ± 0.02
Sylc™	472.8 ± 2.28	4.63 ± 0.01
QMAT1	458.6 ± 2.50	4.49 ± 0.02
QMAT2	458.6 ± 2.50	4.25 ± 0.02
QMAT3	350.4 ± 1.14	3.43 ± 0.01

Results

6.2.4. Glass bioactivity dissolution studies

6.2.4.1. Tris buffer solution studies at pH 7.3 and 9

a. Tris buffer solution (pH = 7.3)

After immersion in Tris buffer solution (pH 7.3) for 1, 3, 6, 9 and 24 hours, the ATR-FTIR spectra of all experimental glasses (QMAT1, QMAT2, QMAT3) showed dramatic changes compared to their corresponding untreated (before immersion) versions (Figure 6.6 and 6.8). These changes were signified by a reduction in the intensity of the non-bridging oxygen (Si-O⁻-alkali⁺, NBO) band at 920cm⁻¹ after immersion for 1 hour. This band disappeared with longer immersion times suggesting rapid glass degradation. In addition, a single P-O vibration band appeared at 560cm⁻¹ after 3 hours, which indicated the presence of apatite precursors (Jones *et al.*, 2001). At 6 hours, the latter band split into prominent twin bands at 560cm⁻¹ and 600cm⁻¹, which became well-defined with longer immersion times. These twin bands indicated the presence of apatitic (PO₄)³⁻ groups, the main characteristic feature of apatite formation, including hydroxyapatite, fluorapatite and carbonated hydroxyapatite (Kim *et al.*, 1989; Peitl Filho *et al.*, 1996). The formation of apatite was confirmed by the presence of a sharp phosphate band at 1030 cm⁻¹ following 6, 9 and 24 hours of immersion (Jones *et al.*, 2001). Conversely, 45S5 and SylcTM did not show any bands at 560cm⁻¹ and 600cm⁻¹, with the further absence of the sharp phosphate band at 1030cm⁻¹ at 6 hours. Apatite formation features (twin bands at 560cm⁻¹ and 600cm⁻¹, and a sharp phosphate band (PO₄)³⁻ at 1030cm⁻¹) in 45S5 and SylcTM glass appeared at 24 hours, but these were less prominent compared to those obtained for all experimental glasses (Figure 6.9 and 6.10).

Results

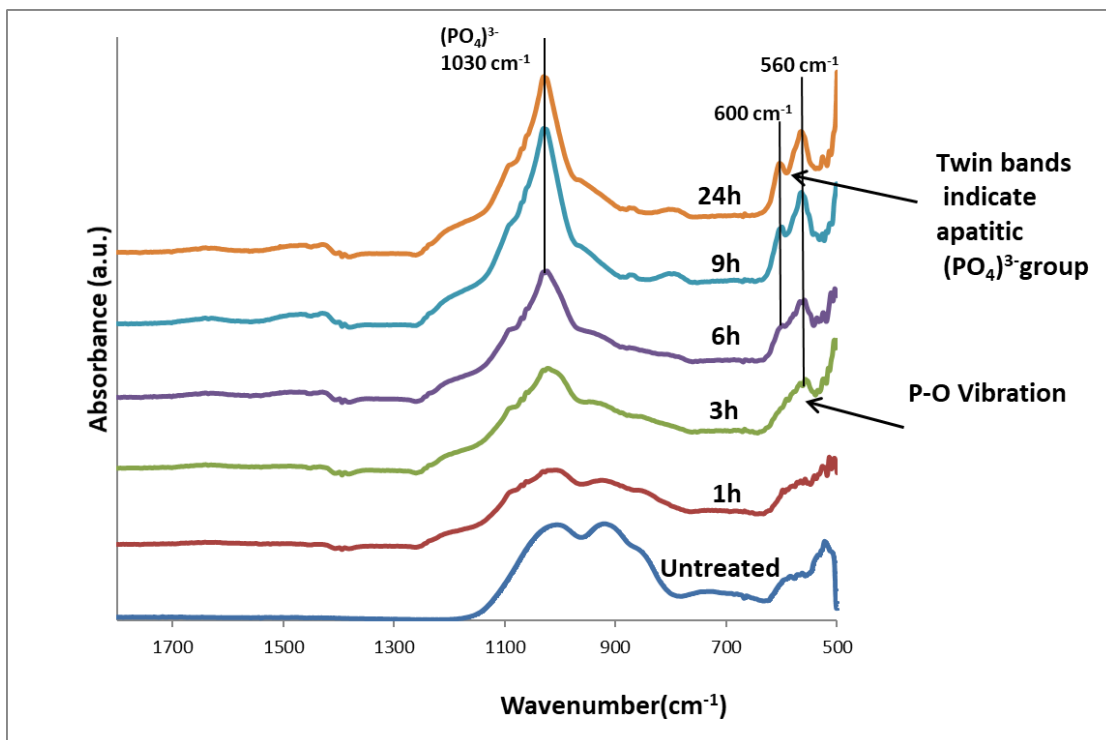


Figure 6.6. ATR-FTIR spectra of QMAT1 glass after immersion in Tris buffer solution (pH=7.3)

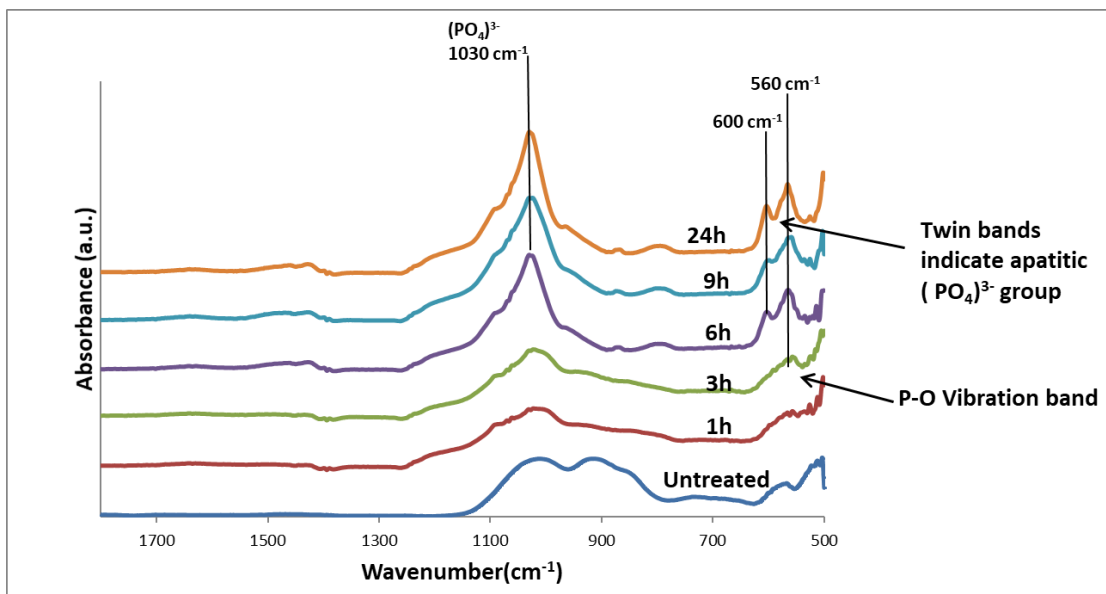


Figure 6.7. ATR-FTIR spectra of QMAT2 glass after immersion in Tris buffer solution (pH=7.3)

Results

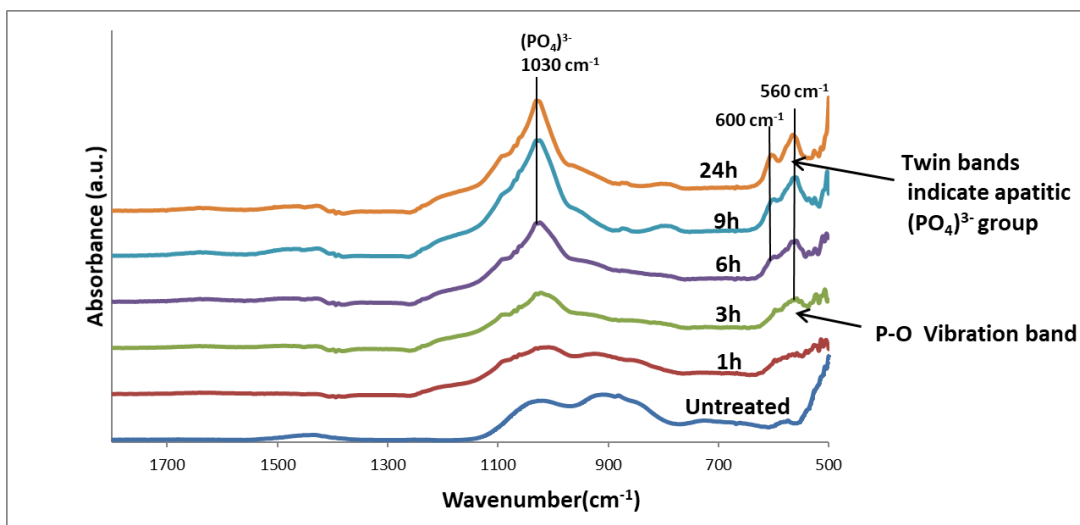


Figure 6.8. ATR-FTIR spectra of QMAT3 glass after immersion in Tris buffer solution (pH=7.3)

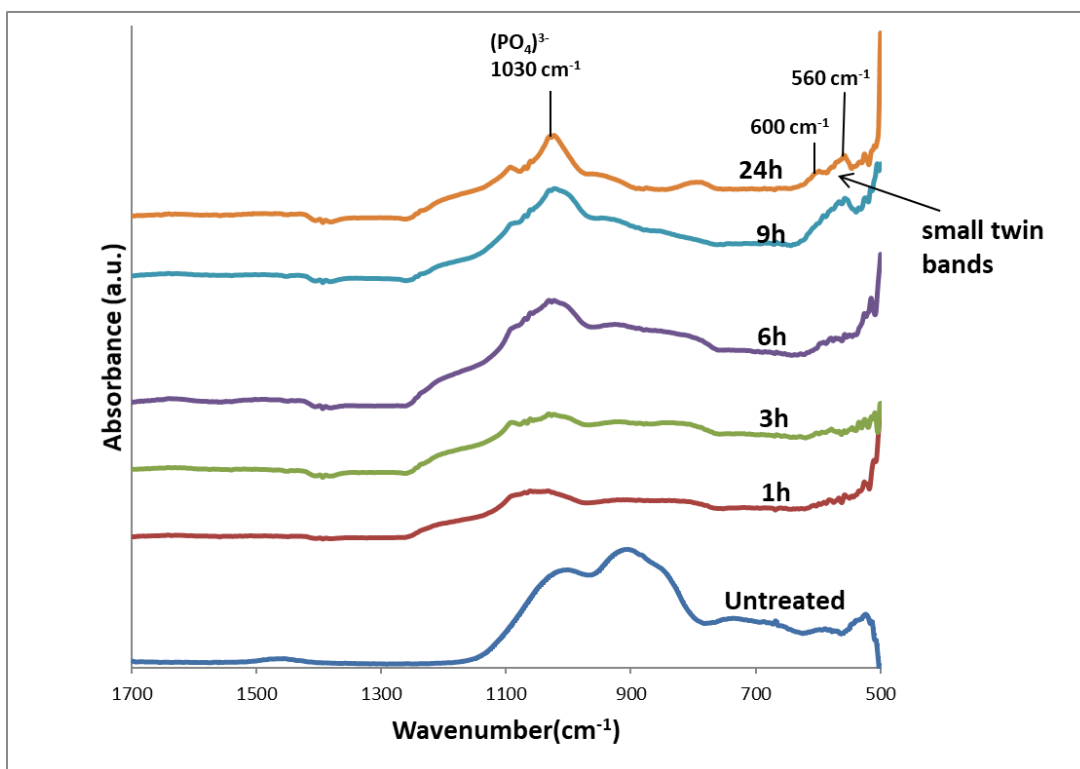


Figure 6.9. ATR-FTIR spectra of 45S5 glass after immersion in Tris buffer solution (pH=7.3)

Results

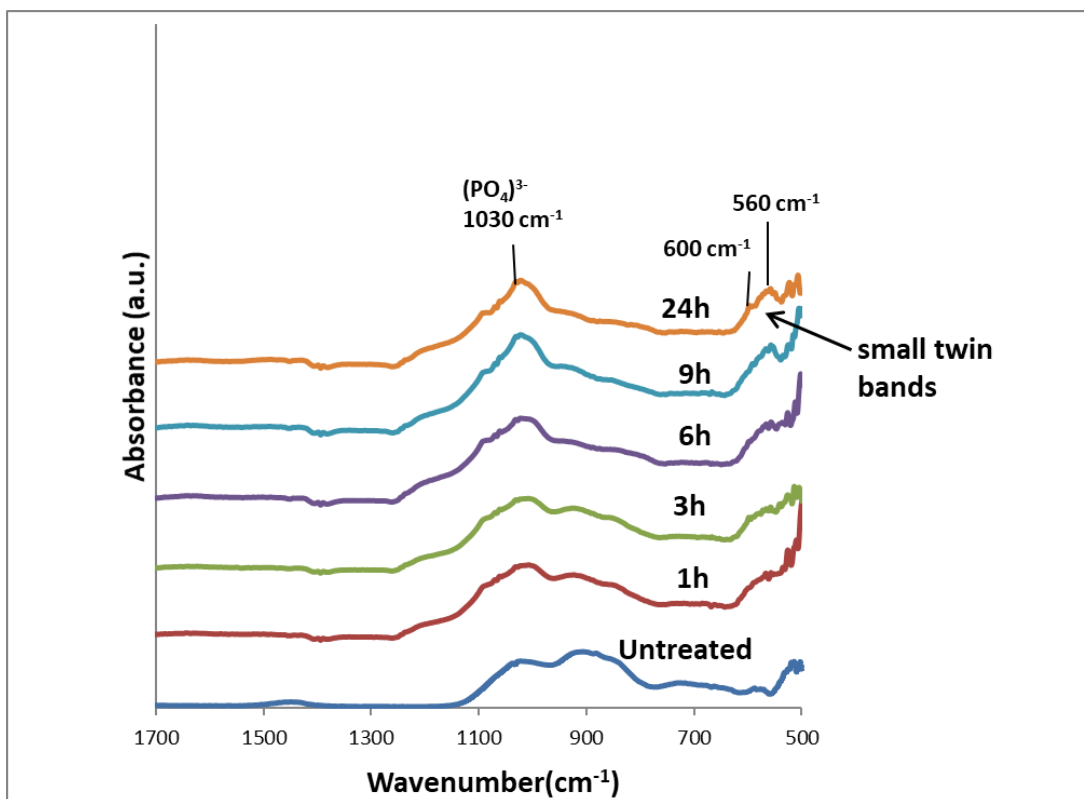


Figure 6.10. ATR-FTIR spectra of Syc™ glass after immersion in Tris buffer solution (pH=7.3)

The XRD patterns of all experimental glasses showed a small peak at 26° and a broad peak from 32° to 34° 2θ, after 6 hours of immersion in Tris buffer solution (pH 7.3), superimposing the amorphous broad peak of untreated glass and the glasses that were immersed for 1 hour and 3 hours, respectively (Figures 6.11 to 6.13). These two peaks, indicating the presence of apatite, became more pronounced as the immersion time increased. However, all the aforementioned peaks were absent in 45S5 and Syc™ (Figures 6.14 and 6.15, respectively) until 24 hours, when much smaller peaks indicative of apatite appeared (Mneimne *et al.*, 2011).

Results

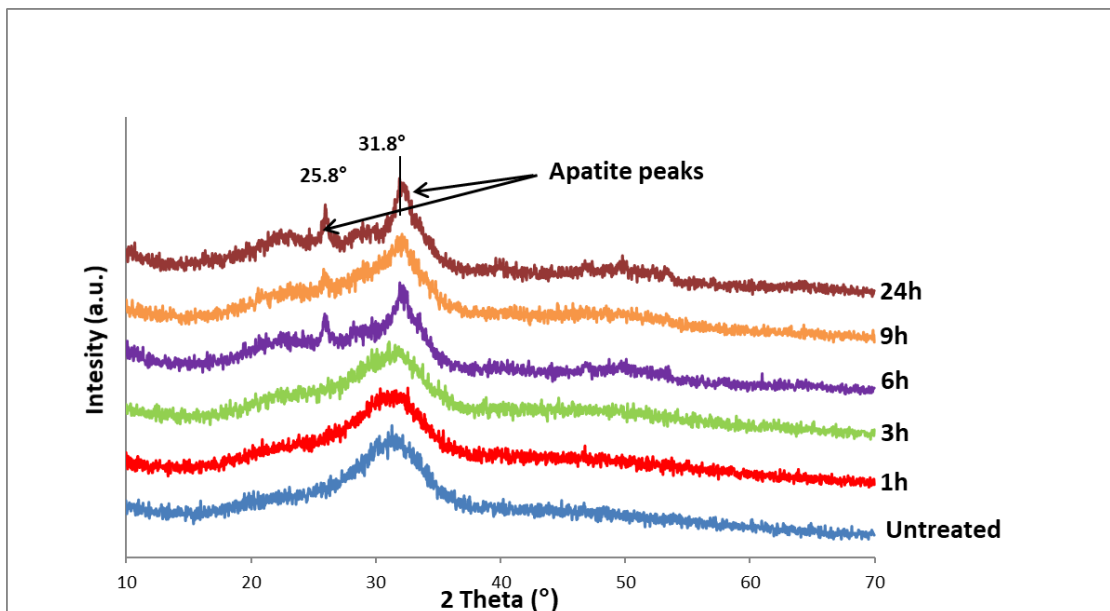


Figure 6.11. XRD patterns of QMAT1 glass after immersion in Tris buffer solution (pH=7.3)

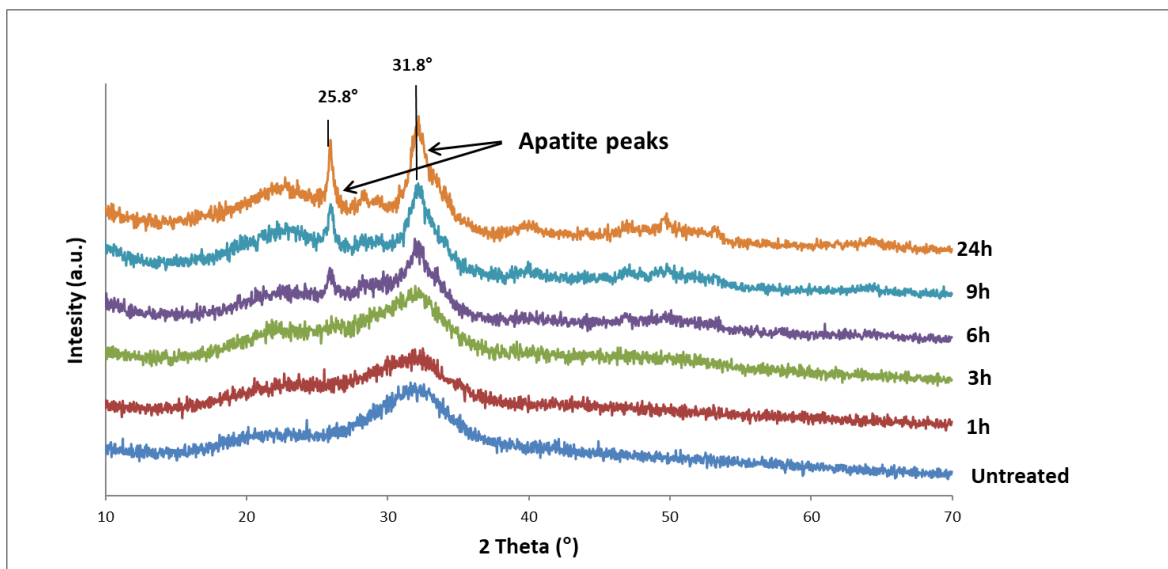


Figure 6.12. XRD patterns of QMAT2 glass after immersion in Tris buffer solution (pH=7.3)

Results

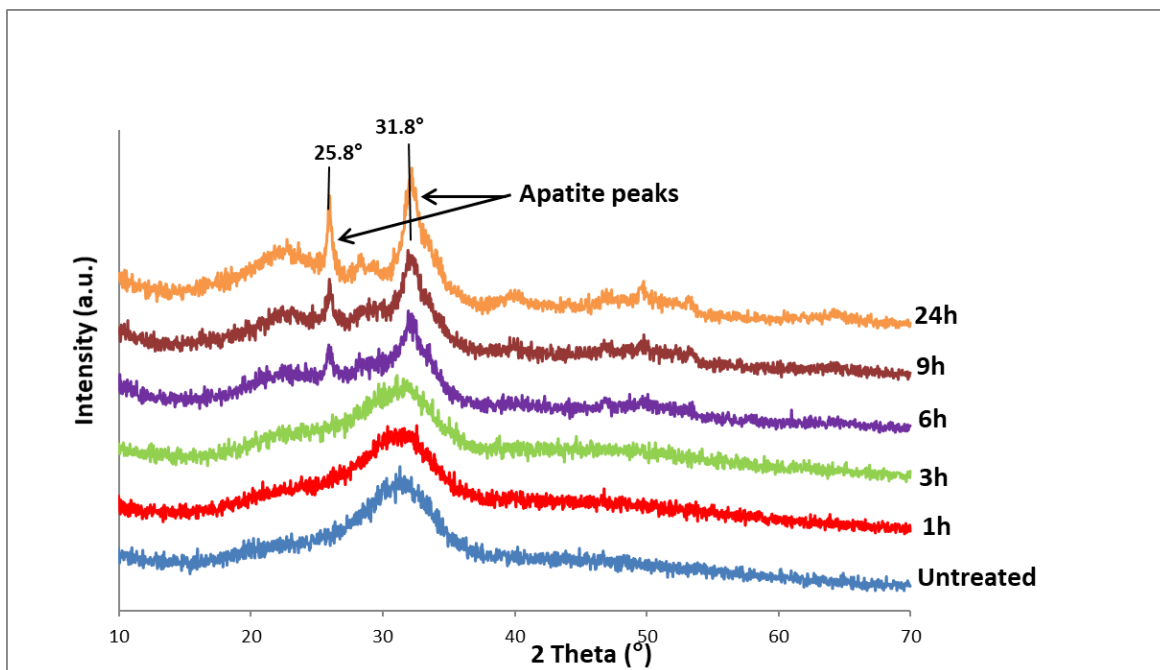


Figure 6.13. XRD patterns of QMAT3 glass after immersion in Tris buffer solution (pH=7.3)

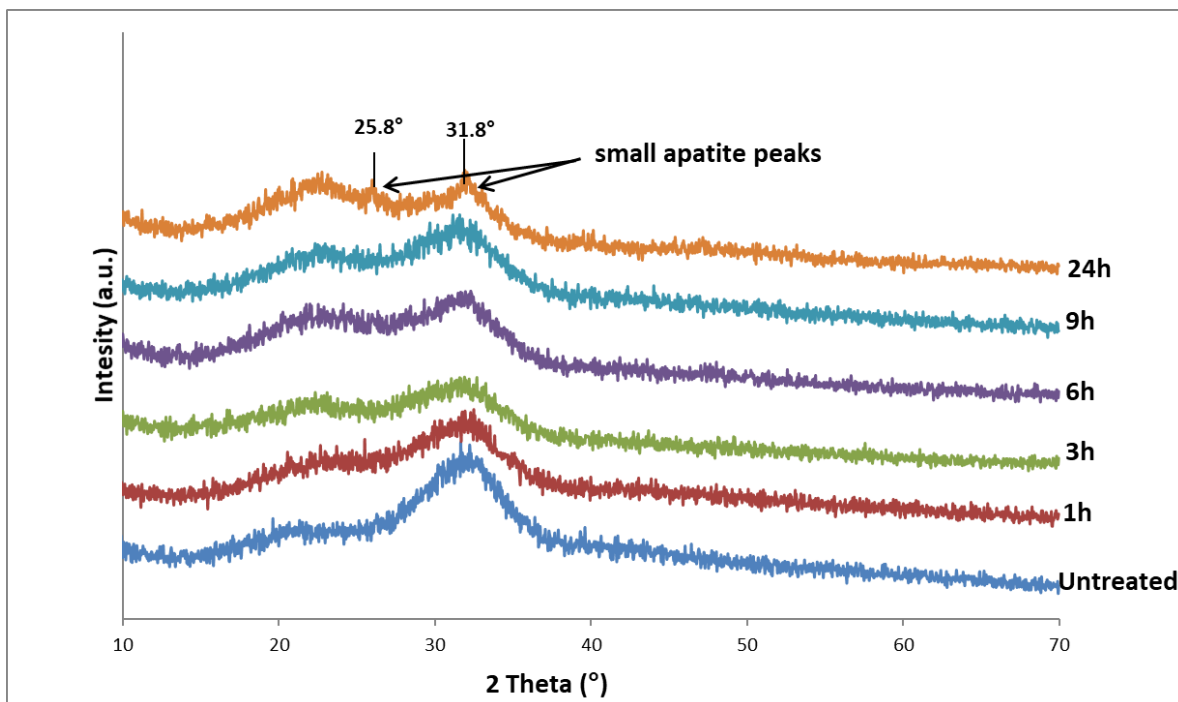


Figure 6.14. XRD patterns of 45S5 glass after immersion in Tris buffer solution (pH=7.3)

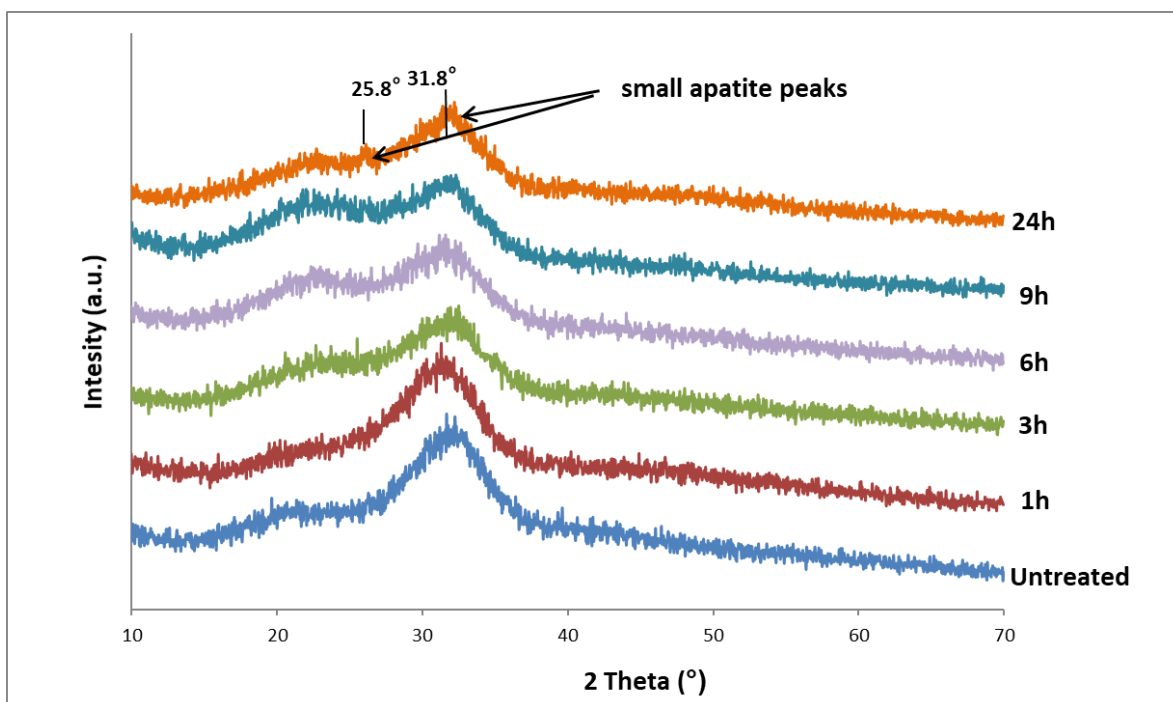


Figure 6.15. XRD patterns of Sylc™ glass after immersion in Tris buffer solution (pH=7.3)

The pH changes of Tris buffer solution (initial pH 7.3) were also recorded for all experimental glasses, 45S5 and Sylc™ to observe their dissolution behaviour. The recorded data (Figure 6.16) clearly indicated a rise in pH for all glasses at each designated time interval in comparison with the control solution (unreacted Tris buffer solution). This rise in pH of Tris buffer solution was significant after 6 hours of immersion for all experimental glasses (QMAT1, QMAT2, and QMAT3), increasing steadily up to 24 hours, peaking at 7.66, 7.75 and 7.82, respectively. Conversely, the rise in pH of Tris buffer solution after immersion of both 45S5 and Sylc™ was limited until 9 hours; thereafter, a sharp increase occurred in the pH level to 7.58 for 45S5 and 7.62 for Sylc™ at 24 hours of immersion.

Results

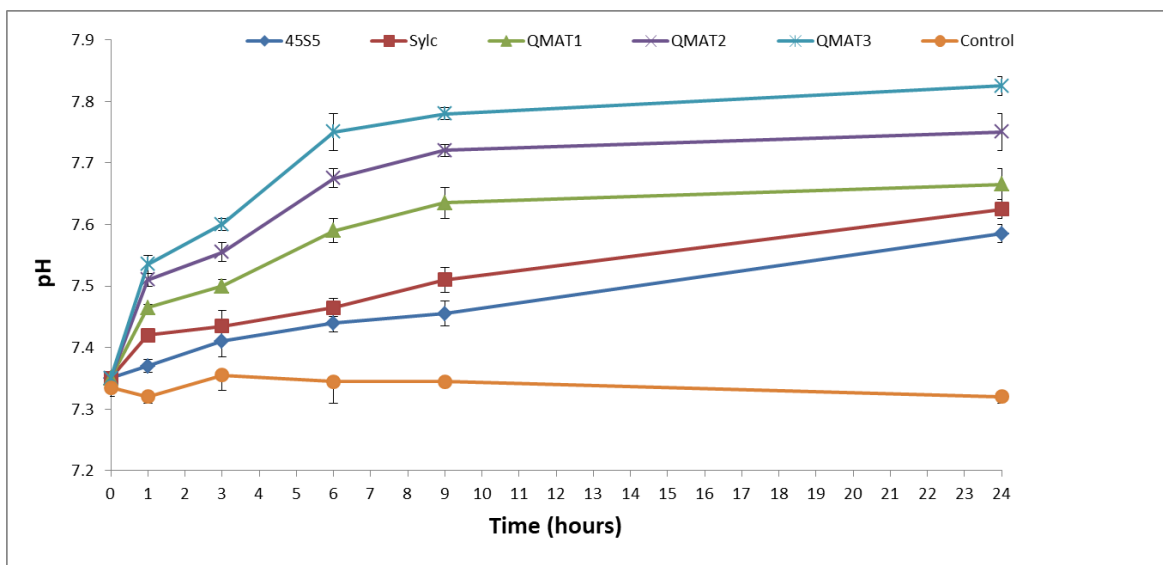


Figure 6.16. The pH change of Tris buffer solution (initial pH=7.3) after immersion of 45S5, Sylc™ and experimental glasses (QMAT1, QMAT2, and QMAT3) plotted against the designated immersion time intervals (1, 3, 6, 9 and 24 hours). * Error bars represent the range of pH measured on 2 independent occasions. Where error bars are not shown, the error was smaller than the data point

b. Tris buffer study (pH=9)

The ATR-FTIR spectra of experimental glasses (QMAT1, QMAT2, and QMAT3) after immersion in Tris buffer solution of initial pH=9 showed no pronounced changes in comparison to their corresponding untreated versions until 6 hours (Figures 6.17 to 6.19). At 6 hours, the intensity of the non-bridging oxygen ($\text{Si}^+\text{-O}^-$ alkali $^+$, NBO) band at 920cm^{-1} slightly decreased suggesting that some ion exchange had occurred. Thereafter, a single P–O vibration band appeared at 560cm^{-1} after 9 hours, which indicated the presence of apatite precursors (Jones *et al.*, 2001). At 24 hours, the latter band split into prominent twin bands at 560cm^{-1} and 600cm^{-1} , corresponding to apatitic $(\text{PO}_4)^{3-}$ groups and indicating the formation of apatite (Kim *et al.*, 1989; Peitl Filho *et al.*, 1996). The formation of apatite was confirmed by the presence of a sharp phosphate band at 1030cm^{-1} . Conversely, both 45S5 and Sylc™ did not show any changes until 24 hours, when a slight reduction in the intensity of the non-bridging oxygen band at 920cm^{-1} was barely observed (Figures 6.20 and 6.21, respectively).

Results

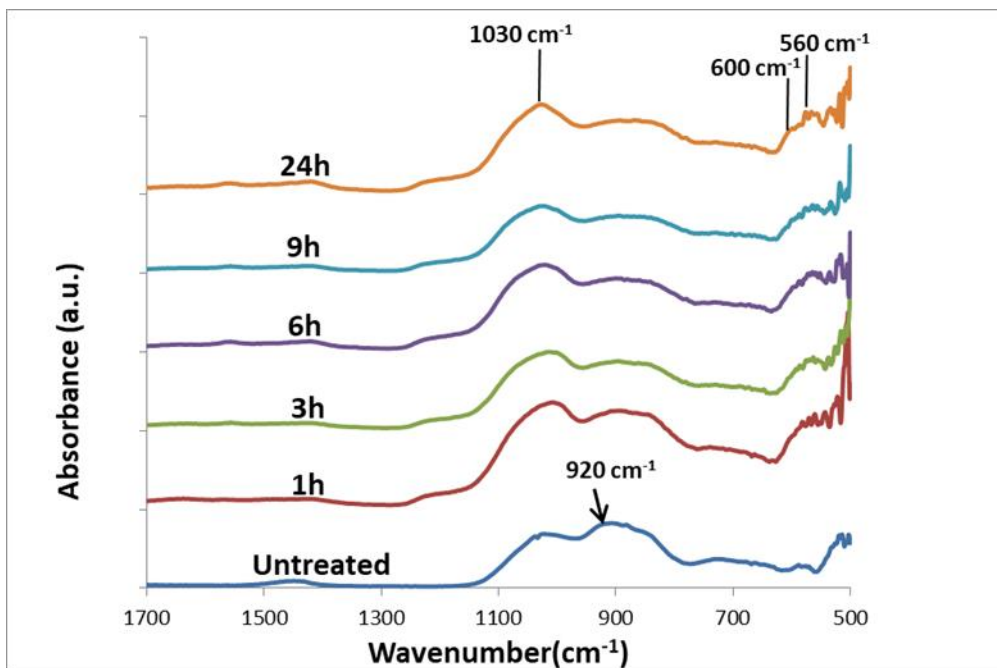


Figure 6.17. ATR-FTIR spectra of QMAT1 glass after immersion in Tris buffer solution (pH=9)

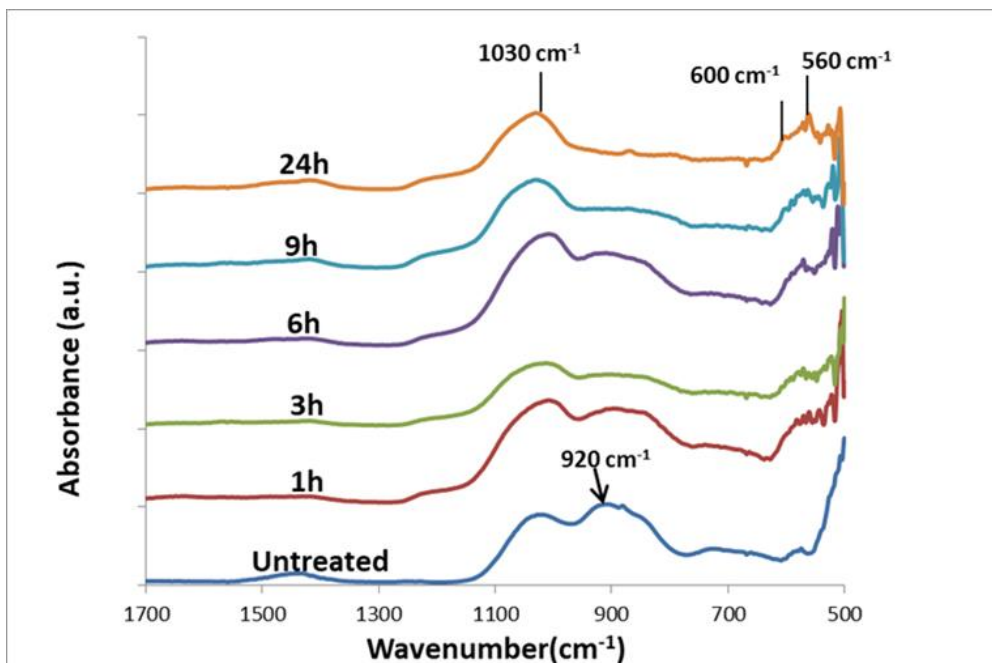


Figure 6.18. ATR-FTIR spectra of QMAT2 glass after immersion in Tris buffer solution (pH=9)

Results

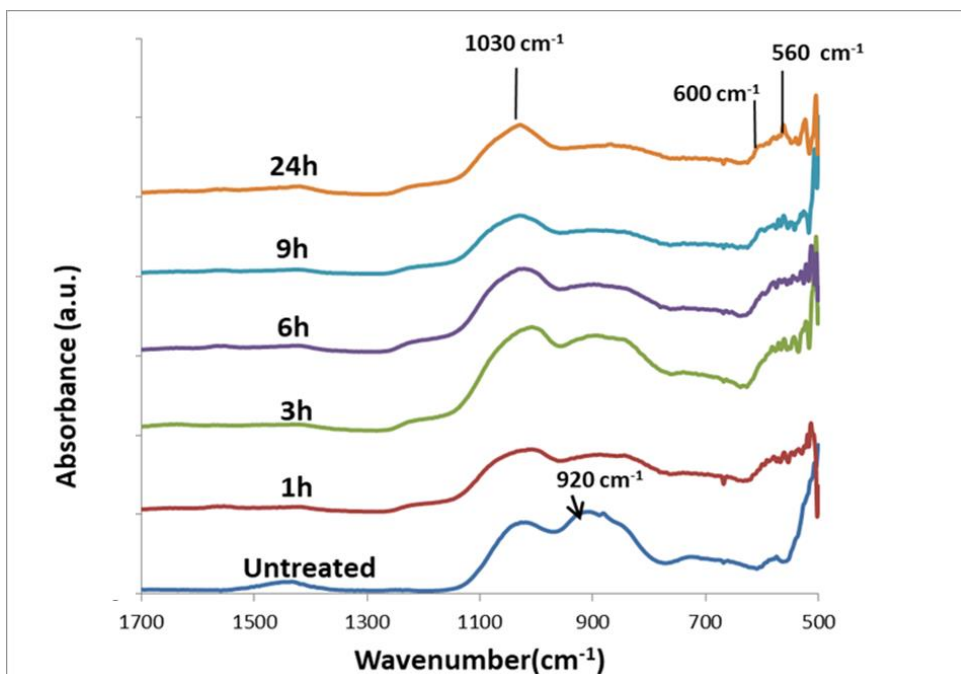


Figure 6.19. ATR-FTIR spectra of QMAT3 glass after immersion in Tris buffer solution (pH=9)

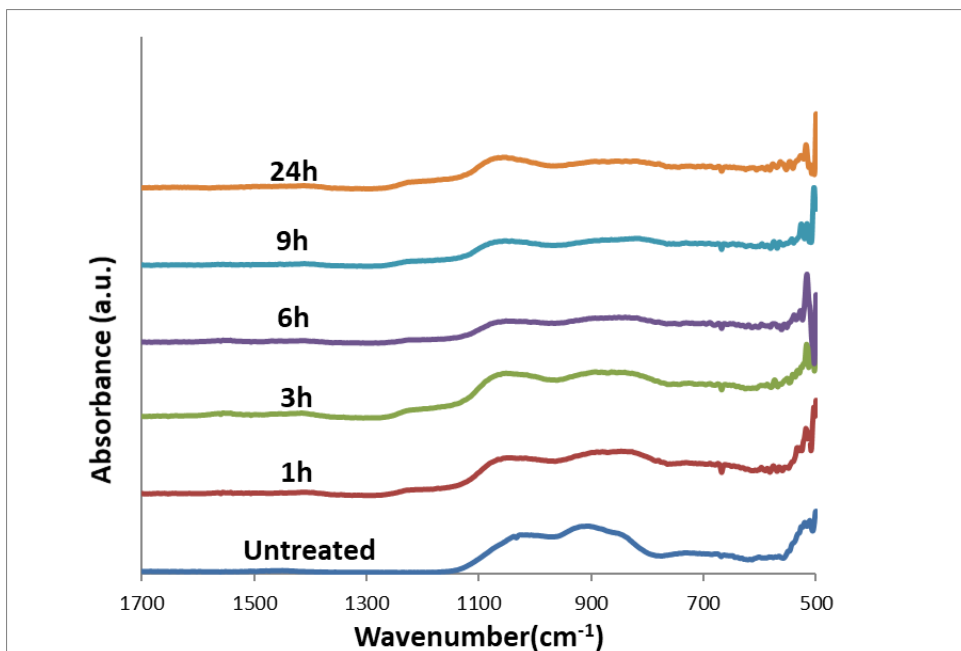


Figure 6.20. ATR-FTIR spectra of 45S5 glass after immersion in Tris buffer solution (pH=9)

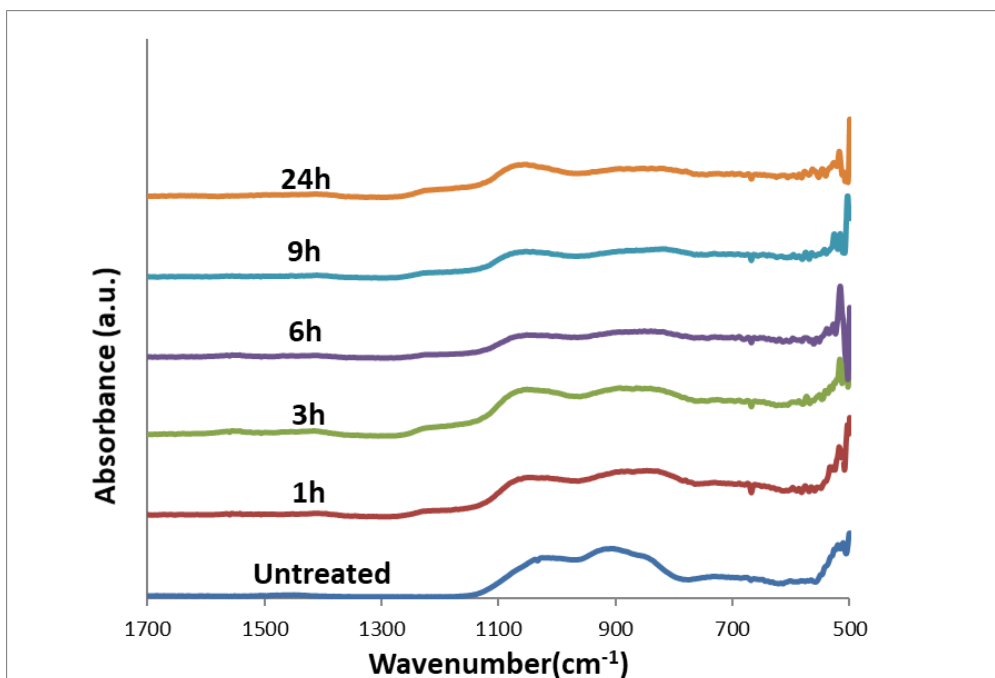


Figure 6.21. ATR-FTIR spectra of Sylc™ glass after immersion in Tris buffer solution (pH=9)

The XRD patterns verified the recorded ATR-FTIR findings for all glasses after immersion in Tris buffer solution of initial pH=9 with the presence of the typical apatite features (a small peak at 25.8° and a broad peak at 31.8°, described earlier in section 5.3.1b) for only experimental glasses (Figures 6.22 to 6.24) at 24 hours of immersion, and the absence of these apatite features for both 45S5 and Sylc™ glasses (Figures 6.25 and 6.26, respectively).

Results

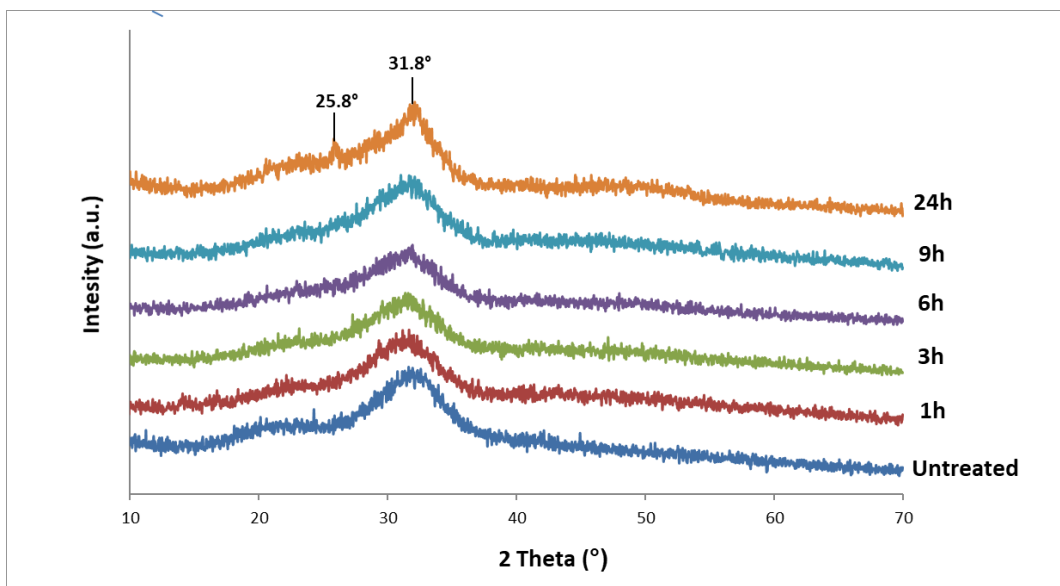


Figure 6.22. XRD patterns of QMAT1 glass after immersion in Tris buffer solution (pH=9)

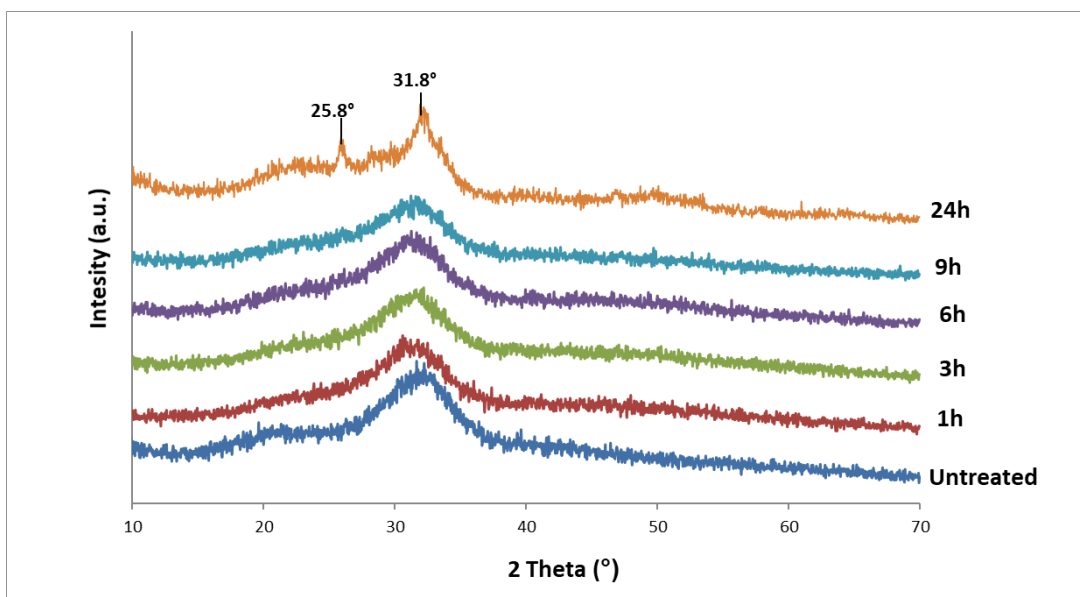


Figure 6.23. XRD patterns of QMAT2 glass after immersion in Tris buffer solution (pH=9)

Results

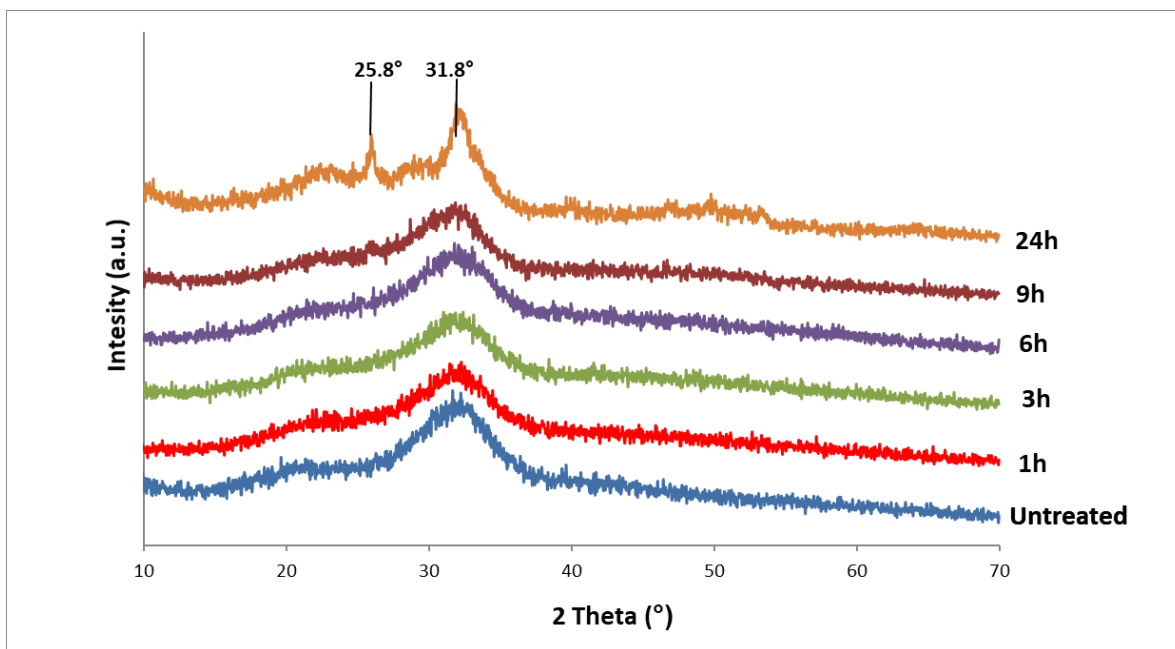


Figure 6.24. XRD patterns of QMAT3 glass after immersion in Tris buffer solution (pH=9)

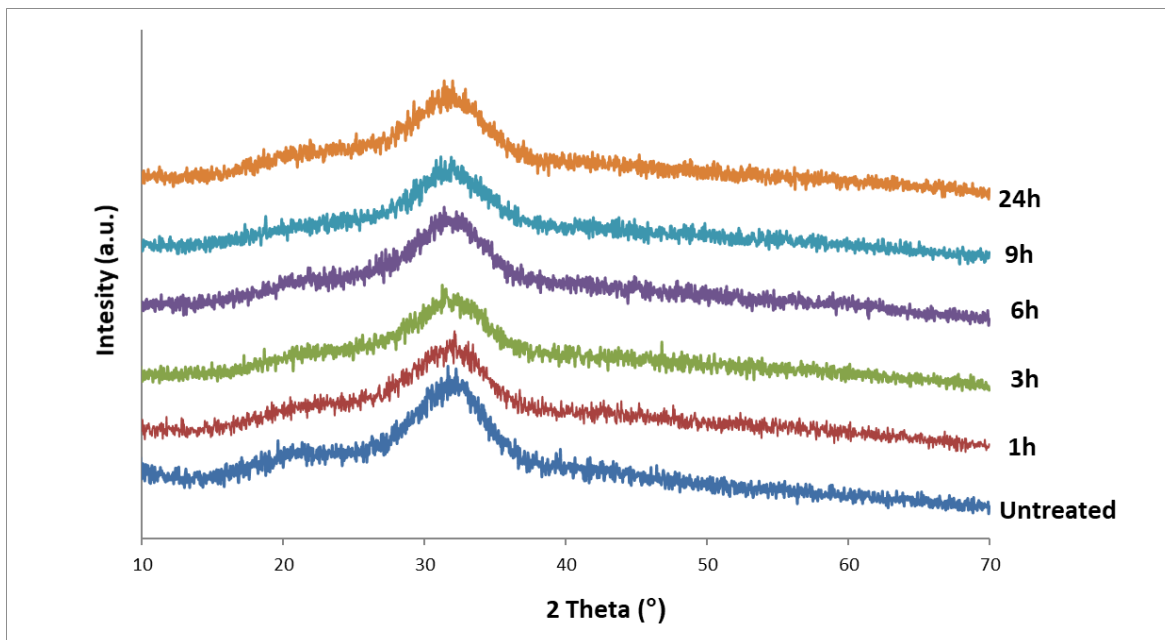


Figure 6.25. XRD patterns of 45S5 glass after immersion in Tris buffer solution (pH=9)

Results

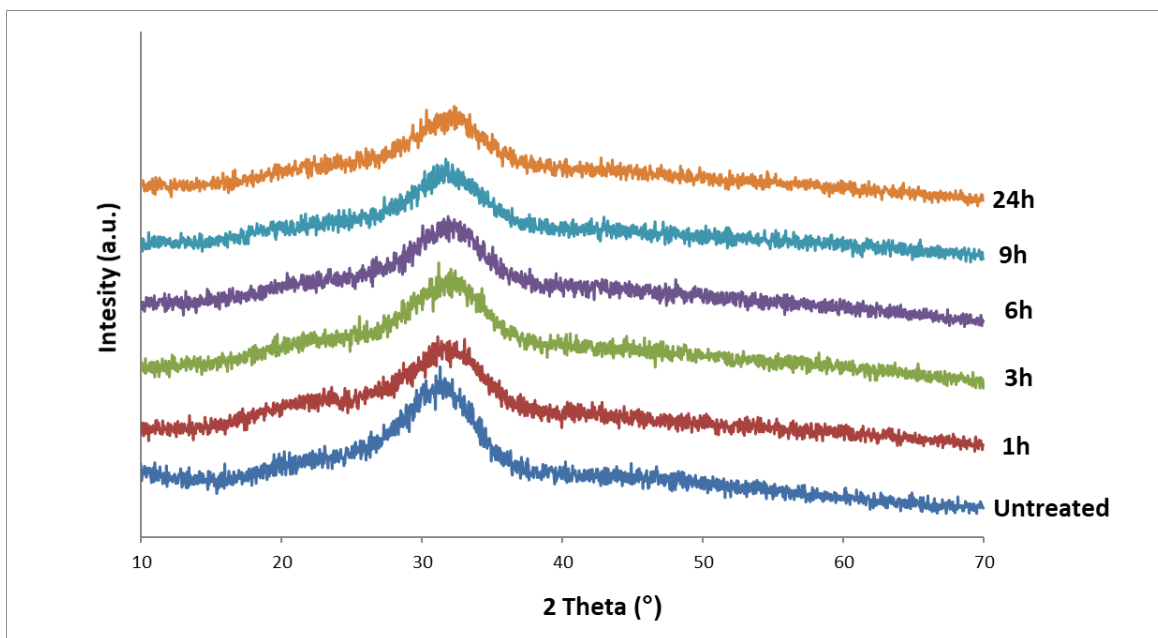


Figure 6.26. XRD patterns of Syc™ glass after immersion in Tris buffer solution (pH=9)

There were limited changes in the pH of Tris buffer solution of initial pH=9 (Figure 6.27) after immersion of both 45S5 and Syc™, while an increase in pH was observed at 24 hours for the experimental glasses only (QMAT1, QMAT2, and QMAT3) to 9.36, 9.43, and 9.51, respectively, indicating apatite formation and suggesting that this took longer at a higher pH (pH 9 compared with pH 7), as the rise in pH of the immersion solution indicated that the ion exchange between the glass (Na^+) and the immersion solution (H^+) occurred. This resulted in a decreased concentration of protons in the immersion solution and consequently a higher pH level.

Results

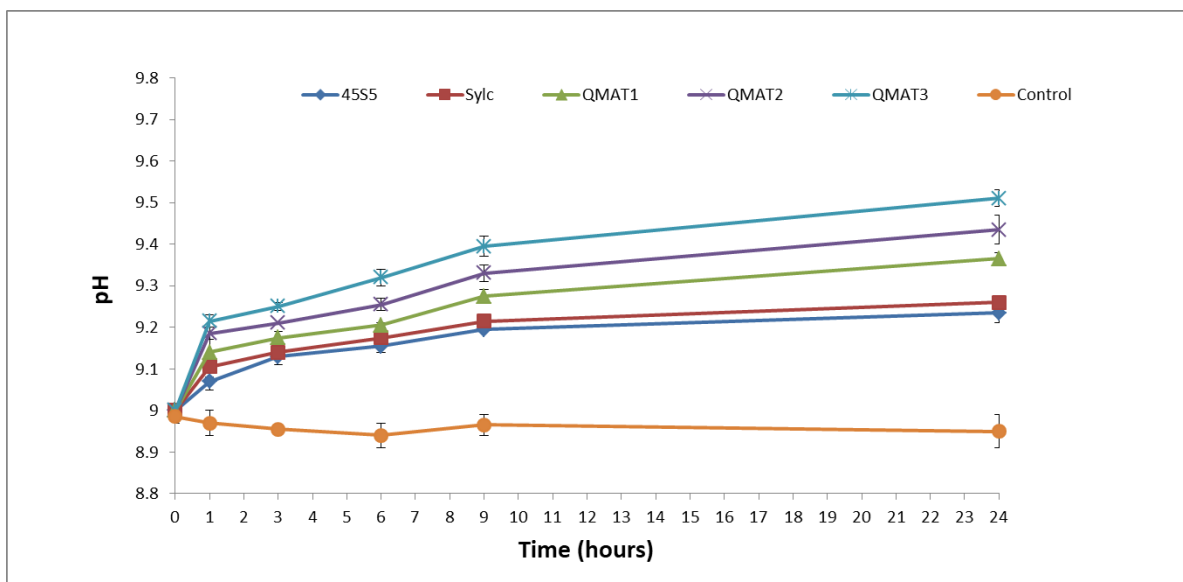


Figure 6.27. The pH change of Tris buffer solution (initial pH=9) after immersion of 45S5, Sylc™ and experimental glasses (QMAT1, QMAT2, and QMAT3) plotted against the designated immersion time intervals (1, 3, 6, 9 and 24 hours). * Error bars represent the range of pH measured on 2 independent occasions. Where error bars are not shown, the error was smaller than the data point

6.2.4.2. Acetic acid study

After immersion in acetic acid solution of initial pH=5, all experimental glasses (QMAT1, QMAT2, QMAT3) clearly showed the disappearance of the non-bridging oxygen ($\text{Si}^+\text{-O}^-$ -alkali $^+$, NBO) band at 920cm^{-1} at the earlier immersion time point (15 minutes). Additionally, a new band appeared at $\sim 790\text{cm}^{-1}$ after 3 hours corresponding to vibration of Si-O-Si bonds between adjacent SiO_4 tetrahedra, and indicating the dissolution of glasses (Brauer *et al.*, 2011). This was accompanied by the appearance of the typical characteristic features of apatite formation in ATR-FTIR spectra (twin bands at 560cm^{-1} and 600cm^{-1} , and a sharp phosphate band (PO_4^{3-} at 1030cm^{-1} ; Figures 6.28 to 6.30). Conversely, both 45S5 and Sylc™ showed these apatite features at 9 hours (Figures 6.31 and 6.32), suggesting that the dissolution of all experimental glasses was faster than with both 45S5 and Sylc™. In addition, the corresponding XRD patterns (Figures 6.33 to 6.37) showed similar trends for rate of apatite formation as observed in their ATR-FTIR spectra.

Results

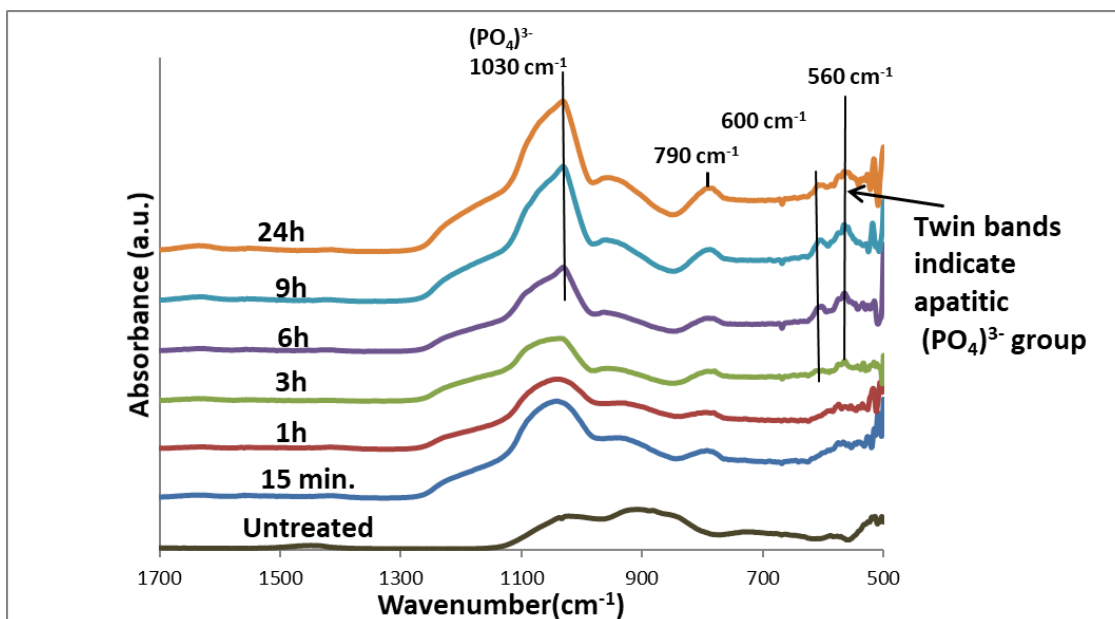


Figure 6.28. ATR-FTIR spectra of QMAT1 glass after immersion in acetic acid (pH=5)

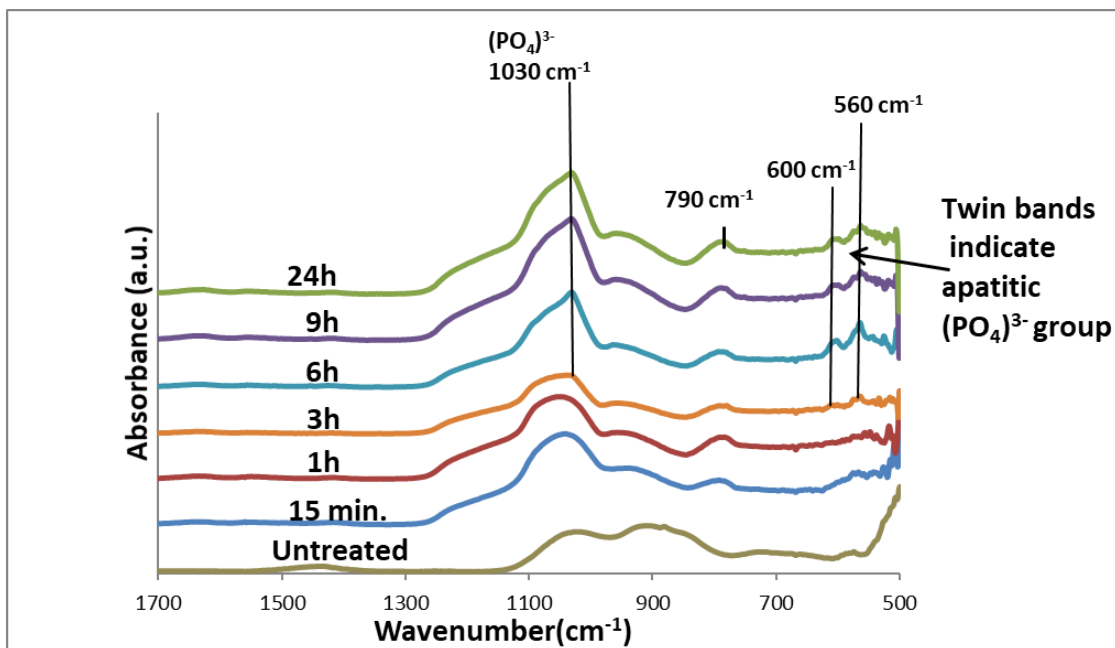


Figure 6.29. ATR-FTIR spectra of QMAT2 glass after immersion in acetic acid (pH=5)

Results

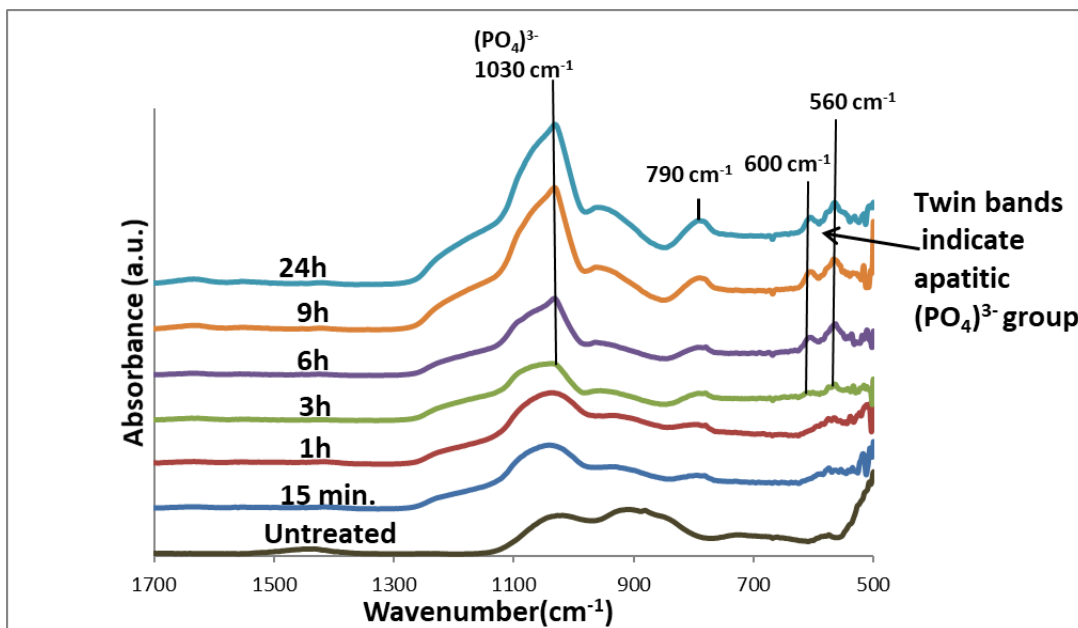


Figure 6.30. ATR-FTIR spectra of QMAT3 glass after immersion in acetic acid (pH=5)

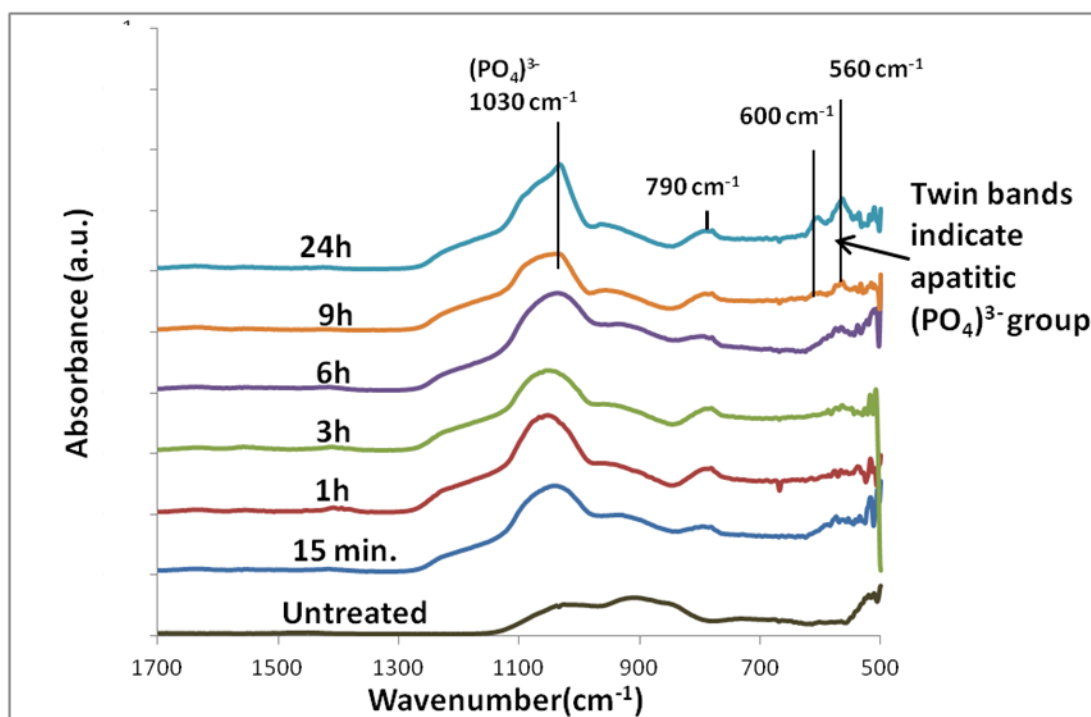


Figure 6.31. ATR-FTIR spectra of 45S5 glass after immersion in acetic acid (pH=5)

Results

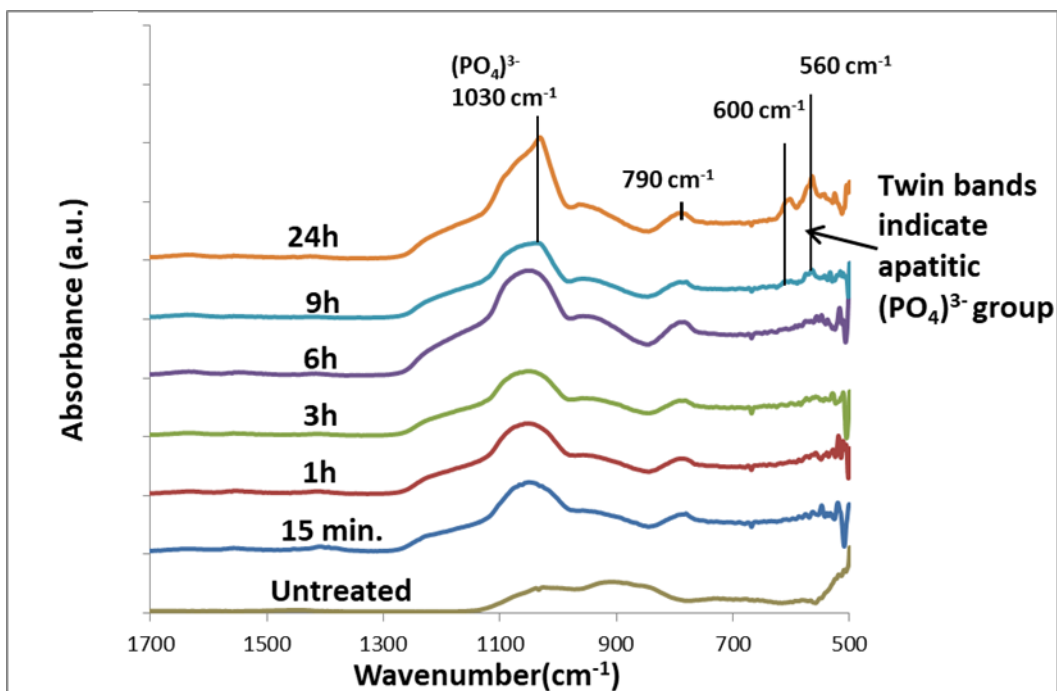


Figure 6.32. ATR-FTIR spectra of Sylc™ glass after immersion in acetic acid (pH=5)

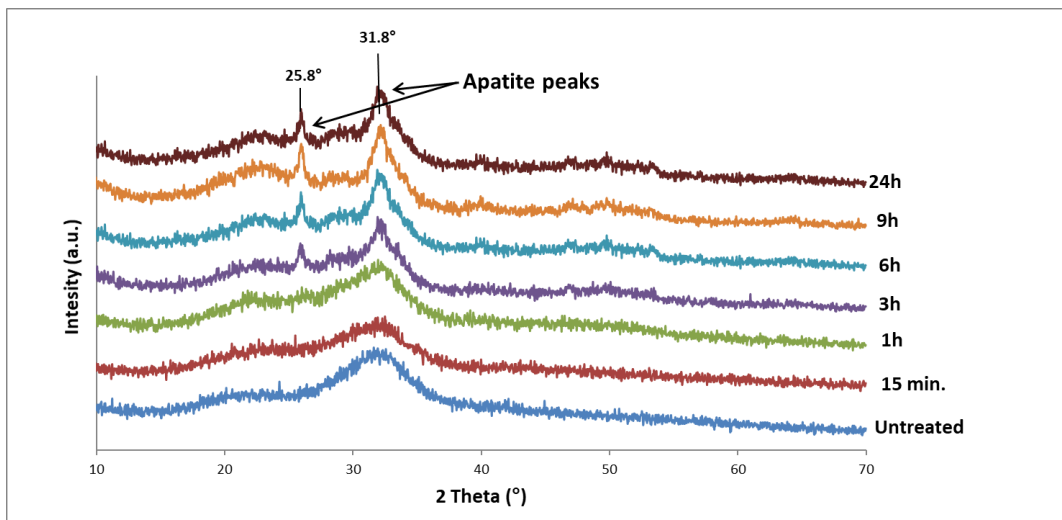


Figure 6.33. XRD patterns of QMAT1 glass after immersion in acetic acid (pH=5)

Results

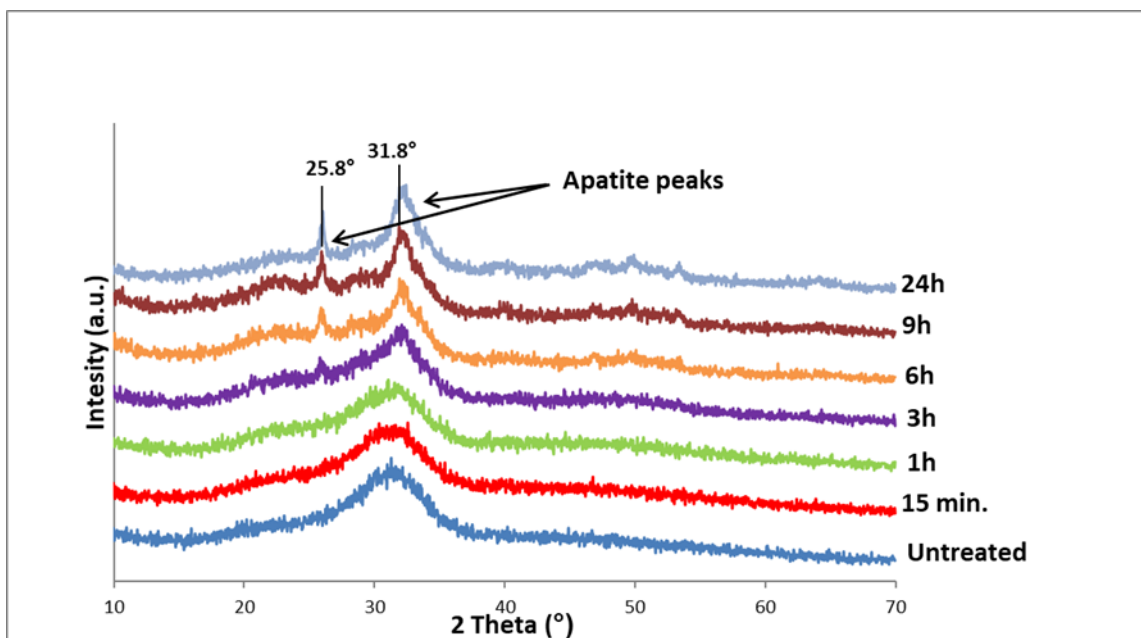


Figure 6.34. XRD patterns of QMAT2 glass after immersion in acetic acid (pH=5)

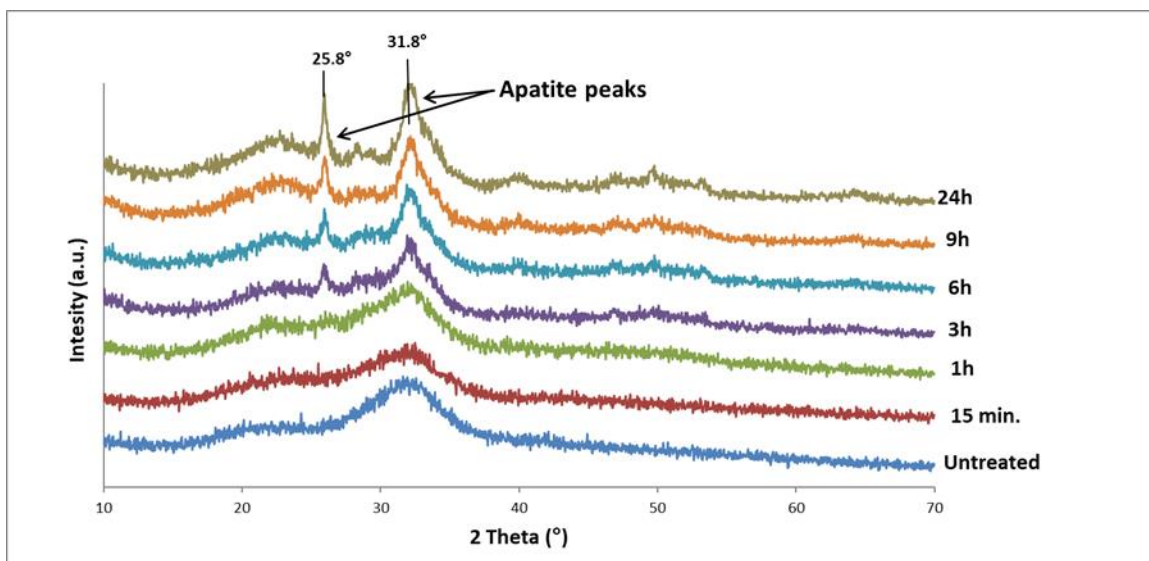


Figure 6.35. XRD patterns of QMAT3 glass after immersion in acetic acid (pH=5)

Results

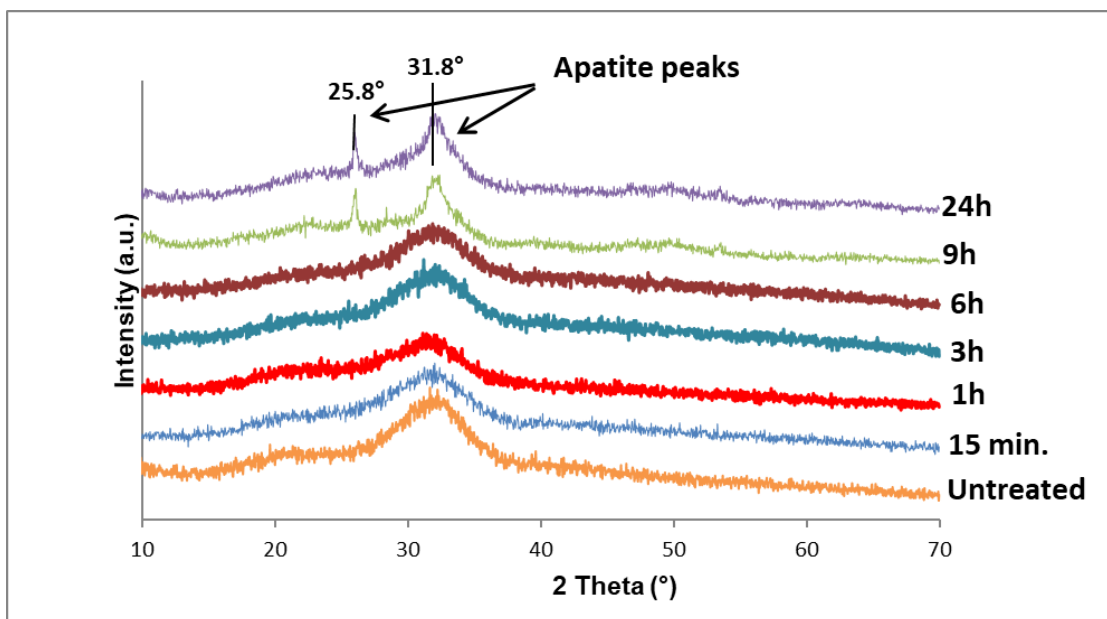


Figure 6.36. XRD patterns of 45S5 glass after immersion in acetic acid (pH=5)

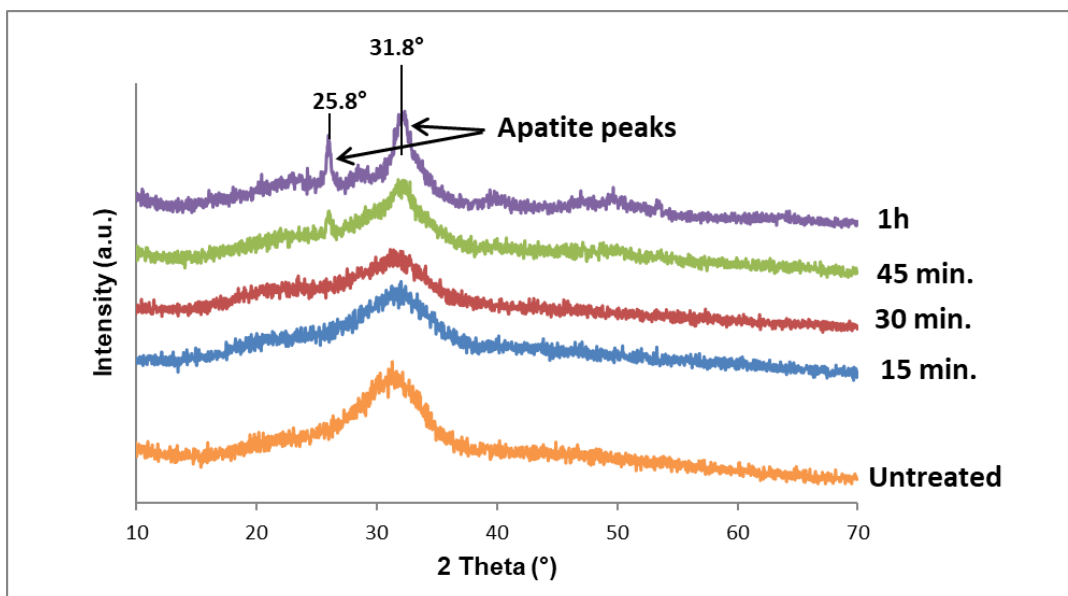


Figure 6.37. XRD patterns of Sylc™ glass after immersion in acetic acid (pH=5)

The change in pH of the acetic acid solution (initial pH 5; Figure 6.38), after immersion of experimental glasses clearly mirrored the ATR-FTIR and XRD observations with a rapid increase in pH level at earlier immersion time points (3 hours), reaching their

Results

highest levels at 6 hours (6.77, 7.13, and 7.34) respectively, followed by a steady pH level. Conversely, the pH of acetic acid solutions for both 45S5 and Sylc™ steadily increased until 6 hours reaching pH levels of 5.57 and 5.73, respectively. This was followed by a sharp increase at 9 hours to 5.97 and 6.2, respectively. As such, the pH rise associated with the experimental glasses was more significant and more rapid than with either 45S5 or Sylc™.

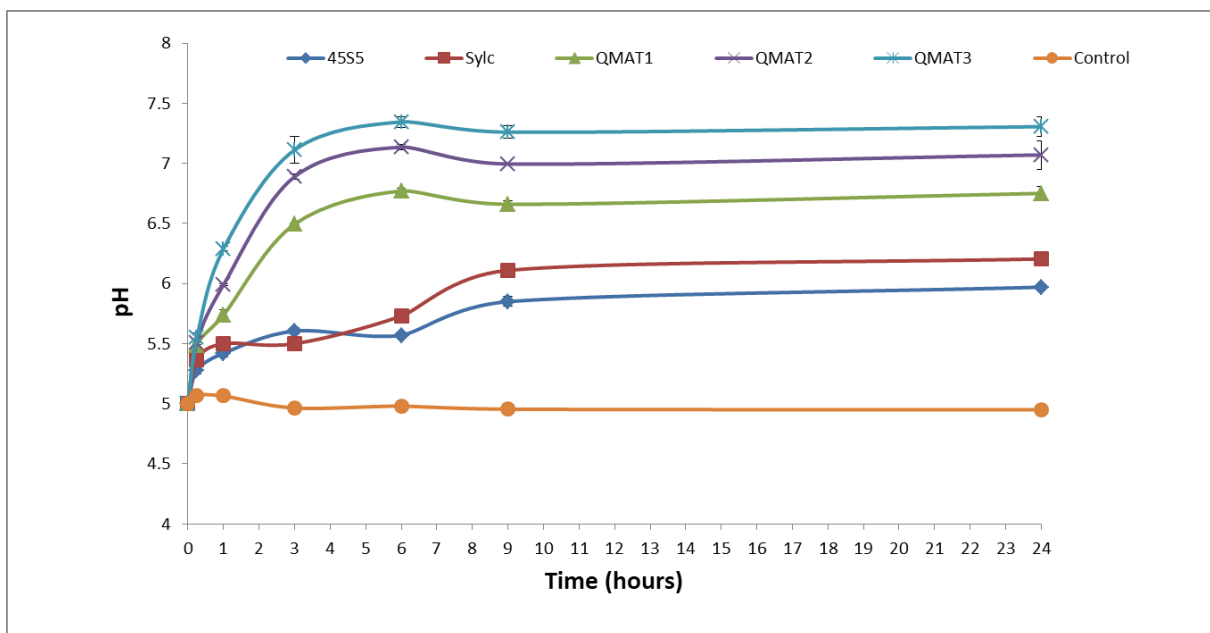


Figure 6.38. The pH change of acetic acid solution (initial pH=5) after immersion of 45S5, Sylc™ and experimental glasses (QMAT1, QMAT2, and QMAT3) plotted against the designated immersion time intervals (15 minutes, 1, 3, 6, 9 and 24 hours). * Error bars represent the range of pH measured on 2 independent occasions. Where error bars are not shown, the error was smaller than the data point

6.2.4.3. Artificial saliva study

The ATR-FTIR spectra of all experimental glasses, 45S5 and Sylc™ immersed in artificial saliva (Figures 6.39 to 6.43) revealed the same characteristic features of apatite formation that were observed in the Tris buffer and acetic acid studies, but the time-dependant transitions were different. In general, all glasses dissolved and formed apatite significantly quicker in artificial saliva (pH 6.5) than in Tris buffer solution of pH 7 and pH 9, respectively, and acetic acid of pH 5. The typical ATR-FTIR apatite features (twin bands at 560cm^{-1} and 600cm^{-1} , and a sharp phosphate band (PO_4^{3-} at 1030cm^{-1})

Results

were observed earlier in all experimental glasses (at 30 minutes) than those obtained in 45S5 and Sylc™ (at 45 minutes). In addition, all XRD patterns (Figures 6.44 to 6.48) of all experimental glasses, 45S5 and Sylc™ exhibited the two apatite peaks, at 26° and in between 32° - $34^\circ 2\theta$, mirroring the ATR-FTIR findings.

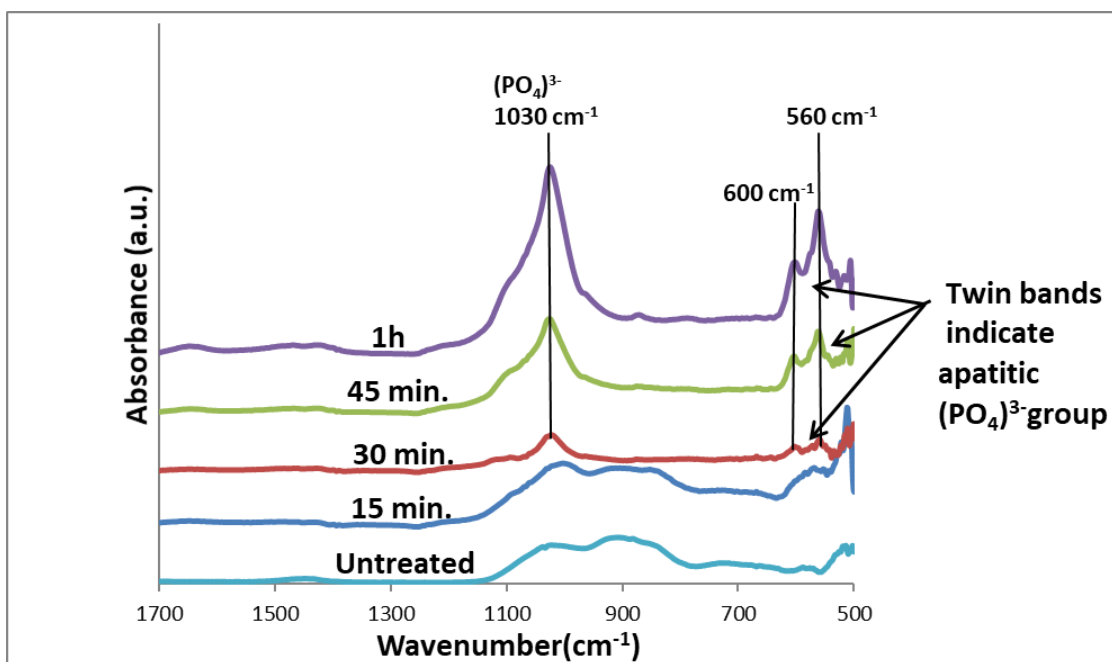


Figure 6.39. ATR-FTIR spectra of QMAT1 glass after immersion in artificial saliva

Results

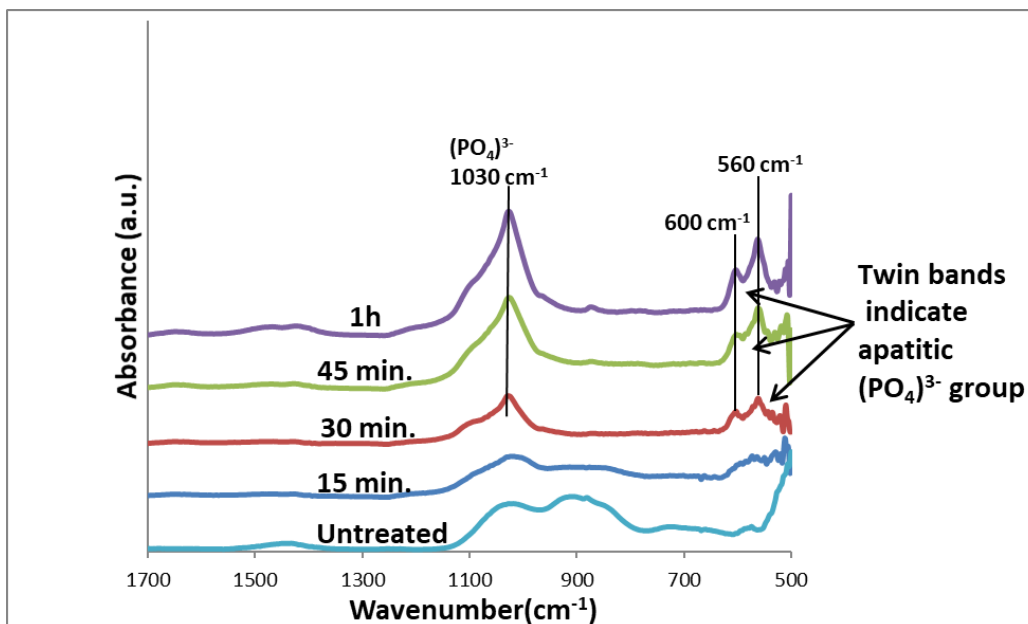


Figure 6.40. ATR-FTIR spectra of QMAT2 glass after immersion in artificial saliva

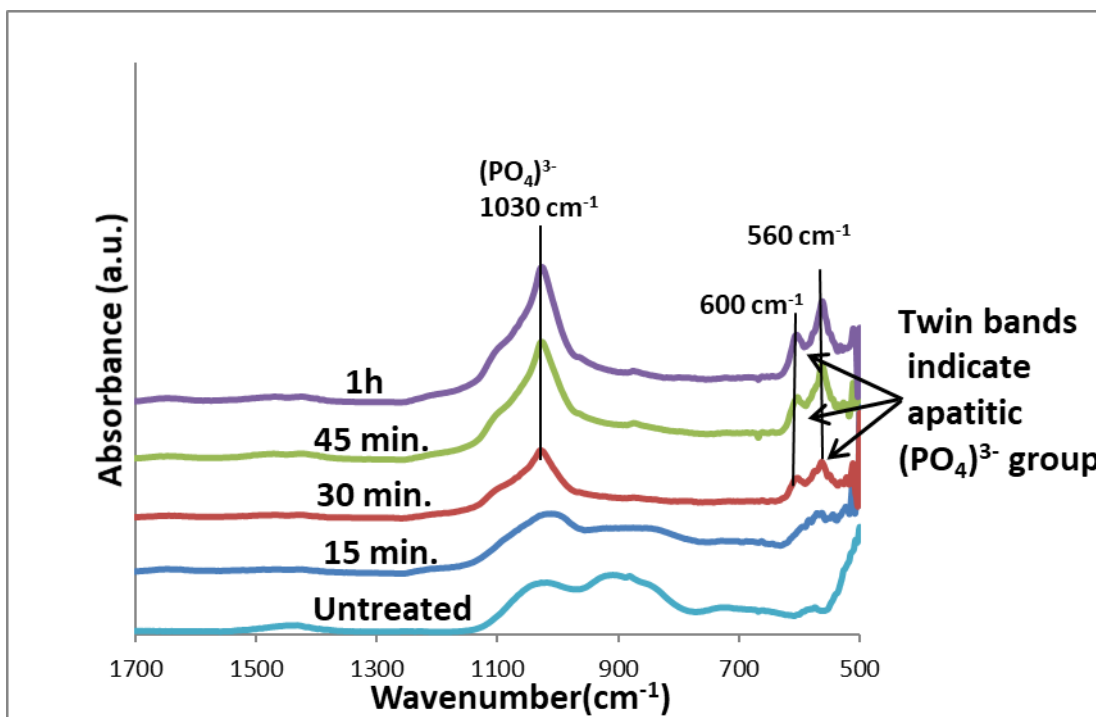


Figure 6.41. ATR-FTIR spectra of QMAT3 glass after immersion in artificial saliva

Results

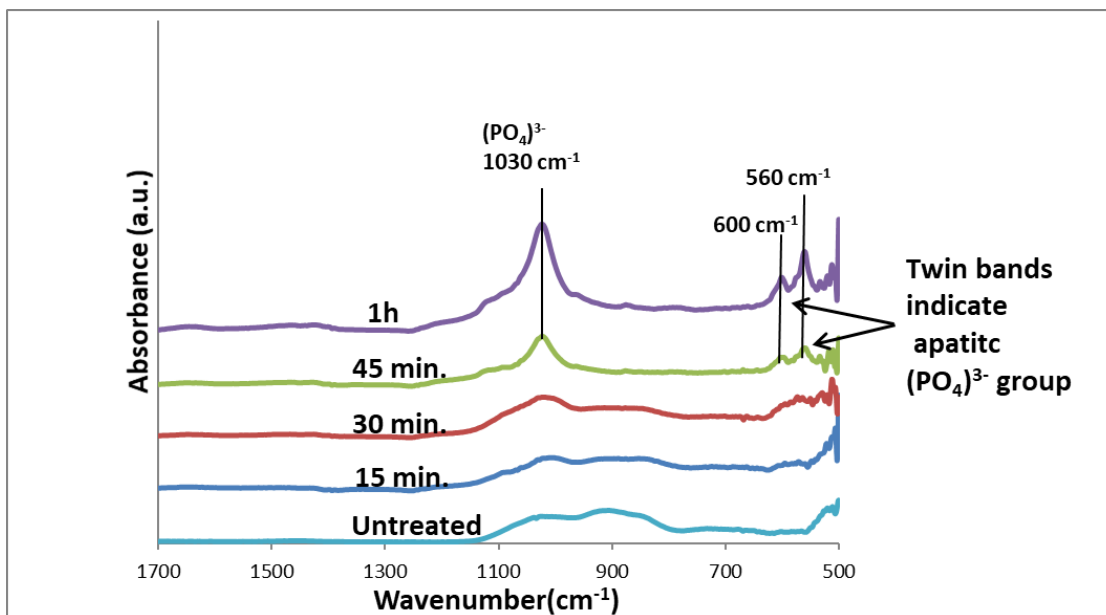


Figure 6.42. ATR-FTIR spectra of 45S5 glass after immersion in artificial saliva

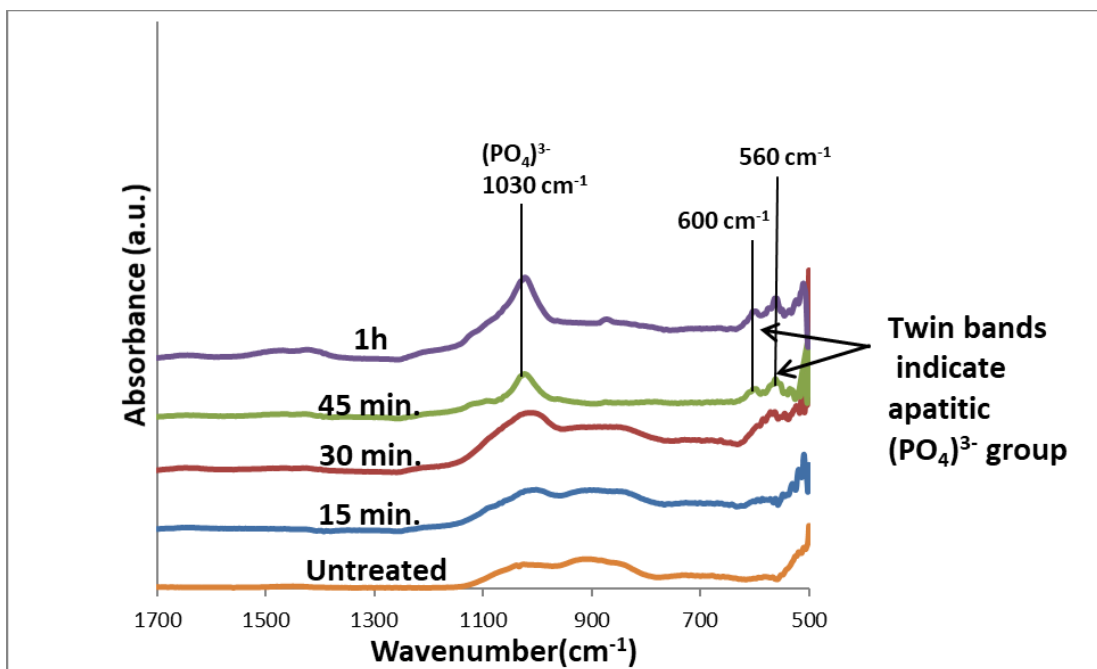


Figure 6.43. ATR-FTIR spectra of Syc™ glass after immersion in artificial saliva

Results

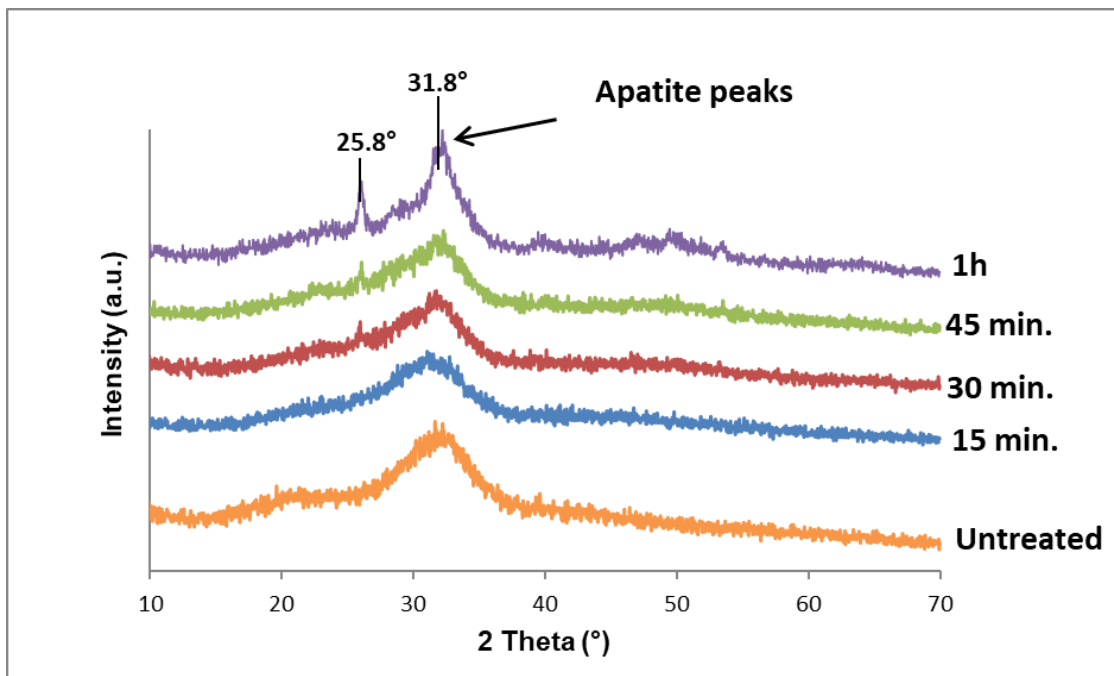


Figure 6.44. XRD patterns of QMAT1 glass after immersion in artificial saliva

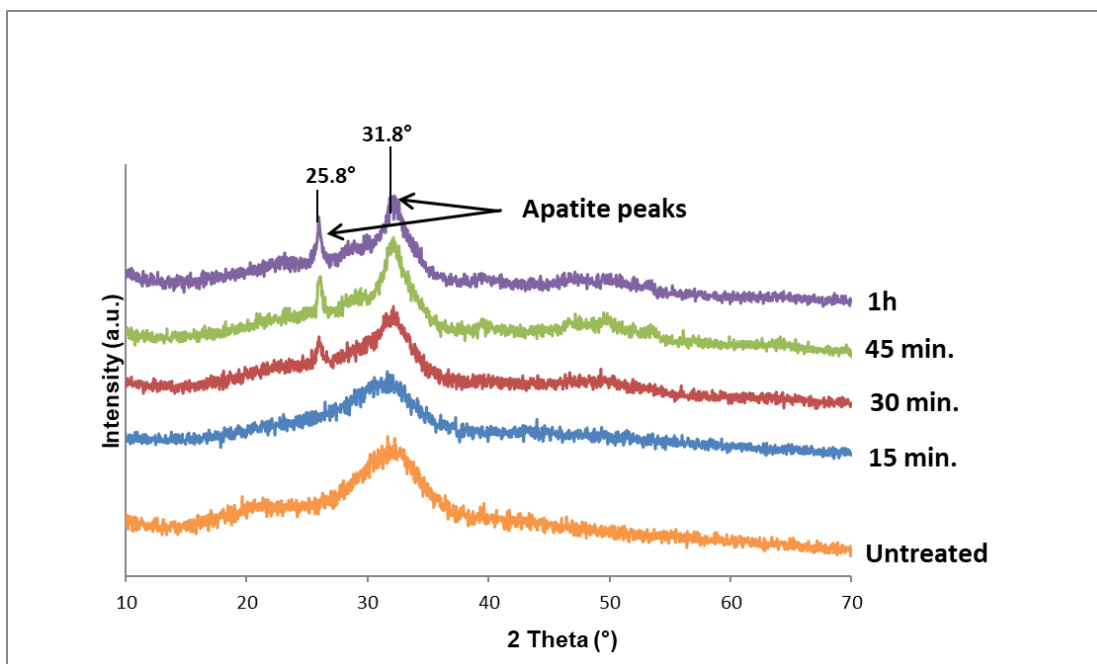


Figure 6.45. XRD patterns of QMAT2 glass after immersion in artificial saliva

Results

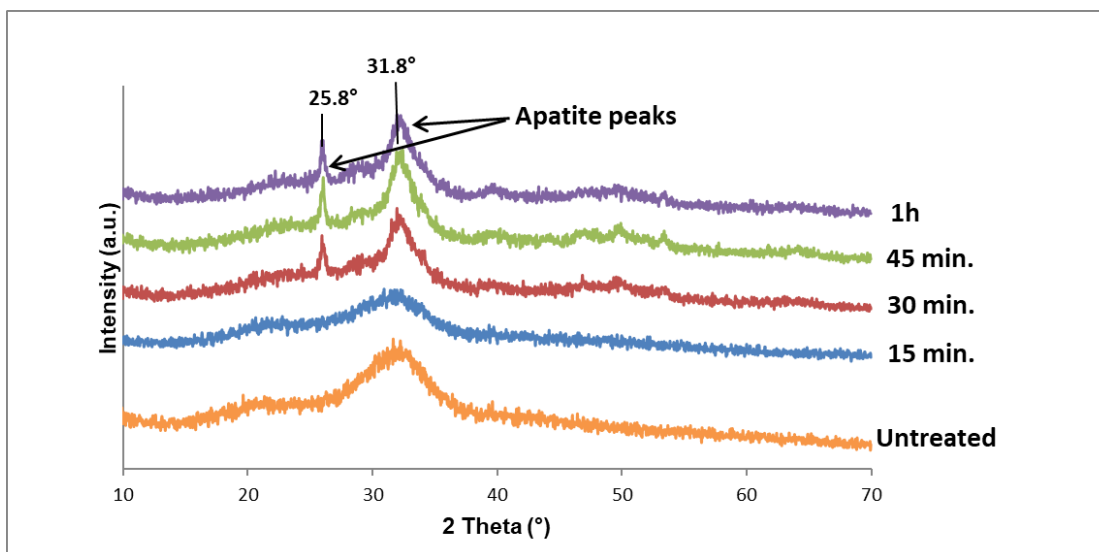


Figure 6.46. XRD patterns of QMAT3 glass after immersion in artificial saliva

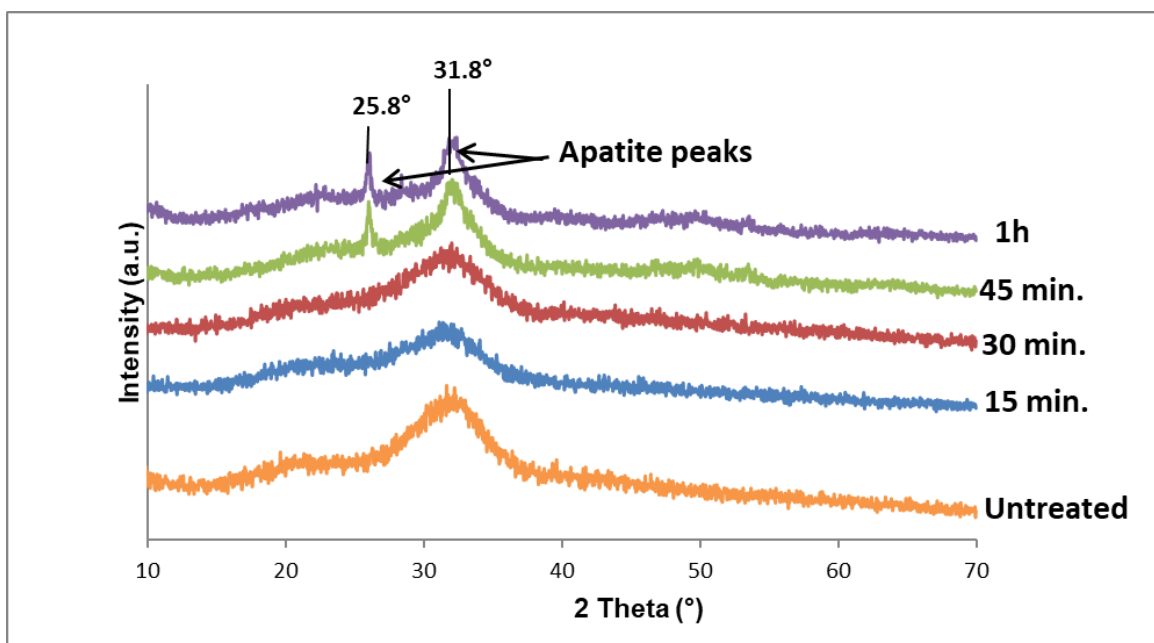


Figure 6.47. XRD patterns of 45S5 glass after immersion in artificial saliva

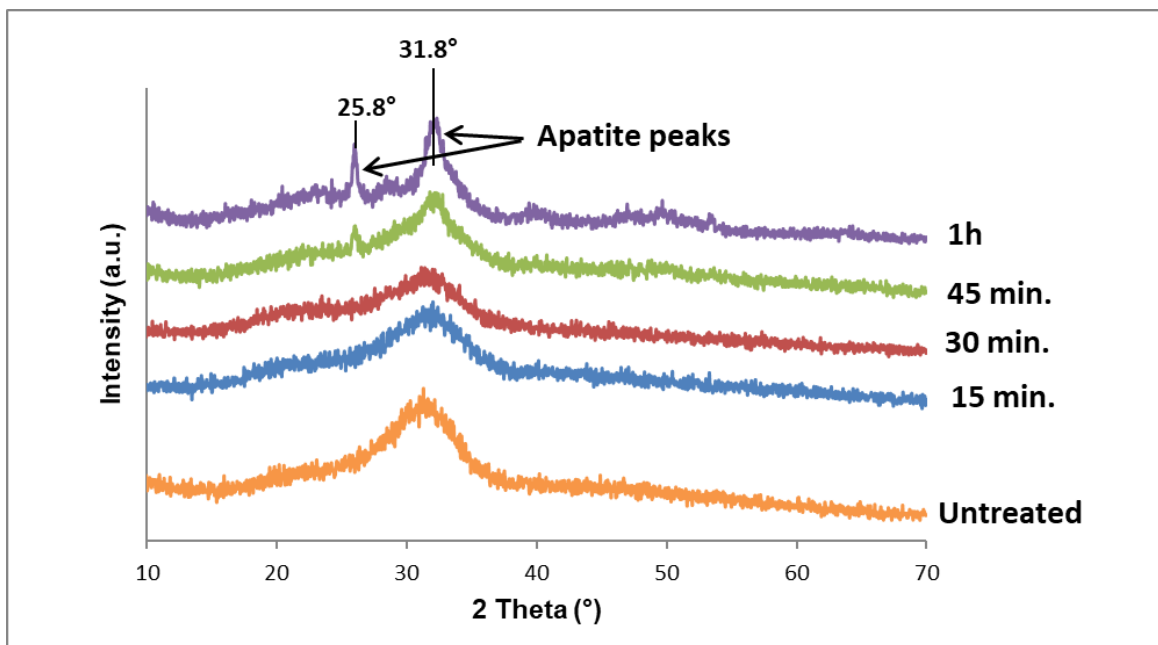


Figure 6.48. XRD patterns of Sylc™ glass after immersion in artificial saliva

The pH change of artificial saliva of initial pH=6.5 after immersion was recorded (Figure 6.49). A pH rise was noted for all glasses, suggesting a reaction between the bioactive glass and the artificial saliva, and reflecting a higher rate of glass dissolution and apatite formation. This rise started rapidly for all experimental glasses (QMAT1, QMAT2, and QMAT3) up to 30 minutes of immersion followed by a gradual increase in pH level for the remaining immersion periods (45 minutes and 1 hour) to levels of 7.01, 7.08, and 7.29, respectively. Conversely, the pH level associated with 45S5 and Sylc™ increased slowly over the first 30 minutes (to pH 6.66 and 6.67) followed by a marked increase at 45 minutes and 1 hour reaching pH 6.87 and 6.94, respectively. These pH changes after immersion of all glasses confirmed the ATR-FTIR and XRD findings.

Results

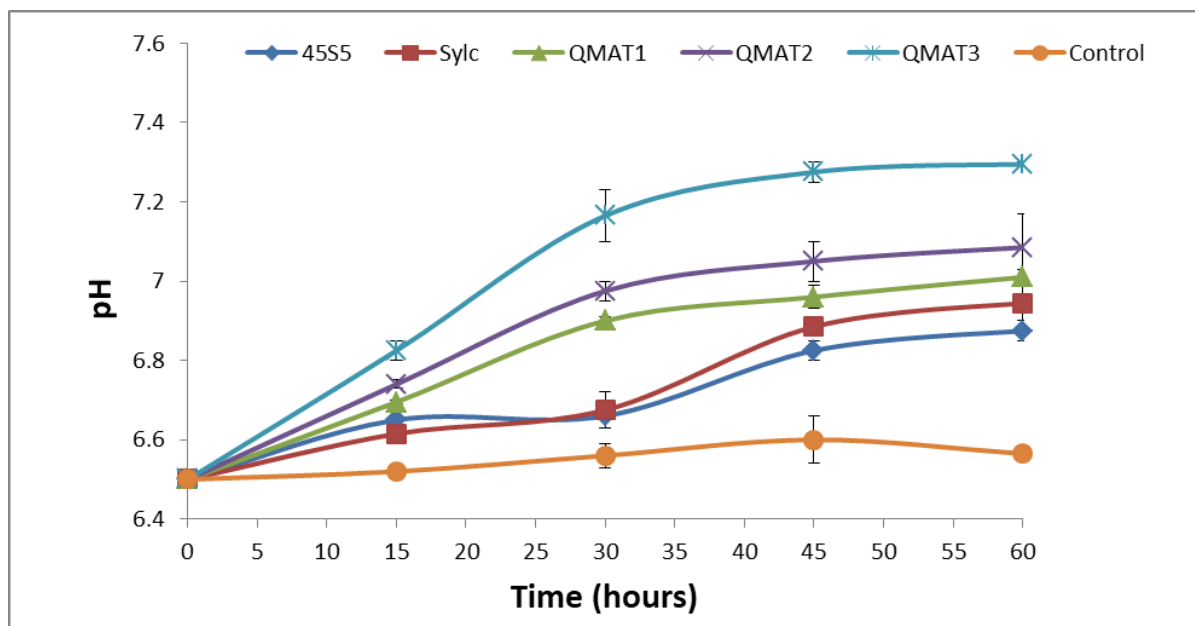


Figure 6.49. The pH change of artificial saliva (initial pH=6.5) after immersion of 45S5, Sylc™ and experimental glasses (QMAT1, QMAT2, and QMAT3) plotted against the designated immersion time intervals (15, 30, 45 minutes and 1 hour). * Error bars represent the range of pH measured on 2 independent occasions. Where error bars are not shown, the error was smaller than the data point

6.2.5. Apatite type detection using ^{19}F MAS-NMR

From the data described above it transpired that QMAT3 had the most potential, particularly with respect to its lower hardness compared to enamel tooth surface and other glasses (experimental, 45S5 and Sylc™), as well as its ability to form apatite earlier than both 45S5 and Sylc™. The ^{19}F MAS-NMR spectrum of this glass powder after 24 hours of immersion in Tris buffer solution and after 1 hour in artificial saliva (Figure 6.50) clearly showed a pronounced peak at -102ppm. This peak was correlated to the characteristic ^{19}F chemical shift (ppm) of the reference peak for fluorapatite (Figure 6.50), confirming the experimental glass QMAT3 formed fluorapatite.

Results

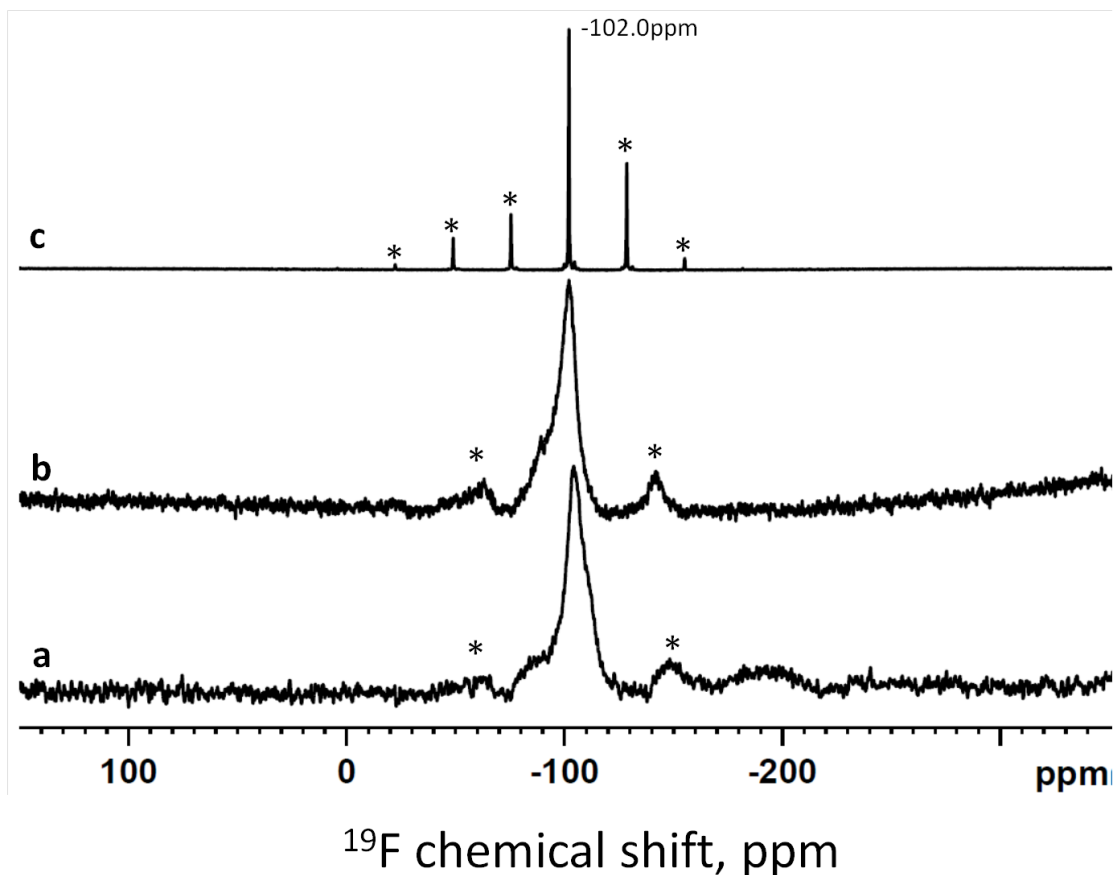


Figure 6.50. ^{19}F MAS-NMR spectra of a) QMAT3 immersed in artificial saliva for 1 hour, b) QMAT3 immersed in Tris buffer solution for 24 hours, and c) fluorapatite reference. (*) Asterisk denotes spinning side bands

The ^{19}F MAS-NMR spectra of the enamel surfaces (Figure 6.51) were assessed under four different conditions: sound, demineralised, after glass propulsion, and after immersing in artificial saliva to induce remineralisation. These spectra appeared as flat lines with no detectable fluoride present in the enamel surfaces in the sound and demineralised states, when immersed in artificial saliva, and after propulsion SylcTM glass followed by immersion in artificial saliva. Conversely, the enamel surface showed the same characteristic fluorapatite peak at -102ppm as the fluorapatite reference peak after propulsion of QMAT3 glass followed by immersion in artificial saliva.

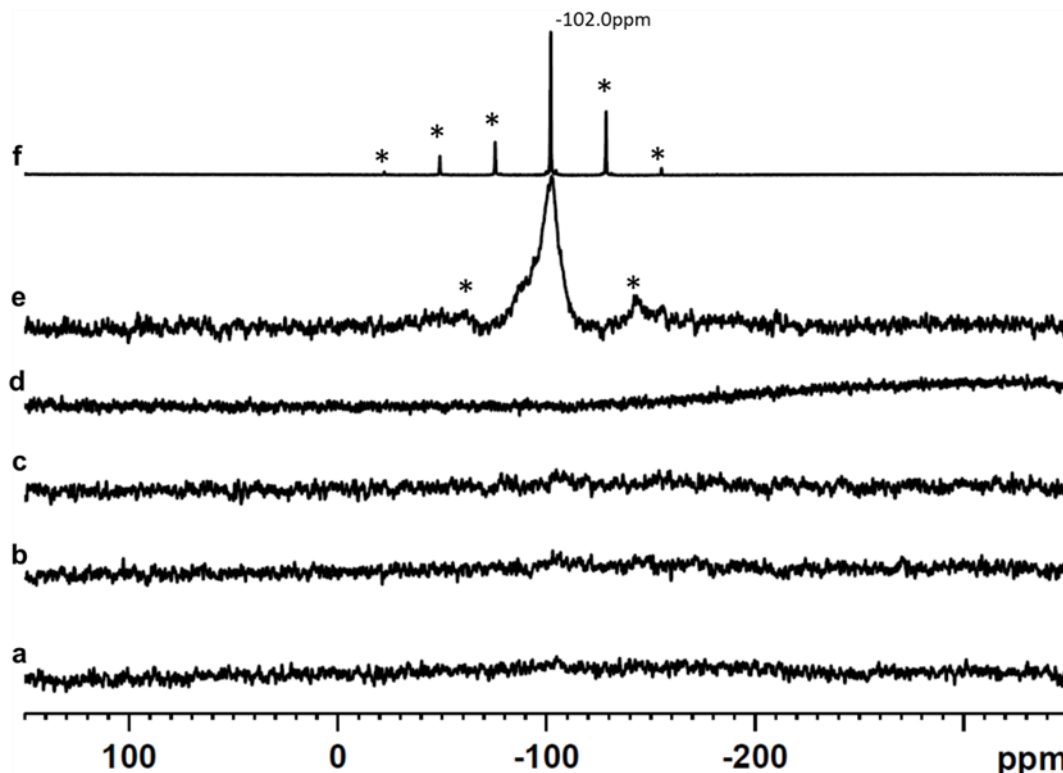


Figure 6.51. ^{19}F MAS-NMR spectra of enamel blocks under various conditions a) sound enamel, b) demineralised enamel, c) remineralised by only immersed in artificial saliva, d) remineralised by propulsion with Sylc[™] glass followed by immersion in artificial saliva, e) remineralised by propulsion with QMAT3 experimental glass followed by immersion in artificial saliva, f) fluorapatite reference. * denotes spinning side bands

6.2.6. Glass particle size analysis

The particle size distribution of 45S5, Sylc[™] and experimental glasses of batches with particle size $<38\mu\text{m}$ are given in Table 6.5 using the Mastersizer 3000 analyser, where D10 represents 10% of the glass particle size, indicating the fine particles within the distribution, D50 represents 50% of the glass particle size, giving a measure of the mean particle size within the distribution and D 90 represents 90% of the glass particle size, reflecting larger particle sizes. All glasses had similar particle size distributions.

Results

Table 6.5. Mean±SD particle size distribution (in micrometres) of 45S5, Sylc™, and experimental glasses of batches with particle size <38µm using Mastersizer 3000 analyser.

Bioactive glasses	Particle size (µm)		
	D10	D50	D90
45S5	5.56±0.06	17.8±0.1	37.1±0.6
Sylc™	5.09±0.03	15.8±0.03	33.9±0.05
QMAT1	5.43±0.06	16.4±0.1	34.3±0.15
QMAT2	5.26±0.02	16.7±0.01	35.0±0.02
QMAT3	5.20±0.03	15.7±0.1	34.0±0.5

The particle size distribution of 45S5, Sylc™ and experimental glasses of batches with particle size ranging between 38µm-90µm are given in Tables 6.6 and 6.7, using a Mastersizer 3000™ analyser and a Malvern/ E Mastersizer analyser, respectively. The two different analysers showed similar pattern for particle size distribution with each glass. The frequency distribution curves for both Sylc™ and QMAT3, obtained from the Mastersizer 3000, are shown in figures 10.1 and 10.2, respectively for batches of particle sizes ranging between 38µm-90µm, and figures 10.3 and 10.4, respectively for batches of particle sizes <38µm in Appendix 5.

Table 6.6. Mean±SD particle size distribution (in micrometres) of 45S5, Sylc™ and experimental glasses of batches with particle size ranging between 38µm-90µm using Mastersizer 3000™ analyser.

Bioactive glasses	Particle size (µm)		
	D10	D50	D90
45S5	33.2±0.05	57.7±0.06	95.1±0.07
Sylc™	31.1±0.02	57.4±0.07	97.1±0.1
QMAT1	33.6±0.1	57.4±0.1	93.0±0.1
QMAT2	33.6±0.1	56.9±0.04	92.1±0.07
QMAT3	34.2±0.28	58.1±0.05	94.6±0.4

Results

Table 6.7. Mean±SD particle size distribution (in micrometres) for 45S5, Sylc™ and experimental glasses of batches with particle size ranging between 38µm-90µm using Malvern/ E Mastersizer analyser.

Bioactive glasses	Particle size (µm)		
	D10	D50	D90
45S5	35.31±0.02	61.98±0.07	75.97±0.1
Sylc™	34.12±0.1	63.47±0.04	76.84±0.05
QMAT1	38.60±0.04	65.52±0.1	77.20±0.28
QMAT2	38.92±0.02	65.50±0.07	77.19±0.04
QMAT3	33.82±0.1	62.69±0.1	76.67±0.02

6.2.7. Glass particle shape analysis

SEM images of 45S5, Sylc™ and experimental glasses (QMAT1, QMAT2, and QMAT3) are presented in Figure 6.52. All images were taken at 250x magnification and showed that all glasses had similar morphology with sharp, angular irregular particles of variable sizes.

Results

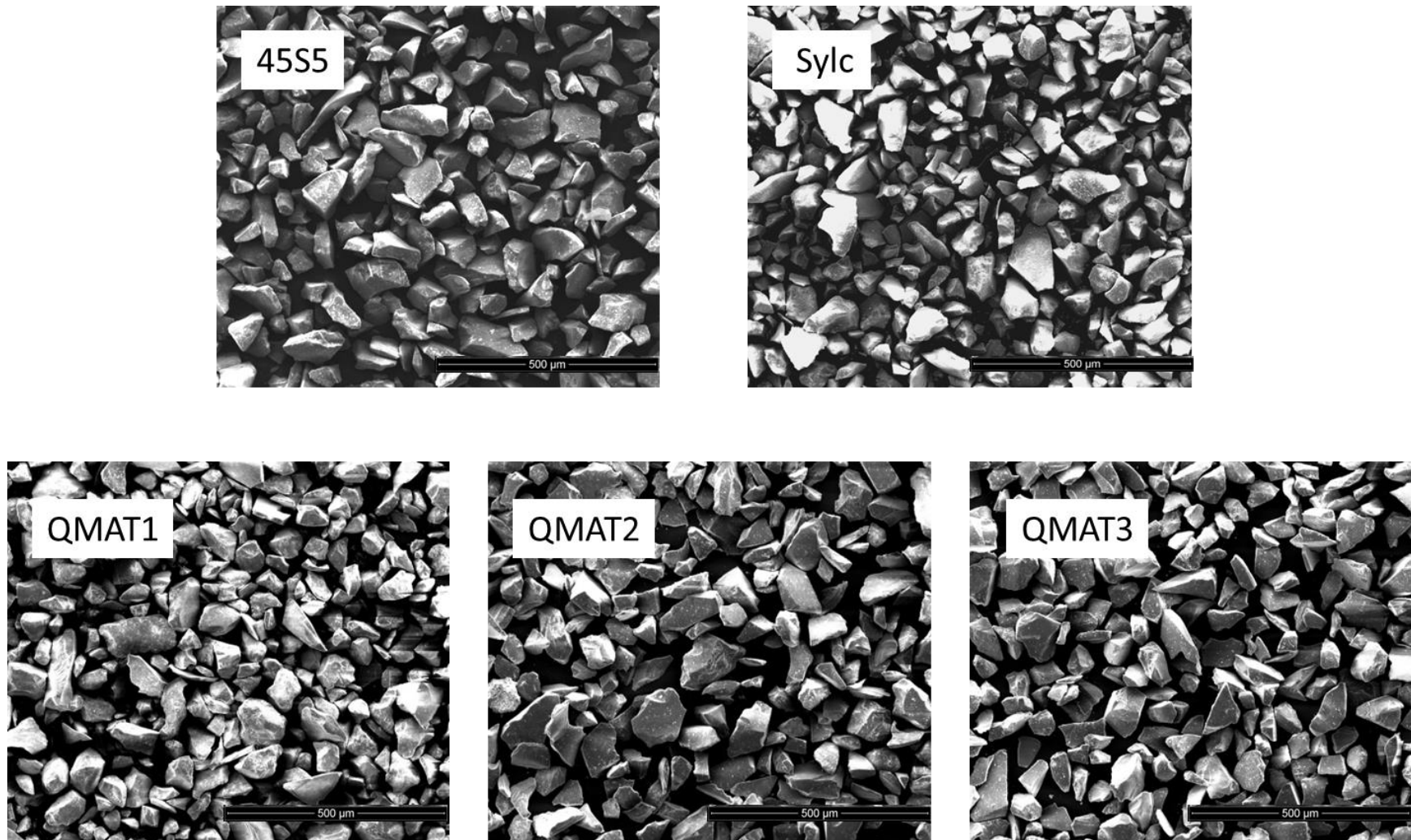


Figure 6.52. SEM images of 45S5, SylcTM and experimental glasses

Results

6.3. Air-abrasion studies performed using the selected novel glass: QMAT 3

6.3.7. Glass cutting efficiency

To assess the cutting efficiency of the commercially-available Sylc™ glass and the most promising novel experimental glass (QMAT3), the cutting time required to cut a hole in orthodontic adhesive (Transbond XT™) discs was recorded five times and then averaged for each glass. The glass was propelled at a fixed operating distance (5mm) via a Velopex Aquacut Quattro™ air-abrasion machine using various parameters. The latter were varied as follows: Air pressure (40psi and 60psi), powder flow rate dials (1, 3, and 5) and nozzle-tip angles (90° and 45°).

No significant differences were observed in the cutting time between the two glass groups using the same parameters (Table 6.8, Figures 6.53 and 6.54). However, the cutting time significantly increased at a nozzle-tip angle of 45° compared to 90° using the same settings ($p < 0.001$). In addition, as the powder flow rate increased (from dial 1 to dial 5), a significant reduction in the cutting time was uniformly recorded using the same air-pressure and angle ($p < 0.001$). Furthermore, increasing the air pressure (from 40psi to 60psi) resulted in a decrease in the cutting time at powder flow rate dial 1 and dial 5 at a nozzle-tip angle of 45°, and at dial 5 at 90° in the Sylc™ groups, while the cutting time was not significantly different between the two air-pressures at each angle with QMAT3.

Results

Table 6.8. Mean \pm SD of the cutting time (in seconds) required to cut a hole within adhesive discs by two propelled glasses using various parameters.

Group No. (n=5)	Glass powder type	Powder flow rate dials	Air Pressure (psi)	Time (sec.) at 90°	Time(sec.) at 45°
1	Sylc™	1	40	30.4 \pm 3.21	62.8 \pm 4.32
2			60	28.6 \pm 2.97	56.4 \pm 4.16
3		3	40	27.6 \pm 2.31	55.4 \pm 3.36
4			60	23.6 \pm 2.61	57.4 \pm 4.88
5		5	40	23.8 \pm 3.11	55.6 \pm 2.41
6			60	18.4 \pm 2.70	50.4 \pm 3.21
7	QMAT3	1	40	28.4 \pm 2.70	56.8 \pm 4.66
8			60	27.4 \pm 2.79	53.6 \pm 4.98
9		3	40	25.6 \pm 2.61	51.8 \pm 2.86
10			60	24.4 \pm 2.51	54.4 \pm 2.88
11		5	40	22.4 \pm 2.70	50.8 \pm 2.95
12			60	19.8 \pm 2.28	48.8 \pm 3.11

Results

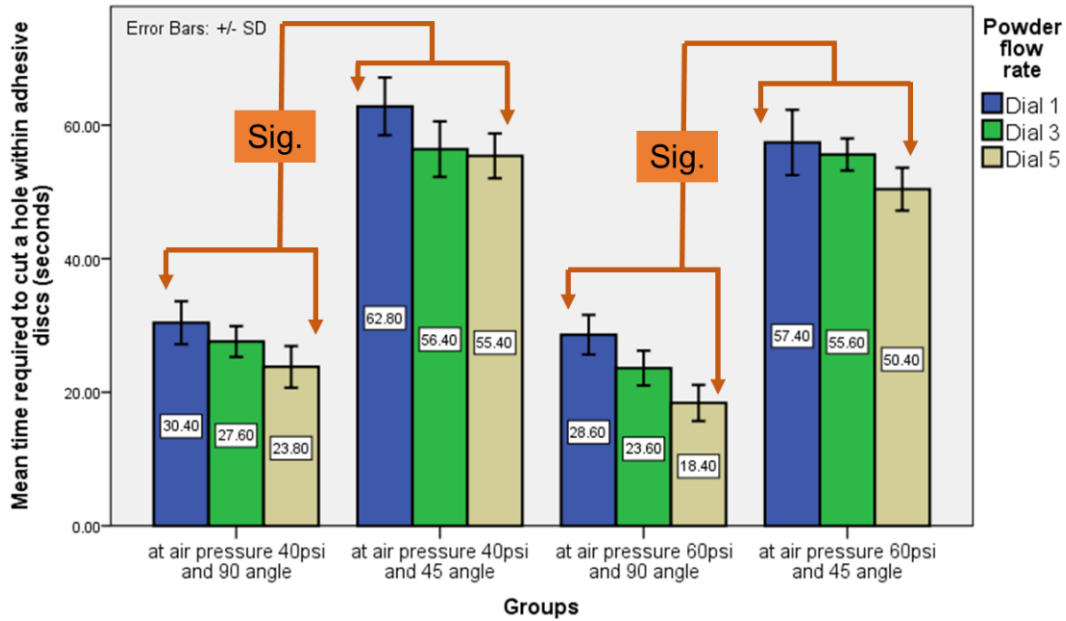


Figure 6.53. Mean \pm SD of the cutting time required to cut a hole within adhesive discs by Sylc™-air-abrasion using various parameters

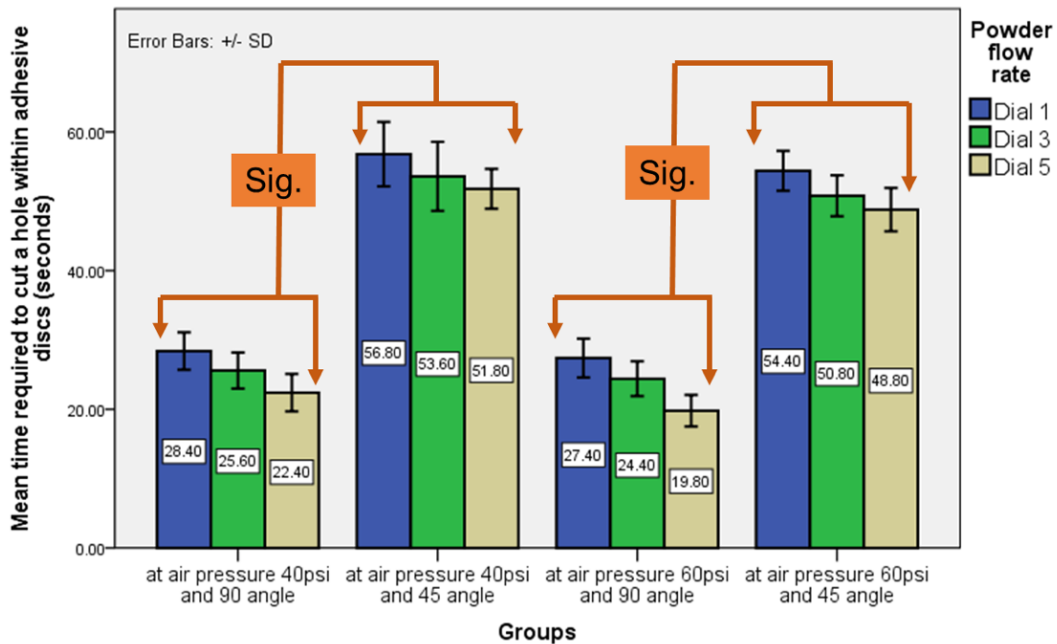


Figure 6.54. Mean \pm SD of the cutting time required to cut a hole within adhesive discs by QMAT3-air-abrasion using various parameters

Results

6.3.8. Glass powder flow rate

To assess the glass powder flow rate of the two air-abrasion systems (Velopex Aquacut Quattro™ air-abrasion machine and BA Ultimate™ air polisher) with an air pressure of 60psi, the amount (in grams) of glass powder (Sylc™ and QMAT3) propelled *via* these two systems was recorded over 1 minute (Table 6.9 and Figure 6.55). No significant differences were observed in the amount of propelled glass powder between the two glass groups using the same air-abrasion system and settings. Within each glass group, the flow rate between the glasses was consistent at dial 5, while a difference was observed at dials 1 and 3 ($p < 0.001$). In addition, adjusting the powder flow rate of the machine from a low (dial 1) to high (dial 5) value led to an increase in the amount of propelled glass within each group ($p < 0.001$).

Table 6.9. Mean \pm SD of the amount (in grams) of glass powder propelled *via* two air-abrasion systems for one minute.

Glass powder type	Velopex Aquacut Quattro™ air-abrasion machine		BA Ultimate™ air polisher
	Powder flow rate dials	Observed powder flow rate (g/min.)	Powder flow rate (g/min.)
Sylc™	1	0.258 \pm 0.12	1.153 \pm 0.020
	3	0.625 \pm 0.16	
	5	1.140 \pm 0.12	
QMAT3	1	0.274 \pm 0.008	1.113 \pm 0.15
	3	0.649 \pm 0.12	
	5	1.126 \pm 0.009	

Results

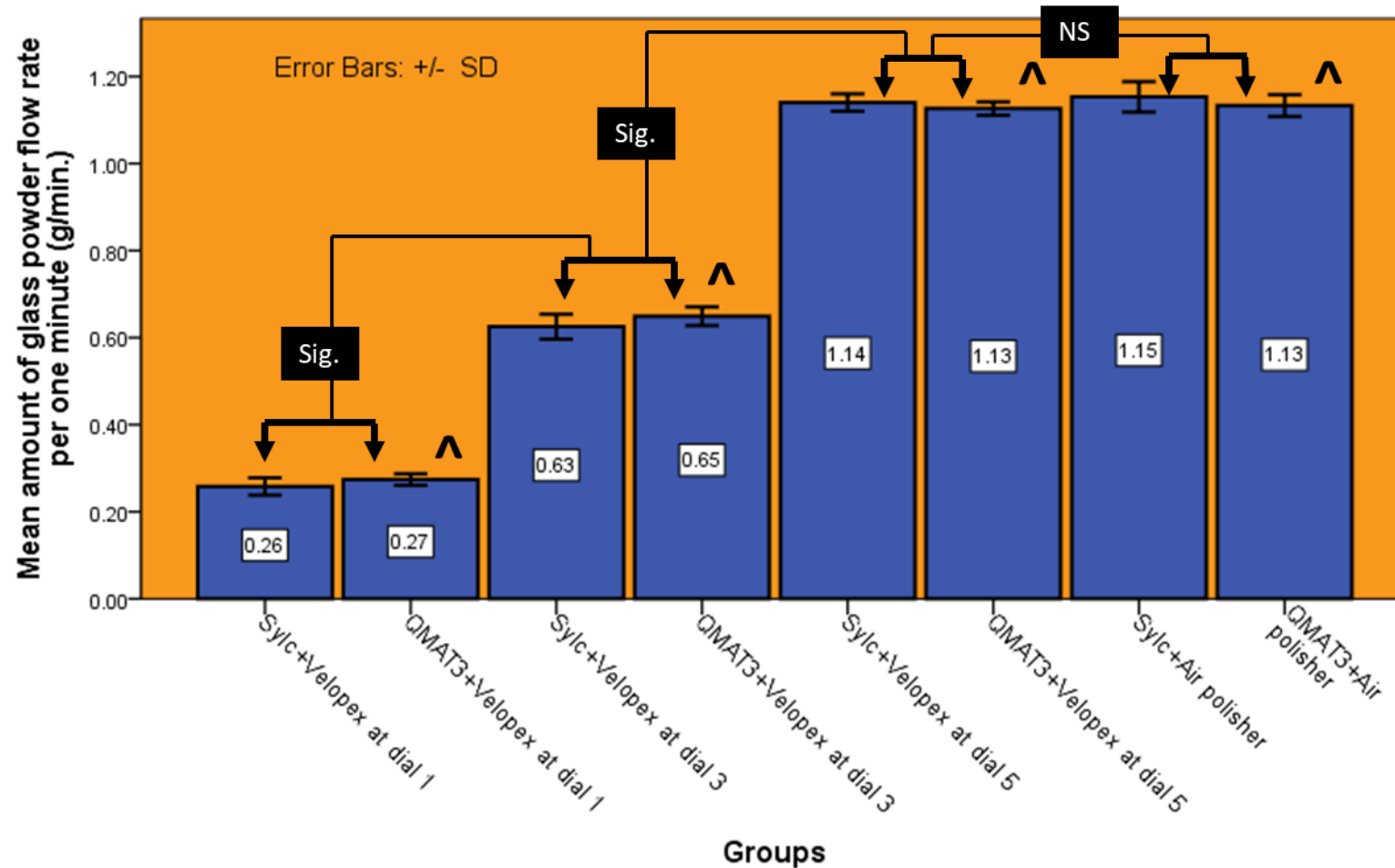


Figure 6.55. Amount (in grams) of glass powder propelled via two air-abrasion systems under air pressure 60 psi over one minute. Sig. refers to significant difference, NS refers to non-significant difference, and (^) denotes no significant difference between the two glasses under the same operating parameters

6.4. Experiments performed using the selected novel glass, QMAT 3

6.4.7. Orthodontic adhesive removal

6.4.7.1. Profilometer results

The profilometer analysis was carried out on three experimental groups (TC bur group, SylcTM-air-abrasion, and QMAT3-air-abrasion) for two orthodontic adhesives (Transbond XTTM and Fuji OrthoTM). The enamel surface roughness under three different conditions (before bracket bonding, after adhesive clean-up following bracket debonding, and after polishing), are presented in Table 6.10 and Figure 6.56. The sound (baseline) measurements did not show any statistically significant differences in enamel roughness among the experimental groups before bracket bonding. For Transbond XTTM resin groups, the enamel roughness significantly increased after post clean-up with both the TC bur ($2.93 \pm 0.13 \mu\text{m}$) and SylcTM ($1.89 \pm 0.15 \mu\text{m}$) compared with their corresponding baseline measurements ($p < 0.001$), while QMAT3-air-abrasion group did not exhibit any significant difference in enamel roughness ($p = 0.927$). In addition, the enamel roughness values after polishing were significantly higher for both the TC bur and SylcTM-air-abrasion groups ($2.73 \pm 0.31 \mu\text{m}$ and $1.81 \pm 0.21 \mu\text{m}$, respectively), than their corresponding baseline measurements ($p < 0.001$). However, no significant difference was shown in the enamel roughness with QMAT3-air-abrasion group relative to baseline either following adhesive removal ($p = 0.983$) or subsequent polishing ($p = 0.998$).

For Fuji OrthoTM, similar patterns were observed for enamel roughness. Roughness was significantly higher after post clean-up in the TC ($2.57 \pm 0.22 \mu\text{m}$) and SylcTM-air-abrasion groups ($1.59 \pm 0.14 \mu\text{m}$) compared to baseline ($p < 0.001$), but the QMAT3-air-abrasion group ($0.51 \pm 0.13 \mu\text{m}$) did not show any significant difference with baseline ($p = 0.249$). In addition, significantly higher enamel roughness values were shown in TC and SylcTM-air-abrasion groups ($2.63 \pm 0.23 \mu\text{m}$ and $1.74 \pm 0.19 \mu\text{m}$, respectively) after polishing than their corresponding baseline measurements ($p < 0.001$), but no significant difference was shown between those of QMAT3-air-abrasion and their corresponding baseline measurements ($p = 0.853$).

Results

Table 6.10. Mean \pm SD of the enamel surface roughness (Ra) in micrometres for each experimental group under three different conditions.

Group (n=10)	Experimental group based on: orthodontic adhesive +post clean-up method used	Before bracket bonding (Baseline)	After post clean-up method	After polishing
1	Transbond XT TM + TC	0.49 \pm 0.09	2.93 \pm 0.13	2.73 \pm 0.31
2	Transbond XTT TM + Sylc TM -air-abrasion	0.51 \pm 0.1	1.89 \pm 0.15	1.81 \pm 0.21
3	Transbond XT TM + QMAT3-air-abrasion	0.49 \pm 0.15	0.58 \pm 0.07	0.56 \pm 0.08
4	Fuji Ortho LC TM + TC	0.54 \pm 0.08	2.57 \pm 0.22	2.63 \pm 0.23
5	Fuji Ortho LC TM + Sylc TM -air-abrasion	0.46 \pm 0.13	1.59 \pm 0.14	1.74 \pm 0.19
6	Fuji Ortho LC TM + QMAT3-air-abrasion	0.36 \pm 0.08	0.51 \pm 0.13	0.45 \pm 0.05

Results

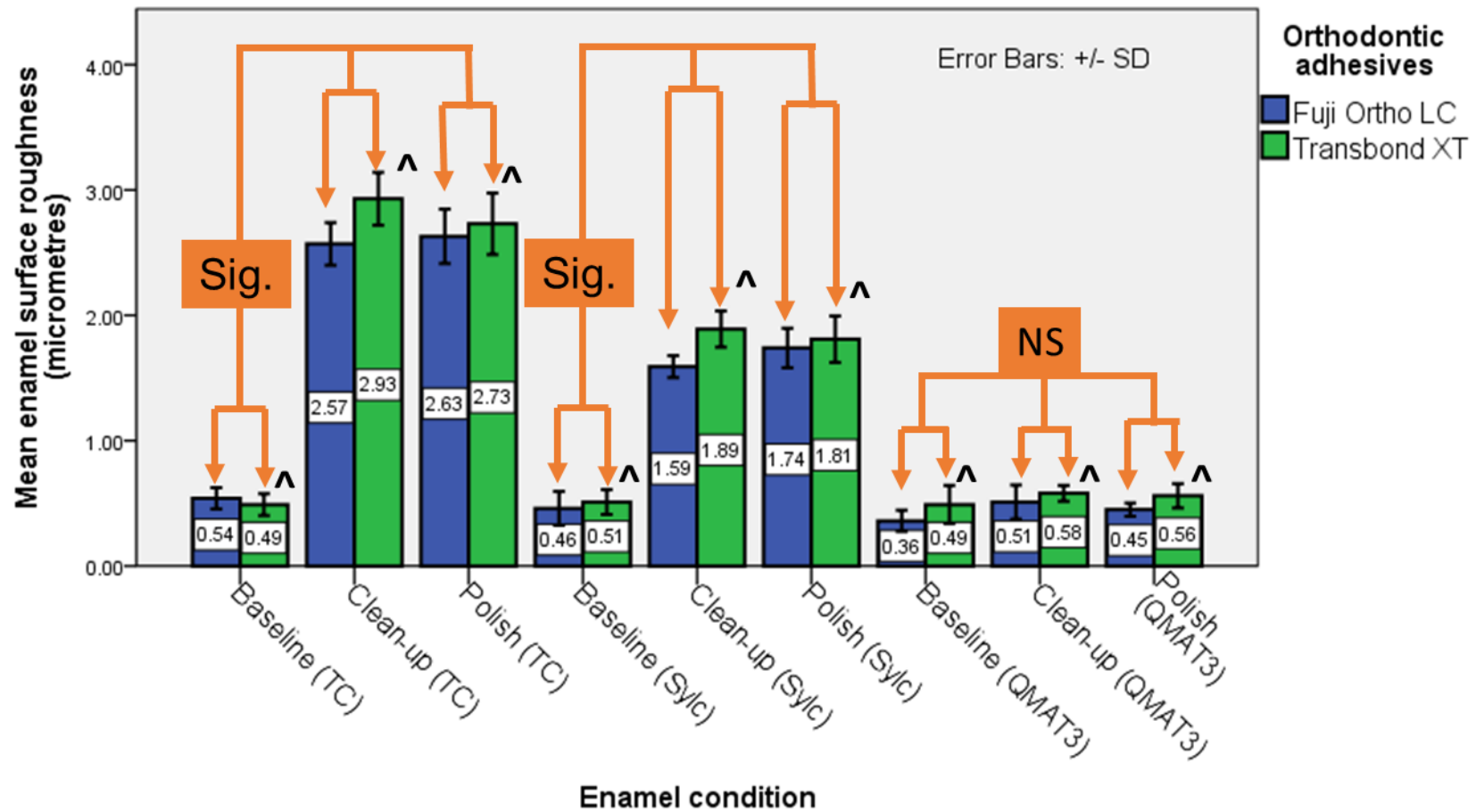


Figure 6.56. Bar graph representing means \pm SD of the enamel surface roughness under three different conditions for two bonding adhesives and three post clean-up methods. (Sig.) refers to significant difference, (NS) refers to Non-significant difference, and (^) denotes no significant differences between the two adhesives under the same enamel condition

6.4.7.2. Scanning electron microscope (SEM) results

With regards to the qualitative SEM assessment of the enamel surface after adhesive clean-up, representative SEM images (at 250x magnification) are shown in Figure 6.57 prior to bracket bonding and following the use of the three approaches (TC bur, Sylc™-air-abrasion and QMAT3-air-abrasion). The sound enamel surface appeared smooth before bracket bonding (Figure 6.57a), whilst it became roughened and pitted after the use of a slow-speed TC bur (Figure 6.57b). In addition, the enamel surface following Sylc™-air-abrasion is seen to have microscopic roughness in some areas (Figure 6.57c), while a uniformly smooth surface was obtained after using QMAT3- air-abrasion (Figure 6.57d).

Results

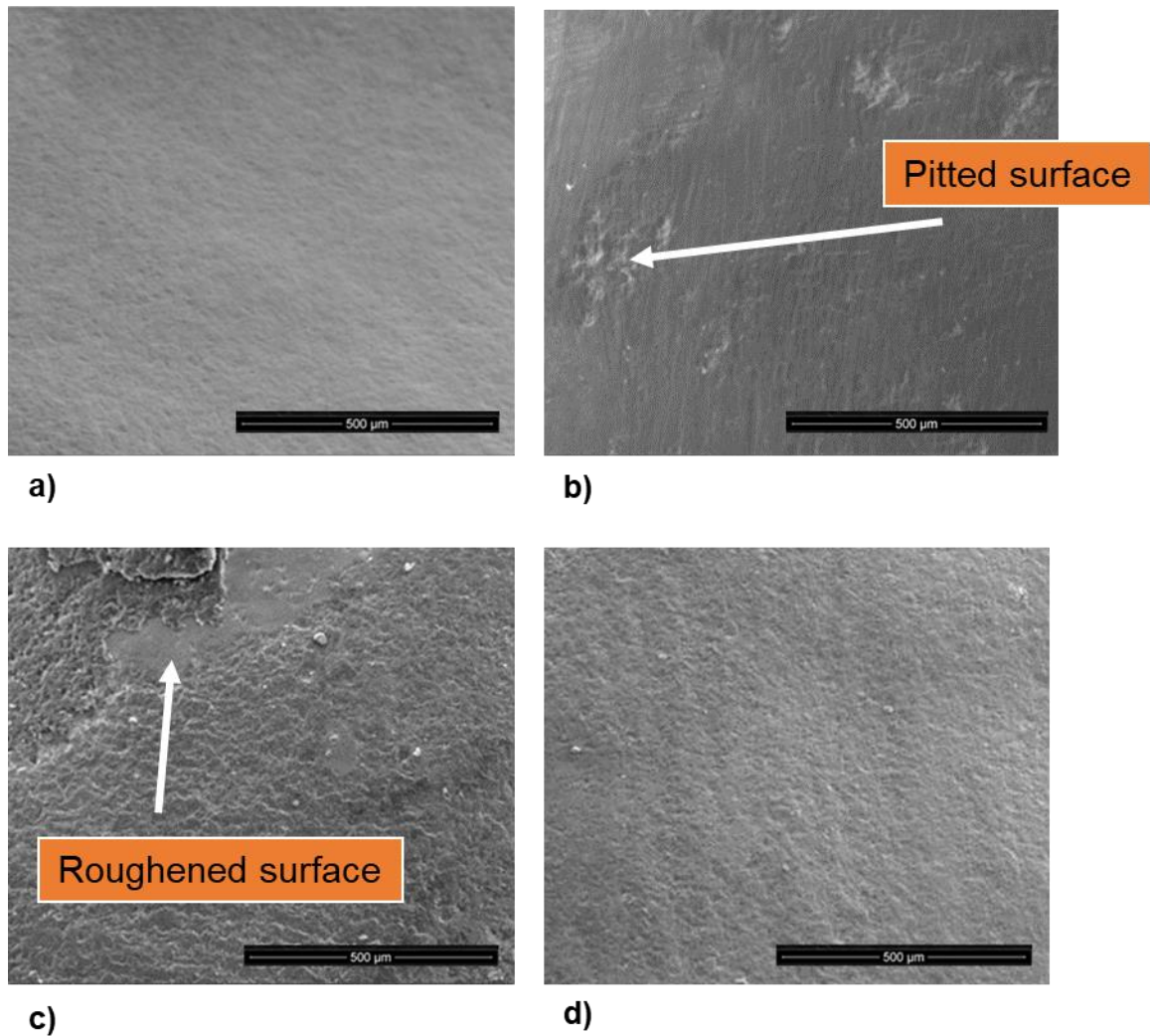


Figure 6.57. Representative SEM images of the enamel surface: a) before bracket bonding; b) after clean-up using the TC bur; c) after clean-up using Sylc™-air-abrasion; d) after clean-up using QMAT3- air-abrasion

6.4.7.3. Time required for adhesive removal

The time required to remove the orthodontic adhesives from the enamel teeth surfaces was recorded for three post clean-up methods: TC bur, Sylc™-air-abrasion, and QMAT3-air-abrasion (Table 6.11 and Figure 6.58). This time was comparable between QMAT3 glass (42.51 ± 3.52 seconds) and Sylc™ (40.72 ± 2.90 seconds) with no statistically significant differences ($p=0.913$) between them in the Transbond XT™ groups. However, both took longer ($p<0.001$) to remove excess Transbond XT™ resin

Results

compared to the TC bur (23.2 ± 4.99 seconds). A similar pattern was observed in the Fuji Ortho LC™ groups with no significant differences found between the time required to remove Fuji Ortho LC™ by both QMAT3 and Sylc™ glasses ($p=0.893$), while both glasses took significantly longer than the TC bur ($p<0.001$). However, a significant difference was observed between Transbond XT™ (53.9 ± 2.38 VHN ~ 0.52 GPa) and Fuji Ortho LC™ (38.1 ± 1.66 VHN ~ 0.37 GPa) in relation to the hardness values of the adhesive discs ($p<0.001$).

Table 6.11. Means \pm SD of the time (seconds) required to remove two residual orthodontic adhesives following bracket debonding by three post clean-up methods.

Group (n=10)	Experimental study group based on: orthodontic adhesive + post clean-up method used	Time (Sec.)
1	Transbond XT™ + TC	23.20 \pm 4.99
2	Transbond XT™ + Sylc™-air-abrasion	40.72 \pm 2.90
3	Transbond XT™ + QMAT3-air-abrasion	42.51 \pm 3.52
4	Fuji Ortho LC™ + TC	22.90 \pm 4.41
5	Fuji Ortho LC™ + Sylc™-air-abrasion	38.43 \pm 4.29
6	Fuji Ortho LC™ + QMAT3-air-abrasion	40.32 \pm 3.36

Results

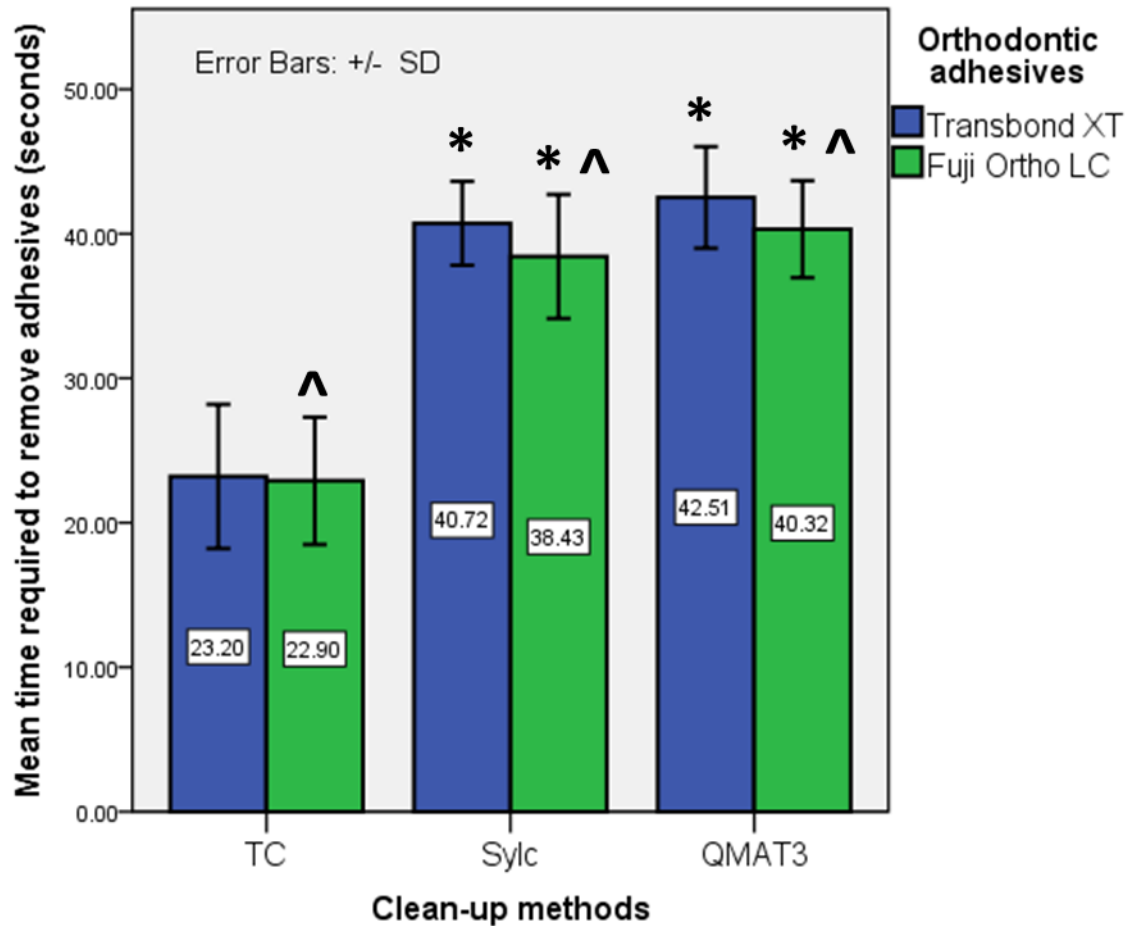


Figure 6.58. Means \pm SD of the time (seconds) required to remove two residual orthodontic adhesives following bracket debonding by three post-clean-up methods. (*) denotes significant difference in comparison with TC group using the same adhesive. (^) denotes no significant differences between two adhesives using the same clean-up method

6.4.8. White spot lesions (WSLs) remineralisation

6.4.8.1. Optical coherence tomography (OCT) results

The mean intensity of light backscattering from the tooth surface did not differ significantly between the experimental groups at baseline and following demineralisation (Table 6.12 and Figure 6.59). In addition, higher light backscattering

Results

intensity values were recorded from demineralised enamel surfaces compared to their corresponding sound values in each experimental group ($p<0.001$). After glass propulsion, a significant reduction was observed in the intensity values of the light backscattered from the tooth surfaces within the QMAT3-air-abrasion group only compared to the corresponding values when demineralised ($p=0.033$). After immersion in artificial saliva, a further significant reduction in the intensity values of QMAT3-air-abrasion was recorded compared to their corresponding values after glass propulsion ($p<0.001$), approximating baseline values ($p=1.000$), while the intensity values within both SylcTM-air-abrasion and control groups remained significantly higher than at baseline ($p<0.001$).

Table 6.12. Means \pm SD of the intensity value of light backscattering for each experimental group under four different conditions.

Group (n=10)	Experimental group based on the treatment method	Sound enamel (Baseline)	Demineralised enamel	After glass propulsion	After immersion in artificial saliva
1	QMAT3-air-abrasion	72.65 \pm 14.06	129.74 \pm 13.97	111.51 \pm 13.03	75.31 \pm 5.49
2	Sylc TM -air-abrasion	72.70 \pm 8.17	130.3 \pm 14.91	116.21 \pm 11.40	93.41 \pm 8.97
3	Untreated (Control)	79.37 \pm 8.50	131.76 \pm 10.95	128.0 \pm 9.36	113.37 \pm 16.32

Results

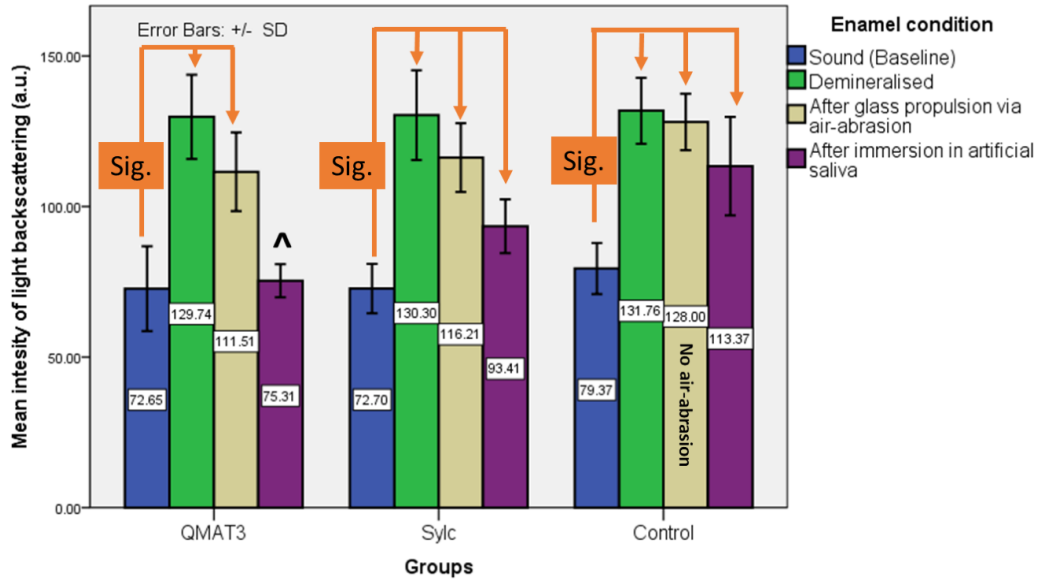


Figure 6.59. Means \pm SD of the intensity value of light backscattering for each experimental group under four different conditions. (^) denotes no significant difference in comparison with the corresponding baseline.

6.4.8.2. Profilometer results

A significant increase in enamel roughness was observed following demineralisation compared to baseline for all experimental groups ($p < 0.001$; Table 6.13 and Figure 6.60). After glass propulsion, the roughness measurements in the SylcTM-air-abrasion group were significantly higher ($3.08 \pm 0.08 \mu\text{m}$) than their corresponding measurements under sound and demineralised conditions ($p < 0.001$). Conversely, there was a significant reduction in the roughness measurements of the QMAT3-air-abrasion group following glass propulsion compared to the demineralised state ($p < 0.001$), approximating their corresponding sound measurements ($p = 1.000$). After immersion in artificial saliva, no significant differences were recorded in the roughness measurements of all experimental groups compared to their corresponding values after glass propulsion ($p = 0.599$ to $p = 1.000$), indicating that immersion in artificial saliva had no effect on the roughness of the enamel surface.

Results

Table 6.13. Means \pm SD of the enamel surface roughness (Ra) in micrometres for each experimental group under four different conditions.

Group (n=10)	Experimental group based on the treatment method	Sound enamel (Baseline)	Demineralised enamel	After glass propulsion	After immersion in artificial saliva
1	QMAT3-air-abrasion	0.52 \pm 0.10	2.07 \pm 0.37	0.55 \pm 0.08	0.54 \pm 0.08
2	Sylc TM -air-abrasion	0.63 \pm 0.09	1.96 \pm 0.37	3.08 \pm 0.27	2.82 \pm 0.18
3	Untreated (Control)	0.60 \pm 0.24	2.01 \pm 0.37	1.89 \pm 0.50	1.73 \pm 0.19

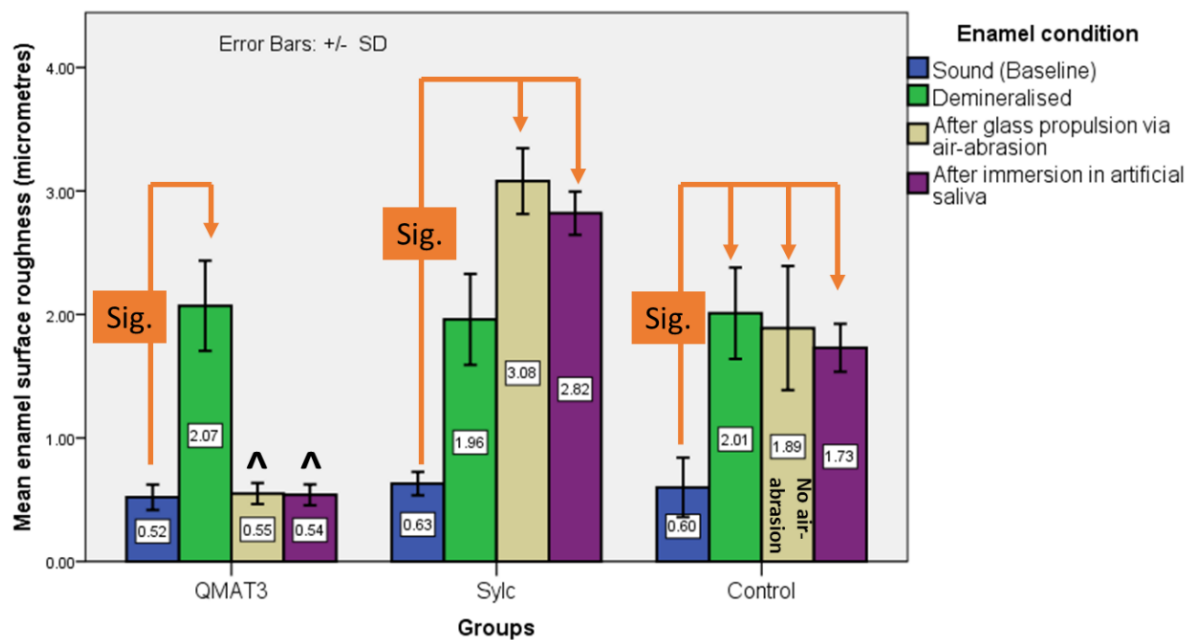


Figure 6.60. Means \pm SD of the enamel surface roughness (Ra) in micrometres for each experimental group under four different conditions. (^) denotes no significant difference in comparison with the corresponding baseline

6.4.8.3. Knoop hardness testing

No significant differences were observed in the Knoop hardness values between the experimental groups at baseline and following demineralisation (Table 6.14 and Figure

Results

6.61). Following demineralisation, the hardness values significantly decreased compared to their corresponding sound values for all experimental groups ($p < 0.001$). After immersion in artificial saliva, a significant increase was observed in the hardness values of both SylcTM-air-abrasion and QMAT3- air-abrasion groups compared to demineralised states and directly after glass propulsion ($p < 0.001$), suggesting that the glass reacted with artificial saliva and enhanced remineralisation of WSLs. Additionally, the hardness values of QMAT3- air-abrasion group were significantly higher than those obtained for the SylcTM-air-abrasion and control groups after immersion in artificial saliva ($p < 0.001$), although they did not reach their corresponding baseline values.

Table 6.14. Means \pm SD of Knoop hardness number (KHN) for each experimental group under four different conditions.

Group (n=10)	Experimental group based on the treatment method	Sound enamel (Baseline)	Demineralised enamel	After glass propulsion	After immersion in artificial saliva
1	QMAT3-air-abrasion	347.91 \pm 11.28	256.28 \pm 15.57	275.55 \pm 12.79	322.31 \pm 7.53
2	Sylc TM -air-abrasion	344.24 \pm 11.61	246.05 \pm 14.70	263.94 \pm 14.52	294.53 \pm 14.09
3	Untreated (Control)	342.25 \pm 12.62	248.45 \pm 15.41	251.67 \pm 9.44	265.19 \pm 16.25

Results

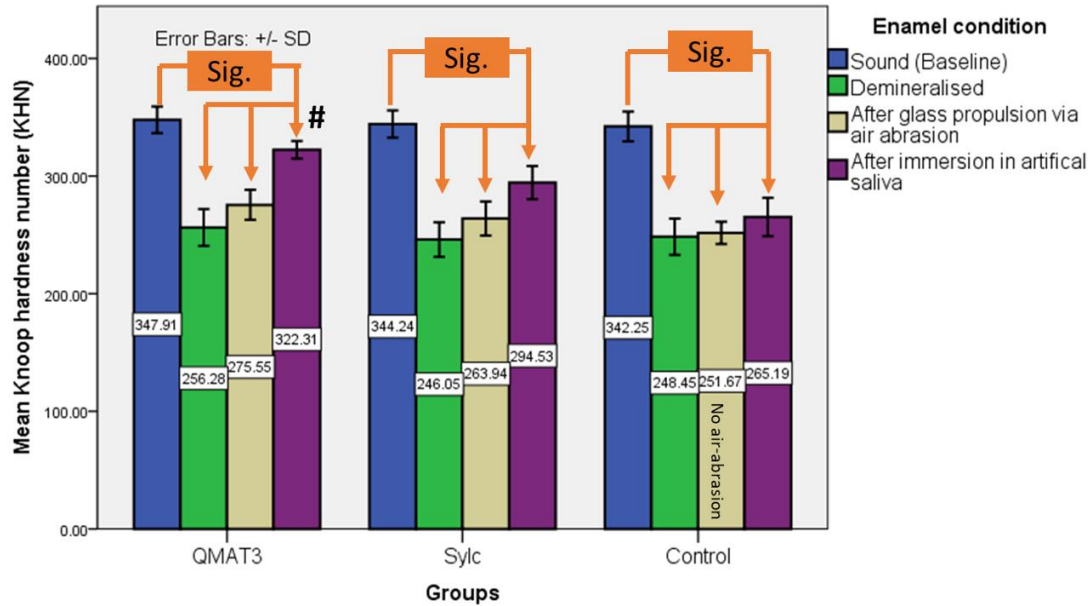


Figure 6.61. Means \pm SD of Knoop hardness number (KHN) for each experimental group under four different conditions. (#) denotes significant increase in enamel hardness compared with SylcTM and control groups after immersion in artificial saliva.

6.4.8.4. Scanning electron microscope (SEM)

Representative SEM images of enamel surfaces from the three experimental groups under different conditions (sound, demineralised, and remineralised following glass propulsion and immersion in artificial saliva) were taken at 3.000x and 20.0000x magnifications. Figure 6.62 showed that the sound enamel surface had a homogenous, flat and smooth surface, while the demineralised enamel surface appeared porous with voids of variable sizes distributed non-uniformly and rough, with irregular patterns of surface destruction due to the demineralisation process. After remineralisation (Figure 6.63), the remineralised enamel surfaces resulting from SylcTM-air-abrasion and QMAT3-air-abrasion were infiltrated by scattered mineral precipitate-like deposits. These apatite-like structures were more evident and distributed more uniformly in QMAT3, completely covering the porosities and resulting in a smoother enamel surface. These deposits were unevenly distributed on a less uniform enamel surface following SylcTM-air-abrasion. No evidence of remineralisation was observed on the rough enamel surfaces of the control (untreated) group.

Results

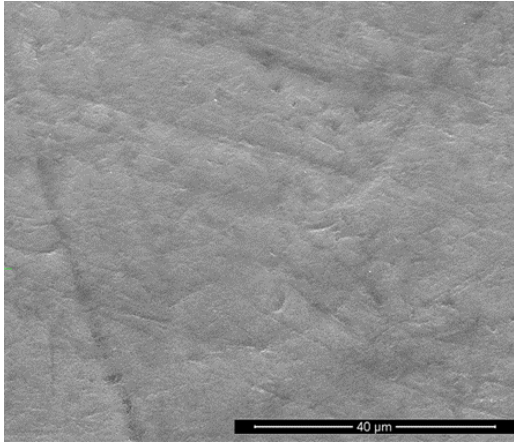
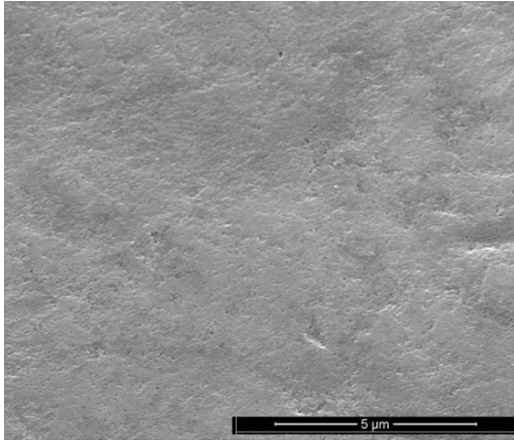
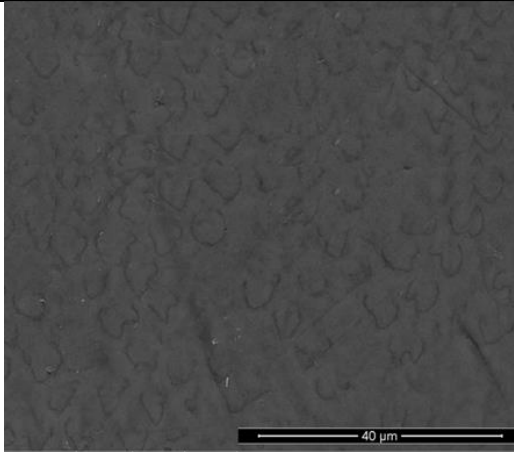
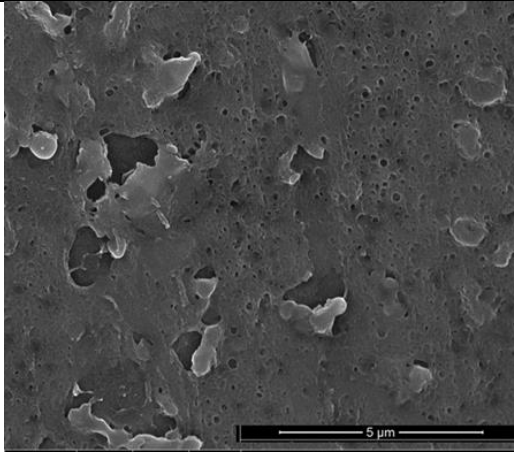
Enamel condition	Images taken at 3000x magnification	Images taken at 20.000x magnification
Sound		
Demineralised		

Figure 6.62. SEM images of sound and demineralised enamel surface

Results

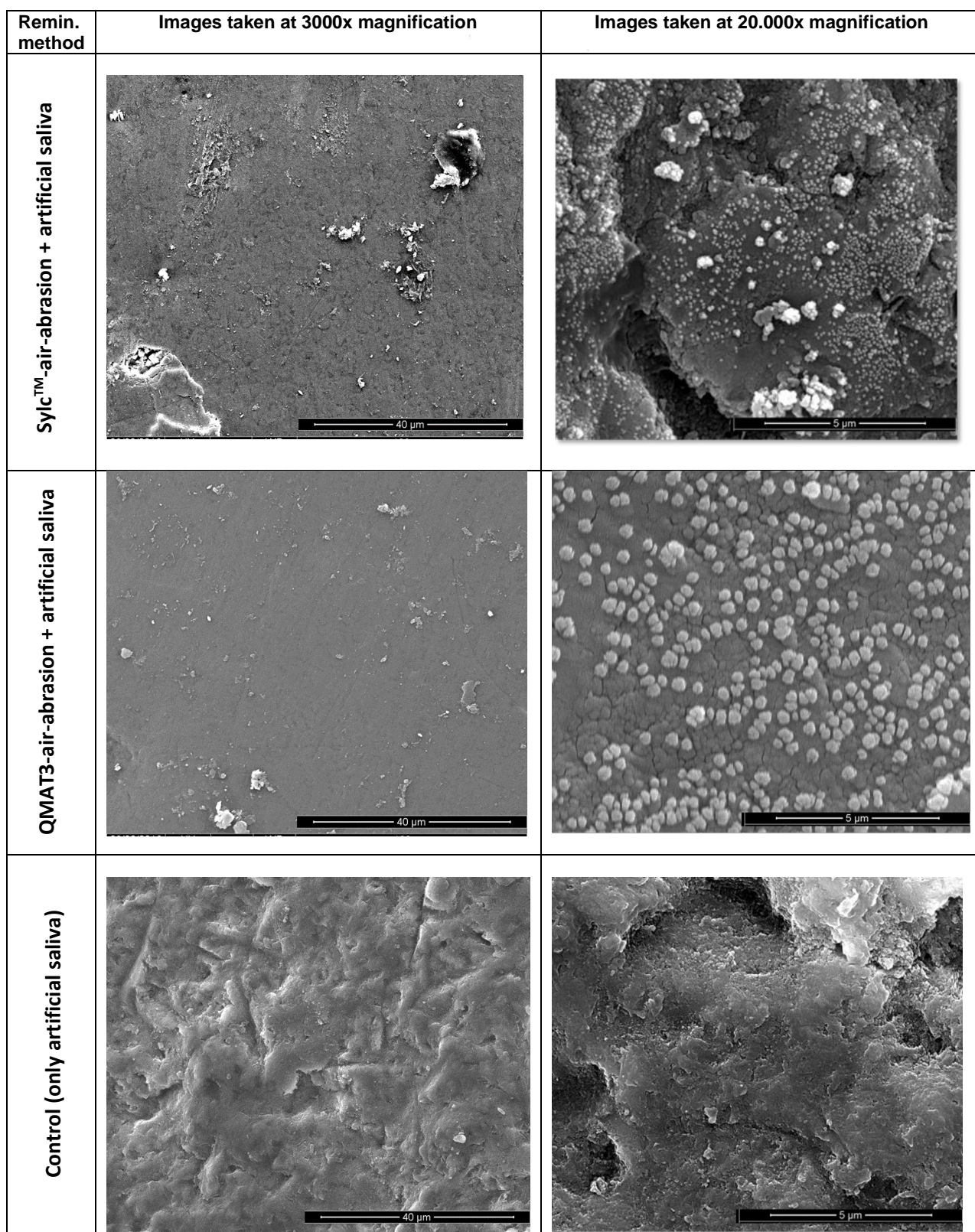


Figure 6.63. SEM images of remineralised enamel surface after using three remineralisation methods

Results

6.4.8.5. Energy dispersive X-ray Spectroscopy (EDX)

Differences in the emission peaks of some elements such as Ca, P, O and Na were observed in EDX spectra when comparing between sound and demineralised enamel surfaces (Figure 6.64). In addition, when the EDX spectra of those obtained after remineralisation involving glass propulsion (Sylc™ or QMAT3) followed by immersion in AS compared with the remineralised enamel surface in artificial saliva (AS) alone in the control group (Figure 6.65), an additional peak for silicon (Si) can be seen for Sylc™ glass at 1.73 keV in the Sylc™-air-abrasion group, and two additional peaks, at 1.73 keV and 0.65 keV representing (Si) and fluoride (F), respectively, can be seen for QMAT3 glass in the QMAT3-air-abrasion group.

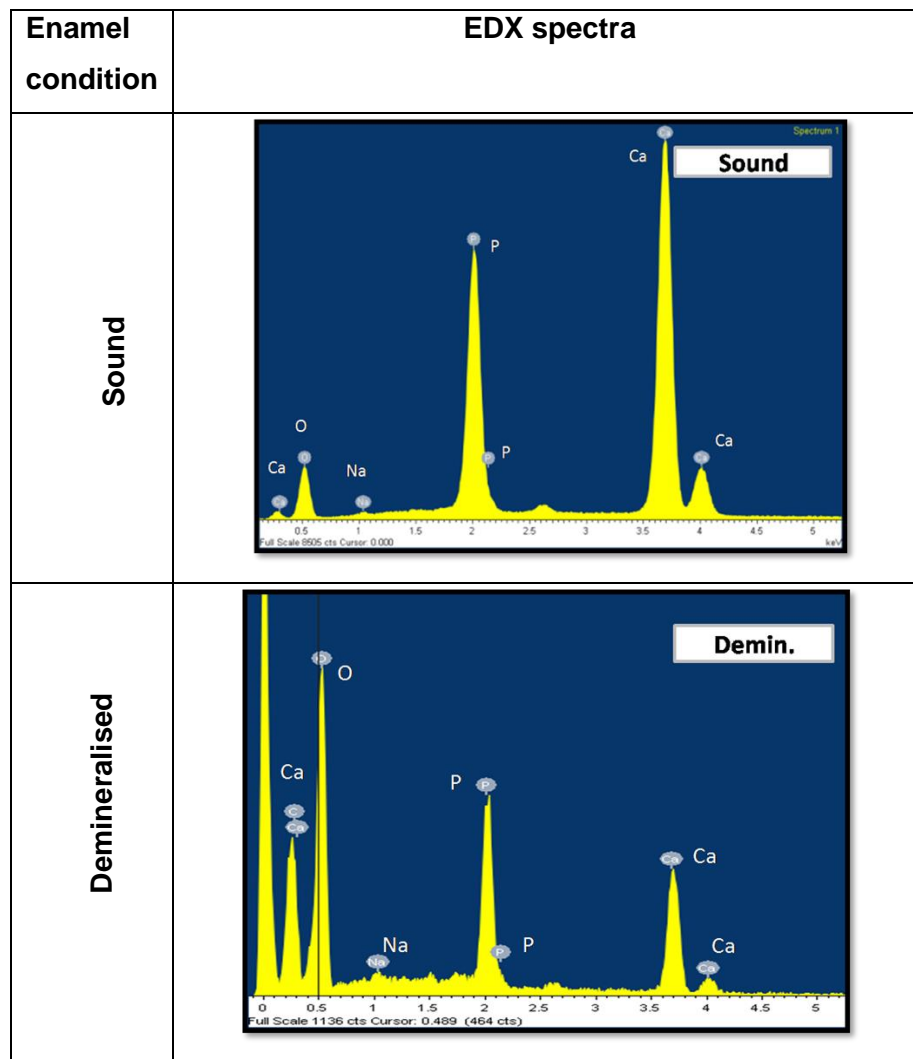


Figure 6.64. EDX spectra of sound and demineralised enamel surface

Results

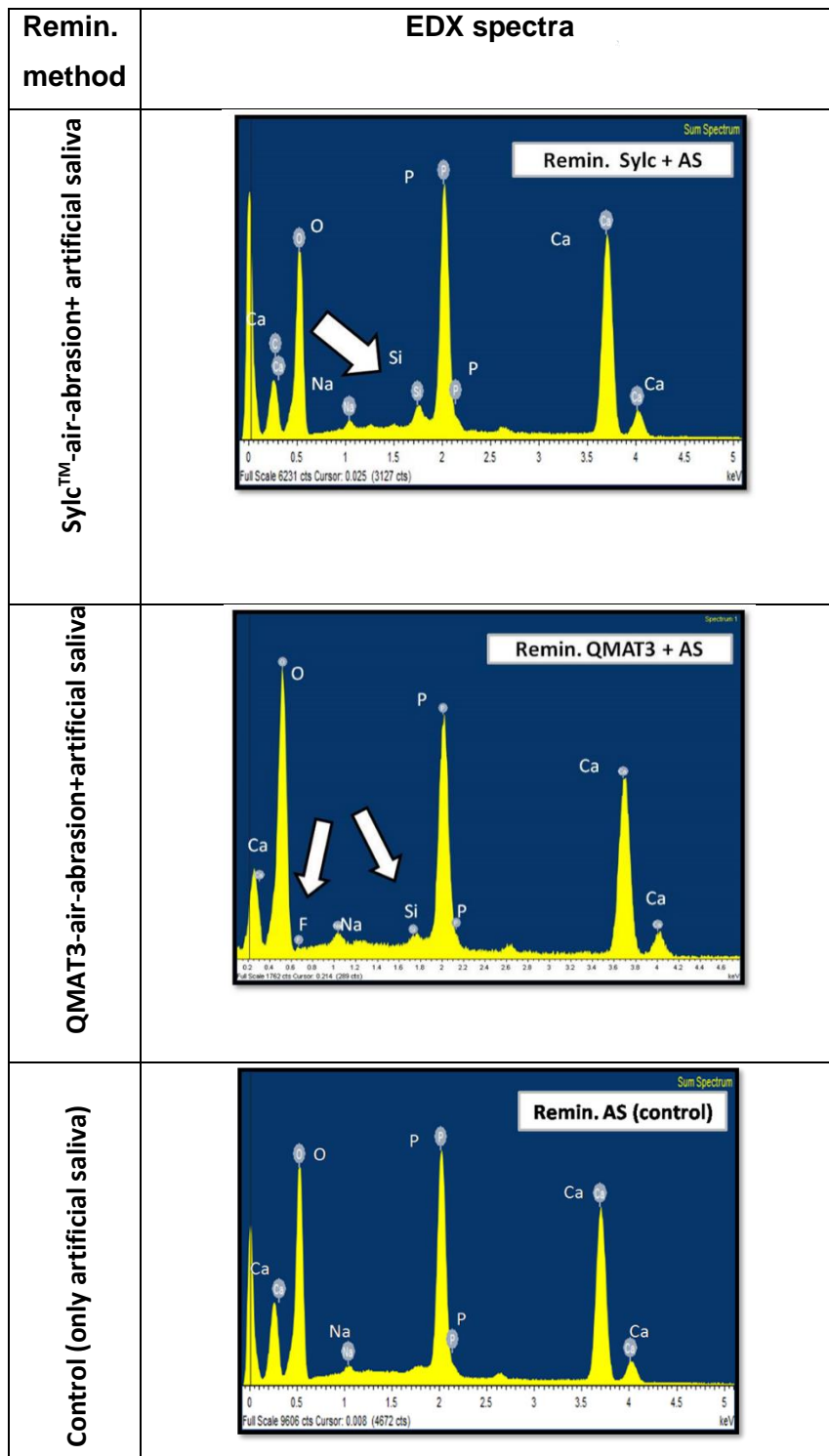


Figure 6.65. SEM images of remineralised enamel surface after using three remineralisation methods

7. DISCUSSION

7.1. Glass development and characterisation

7.2.7. Characterization of amorphous nature of glasses, glass thermal analysis, and hardness measurements

Bioactive glass, 45S5, has been used in a number of commercial medical (NovaBone™), and dental (Perioglas™, Sylc™ and NovaMin™) applications (Hench, 2006). Furthermore, preliminary *in vitro* research has been undertaken on its use *via* propulsion using air-abrasion, in order to cut sound and carious enamel and dentine (Paolinelis *et al.*, 2008; Banerjee *et al.*, 2011), remove residual orthodontic adhesives following bracket debonding from enamel surfaces (Banerjee *et al.*, 2008), and potentially to remineralise white spot lesions (Milly *et al.*, 2014b; 2015). However, these preliminary *in vitro* studies have yet to prompt widespread clinical application due to problems including excessive hardness of the glass above that of sound enamel (~3.5GPa) risking enamel damage (O'Donnell, 2011), with reported values varying between 4.5GPa (Cook *et al.*, 2008) and 5.75GPa (Lopez-Esteban *et al.*, 2003). Therefore, it is desirable to develop glasses with similar or lower hardness to that of enamel.

A number of alterations to the glass formulation to modify the hardness of bioactive glasses are possible. It has, for example, been reported that increasing Na₂O content from zero mol% to 26.5mol% (in exchange for CaO), across a series of bioactive glasses, with a constant network connectivity value close to two (NC=2.04), resulted in a linear decrease in the glass transition temperature (T_g; from 750°C to 500°C) (Wallace *et al.*, 1999). This was attributed to the substitution of CaO producing a more disrupted silicate glass network as one Ca²⁺ was replaced by two Na⁺ ions. The latter resulted in the loss of the ionic bridges that Ca²⁺ ions provided between two adjacent non-bridging oxygens, thus contributing to a decrease in the packing density of the glass. Additionally, it has also been reported that a reduction in silica content led to a decrease in T_g (O'Donnell *et al.*, 2009) in two glass series, from 513°C to 482°C and from 519°C to 491°C, respectively, when the phosphate content was increased from 1.07mol% to 9.25mol% and from zero mol% to 6.33mol%, respectively, to replace the reduced silica content. Similarly, Brauer *et al.* (2009) reported a decrease in T_g values

Discussion

(from 520°C to 400°C) after reducing the silica content (from 49.47mol% to 33.29mol%), while increasing the fluoride content (from zero mol% to 32.71mol%). The authors attributed this to the formation of complexes between fluoride and calcium ions (hypothetical CaF^+ complexes) in the glass network structure. These complexes reduced the positive charge of the calcium ion from two to one allowing the complex to bond only to one non-bridging oxygen instead of two. Hence, the electronegative forces between the two non-bridging oxygens reduced, weakening the durability of the glass and decreasing its T_g . Furthermore, both Farooq *et al.* (2013) and Mneimne *et al.* (2011) reported that glasses containing fluoride with a lower silica content and higher phosphate content increased the rate of glass degradation and apatite formation.

Hence, this concept of increasing Na_2O content (to 30mol%, in exchange for CaO content to 23.9mol%, compared to those in 45S5 glass; $\text{Na}=24.4\text{mol\%}$ and $\text{Ca}=26.9\text{mol\%}$), decreasing the silica content (from 46.1mol% for 45S5 to 37mol%), increasing phosphate content (from 2.6mol% for 45S5 to 6.1mol%) and the incorporation of calcium fluoride (constant ratio of fluoride; 3mol%). This formulation was preferred in the present study to develop glasses with lower T_g values, and higher rates of degradation and apatite formation. The latter two modifications were a consequence of the aforementioned reported studies with Mneimne *et al.* (2011) and Farooq *et al.* (2013) suggested that increased phosphate content (to approximately 6mol% in fluoride-containing glasses) led to a rapid release of calcium (Ca^{2+}) and orthophosphate (PO_4^{3-}) ions to the surrounding solution promoting early fluorapatite formation (6 hours). The fluoride content was kept constant, not only to enhance fluorapatite formation, but to prevent fluorite development as a consequence of excessive fluoride above levels of $\geq 5\text{mol\%}$ (Lusvardi *et al.*, 2009; Brauer *et al.*, 2009; Brauer *et al.*, 2010; Mneimne *et al.*, 2011). The formation of fluorite indicates crystallisation of the glass, resulting in inhibition of its bioactive properties; the presence of crystalline phases gives rise to increased resistance to ion exchange reactions between the glass surface and the physiological solution, which in turn affect apatite formation.

Hence, these modifications to the experimental glasses resulted in fluorapatite formation and absence of fluorite, which is discussed in detail later. They also resulted in a significant decrease in T_g values (355°C for QMAT3) compared with the 45S5

Discussion

glass (530°C), Sylc™ glass (530°C) and those reported above by O'Donnell *et al.*, (2009) and Brauer *et al.* (2009). A corresponding decrease in hardness values (3.43GPa for QMAT3) compared with 45S5 (4.66 GPa) and Sylc™ (4.63 GPa) was also noted. These hardness values, and those published, vary significantly from one study to another; for example, the hardness of bioactive glass, 45S5 reported by Lopez-Esteban *et al.* (2003) and Farooq *et al.* (2013) were 5.75GPa and 5.84GPa, respectively. This variation may be associated with the differences in the methodology used to prepare these glasses, and the indenter load used to measure the hardness, although a Vickers's instrument was used in all studies. In the current study the indenter load was 2.9kg while the indenter loads used by Lopez-Esteban *et al.* (2003) and Farooq *et al.* (2013) were 0.5-1.2kg, and 0.01kg, respectively. It was also evident from the T_g and hardness data in this study that QMAT3 conserved the enamel surface while removing the residual adhesives, without inducing undesirable surface enamel loss (discussed later).

Despite taking into consideration the aforementioned factors, two out of the five experimental glasses (QMAT4 and QMAT5) formed a crystalline structure when the sodium content was increased to 40 mol% with a commensurate reduction in calcium content. The crystalline structure of these glasses (verified by ATR-FTIR and XRD techniques) would have consequently affected the ion exchange process between their surface and the immersion solution, and their dissolution behaviour (apatite formation), as reported in previous studies (Ducheyne *et al.*, 1997; O'Donnell *et al.*, 2009; Brauer *et al.*, 2010; Mneimne *et al.*, 2011). Therefore, it was decided to exclude these two glasses from further experiments.

7.1.2. Glass bioactivity dissolution studies

Dissolution studies have been widely used for assessing the bioactivity of glasses and their potential ability to form apatite (O'Donnell *et al.* 2009; Brauer *et al.* 2010; Mneimne *et al.*, 2011; Farooq *et al.*, 2013; Mneimne, 2014; Bingel *et al.* 2015). These *in vitro* studies involved immersion of bioactive glasses in solutions, such as Tris buffer, artificial saliva and simulated body fluid, to assess their potential ability to form apatite *in vitro* prior to any subsequent *in vivo* studies.

Discussion

In the present study, three different solutions were used to examine the behaviour of three experimental (QMAT 1, 2 and 3; fluoride-containing glasses), 45S5 and Sylc™ glasses *in vitro*. These were: i) Tris buffer solution, which is a simple physiological solution mimicking diluted saliva or buffered water, with two different pH levels (7, and 9, respectively), ii) acetic acid of pH 5, which is an ideal caries-simulating system providing the same acidic medium that cariogenic bacteria thrive in and release acid by-products inducing enamel demineralisation and WSL formation, and iii) artificial saliva of pH 6.5, a solution simulating the composition and pH level of natural saliva, which is commonly used to assess the bioactivity of glasses *in vitro* (Earl *et al.*, 2010a; 2010b; Mneimne, 2014).

Prior to commencing the glass bioactivity dissolution studies, ATR-FTIR and XRD techniques were used to confirm their amorphous nature, and to identify any changes in the glass characteristics after reaction with the immersion solution. The immersion time intervals and the size of the glass particles used (<38µm) in the dissolution studies within the present research were similar to those reported in a number of studies (Mneimne *et al.*, 2011; Farooq *et al.*, 2013; Bingel *et al.*, 2015). The decision to incorporate a variety of intervals allowed a fair range of immersion time points to be used in order to pinpoint when apatite formation commenced and how this varied over time, allowing comparison with other published work.

According to the ATR-FTIR, XRD, and pH results, all experimental glasses (QMAT1, QMAT2 and QMAT3), after immersion in Tris buffer solution of pH=7, clearly showed dramatic changes in comparison to their unreacted versions, particularly in the timing of apatite formation. The latter occurred after 6 hours of immersion and was accompanied by a sudden rise in the pH level of the reacted Tris buffer solution, followed by a gradual increase in pH over the remaining immersion time periods (9 hours and 24 hours). However, these changes were barely observed at 24 hours for both 45S5 and Sylc™ glasses, suggesting that experimental glasses (containing fluoride) began to degrade early. This pattern could be explained based on Hench's mechanism of glass degradation (dissolution) and apatite formation (Hench, 1991) with the ion exchange process, particularly the exchange of sodium cations from the bioactive glass with hydrated protons (H^+) from the immersion solution, leaving behind residual hydroxyl ions (OH^-). The loss of protons from the immersion solution resulted in an increase in

Discussion

its pH, while the residual hydroxyl ions hydrolysed the Si-O-Si bonds in glasses, forming silanol groups $\text{Si}(\text{OH})_4$ that later condensed to form a silica-rich gel layer. The latter is usually accompanied by leaching of calcium and phosphate from the glass and into the immersion solution, followed by the formation of a precipitate on the silica rich gel layer, identified as amorphous calcium phosphate, which mineralises later to form apatite. In the present study, it is inferred that this ion exchange mechanism was achieved for all glasses after immersion in solutions.

The ability of experimental glasses (fluoride-containing QMAT1, 2 and 3) to form apatite faster (at 6 hours) than both 45S5 and SylcTM (at 24 hours) after immersion in Tris buffer solution of pH=7 were consistent with previous findings (Mneimne *et al.*, 2011, Farooq *et al.*, 2013). The glasses in the latter two studies included the addition of fluoride (up to 25.54mol% and 3mol%, respectively), reduced silica content (up to 28.40mol% and 37mol%, respectively) and increased phosphate content (up to 6.33mol% and 6.1mol%, respectively) with a constant network connectivity (NC=2.08) for each, compared to 45S5 glass (silica=46.1mol%, phosphate= 2.6mol%, fluoride=zero mol% and NC=2.1). Both studies involved decreased sodium and calcium content but only one glass was amorphous in Mneimne *et al.* (2011), where the sodium and calcium contents were similar to 45S5, while all of Farooq *et al.*'s (2013) glasses were amorphous. In the latter, the sodium content was reduced to zero mol% in exchange for increased calcium content (53.9mol%). In the present study, the strategies used in preparing the experimental glasses were derived from these two studies, but the sodium content was increased across the glass series up to 30mol% with a commensurate reduction in calcium content up to 23.9mol% to maintain the network connectivity at a constant level (2.08). This approach may have led to earlier apatite formation than with both 45S5 and SylcTM.

Similar changes (apatite formation with a rise in pH of the immersion solution) were also observed for all glasses after immersion in acetic acid of pH=5, but at earlier immersion time points (at 3 hours for experimental glasses and at 9 hours for both 45S5 and SylcTM glasses) compared to those in Tris of pH=7 (at 6 hours for experimental glasses and at 24 hours for both 45S5 and SylcTM). This 'smart' property relates to the high concentration of protons (H^+) in acetic acid (pH =5) promoting a rapid exchange of protons with the sodium cations from the reacted glass. This was

Discussion

accompanied by a decrease in the concentration of protons, an increase in the pH level of acetic acid and the early formation of apatite. Conversely, due to the low concentration of protons in Tris buffer of pH=9, apatite formation and the rise in pH level required prolonged immersion periods, of up to 24 hours for experimental glasses, suggesting a gradual ion exchange between sodium cations and the protons in the immersion solution. However, no dramatic changes were observed for both 45S5 and SylcTM after immersion in Tris buffer of pH=9. Only one previous study has reported the effects of various immersion solutions pH on the release of ions and apatite formation with Bioglass[®](45S5) (Bingel *et al.*, 2015). The findings for both 45S5 and Sylc in the present study showed similar trends to those reported by Bingel *et al.* (2015) but apatite formed earlier (after 3 hours in acetic acid of pH=5) in the latter study, while it took 9 hours in the present study. This discrepancy may relate to the use of potassium hydroxide as a buffer to adjust the pH of acetic acid in the present study, while Bingel *et al.* (2015) used sodium hydroxide. It is suggested that the latter study resulted in a higher amount of sodium cations in the acetic acid solution prior to reaction with the glass, which masked the amount of sodium cations released. Hence, there was a higher concentration of sodium cations available for exchange with the protons in the solution, which may have accelerated apatite formation.

In the present study, accelerated apatite formation with all glasses was found with artificial saliva (as an immersion solution) compared with the other immersion solutions (Tris buffer and acetic acid). Specifically, experimental glasses formed apatite in 30 minutes while both 45S5 and SylcTM glasses required 45 minutes in artificial saliva. This may relate to the composition of the artificial saliva, which was supersaturated with calcium and phosphate ions. These ions, together with the calcium and phosphate ions released from the glasses on immersion, led to the formation of an amorphous calcium phosphate layer. This layer mineralised to form crystalline hydroxyapatite/fluorapatite in the experimental glasses and crystalline hydroxyapatite in both 45S5 and SylcTM glasses in line with reported findings by Mneimne (2014). The latter compared 45S5 glass and two experimental glasses of similar chemical composition to 45S5, but with reduced silica content (from 46.1mol%; 45S5 to 38.5mol% and 35.9mol%, respectively), increased phosphate content (from 2.6mol%; 45S5 to 6.3mol% for both), and the addition of fluoride (5.0mol%) to one of the glasses. Both experimental glasses formed apatite after 30 minutes of immersion in artificial saliva, while 45S5 glass

Discussion

produced apatite after 45 minutes. As mentioned earlier, Mneimne *et al.*'s (2014) second glass was comparable to that used in the present study. The chief difference between the two glass formulations was related to the increased sodium content (from 24.4mol%-45S5 to 30mol%), and a commensurate reduction in calcium (from 26.9mol%-45S5 to 23.9mol%) in the present study.

Although all experimental glasses presented with higher hardness values compared with the orthodontic adhesives, the experimental glass, QMAT3 was selected to be the most promising novel bioactive glass in the present research as it also presented with accelerated apatite formation, and lower hardness than that of sound enamel (~3.5GPa) (O'Donnell, 2011) and the commercially-available SycTM. It was therefore assumed that it would remove the residual adhesive safely and effectively without damaging the enamel surface. As a consequence, ¹⁹F MAS-NMR spectroscopy was used to detect the type of apatite formed on this selected glass after 24 hours of immersion in Tris buffer solution of pH=7 and after 1 hour of immersion in artificial saliva of pH=6.5, respectively. These immersion solutions, pH levels and immersion times were similar to those used in analogous studies (Mneimne *et al.*, 2011; Mneimne, 2014). The findings of the latter two studies using ¹⁹F MAS-NMR were in accordance with those of the present study confirming fluorapatite formation. It can be assumed that the presence of apatite detected after 6 hours in Tris buffer and 30 minutes in artificial saliva were also fluorapatite. Identical protocols for preparing the two immersion solutions were used in all studies. The formation of fluorapatite from fluoride-containing glasses (QMAT3) also corresponded with Okazaki and Sato (1990), who studied crystal models of hydroxyapatite and fluorapatite using computer graphics. They found that fluoride ions combined with the amorphous calcium phosphate layer (instead of OH⁻ ions) and suggested that this was due to the fluoride ions being smaller than the hydroxyl ions (OH⁻), and so they readily packed into the apatite lattice to form fluorapatite. The latter is chemically more stable than hydroxyapatite and more resistant to acid attack, caused by cariogenic bacteria, which may otherwise induce enamel demineralisation and WSL formation on the tooth surface (Featherstone, 2000; Robinson *et al.*, 2000).

7.3. Studies performed with glass particles between 38µm - 90µm in size

7.3.7. Glass particle size distribution analysis

It was necessary to produce a second batch of glasses with a larger particle size distribution (D90) for use in the air abrasion studies. Horiguchi *et al.*, (1998) reported that a larger mass (particle size) of glass was required to produce a higher kinetic energy, which increases the effectiveness of particle removal from the target surface. It took a number of attempts to increase the amount of large particles within the glass particle size distribution, since the presence of fine particles resulted in clumping and stagnation of the glass powder within the nozzle tip of the air abrasion hand-piece, and thus hindered the air-abrasion process; the presence of large particles prevented agglomeration of the glass powder.

7.3.8. Glass particle shape analysis

SEM images revealed the morphology of the commercially-available SycTM glass, 45S5 and experimental glasses to be very similar in appearance, characterised by sharp, angular and irregular particles. These in turn aided in removing residual orthodontic adhesives. Similar conclusions were reached by Horiguchi *et al.* (1998), who also used scanning electron microscopy to study the effects of either crushed glass powder (angular shape) or glass beads (spherical shape) in the removal of a layer of tissue from the target surface. They found that the crushed glass powder removed approximately three times more tissue than the glass beads, although both glass particles had the same size. These observations suggested that the angular shaped particles increased their cutting efficacy.

7.4. Air-abrasion studies performed using the selected novel glass, QMAT 3

Studies have been published which characterise the efficacy of bioactive glass (45S5) in the form of different particle sizes, ranging from 10µm -178µm in diameter, propelled *via* different air-abrasion systems (AbradentTM, HeraeusTM, and Aquacut VelopexTM, as

Discussion

described in the Literature Review; section 2.13.2) to cut (remove) sound and carious enamel and dentine (Horiguchi *et al.*, 1998; Paolinelis *et al.*, 2008; Banerjee *et al.*, 2011), removal of residual orthodontic adhesives (Banerjee *et al.*, 2008) and remineralisation of WSLs (Milly *et al.*, 2014b; 2015). In the present study QMAT3, of a particle size ranging between 38-90µm, was selected to be the most promising novel experimental glass for air abrasion studies because of its lower hardness compared to enamel and other glasses, and faster apatite (fluorapatite) formation compared to both 45S5 and Sylc™. The cutting efficiency of Sylc™ and QMAT3 experimental glasses were assessed by calculating the time required to cut a hole within prepared orthodontic adhesive discs using the Velopex Aquacut Quattro™ air-abrasion machine to propel them. This air-abrasion system facilitated precise control, providing known operating parameters to influence the cutting efficiency with particulate streams, thus allowing detection of minor differences that were present between the two glasses; this could not be achieved by using other air-abrasion systems.

In the present study, the results clearly showed that there were no significant differences between the two glasses when the same operating parameters were used, suggesting that QMAT3 is a potential alternative to Sylc™. However, on varying the parameters of the machine, such as different air-pressures (40 and 60 psi) and powder flow rate dials (1, 3, and 5), the cutting efficiency (cutting time) of each glass was increased with a change in the nozzle tip angle from 90° to 45°. The use of a 45° angle produced shallow preparations with a larger surface area and required more time to reach the base of the hole, while a 90° angle created narrow, deep preparations, which resulted in reaching the base of the hole within a short period of time. Similar findings were reported by Santos-Pinto *et al.* (2001), who used a PrepStar air-abrasion system (Danville Eng, San Ramon, CA, USA) and aluminium oxide powder (particle size 27µm) at two nozzle tip angles (80° and 45° under 80psi air-pressure) for 15 seconds, at an operating distance of 2mm, to cut surfaces on 72 of extracted human molars, which were assessed using SEM. Furthermore, a significant reduction in the cutting time was observed when the air pressure was increased from 40psi to 60psi. This finding agreed with those reported by Paolinelis *et al.*, (2009) and Milly *et al.* (2014a), who found a linear relationship between the increased kinetic energy and the increased velocity of the glass particles, as a result of the increased propellant pressure. Adjusting the powder flow rate from the minimum value (dial 1) to the maximum (dial 5) resulted in a

Discussion

reduction in the cutting time with QMAT3, while other parameters were kept constant. Similar observations were reported by Paolinelis *et al.* (2009) using alumina powder (particle size 27 μ m) propelled *via* an Abradent™ air-abrasion machine (Crystalmark, CA, USA) to examine the cutting characteristics under various operating parameters, on flat Macor™ sheets of 6mm thickness. This can be explained by the fact that increasing powder flow rate resulted in an increase in the number of the glass particles coming into contact with the surface, leading to abrade it within a short period of time. As such, the importance of controlling the operating setting parameters of the air-abrasion machine prior to its use is clear.

Although the Velopex Aquacut Quattro™ air-abrasion machine is commercially-available and permits control of key setting parameters, BA Ultimate™ air polisher was used further for *in vitro* studies as it is more suited to the dental clinic. Moreover, no significant differences in the powder flow rate were observed between the polisher and the machine when the latter was set at a powder flow rate dial 5, as well as between the two glasses using the same air-abrasion system, suggesting that any difference between the two glasses in subsequent experiments related primarily to the properties of the propelled glass itself rather than to the physics of the air-abrasion system.

7.4. Experiments performed using the selected novel glass, QMAT 3

7.4.1. Orthodontic adhesive removal

Extracted human premolar teeth were used instead of bovine teeth due to the structural differences between them, such as thicker crystallites, lower fluoride concentration and increased enamel porosity in the latter. In addition, they are not subjected to the same genetic as well as environmental and dietary factors as human material and, as such, will behave differently in a physical and chemical manner (Melberg, 1992; Laurance-Young *et al.*, 2011). Moreover, Yassen *et al.* (2011) indicated that inconsistent data are available in relation to the use of bovine teeth as an alternative to human teeth in *in vitro* research, and the differences in the morphological structures, physical properties and chemical compositions between them should not be overlooked.

Discussion

It has previously been reported that the use of TC burs increased enamel roughness compared to composite burs (Karan *et al.*, 2010), white stone (Mohebi *et al.*, 2017), stainburster burs (Erdur *et al.*, 2016) and a bespoke adhesive residue remover (Jaiszewska-Olszowska *et al.*, 2015). These authors compared their results with atomic force microscopy, profilometer, and 3D scanning using blue-light technology. In the present study, the profilometer data revealed that the use of the TC bur increased enamel surface roughness regardless of the type of adhesive used. Sylc™-air-abrasion also produced an increase in the enamel roughness to some extent. These findings are in agreement with those of Banerjee *et al.* (2008), who demonstrated that removal of residual adhesive resin (Unite™) using alumina air-abrasion caused more enamel loss (0.039 mm³), followed by the TC bur (0.285 mm³) and finally 45S5 air-abrasion (0.135 mm³) using an Abradent™ (Crystalmark, CA, USA) air-abrasion machine. In the present study, the novel experimental glass (QMAT3) induced less enamel roughness compared with the TC bur and Sylc™-air-abrasion, irrespective of the adhesive material used, a finding which was corroborated using SEM imaging. This finding relates to the lower hardness value of QMAT3 which approximates but does not exceed that of the enamel surface. Therefore, this glass powder was less likely to roughen the enamel surface, mitigating the associated risk of plaque accumulation and caries formation. Furthermore, the handling technique used in this study was similar to that used by Paolinelis *et al.* (2009), who confirmed that using the aforementioned operating parameters increased the cutting efficiency of the air-abrasion technique. Consequently, using accepted clinical handling parameters it appears that QMAT3 novel glass powder may be capable of selective removal of orthodontic adhesives without inducing deleterious abrasion of the enamel surface, although quantification of the volume of loss was not undertaken.

Enamel surface roughness measurements were not affected by polishing subsequent to each clean-up method with either adhesive. Polishing of the enamel surface does not appear to penetrate the grooves and pits produced by the clean-up, particularly with the tungsten-carbide bur in the present study. Similarly, previous studies reported that polishing (by pumicing using a rubber cup with non-fluoridated pumice for a period ranging from 10 to 30 seconds, and similar to the methodology used in the present study for 20 seconds) had no effect on the enamel roughness induced by adhesive

Discussion

removal using profilometer and scanning electron microscope (Roush *et al.*, 1977; Gwinnett and Gorelick, 1997; Vieira *et al.*, 1993; Ahrari *et al.*, 2013).

Further laboratory research in relation to the cutting efficiency of this approach is required prior to clinical application, although preliminary data suggests comparable levels of efficiency to other bioactive glass formulations. Although a significant difference was recorded for the hardness of both adhesives (Transbond XT™, ~0.52GPa; Fuji Ortho LC™, ~0.37GPa), glass-air abrasion, with both Sylc and QMAT3, resulted in removing both adhesives, since their hardness values were much higher (Sylc=4.63GPa and QMAT3=3.43GPa). Additionally, adhesive removal took approximately half the time with the TC bur. This discrepancy might relate to the aggressive cutting associated with sharp cutting blades of TC bur while bioactive glass propulsion works by means of abrasion. Similar conclusions were reached by both Karan *et al.* (2010) and Mohebi *et al.* (2016), who reported that TC burs removed adhesive remnants faster than composite bur and white stone, respectively.

It is important to emphasise that the present research is limited by its *ex vivo* nature; as such, replication within an *in vivo* situation is required. In addition, teeth were stored in deionised water rather than undergoing a simulated artificial aging process involving thermo-mechanical cycling; the latter approach may have been more clinically representative, although use of water storage remains an accepted approach (Amaral *et al.*, 2007).

7.4.2. White spot lesion (WSL) remineralisation

Artificial WSLs were induced in human premolars instead of using teeth with natural WSLs, since the latter vary widely in shape, size and mineral content, which may in turn influence the outcome of the remineralisation studies (Silverstone *et al.*, 1981; Huang *et al.*, 2007; Cochrane *et al.*, 2012). Therefore, artificial WSLs were induced *in vitro* for the remineralisation part of the study to avoid biological variations that may affect the pattern and efficacy of the remineralisation treatment. The bi-layer demineralisation protocol used in this study, which involved the application of a methyl cellulose gel layer on the tooth surface, to slow the penetration of lactic acid (where the former layer buffered the effect of the acid) for 14 days at 37°C, created a subsurface carious lesion

Discussion

with an intact outer surface and an average depth of 70-100µm. These features were in line with a protocol used in two *in vitro* studies (Lynch *et al.*, 2007; Magalhaes *et al.*, 2009), which reported that the features of the lesions induced by bi-layer demineralisation approximated to those of natural lesions. They used transverse microradiography utilising a computerised image-analysis system to measure the mineral content profiles in different types of artificially-induced lesions.

Kang *et al.* (2012) found that the porous demineralised surfaces of enamel had high intensity light backscattering values due to the increased number and size of pores compared with those of sound enamel using OCT. Conversely, the light associated with both sound and remineralised enamel surfaces is scattered from well-ordered prism (rod) structures resulting in less time for the light to travel within the enamel structure of extracted human teeth and leading to low intensity values (Jones and Fried, 2006; Milly *et al.*, 2014b; Milly *et al.*, 2015). The OCT findings in the present study were in accordance with the aforementioned studies. After glass propulsion and immersion in artificial saliva, it was clear that the QMAT3-air-abrasion group presented with lower light intensity backscattering values on remineralised enamel surfaces compared with those obtained for the SylcTM-air-abrasion and control (untreated) groups. This may be due to evenly distributed and profusely scattered QMAT3 glass particles forming a new mineral layer on enamel that fully covered the porous lesion, as observed in SEM images, while the particles of SylcTM glass diffused unevenly on the remineralised enamel surfaces. The high intensity light backscattering values obtained for the control group reflect the low potential for remineralisation associated with artificial saliva and therefore a lack of remineralisation.

The current profilometer findings showed that after propulsion of SylcTM *via* air-abrasion, enamel surface roughness increased compared to sound enamel. This may relate to the hardness of this glass (4.6GPa), which was higher than that of enamel (3.5GPa), thus leading to abrasion of the enamel surface. Conversely, due to the lower hardness of QMAT3 (3.4GPa; approximating but not exceeding that of the enamel surface), the surface roughness of previously demineralised enamel was significantly reduced after propulsion and found to be similar to that of sound enamel. These findings were in accordance with Milly *et al.* (2014; 2015). The authors used 45S5 powder in the form of a slurry and paste (mixed with polyacrylic acid) for 21 days

Discussion

(applied twice daily for 5 minutes) to enhance remineralisation of demineralised human enamel surfaces, either with or without adjunctive pre-conditioning (using air-abrasion with the same glass). The protocol used in the present study was simpler, less time-consuming and therefore potentially of greater clinical appeal.

The Knoop hardness number (KHN) values of sound enamel obtained in the present study (338-351 KHN) were in accordance with previous studies ranging from 270-350 KHN (Meredith *et al.* 1996), 322-353 KHN (Lupi-Pegurier *et al.*, 2003) and 314-361 KHN (Jennett *et al.*, 1994). These variations may be attributed to factors such as the chemical composition and histological features of the enamel surface, enamel sample preparation, the tested site on the enamel, load applied and reading error in respect of long-axis indentation length. After demineralisation, the KHN values were lower than their corresponding sound surfaces. Davidson *et al.* (1974) also demonstrated that the KHN values of demineralised enamel surfaces was 50% less than with sound surfaces. They suggested that the decrease in KHN value was associated with a decrease in the concentration of calcium after acid attack. After glass propulsion and immersion in artificial saliva to induce remineralisation, an increase in the enamel microhardness was observed, suggesting an increase in the mineral content, particularly after using QMAT3. These findings agree with Milly *et al.* (2015), who reported increased KHN values after applying 45S5 powder in the form of a slurry or a paste (for 21 days) to the pre-conditioning surface. In the current study, 24 hours of immersion in artificial saliva was sufficient to observe an increase in KHN values of human enamel surfaces remineralised after glass propulsion *via* air-abrasion.

The surface characteristics of sound and demineralized enamel (via SEM) were similar to those reported in the literature (Dong *et al.*, 2011; Ferrazzano *et al.*, 2011; Jayarajan, 2011; Gjorgievska *et al.*, 2013; Milly *et al.*, 2015). After glass (QMAT3) propulsion and immersion in artificial saliva to induce remineralisation, SEM images showed mineral precipitations completely covering the enamel surface suggesting that the bioactive glass particles were embedded in the treated enamel surface and effectively led to its remineralisation. This occurred despite the teeth samples being rinsed with deionised water, dried for 48h at room temperature and sputter-coated prior to imaging. These precipitations presented as dumbbell-like crystallites aggregated as a bunch of flowers; similar effects have also been reported in a number of studies where bioactive glass

Discussion

(45S5) was either applied as a paste or slurry (Pulido *et al.*, 2012; Gjorgievska *et al.*, 2013; Bakry *et al.*, 2014a; Bakry *et al.*, 2014b; Milly *et al.*, 2014; Narayana *et al.*, 2014; Milly *et al.*, 2015). However, these precipitations only partially filled the pores in the enamel surfaces propelled with Sylc™ indicating that partial enamel remineralisation occurred.

The findings from the EDX spectra in the present study supported the appearance of the SEM images, with the presence of an additional peak of silicon (Si) after propelling Sylc™ glass, and the presence of two additional peaks, for silicon (Si) and fluoride (F), after propelling QMAT3 glass. These peaks confirmed the incorporation of the glass particles within the enamel surface, which was not detected prior to propulsion of these glasses. This implies that the embedded particles were apatite-like structures of reacted bioactive glass particles and did not simply represent deposits of non-reacted bioactive glass particles. The additional Si peak was an indication of the formation of silica gel layer, while two additional peaks for Si and F, after propelling experimental glass (QMAT3) suggest the formation of silica gel layer and fluorapatite.

Hence, the findings of OCT, non-contact profilometer, Knoop hardness testing, SEM, and EDX were consistent in suggesting the remineralisation of WSLs after QMAT3-air-abrasion followed by immersion in artificial saliva for 24 hours. These five techniques provided a more comprehensive perspective on the overall performance of QMAT3 glass for WSL remineralisation in comparison with the commercially-available Sylc™ propelled *via* air-abrasion. The surface characteristics of sound (baseline) and remineralised enamel with QMAT3 surfaces were comparable. These included lower intensity light backscattering values (detected by OCT), lower surface roughness values (by non-contact profilometer) and higher Knoop hardness values compared to those corresponding to demineralised surfaces.

¹⁹F MAS-NMR spectroscopy confirmed the presence of fluorapatite in remineralised enamel blocks after QMAT3-air-abrasion followed by immersion in artificial saliva for 24 hours. This type of apatite was not detected in sound or demineralised enamel, or enamel remineralised either by artificial saliva only, or remineralised with Sylc™ glass. This confirmed that the mineral deposits observed with SEM after propelling QMAT3 were fluorapatite. Similar findings using ¹⁹F MAS-NMR were obtained by Mohammed *et*

Discussion

al. (2013), who studied the effect of immersion, on demineralised enamel blocks, in a remineralising solution (0.1 M acetic acid buffered with NaOH to pH=4) containing NaF of different concentrations. The authors found that fluorapatite was formed on these blocks after immersion (solution containing 11 ppm fluoride) for 96 hours, at 37°C. Hill *et al.* (2015) also detected the formation of fluorapatite by ^{19}F MAS-NMR on demineralised enamel blocks after immersion for 96 hours at 37°C in a remineralising solution (0.1 M acetic acid of pH=4) containing either a commercial mouthwash or a toothpaste (Ultradex®, Perioducts Ltd, Ruslip HA4 6SA, UK; diluted to 10%). Both products contained nano hydroxyapatite powder (5%, 7.5%, respectively) and fluoride in the form of sodium mono fluorophosphate (600 ppm and 1000 ppm, respectively). Compared to the studies described above, fluorapatite formed earlier in the current study (at 24 hours; end-point of the experiment). It can be also assumed that it may have actually begun to form prior to 24 hours, since the glass dissolution studies verified apatite presence at 6 hours in Tris buffer and 30 minutes in artificial saliva.

All experimental glasses with increased sodium and phosphate contents, decreased silica content and a constant level of fluoride, particularly QMAT3, performed exceptionally well compared with 45S5 and Sylc™. The chemical composition of these experimental glasses increased their dissolution rates and subsequently invoked rapid apatite formation in all immersion solutions. The high sodium content reduced the hardness of QMAT3 avoiding enamel damage on removing residual orthodontic adhesive. Finally, the presence of a constant level of fluoride prevented the formation of unwanted fluorite, but instead, fluorapatite was formed, denoting a very positive finding. This is particularly beneficial since fluorapatite is more chemically stable than hydroxyapatite and has more resistance to acid attack associated with cariogenic bacteria, which might otherwise trigger enamel demineralisation and WSL formation (Featherstone, 2000; Robinson *et al.*; 2000).

8. CONCLUSIONS AND FUTURE WORK

8.1. CONCLUSIONS

- Based on 11 *in vitro* studies in a systematic review, it appears that bioactive glasses may be capable of promoting enamel remineralisation in various formulations, compared with other topical remineralising materials including fluoride and CPP-ACP. However, further clinical research to confirm their effectiveness is now overdue.
- A bioactive glass (45S5) mirroring the formula of the commercially-available 45S5 glass (Sylc™) was developed with similar properties and behaviour. Specifically, three amorphous experimental glasses had similar particle size distributions and shape to both the laboratory-prepared 45S5 glass and Sylc™.
- The bioactivity of these amorphous experimental glasses was proven by accelerated apatite formation after immersion in solutions of varying pH (6 hours in Tris buffer of pH 7, 3 hours in acetic acid of pH 5 and 30 minutes in artificial saliva of pH 6.5) relative both to Sylc™ and 45S5 (24 hours, 9 hours, 45 minutes, respectively).
- The most promising novel experimental glass (QMAT3) had a glass transition temperature (355°C) lower than experimental QMAT1 and 2, laboratory-prepared 45S5 and Sylc™ (530°C). Its hardness was also lower than experimental QMAT1 and 2, 45S5 and Sylc™, but higher than orthodontic adhesives and comparable to that of enamel.
- The cutting efficiency and powder flow rate of both Sylc™ and QMAT3 were similar using the same air-abrasion system and settings. Moreover, the use of various settings and operating parameters during use with the air-abrasion machine affected the cutting efficiency of both Sylc™ and the QMAT3 in a similar manner.
- QMAT3-air-abrasion was capable of selectively removing residual orthodontic adhesives without inducing enamel damage, compared with Sylc™-air-abrasion and the tungsten-carbide bur. It therefore shows promise as a viable alternative to the most common rotary method (TC bur) for removal of adhesive. However,

Conclusions and Future work

QMAT3-air-abrasion took approximately twice the time to remove adhesive remnants compared with the TC bur. As such, further laboratory research is required to improve the cutting efficiency of this glass prior to its clinical application.

- QMAT3 was capable of enhancing enamel remineralisation more effectively than Sylc™ suggesting its potential utility in promoting enamel remineralisation *in vivo*, particularly as it formed fluorapatite when coming into contact with solutions simulating the physiological solution.
- Fluorapatite was formed on human enamel by QMAT3. This is particularly beneficial as fluorapatite is more chemically stable and more resistant to acid attack compared to hydroxyapatite formed by both Sylc™ and 45S5. Therefore, this formation of fluorapatite was a positive and encouraging finding.
- Overall, a novel glass (QMAT3) with comparable, if not superior, bench properties to Sylc™ has been developed. This experimental work shows promise in the area of adhesive removal after orthodontic bracket debonding and, according to SEM evidence, remineralisation of artificially introduced WSL on enamel surfaces under laboratory conditions.

8.2. FUTURE WORK

- QMAT3-air-abrasion took approximately twice the time to remove adhesive remnants compared with the TC bur. Therefore, evaluation of glasses with similar chemical composition to the most promising glass (QMAT3), but with different ranges of particle size should be undertaken. This will allow evaluation and further improvement of cutting efficiency in the removal of residual orthodontic adhesives.
- To study the remineralisation potential of QMAT3 on artificial WSLs of different lesion depths, induced by different demineralisation protocols.
- To study the remineralising potential of QMAT3 on natural WSLs and on carious dentine (natural/artificial).

Conclusions and Future work

- It would be useful to study the potential ability of QMAT3 as a polishing powder for enamel surface to remove staining.
- To design a series of bioactive glasses incorporating strontium and fluoride (strontium will be exchanged for calcium). Strontium has bacteriostatic effects (Liu *et al.*, 2016). Furthermore, it has a high molar mass compared with calcium; this will result in the formation of glasses with lower hardness and higher kinetic energy, thus potentially improving their cutting efficiency.
- To undertake a clinical trial assessing the cutting efficiency of QMAT3 in removing residual orthodontic adhesives and to allow evaluation of the associated remineralisation characteristics.

References

REFERENCES

- Adeyemi, A. A., Jarad, F. D., Pender, N., & Higham, S. M. (2006). Comparison of quantitative light-induced fluorescence (QLF) and digital imaging applied for the detection and quantification of staining and stain removal on teeth. *Journal of Dentistry*, 34(7), 460-466.
- Ahrari, F., Akbari, M., Akbari, J., & Dabiri, G. (2013). Enamel surface roughness after debonding of orthodontic brackets and various clean-up techniques. *Journal of Dentistry of Tehran University of Medical Sciences*, 10(1), 82-93.
- Aina, V., Malavasi, G., Pla, A. F., Munaron, L., & Morterra, C. (2009). Zinc-containing bioactive glasses: surface reactivity and behaviour towards endothelial cells. *Acta Biomaterialia*, 5(4), 1211-1222.
- Alexander, S. A., & Ripa, L. W. (2000). Effects of self-applied topical fluoride preparations in orthodontic patients. *The Angle Orthodontist*, 70(6), 424-430.
- Aljehani, A., Tranæus, S., Forsberg, C. M., Angmar-Månsson, B., & Shi, X. Q. (2004). In vitro quantification of white spot enamel lesions adjacent to fixed orthodontic appliances using quantitative light- induced fluorescence and DIAGNOdent. *Acta Odontologica Scandinavica*, 62(6), 313-318.
- Aljehani, A., Yousif, M. A., Angmar-Månsson, B., & Shi, X. Q. (2006). Longitudinal quantification of incipient carious lesions in postorthodontic patients using a fluorescence method. *European Journal of Oral Sciences*, 114(5), 430-434.
- Aljubouri, Y. D., Millett, D. T., & Gilmour, W. H. (2003). Laboratory evaluation of a self-etching primer for orthodontic bonding. *The European Journal of Orthodontics*, 25(4), 411-415.
- Aljubouri, Y. D., Millett, D. T., & Gilmour, W. H. (2004). Six and 12 months' evaluation of a self-etching primer versus two-stage etch and prime for orthodontic bonding: a randomized clinical trial. *The European Journal of Orthodontics*, 26(6), 565-571.
- Al-Khateeb, S., Exterkate, R., Angmar-Månsson, B., & ten Cate, B. (2000). Effect of acid-etching on remineralization of enamel white spot lesions. *Acta Odontologica Scandinavica*, 58(1), 31-36.

References

- Alkire, R. G., Bagby, M. D., Gladwin, M. A., & Kim, H. (1997). Torsional creep of polycarbonate orthodontic brackets. *Dental Materials*, 13(1), 2-6.
- Amaechi, B. T., Porteous, N., Ramalingam, K., Mensinkai, P. K., Ccahuana Vasquez, R. A., Sadeghpour, A., & Nakamoto, T. (2013). Remineralization of artificial enamel lesions by theobromine. *Caries Research*, 47(5), 399-405.
- Amaral, M., Lopes, M. A., Silva, R. F., & Santos, J. D. (2002). Densification route and mechanical properties of Si₃N₄-bioglass biocomposites. *Biomaterials*, 23(3), 857-862.
- Amaral, F. L., Colucci, V., PALMA-DIBB, R. G., & Corona, S. A. (2007). Assessment of in vitro methods used to promote adhesive interface degradation: a critical review. *Journal of Esthetic and Restorative Dentistry*, 19(6), 340-353.
- Anderson, A. M., Kao, E., Gladwin, M., Benli, O., & Ngan, P. (2002). The effects of argon laser irradiation on enamel decalcification: An in vivo study. *American journal of orthodontics and dentofacial orthopedics*, 122(3), 251-259.
- Andersson, A., Skold-Larsson, K., Hallgren, A., Petersson, L. G., & Twetman, S. (2004). Measurement of enamel lesion regression with a laser fluorescence device (DIAGNOdent): a pilot study. *Orthodontics*, 1, 201-206.
- Anderson, A., Skold-Larsson, K., Hallgren, A., Petersson, L. G., & Twetman, S. (2007). Effect of a dental cream containing amorphous calcium phosphate complexes on white spot lesion regression assessed by laser fluorescence. *Oral Health Prev Dent*, 5, 229-233.
- Ang, S. F., Saadatmand, M., Swain, M. V., Klocke, A., & Schneider, G. A. (2012). Comparison of mechanical behaviors of enamel rod and interrod regions in enamel. *Journal of Materials Research*, 27(2), 448-456.
- Angmar-Månsson, B., & Ten Bosch, J. J. (1987). Optical methods for the detection and quantification of caries. *Advances in Dental Research*, 1(1), 14-20.
- Angmar-Mansson, B., Al-Khateeb, S., & Tranaeus, S. (1996). Monitoring the caries process Optical methods for clinical diagnosis and quantification of enamel caries. *European Journal of Oral Sciences*, 104(4), 480-485.

References

- Angmar-Mansson, B., & Bosch, J. T. (2001). Quantitative light-induced fluorescence (QLF): a method for assessment of incipient caries lesions. *Dentomaxillofacial Radiology*, 30(6), 298-307.
- Arhun, N., & Arman, A. (2007). Effects of orthodontic mechanics on tooth enamel: a review. *Seminars in Orthodontics*, 13(4), 281-291.
- Arends, J., Dijkman, T., & Christoffersen, J. (1987). Average mineral loss in dental enamel during demineralization. *Caries Research*, 21(3), 249-254.
- Argenta, R. M. O., Tabchoury, C. P. M., & Cury, J. A. (2003). A modified pH-cycling model to evaluate fluoride effect on enamel demineralization. *Pesquisa Odontológica Brasileira*, 17(3), 241-246.
- Arici, S. (1998). Orthodontic brackets (A Literature Review). *Turkish Journal of Orthodontics*, 11(2), 175-187.
- Arora, V., Arora, P. & Jawa, S. (2012). Microabrasive Technology for Minimal Restorations. *International Journal of Scientific and Research Publications*, 2, 1-7.
- Artun, J., & Bergland, S. (1984). Clinical trials with crystal growth conditioning as an alternative to acid-etch enamel pretreatment. *American Journal of Orthodontics*, 85(4), 333-340.
- Atsü, S. S., Gelgör, İ. E., & Sahin, V. (2006). Effects of silica coating and silane surface conditioning on the bond strength of metal and ceramic brackets to enamel. *The Angle Orthodontist*, 76(5), 857-862.
- Azzeh, E., & Feldon, P. J. (2003). Laser debonding of ceramic brackets: a comprehensive review. *American Journal of Orthodontics and Dentofacial Orthopedics*, 123(1), 79-83.
- Baeshen, H. A., Lingström, P., & Birkhed, D. (2011). Effect of fluoridated chewing sticks (Miswaks) on white spot lesions in post orthodontic patients. *American Journal of Orthodontics and Dentofacial Orthopedics*, 140(3), 291-297.
- Bailey, D. L., Adams, G. G., Tsao, C. E., Hyslop, A., Escobar, K., Manton, D. J., Morgan, M. V. (2009). Regression of post-orthodontic lesions by a remineralizing cream. *Journal of Dental Research*, 88(12), 1148-1153.

References

- Bakhadher, W., Halawany, H., Talic, N., Abraham, N., & Jacob, V. (2015). Factors affecting the shear bond strength of orthodontic brackets- A review of in vitro studies. *Acta Medica*, 58(2), 43-48.
- Bakry, A. S., Marghalani, H. Y., Amin, O. A., Tagami, J. (2014a). The effect of a bioglass paste on enamel exposed to erosive challenge. *Journal of Dentistry*, 42(11), 1458-1463.
- Bakry, A. S., Takahashi, H., Otsuki, M., Tagami, J. (2014b). Evaluation of new treatment for incipient enamel demineralization using 45S5 bioglass. *Dental Materials*, 30(3), 314-320.
- Banerjee, A., Paolinelis, G., Socker, M., McDonald, F., & Watson, T. F. (2008). An in vitro investigation of the effectiveness of bioactive glass air-abrasion in the 'selective' removal of orthodontic resin adhesive. *European Journal of Oral Sciences*, 116(5), 488-492.
- Banerjee, A., Hajatdoost-Sani, M., Farrell, S., & Thompson, I. (2010). A clinical evaluation and comparison of bioactive glass and sodium bicarbonate air-polishing powders. *Journal of Dentistry*, 38(6), 475-479.
- Banerjee, A., Thompson, I. D., & Watson, T. F. (2011). Minimally invasive caries removal using bio-active glass air-abrasion. *Journal of Dentistry*, 39(1), 2-7.
- Banks, P. A., & Richmond, S. (1994). Enamel sealants: a clinical evaluation of their value during fixed appliance therapy. *The European Journal of Orthodontics*, 16(1), 19-25.
- Banks, P. A., Burn, A., & O'Brien, K. (1997). A clinical evaluation of the effectiveness of including fluoride into an orthodontic bonding adhesive. *The European Journal of Orthodontics*, 19(4), 391-395.
- Banks, P. A., Chadwick, S. M., Asher-McDade, C., & Wright, J. L. (2000). Fluoride-releasing elastomerics-a prospective controlled clinical trial. *The European Journal of Orthodontics*, 22(4), 401-407.
- Barbour, M. E., & Rees, J. S. (2004). The laboratory assessment of enamel erosion: a review. *Journal of Dentistry*, 32(8), 591-602.

References

- Barry, G. R. P. (1995). A clinical investigation of the effects of omission of pumice prophylaxis on band and bond failure. *British Journal of Orthodontics*, 22(3), 245-248.
- Basdra, E. K., Huber, H., & Komposch, G. (1996). Fluoride released from orthodontic bonding agents alters the enamel surface and inhibits enamel demineralization in vitro. *American Journal of Orthodontics and Dentofacial Orthopedics*, 109(5), 466-472.
- Beerens, M. W., Van Der Veen, M. H., Van Beek, H., & Ten Cate, J. M. (2010). Effects of casein phosphopeptide amorphous calcium fluoride phosphate paste on white spot lesions and dental plaque after orthodontic treatment: a 3-month follow-up. *European Journal of Oral Sciences*, 118(6), 610-617.
- Benham, A. W., Campbell, P. M., & Buschang, P. H. (2009). Effectiveness of pit and fissure sealants in reducing white spot lesions during orthodontic treatment: A Pilot study. *The Angle Orthodontist*, 79(2), 338-345.
- Benson, P. E., Pender, N., & Higham, S. M. (1999). An in situ caries model to study demineralisation during fixed orthodontics. *Clinical Orthodontics and Research*, 2(3), 143-153.
- Benson, P. E., Pender, N., & Higham, S. M. (2003). Quantifying enamel demineralization from teeth with orthodontic brackets—a comparison of two methods. Part 1: repeatability and agreement. *The European Journal of Orthodontics*, 25(2), 149-158.
- Benson, P. E., Parkin, N., Millett, D. T., Dyer, F. E., Vine, S., & Shah, A. (2004a). Fluorides for the prevention of white spots on teeth during fixed brace treatment. *Cochrane Database Syst Rev*, 3, Art. No.: CD003809, 1-47.
- Benson, P. E., Douglas, C. I., & Martin, M. V. (2004b). Fluoridated elastomers: effect on the microbiology of plaque. *American Journal of Orthodontics and Dentofacial Orthopedics*, 126(3), 325-330.
- Benson, P. E., Shah, A. A., Millett, D. T., Dyer, F., Parkin, N., & Vine, R. S. (2005). Fluorides, orthodontics and demineralization: a systematic review. *Journal of Orthodontics*, 32(2), 102-114.

References

- Benson, P. (2008). Evaluation of white spot lesions on teeth with orthodontic brackets. *Seminars in Orthodontics*, 14(3), 200-208.
- Benson, P. E., Parkin, N., Dyer, F., Millett, D. T., Furness, S., & Germain, P. (2013). Fluorides for the prevention of early tooth decay (demineralised white lesions) during fixed brace treatment. *Cochrane Database Syst Rev*, 12. Art. No.: CD003809, 1-33.
- Berkovitz, B. K., Holland, G. R., & Moxham, B. J. (2005). *Oral anatomy, histology and embryology*. Mosby.
- Bingel, L., Groh, D., Karpukhina, N., & Brauer, D. S. (2015). Influence of dissolution medium pH on ion release and apatite formation of Bioglass® 45S5. *Materials Letters*, 143, 279-282.
- Bishara, S. E., & Trulove, T. S. (1990). Comparisons of different debonding techniques for ceramic brackets: An in vitro study: Part II. Findings and clinical implications. *American Journal of Orthodontics and Dentofacial Orthopedics*, 98(3), 263-273.
- Bishara, S. E., Ortho, D., & Fehr, D. E. (1993). Comparisons of the effectiveness of pliers with narrow and wide blades in debonding ceramic brackets. *American Journal of Orthodontics and Dentofacial Orthopedics*, 103(3), 253-257.
- Bishara, S. E., VonWald, L., Laffoon, J. F., & Jakobsen, J. R. (2000). Effect of changing enamel conditioner concentration on the shear bond strength of a resin-modified glass ionomer adhesive. *American Journal of Orthodontics and Dentofacial Orthopedics*, 118(3), 311-316.
- Bishara, S. E., VonWald, L., Laffoon, J. F., & Warren, J. J. (2001). Effect of a self-etch primer/adhesive on the shear bond strength of orthodontic brackets. *American Journal of Orthodontics and Dentofacial Orthopedics*, 119(6), 621-624.
- Bishara, S. E., Soliman, M. M., Oonsombat, C., Laffoon, J. F., & Ajlouni, R. (2004). The effect of variation in mesh-base design on the shear bond strength of orthodontic brackets. *The Angle Orthodontist*, 74(3), 400-404.
- Bishara, S. E., & Ostby, A. W. (2008). White spot lesions: formation, prevention, and treatment. In *Seminars in Orthodontics*, 14(3), 174-182.

References

- Black, R. B. (1950). Airbrasive: some fundamentals. *The Journal of the American Dental Association*, 41(6), 701-710. Cited by: Cook, R. J., Azzopardi, A., Thompson, I. D., & Watson, T. F. (2001). Real-time confocal imaging, during active air abrasion-substrate cutting. *Journal of Microscopy*, 203(2), 199-207.
- Boersma, J. G., Van der Veen, M. H., Lagerweij, M. D., Bokhout, B., & Prahl-Andersen, B. (2004). Caries prevalence measured with QLF after treatment with fixed orthodontic appliances: influencing factors. *Caries Research*, 39(1), 41-47.
- Bollen, C. M., Lambrechts, P., & Quirynen, M. (1997). Comparison of surface roughness of oral hard materials to the threshold surface roughness for bacterial plaque retention: a review of the literature. *Dental Materials*, 13(4), 258-269.
- Bonetti, G. A., Zanarini, M., Parenti, S. I., Lattuca, M., Marchionni, S., & Gatto, M. R. (2011). Evaluation of enamel surfaces after bracket debonding: an in-vivo study with scanning electron microscopy. *American Journal of Orthodontics and Dentofacial Orthopedics*, 140(5), 696-702.
- Bowman, S. J., & Ramos, A. L. (2005). The effectiveness of a fluoride varnish in preventing the development of white spot lesions. *World Journal of Orthodontics*, 7(2), 138-144.
- Boyd, R. L. (1991). Two-year longitudinal study of a peroxide-fluoride rinse on decalcification in adolescent orthodontic patients. *The Journal of Clinical Dentistry*, 3(3), 83-87.
- Boyd, R. L., & Chun, Y. S. (1994). Eighteen-month evaluation of the effects of a 0.4% stannous fluoride gel on gingivitis in orthodontic patients. *American Journal of Orthodontics and Dentofacial Orthopedics*, 105(1), 35-41.
- Boyde, A. (1997). Microstructure of enamel. *Dental Enamel*, 205, 18-31.
- Boyer, D. B., Engelhardt, G., & Bishara, S. E. (1995). Debonding orthodontic ceramic brackets by ultrasonic instrumentation. *American Journal of Orthodontics and Dentofacial Orthopedics*, 108(3), 262-266.

References

- Brackett, W. W., Gunnin, T. D., Gilpatrick, R. O., & Browning, W. D. (1998). Microleakage of class V compomer and light-cured glass ionomer restorations. *Journal of Prosthetic Dentistry*, 79(3), 261-263.
- Brantley, W.A., Eliades, T (2001). *Orthodontic materials: scientific and clinical aspects*. Stuttgart: Thieme.
- Brauer, D. S., Karpukhina, N., Law, R. V., & Hill, R. G. (2009). Structure of fluoride-containing bioactive glasses. *Journal of Materials Chemistry*, 19(31), 5629-5636.
- Brauer, D. S., Karpukhina, N., O'Donnell, M. D., Law, R. V., & Hill, R. G. (2010). Fluoride-containing bioactive glasses: effect of glass design and structure on degradation, pH and apatite formation in simulated body fluid. *Acta Biomaterialia*, 6(8), 3275-3282.
- Bröchner, A., Christensen, C., Kristensen, B., Tranæus, S., Karlsson, L., Sonnesen, L., & Twetman, S. (2011). Treatment of post-orthodontic white spot lesions with casein phosphopeptide-stabilised amorphous calcium phosphate. *Clinical Oral Investigations*, 15(3), 369-373.
- Brouns, E. M., Schopf, P. M., & Kocjancic, B. (1993). Electrothermal debonding of ceramic brackets. An in vitro study. *The European Journal of Orthodontics*, 15(2), 115-123.
- Buchalla, W., Imfeld, T., Attin, T., Swain, M. V., & Schmidlin, P. R. (2008). Relationship between nanohardness and mineral content of artificial carious enamel lesions. *Caries Research*, 42(3), 157-163.
- Buonocore, M. G. (1955). A simple method of increasing the adhesion of acrylic filling materials to enamel surfaces. *Journal of Dental Research*, 34(6), 849-853.
- Buonocore, M. G. (1963). Principles of adhesive retention and adhesive restorative materials. *The Journal of the American Dental Association*, 67(3), 382-391.
- Buonocore, M. (1970). Adhesive sealing of pits and fissures for caries prevention, with use of ultraviolet light. *The Journal of the American Dental Association*, 80(2), 324-328.

References

- Burwell, A. K., Litkowski, L. J., & Greenspan, D. C. (2009). Calcium sodium phosphosilicate (NovaMin®): remineralization potential. *Advances in Dental Research*, 21(1), 35-39.
- Cacciafesta, V., Sfondrini, M. F., Baluga, L., Scribante, A., & Klersy, C. (2003). Use of a self-etching primer in combination with a resin-modified glass ionomer: effect of water and saliva contamination on shear bond strength. *American Journal of Orthodontics and Dentofacial Orthopedics*, 124(4), 420-426.
- Can, A. M., Darling, C. L., Ho, C., & Fried, D. (2008). Non-destructive assessment of inhibition of demineralization in dental enamel irradiated by a $\lambda = 9.3\text{-}\mu\text{m}$ CO₂ laser at ablative irradiation intensities with PS-OCT. *Lasers in Surgery and Medicine*, 40(5), 342-349.
- Canli, S. (2010). *Thickness Analysis of Thin Films by Energy Dispersive X-Ray Spectroscopy* (Doctoral dissertation, Middle East Technical University).
- Carpenter, G., Cotroneo, E., Moazzez, R., Rojas-Serrano, M., Donaldson, N., Austin, R., & Proctor, G. (2014). Composition of enamel pellicle from dental erosion patients. *Caries Research*, 48(5), 361-367.
- Castellano, J. B., & Donly, K. J. (2004). Potential remineralization of demineralized enamel after application of fluoride varnish. *American Journal of Dentistry*, 17(6), 462-464.
- Caverzasio, J., Palmer, G., & Bonjour, J. P. (1998). Fluoride: mode of action. *Bone*, 22(6), 585-589.
- Cerruti, M., Greenspan, D., & Powers, K. (2005). Effect of pH and ionic strength on the reactivity of Bioglass® 45S5. *Biomaterials*, 26(14), 1665-1674.
- Chambers, C., Stewart, S., Su, B., Sandy, J., & Ireland, A. (2013). Prevention and treatment of demineralisation during fixed appliance therapy: a review of current methods and future applications. *British Dental Journal*, 215(10), 505-511.
- Chapman, J. A., Roberts, W. E., Eckert, G. J., Kula, K. S., & González-Cabezas, C. (2010). Risk factors for incidence and severity of white spot lesions during treatment

References

with fixed orthodontic appliances. *American Journal of Orthodontics and Dentofacial Orthopedics*, 138(2), 188-194.

Chatterjee, R., & Kleinberg, I. (1979). Effect of orthodontic band placement on the chemical composition of human incisor tooth plaque. *Archives of Oral Biology*, 24(2), 97-100.

Chen, Q., Zhu, C., & Thouas, G. A. (2012). Progress and challenges in biomaterials used for bone tissue engineering: bioactive glasses and elastomeric composites. *Progress in Biomaterials*, 1(1), 1-22.

Cheng, H. Y., Chen, C. H., Li, C. L., Tsai, H. H., Chou, T. H., & Wang, W. N. (2011). Bond strength of orthodontic light-cured resin-modified glass ionomer cement. *The European Journal of Orthodontics*, 33(2), 180-184.

Chitnis, D., Dunn, W. J., & Gonzales, D. A. (2006). Comparison of in-vitro bond strengths between resin-modified glass ionomer, polyacid-modified composite resin, and giomer adhesive systems. *American Journal of Orthodontics and Dentofacial Orthopedics*, 129(3), 330.e11-330.e16.

Chung, C. H., Cuozzo, P. T., & Mante, F. K. (1999). Shear bond strength of a resin-reinforced glass ionomer cement: an in vitro comparative study. *American Journal of Orthodontics and Dentofacial Orthopedics*, 115(1), 52-54.

Cochran, J. A., Ketley, C. E., Sanches, L., Mamai-Homata, E., Oila, A. M., Árnadóttir, I. B., & O'Mullane, D. M. (2004). A standardized photographic method for evaluating enamel opacities including fluorosis. *Community Dentistry and Oral Epidemiology*, 32(1), 19-27.

Cochrane, N. J., Cai, F., Huq, N. L., Burrow, M. F., & Reynolds, E. C. (2010). New approaches to enhanced remineralization of tooth enamel. *Journal of Dental Research*, 89(11), 1187-1197.

Cochrane, N. J., Anderson, P., Davis, G. R., Adams, G. G., Stacey, M. A., & Reynolds, E. C. (2012). An X-ray microtomographic study of natural white-spot enamel lesions. *Journal of Dental Research*, 91(2), 185-191.

References

- Cook, P. A. (1990). Direct bonding with glass ionomer cement. *Journal of Clinical Orthodontics*, 24(8), 509-511.
- Cook, R. J., Azzopardi, A., Thompson, I. D., & Watson, T. F. (2001). Real-time confocal imaging, during active air abrasion–substrate cutting. *Journal of Microscopy*, 203(2), 199-207.
- Cook RJ, Watson TF, Hench LL, Thompson ID. U.S. Patent No. 7,329,126. (2008) Washington, DC: U.S. Patent and Trademark Office.
- Cozza, P., Martucci, L., De Toffol, L., & Penco, S. I. (2006). Shear bond strength of metal brackets on enamel. *The Angle Orthodontist*, 76(5), 851-856.
- Cramer, N. B., Stansbury, J. W., & Bowman, C. N. (2011). Recent advances and developments in composite dental restorative materials. *Journal of Dental Research*, 90(4), 402-416.
- Croll, T. P., & Bullock, G. A. (1994). Enamel microabrasion for removal of smooth surface decalcification lesions. *Journal of Clinical Orthodontics*, 28(6), 365-370.
- Cross, S. E., Kreth, J., Wali, R. P., Sullivan, R., Shi, W., & Gimzewski, J. K. (2009). Evaluation of bacteria-induced enamel demineralization using optical profilometry. *Dental Materials*, 25(12), 1517-1526.
- Cucu, M., Driessen, C. H., & Ferreira, P. D. (2002). The influence of orthodontic bracket base diameter and mesh size on bond strength. *SADJ: journal of the South African Dental Association*, 57(1), 16-20.
- da Rosa, W. L. D. O., Piva, E., & da Silva, A. F. (2015). Bond strength of universal adhesives: A systematic review and meta-analysis. *Journal of Dentistry*, 43(7), 765-776.
- Davidson, C. L., Hoekstra, I. S., & Arends, J. (1974). Microhardness of sound, decalcified and etched tooth enamel related to the calcium content. *Caries Research*, 8(2), 135-144.

References

- de Dios Teruel, J., Alcolea, A., Hernández, A., & Ruiz, A. J. O. (2015). Comparison of chemical composition of enamel and dentine in human, bovine, porcine and ovine teeth. *Archives of Oral Biology*, 60(5), 768-775.
- De Josselin de Jong, E., Sundström, F., Westerling, H., Tranaeus, S., Ten Bosch, J. J., & Angmar-Månsson, B. (1995). A new method for in vivo quantification of changes in initial enamel caries with laser fluorescence. *Caries Research*, 29(1), 2-7.
- de Mello Vieira, A. E., Delbem, A. C. B., Sasaki, K. T., Rodrigues, E., Cury, J. A., & Cunha, R. F. (2005). Fluoride dose response in pH-cycling models using bovine enamel. *Caries Research*, 39(6), 514-520.
- Deng, M., Wen, H. L., Dong, X. L., Li, F., Xu, X., Li, H., & Zhou, X. D. (2013). Effects of 45S5 bioglass on surface properties of dental enamel subjected to 35% hydrogen peroxide. *International Journal of Oral Science*, 5(2), 103-110.
- Dirks, O. B. (1966). Posteruptive changes in dental enamel. *J Dent Res*, 45(3), 503-511.
- Dong, Z., Chang, J., Zhou, Y., & Lin, K. (2011). In vitro remineralization of human dental enamel by bioactive glasses. *Journal of Materials Science*, 46(6), 1591-1596.
- Donnan, M. F., & Ball, I. A. (1988). A double-blind clinical trial to determine the importance of pumice prophylaxis on fissure sealant retention. *British Dental Journal*, 165(8), 283-286.
- Dowker, S. E. P., Elliott, J. C., Davis, G. R., & Wassif, H. S. (2003). Longitudinal study of the three-dimensional development of subsurface enamel lesions during in vitro demineralisation. *Caries Research*, 37(4), 237-245.
- Du, M., Cheng, N., Tai, B., Jiang, H., Li, J., & Bian, Z. (2012). Randomized controlled trial on fluoride varnish application for treatment of white spot lesion after fixed orthodontic treatment. *Clinical Oral Investigations*, 16(2), 463-468.
- Du Min, Q., Bian, Z., Jiang, H., Greenspan, D. C., Burwell, A. K., Zhong, J., & Tai, B. J. (2008). Clinical evaluation of a dentifrice containing calcium sodium phosphosilicate (novamin) for the treatment of dentine hypersensitivity. *American Journal of Dentistry*, 21(4), 210-214.

References

- Ducheyne, P., El-Ghannam, A., & Shapiro, I. (1997). *U.S. Patent No. 5,676,720*. Washington, DC: U.S. Patent and Trademark Office.
- Earl, J. S., Leary, R. K., Muller, K. H., Langford, R. M., & Greenspan, D. C. (2010a). Physical and chemical characterization of dentine surface following treatment with NovaMin technology. *The Journal of Clinical Dentistry*, 22(3), 62-67.
- Earl, J. S., Topping, N., Elle, J., Langford, R. M., & Greenspan, D. C. (2010b). Physical and chemical characterization of the surface layers formed on dentine following treatment with a fluoridated toothpaste containing NovaMin. *The Journal of Clinical Dentistry*, 22(3), 68-73.
- Eberhard, H., Hirschfelder, U., & Sindel, J. (1997). Compomers-a new bracket bonding generation in orthodontics? *Journal of Orofacial Orthopedics*, 58(1), 62-69.
- Edén, M. (2011). The split network analysis for exploring composition–structure correlations in multi-component glasses: I. Rationalizing bioactivity-composition trends of bioglasses. *Journal of Non-Crystalline Solids*, 357(6), 1595-1602.
- Ehrlich, H., Koutsoukos, P. G., Demadis, K. D., & Pokrovsky, O. S. (2008). Principles of demineralization: modern strategies for the isolation of organic frameworks: Part I. Common definitions and history. *Micron*, 39(8), 1062-1091.
- Elaut, J., & Wehrbein, H. (2004). The effects of argon laser curing of a resin adhesive on bracket retention and enamel decalcification: a prospective clinical trial. *The European Journal of Orthodontics*, 26(5), 553-560.
- Elgayar, I., Aliev, A. E., Boccaccini, A. R., & Hill, R. G. (2005). Structural analysis of bioactive glasses. *Journal of Non-Crystalline Solids*, 351(2), 173-183.
- Eliades, T., & Brantley, W. A. (2000). The inappropriateness of conventional orthodontic bond strength assessment protocols. *European Journal of Orthodontics*, 22(1), 13-23.
- Elliott, J. C. (2013). *Structure and chemistry of the apatites and other calcium orthophosphates* (Vol. 18). Elsevier.

References

- Erdur, E. A., Akin, M., Cime, L., & İleri, Z. (2016). Evaluation of Enamel Surface Roughness after Various Finishing Techniques for Debonding of Orthodontic Brackets. *Turkish J Orthod*, 29(1): 1-5.
- Erol-Taygun, M., Zheng, K., & Boccaccini, A. R. (2013). Nanoscale bioactive glasses in medical applications. *International Journal of Applied Glass Science*, 4(2), 136-148.
- Farooq, I., Tylkowski, M., Müller, S., Janicki, T., Brauer, D. S., & Hill, R. G. (2013). Influence of sodium content on the properties of bioactive glasses for use in air abrasion. *Biomedical Materials*, 8(6), 065008-065031.
- Fava, M., Watanabe, I. S., Fava de Moraes, F., & da Costa, R. D. R. S. (1997). Observations on etched enamel in non-erupted deciduous molars: a scanning electron microscopic study. *Revista de Odontologia da Universidade de São Paulo*, 11(3), 157-160.
- Feagin, F., Koulourides, T., & Pigman, W. (1969). The characterization of enamel surface demineralization, remineralization, and associated hardness changes in human and bovine material. *Archives of Oral Biology*, 14(12), 1407-1417.
- Featherstone, J. D. B., Ten Cate, J. M., Shariati, M., & Arends, J. (1983). Comparison of artificial caries-like lesions by quantitative microradiography and microhardness profiles. *Caries research*, 17(5), 385-391.
- Featherstone, J. D. (2000). The science and practice of caries prevention. *Journal of the American Dental Association*, 131(7), 887-899.
- Fejerskov, O., Nyvad, B., & Kidd, E. A. M. (2003). Clinical and histological manifestations of dental caries. In *Dental Caries* (pp.71-79). Blackwell Publishing Ltd.
- Feldner, J. C., Sarkar, N. K., Sheridan, J. J., & Lancaster, D. M. (1994). In vitro torque-deformation characteristics of orthodontic polycarbonate brackets. *American Journal of Orthodontics and Dentofacial Orthopedics*, 106(3), 265-272.
- Fernandez, L., & Canut, J. A. (1999). In vitro comparison of the retention capacity of new aesthetic brackets. *The European Journal of Orthodontics*, 21(1), 71-77.
- Ferracane, J. L. (2011). Resin composite—state of the art. *Dental Materials*, 27(1), 29-38.

References

- Ferracane, J. L., Pfeifer, C. S., & Hilton, T. J. (2014). Microstructural Features of Current Resin Composite Materials. *Current Oral Health Reports*, 1(4), 205-212.
- Ferrazzano, G. F., Amato, I., Cantile, T., Sangianantoni, G., & Ingenito, A. (2011). In vivo remineralising effect of GC tooth mousse on early dental enamel lesions: SEM analysis. *International Dental Journal*, 61(4), 210-216.
- Field, J., Waterhouse, P., & German, M. (2010). Quantifying and qualifying surface changes on dental hard tissues in vitro. *Journal of Dentistry*, 38(3), 182-190.
- Finke, M., Jandt, K. D., & Parker, D. M. (2000). The early stages of native enamel dissolution studied with atomic force microscopy. *Journal of Colloid and Interface Science*, 232(1), 156-164.
- Fleming, P. S., Johal, A., & Pandis, N. (2012). Self-etch primers and conventional acid-etch technique for orthodontic bonding: a systematic review and meta-analysis. *American Journal of Orthodontics and Dentofacial Orthopedics*, 142(1), 83-94.
- Flores, D. A., Choi, L. K., Caruso, J. M., Tomlinson, J. L., Scott, G. E., & Jeiroudi, M. T. (1994). Deformation of metal brackets: a comparative study. *The Angle Orthodontist*, 64(4), 283-290.
- Fontana, M., Li, Y., Dunipace, A. J., Noblitt, T. W., Fischer, G., Katz, B. P., & Stookey, G. K. (1996). Measurement of enamel demineralization using microradiography and confocal microscopy. *Caries Research*, 30(5), 317-325.
- Fornell, A. C., Sköld-Larsson, K., Hallgren, A., Bergstrand, F., & Twetman, S. (2002). Effect of a hydrophobic tooth coating on gingival health, mutans streptococci, and enamel demineralization in adolescents with fixed orthodontic appliances. *Acta Odontologica Scandinavica*, 60(1), 37-41.
- Forsberg, C. M., & Hagberg, C. (1992). Shear bond strength of ceramic brackets with chemical or mechanical retention. *British Journal of Orthodontics*, 19(3), 183-189.
- Garcia-Godoy, F., & Gwinnett, A. J. (1991). Effect of etching times and mechanical pretreatment on the enamel of primary teeth: an SEM study. *American Journal of Dentistry*, 4(3), 115-118.

References

- García-Godoy, F., & Hicks, M. J. (2008). Maintaining the integrity of the enamel surface: the role of dental biofilm, saliva and preventive agents in enamel demineralization and remineralization. *The Journal of the American Dental Association*, 139, 25S-34S.
- Gardner, A., & Hobson, R. (2001). Variations in acid-etch patterns with different acids and etch times. *American Journal of Orthodontics and Dentofacial Orthopedics*, 120(1), 64-67.
- Gaworski, M., Weinstein, M., Borislow, A. J., & Braitman, L. E. (1999). Decalcification and bond failure: a comparison of a glass ionomer and a composite resin bonding system in vivo. *American Journal of Orthodontics and Dentofacial Orthopedics*, 116(5), 518-521.
- Geiger, A. M., Gorelick, L., Gwinnett, A. J., & Griswold, P. G. (1988). The effect of a fluoride program on white spot formation during orthodontic treatment. *American Journal of Orthodontics and Dentofacial Orthopedics*, 93(1), 29-37.
- Geiger, A. M., Gorelick, L., Gwinnett, A. J., & Benson, B. J. (1992). Reducing white spot lesions in orthodontic populations with fluoride rinsing. *American Journal of Orthodontics and Dentofacial Orthopedics*, 101(5), 403-407.
- Gentleman, E., Stevens, M. M., Hill, R. G., & Brauer, D. S. (2013). Surface properties and ion release from fluoride-containing bioactive glasses promote osteoblast differentiation and mineralization in vitro. *Acta Biomaterialia*, 9(3), 5771-5779.
- Gerrard, W. A., & Winter, P. J. (1986). Evaluation of toothpastes by their ability to assist rehardening of enamel in vitro. *Caries Research*, 20(3), 209-216.
- Gill, P., Moghadam, T. T., & Ranjbar, B. (2010). Differential scanning calorimetry techniques: applications in biology and nanoscience. *J Biomol Tech*, 21(4), 167-193.
- Gillgrass, T. J., Benington, P. C. M., Millett, D. T., Newell, J., & Gilmour, W. H. (2001). Modified composite or conventional glass ionomer for band cementation. A comparative clinical trial. *American Journal of Orthodontics and Dentofacial Orthopedics*, 120(1), 49-53.

References

- Gjorgievska, E. S., Nicholson, J. W., Slipper, I. J., & Stevanovic, M. M. (2013). Remineralization of demineralized enamel by toothpastes: a scanning electron microscopy, energy dispersive X-ray analysis, and three-dimensional stereo-micrographic study. *Microscopy and Microanalysis*, 19(03), 587-595.
- Gladys, S., Van Meerbeek, B., Braem, M., Lambrechts, P., & Vanherle, G. (1997). Comparative physio-mechanical characterization of new hybrid restorative materials with conventional glass-ionomer and resin composite restorative materials. *Journal of Dental Research*, 76(4), 883-894.
- Gomez, J., Pretty, I. A., Santarpia Iii, R. P., Cantore, B., Rege, A., Petrou, I., & Ellwood, R. P. (2014). Quantitative light-induced fluorescence to measure enamel remineralization in vitro. *Caries Research*, 48(3), 223-227.
- Gorelick, L., Geiger, A. M., & Gwinnett, A. J. (1982). Incidence of white spot formation after bonding and banding. *American Journal of Orthodontics*, 81(2), 93-98.
- Gorton, J., & Featherstone, J. D. (2003). In vivo inhibition of demineralization around orthodontic brackets. *American Journal of Orthodontics and Dentofacial Orthopedics*, 123(1), 10-14.
- Gray, J. A. (1966). Kinetics of enamel dissolution during formation of incipient caries-like lesions. *Archives of Oral Biology*, 11(4), 397IN5-421IN7.
- Greenspan, D. C. (1999). Developments in biocompatible glass compositions. *Medical Device and Diagnostic Industry*, 21, 150-159.
- Grubisa, H. S., Heo, G., Raboud, D., Glover, K. E., & Major, P. W. (2004). An evaluation and comparison of orthodontic bracket bond strengths achieved with self-etching primer. *American Journal of Orthodontics and Dentofacial Orthopedics*, 126(2), 213-219.
- Guan, G., Takano-Yamamoto, T., Miyamoto, M., Hattori, T., Ishikawa, K., & Suzuki, K. (2000). Shear bond strengths of orthodontic plastic brackets. *American Journal of Orthodontics and Dentofacial Orthopedics*, 117(4), 438-443.
- Gwinnett, A. J., & Gorelick, L. (1977). Microscopic evaluation of enamel after debonding: clinical application. *American Journal of Orthodontics*, 71(6), 651-665.

References

- Gwinnett, A. J., & Ceen, R. F. (1979). Plaque distribution on bonded brackets: a scanning microscope study. *American Journal of Orthodontics*, 75(6), 667-677. Cited by: Øgaard, B., Alm, A. A., Larsson, E., & Adolfsson, U. (2006). A prospective, randomized clinical study on the effects of an amine fluoride/stannous fluoride toothpaste/mouth rinse on plaque, gingivitis and initial caries lesion development in orthodontic patients. *The European Journal of Orthodontics*, 28(1), 8-12
- Gwinnett, A. J. (1988). A comparison of shear bond strengths of metal and ceramic brackets. *American Journal of Orthodontics and Dentofacial Orthopedics*, 93(4), 346-348.
- Habibi, M., Nik, T. H., & Hooshmand, T. (2007). Comparison of debonding characteristics of metal and ceramic orthodontic brackets to enamel: an in-vitro study. *American Journal of Orthodontics and Dentofacial Orthopedics*, 132(5), 675-679.
- Hahn, S. K., Kim, J. W., Lee, S. H., Kim, C. C., Hahn, S. H., & Jang, K. T. (2004). Microcomputed tomographic assessment of chemomechanical caries removal. *Caries Research*, 38(1), 75-78.
- Hannig, M., & Hannig, C. (2010). Nanomaterials in preventive dentistry. *Nature Nanotechnology*, 5(8), 565-569.
- Harazaki, M., Haykawa, K., Fukui, T., Isshiki, Y., Powell, L. G. (2001). The Nd-YAG laser is useful in prevention of dental caries during orthodontic treatment. *The Bulletin of Tokyo Dental College*, 42(2), 79-86.
- Hariri, I., Sadr, A., Shimada, Y., Tagami, J., Sumi, Y. (2012). Effects of structural orientation of enamel and dentine on light attenuation and local refractive index: an optical coherence tomography study. *Journal of Dentistry*, 40(5), 387-396.
- Hay, D. I., Smith, D. J., Schluckebier, S. K., & Moreno, E. C. (1984). Relationship between concentration of human salivary statherin and inhibition of calcium phosphate precipitation in stimulated human parotid saliva. *Journal of Dental Research*, 63(6), 857-863.
- Hayakawa, K. (2005). Nd: YAG laser for debonding ceramic orthodontic brackets. *American Journal of Orthodontics and Dentofacial Orthopedics*, 128(5), 638-647.

References

- He, B., Huang, S., Jing, J., & Hao, Y. (2010). Measurement of hydroxyapatite density and Knoop hardness in sound human enamel and a correlational analysis between them. *Archives of Oral Biology*, 55(2), 134-141.
- Hegarty, D. J., & Macfarlane, T. V. (2002). In vivo bracket retention comparison of a resin-modified glass ionomer cement and a resin-based bracket adhesive system after a year. *American Journal of Orthodontics and Dentofacial Orthopedics*, 121(5), 496-501.
- Hegde, V. S., & Khatavkar, R. A. (2010). A new dimension to conservative dentistry: Air abrasion. *Journal of Conservative Dentistry*, 13(1), 4-8.
- Heinig, N., & Hartmann, A. (2008). Efficacy of a sealant. *Journal of Orofacial Orthopedics*, 69(3), 154-167.
- Hench, L. L., Splinter, R. J., Allen, W. C., & Greenlee, T. K. (1971). Bonding mechanisms at the interface of ceramic prosthetic materials. *Journal of Biomedical Materials Research*, 5(6), 117-141.
- Hench, L. L., & Wilson, J. (Eds.). (1993). *An introduction to bioceramics* (Vol. 1). World Scientific.
- Hench, L. L. & June, W. (1999). *An Introduction to bioceramics*, World Scientific.
- Hench, L. L. (1991). Bioceramics: from concept to clinic. *Journal of the American Ceramic Society*, 74(7), 1487-1510.
- Hench, L. L. (2006). The story of Bioglass®. *Journal of Materials Science: Materials in Medicine*, 17(11), 967-978.
- Hench, L. L. (2013). Chronology of bioactive glass development and clinical applications, *New Journal of Glass and Ceramics*, 3(2), 67-73.
- Hicks, M. J., & Silverstone, L. M. (1984). Acid-etching of caries-like lesions of enamel: a polarized light microscopic study. *Caries Research*, 18(4), 315-326.
- Hicks, J., Winn, I. I., Flaitz, C., & Powell, L. (2004). In vivo caries formation in enamel following argon laser irradiation and combined fluoride and argon laser treatment: A clinical pilot study. *Quintessence International*, 35(1), 15-20.

References

- Hill, R. G., De Barra, E., Griffin, S., Henn, G., Devlin, J., Hatton, P. V., & Craig, G. (1995). Fluoride release from glass polyalkenoate (ionomer) cements. In *Key Engineering Materials*, 99, 315-322.
- Hill, R. (1996). An alternative view of the degradation of bioglass. *Journal of Materials Science Letters*, 15, 1122-1125.
- Hill, R. G., & Brauer, D. S. (2011). Predicting the bioactivity of glasses using the network connectivity or split network models. *Journal of Non-Crystalline Solids*, 357(24), 3884-3887.
- Hill, R. G., Gillam, D. G., & Chen, X. (2015). The ability of a nano hydroxyapatite toothpaste and oral rinse containing fluoride to protect enamel during an acid challenge using ¹⁹F solid state NMR spectroscopy. *Materials Letters*, 156, 69-71.
- Holmen, L., Thylstrup, A., Featherstone, J. D. B., Fredebo, L., & Shariati, M. (1985). A scanning electron microscopic study of surface changes during development of artificial caries. *Caries Research*, 19(1), 11-21.
- Holmen, L., Mejare, I., Malmgren, B., & Thylstrup, A. (1988). The effect of regular professional plaque removal on dental caries in vivo. *Caries Research*, 22(4), 250-256.
- Horiguchi S, Yamada T, Inokoshi S & Tagami J (1998). Selective caries removal with air abrasion. *Operative Dentistry* 23(5), 236-243.
- Hosoya, Y., Taguchi, T., & Tay, F. R. (2007). Evaluation of a new caries detecting dye for primary and permanent carious dentine. *Journal of Dentistry*, 35(2), 137-143.
- Huang, T. H., Ding, S. J., Min, Y., & Kao, C. T. (2004). Metal ion release from new and recycled stainless steel brackets. *The European Journal of Orthodontics*, 26(2), 171-177.
- Huang, T. T., Jones, A. S., He, L. H., Darendeliler, M. A., & Swain, M. V. (2007). Characterisation of enamel white spot lesions using X-ray micro-tomography. *Journal of Dentistry*, 35(9), 737-743.
- Huang, G. J., Roloff-Chiang, B., Mills, B. E., Shalchi, S., Spiekerman, C., Korpak, A. M., & Matunas, J. C. (2013). Effectiveness of MI Paste Plus and PreviDent fluoride varnish

References

for treatment of white spot lesions: a randomized controlled trial. *American Journal of Orthodontics and Dentofacial Orthopedics*, 143(1), 31-41.

Ilharreborde, B., Morel, E., Fitoussi, F., Presedo, A., Souchet, P., Penneçot, G. F., & Mazda, K. (2008). Bioactive glass as a bone substitute for spinal fusion in adolescent idiopathic scoliosis: a comparative study with iliac crest autograft. *Journal of Pediatric Orthopaedics*, 28(3), 347-351.

Imazato, S., Ebi, N., Takahashi, Y., Kaneko, T., Ebisu, S., & Russell, R. R. (2003). Antibacterial activity of bactericide-immobilized filler for resin-based restoratives. *Biomaterials*, 24(20), 3605-3609.

Ingram, G. S., & Silverstone, L. M. (1981). A chemical and histological study of artificial caries in human dental enamel in vitro. *Caries Research*, 15(5), 393-398.

Ireland, A. J., & Sherriff, M. (2002). An investigation into the use of pumice prior to bonding with a filled diacrylate or resin modified glass polyalkenoate cement. *J Orthod*, 29, 217-220.

Ireland, A. J., Hosein, I., & Sherriff, M. (2005). Enamel loss at bond-up, debond and clean-up following the use of a conventional light-cured composite and a resin-modified glass polyalkenoate cement. *European Journal of Orthodontics*, 27(4), 413-419.

Ireland, A. J., McNamara, C., Clover, M. J., House, K., Wenger, N., Barbour, M. E., Sandy, J. R. (2008). 3D surface imaging in dentistry—what we are looking at. *British Dental Journal*, 205(7), 387-392.

Jahanbin, A., Ameri, H., Shahabi, M., & Ghazi, A. (2015). Management of Post-orthodontic White Spot Lesions and Subsequent Enamel Discoloration with Two Microabrasion Techniques. *Journal of Dentistry*, 16(1), 56-60.

Janiszewska-Olszowska, J., Szatkiewicz, T., Tomkowski, R., Tandecka, K., & Grocholewicz, K. (2014). Effect of orthodontic debonding and adhesive removal on the enamel—current knowledge and future perspectives—a systematic review. *Medical Science Monitor Basic Research*, 20, 1991-2001.

Janiszewska-Olszowska, J., Tandecka, K., Szatkiewicz, T., Stępień, P., Sporniak-Tutak, K., & Grocholewicz, K. (2015). Three-dimensional analysis of enamel surface

References

- alteration resulting from orthodontic clean-up—comparison of three different tools. *BMC Oral Health*, 15(1), 146-153.
- Jena, A. K., Duggal, R., & Mehrotra, A. K. (2007). Physical properties and clinical characteristics of ceramic brackets: a comprehensive review. *Trends Biomater Artif Organs*, 20(2), 101-115.
- Jennett, E., Motamedi, M., Rastegar, S., Frederickson, C., Arcoria, C., & Powers, J. M. (1994). Dye-enhanced ablation of enamel by pulsed lasers. *Journal of Dental Research*, 73(12), 1841-1847.
- Jones, J. R., Sepulveda, P., & Hench, L. L. (2001). Dose-dependent behavior of bioactive glass dissolution. *Journal of Biomedical Materials Research*, 58(6), 720-726.
- Jones, J., & Clare, A. (Eds.). (2012). *Bio-glasses: an introduction*. John Wiley & Sons.
- Jones, R. S., & Fried, D. (2006). Remineralization of enamel caries can decrease optical reflectivity. *Journal of Dental Research*, 85(9), 804-808.
- Jones, R. S., Darling, C. L., Featherstone, J. D., Fried, D. (2006). Remineralization of in vitro dental caries assessed with polarization-sensitive optical coherence tomography. *Journal of Biomedical Optics*, 11(1), 014016-014016.
- Jost-Brinkmann, P. G., Stein, H., Miethke, R. R., & Nakata, M. (1992). Histologic investigation of the human pulp after thermodebonding of metal and ceramic brackets. *American Journal of Orthodontics and Dentofacial Orthopedics*, 102(5), 410-417.
- Kang, H., Darling, C. L., & Fried, D. (2012). Nondestructive monitoring of the repair of enamel artificial lesions by an acidic remineralization model using polarization-sensitive optical coherence tomography. *Dental Materials*, 28(5), 488-494.
- Kapur, R., Sinha, P. K., & Nanda, R. S. (1999). Comparison of frictional resistance in titanium and stainless steel brackets. *American Journal of Orthodontics and Dentofacial Orthopedics*, 116(3), 271-274.
- Karadas, M., Cantekin, K., & Celikoglu, M. (2011). Effects of orthodontic treatment with a fixed appliance on the caries experience of patients with high and low risk of caries. *Journal of Dental Sciences*, 6(4), 195-199.

References

- Karan, S., Kircelli, B. H., & Tasdelen, B. (2010). Enamel surface roughness after debonding: comparison of two different burs. *The Angle Orthodontist*, 80(6), 1081-1088.
- Karlinsey, R. L., Mackey, A. C., Stookey, G. K., & Pfarrer, A. M. (2009). In vitro assessments of experimental NaF dentifrices containing a prospective calcium phosphate technology. *American Journal of Dentistry*, 22(3), 180-184.
- Kazarian, S. G., & Chan, K. L. A. (2006). Applications of ATR-FTIR spectroscopic imaging to biomedical samples. *Biochimica et Biophysica Acta (BBA)-Biomembranes*, 1758(7), 858-867.
- Kazarian, S. G., & Chan, K. A. (2013). ATR-FTIR spectroscopic imaging: recent advances and applications to biological systems. *Analyst*, 138(7), 1940-1951.
- Keim, R. G., Gottlieb, E. L., Nelson, A. H., & VOGELS III, D. S. (2002). 2002 JCO study of orthodontic diagnosis and treatment procedures. *J Clin Orthod*, 36, 553-568.
- Khalaf, K. (2014). Factors affecting the formation, severity and location of white spot lesions during orthodontic treatment with fixed appliances. *Journal of Oral & Maxillofacial Research*, 5(1), e4-e9.
- Kidd, E. A. M., & Fejerskov, O. (2004). What constitutes dental caries? Histopathology of carious enamel and dentine related to the action of cariogenic biofilms. *Journal of Dental Research*, 83(1), C35-C38.
- Kielbassa, A. M., Wrbas, K. T., Schulte-Mönting, J., & Hellwig, E. (1999). Correlation of transversal microradiography and microhardness on in situ-induced demineralization in irradiated and nonirradiated human dental enamel. *Archives of Oral Biology*, 44(3), 243-251.
- Kielbassa, A. M., Gillmann, L., Zantner, C., Meyer-Lueckel, H., Hellwig, E., & Schulte-Mönting, J. (2005). Profilometric and microradiographic studies on the effects of toothpaste and acidic gel abrasivity on sound and demineralized bovine dental enamel. *Caries Research*, 39(5), 380-386.
- Kim, C. Y., Clark, A. E., & Hench, L. L. (1989). Early stages of calcium-phosphate layer formation in bioglasses. *Journal of Non-crystalline Solids*, 113 (3), 195-202.

References

- Kim, S. S., Park, W. K., Son, W. S., Ahn, H. S., Ro, J. H., & Kim, Y. D. (2007). Enamel surface evaluation after removal of orthodontic composite remnants by intraoral sandblasting: a 3-dimensional surface profilometry study. *American Journal of Orthodontics and Dentofacial Orthopedics*, 132(1), 71-76.
- Kim, S., KIM, E. Y., JEONG, T. S., & KIM, J. W. (2011). The evaluation of resin infiltration for masking labial enamel white spot lesions. *International Journal of Paediatric Dentistry*, 21(4), 241-248.
- Kim, S. (2015). *Predicting Improvement of Post-Orthodontic White Spot Lesions* (Doctoral dissertation).
- Knösel, M., Attin, R., Becker, K., & Attin, T. (2007). External bleaching effect on the color and luminosity of inactive white-spot lesions after fixed orthodontic appliances. *The Angle Orthodontist*, 77(4), 646-652.
- Knösel, M., Mattysek, S., Jung, K., Sadat-Khonsari, R., Kubein-Meesenburg, D., Bauss, O., & Ziebolz, D. (2010). Impulse debracketing compared to conventional debonding: Extent of enamel damage, adhesive residues and the need for post processing. *The Angle Orthodontist*, 80(6), 1036-1044.
- Knösel, M., Eckstein, A., & Helms, H. J. (2013). Durability of esthetic improvement following Icon resin infiltration of multibracket-induced white spot lesions compared with no therapy over 6 months: a single-center, split-mouth, randomized clinical trial. *American Journal of Orthodontics and Dentofacial Orthopedics*, 144(1), 86-96.
- Knox, J., Hubsch, P., Jones, M. L., & Middleton, J. (2000). The influence of bracket base design on the strength of the bracket–cement interface. *Journal of Orthodontics*, 27(3), 249-254.
- Kokubo, T., Kim, H. M., & Kawashita, M. (2003). Novel bioactive materials with different mechanical properties. *Biomaterials*, 24(13), 2161-2175.
- Krell, K. V., Courey, J. M., & Bishara, S. E. (1993). Orthodontic bracket removal using conventional and ultrasonic debonding techniques, enamel loss, and time requirements. *American Journal of Orthodontics and Dentofacial Orthopedics*, 103(3), 258-266.

References

- Kronenberg, O., Lussi, A., & Ruf, S. (2009). Preventive effect of ozone on the development of white spot lesions during multibracket appliance therapy. *The Angle Orthodontist*, 79(1), 64-69.
- Kukleva, M. P., Shetkova, D. G., & Beev, V. H. (2001). Comparative age study of the risk of demineralization during orthodontic treatment with brackets. *Folia Medica*, 44(1-2), 56-59.
- Kusy, R. P., Whitley, J. Q., Ambrose, W. W., & Newman, J. G. (1998). Evaluation of titanium brackets for orthodontic treatment: Part I. The passive configuration. *American Journal of Orthodontics and Dentofacial Orthopedics*, 114(5), 558-572.
- Kusy, R. P., & O'grady, P. W. (2000). Evaluation of titanium brackets for orthodontic treatment: part II—the active configuration. *American Journal of Orthodontics and Dentofacial Orthopedics*, 118(6), 675-684.
- Laurance-Young, P., Bozec, L., Gracia, L., Rees, G., Lippert, F., Lynch, R. J. M., & Knowles, J. C. (2011). A review of the structure of human and bovine dental hard tissues and their physicochemical behaviour in relation to erosive challenge and remineralisation. *Journal of Dentistry*, 39(4), 266-272.
- Laurell, K. A., & Hess, J. A. (1995). Scanning electron micrographic effects of air-abrasion cavity preparation on human enamel and dentine. *Quintessence International*, 26(2), 139-144.
- Le, P. T., Weinstein, M., Borislow, A. J., & Braitman, L. E. (2003). Bond failure and decalcification: a comparison of a cyanoacrylate and a composite resin bonding system in vivo. *American Journal of Orthodontics and Dentofacial Orthopedics*, 123(6), 624-627.
- Lei, J., Guo, J., Fu, D., Wang, Y., Du, X., Zhou, L., & Huang, C. (2014). Influence of three remineralization materials on physicochemical structure of demineralized enamel. *Journal of Wuhan University of Technology. Materials Science Edition*, 29(2), 410-416.
- Linton, J. L. (1996). Quantitative measurements of remineralization of incipient caries. *American Journal of Orthodontics and Dentofacial Orthopedics*, 110(6), 590-597.

References

- Lippert, F., & Lynch, R. J. M. (2014). Comparison of Knoop and Vickers surface microhardness and transverse microradiography for the study of early caries lesion formation in human and bovine enamel. *Archives of Oral Biology*, 59(7), 704-710.
- Lippitz, S. J., Staley, R. N., & Jakobsen, J. R. (1998). In vitro study of 24-hour and 30-day shear bond strengths of three resin–glass ionomer cements used to bond orthodontic brackets. *American Journal of Orthodontics and Dentofacial Orthopedics*, 113(6), 620-624.
- Littlewood, S. J., Mitchell, L., & Greenwood, D. C. (2001). A randomized controlled trial to investigate brackets bonded with a hydrophilic primer. *Journal of Orthodontics*, 28(4), 301-305.
- Liu, J. K., Chuang, S. F., Chang, C. Y., & Pan, Y. J. (2004). Comparison of initial shear bond strengths of plastic and metal brackets. *European Journal of Orthodontics*, 26(5), 531-534.
- Liu, J., Rawlinson, S. C., Hill, R. G., & Fortune, F. (2016). Strontium-substituted bioactive glasses in vitro osteogenic and antibacterial effects. *Dental Materials*, 32(3), 412-422.
- Lloyd, B. A., Christensen, D. O., & Brown, W. S. (1976). Energy inputs and thermal stresses during cutting in dental materials. *The Cutting Edge, Pearlman, S., Ed., DHEW Publication (NIH)*, 76-670.
- Lo, E. C. M., Zhi, Q. H., & Itthagarun, A. (2010). Comparing two quantitative methods for studying remineralization of artificial caries. *Journal of Dentistry*, 38(4), 352-359.
- Lockyer, M. W. G., Holland, D., & Dupree, R. (1995). NMR investigation of the structure of some bioactive and related glasses. *Journal of Non-Crystalline Solids*, 188(3), 207-219.
- Lombardo, L., Ortan, Y. Ö., Gorgun, Ö., Panza, C., Scuzzo, G., & Siciliani, G. (2013). Changes in the oral environment after placement of lingual and labial orthodontic appliances. *Progress in Orthodontics*, 14(1), 1-8.

References

- Lopez, J. I. (1980). Retentive shear strengths of various bonding attachment bases. *American Journal of Orthodontics*, 77(6), 669-678.
- Lopez-Esteban, S., Saiz, E., Fujino, S., Oku, T., Suganuma, K., & Tomsia, A. P. (2003). Bioactive glass coatings for orthopedic metallic implants. *Journal of The European Ceramic Society*, 23(15), 2921-2930.
- Lovrov, S., Hertrich, K., & Hirschfelder, U. (2007). Enamel demineralization during fixed orthodontic treatment—incidence and correlation to various oral-hygiene parameters. *Journal of Orofacial Orthopedics*, 68(5), 353-363.
- Lucchese, A., & Gherlone, E. (2013). Prevalence of white-spot lesions before and during orthodontic treatment with fixed appliances. *The European Journal of Orthodontics*, 35(5), 664-668.
- Lupi-Pegurier, L., Muller, M., Leforestier, E., Bertrand, M. F., & Bolla, M. (2003). In vitro action of Bordeaux red wine on the microhardness of human dental enamel. *Archives of Oral Biology*, 48(2), 141-145.
- Lussi, A., Hibst, R., & Paulus, R. (2004). DIAGNOdent: an optical method for caries detection. *Journal of Dental Research*, 83(1), C80-C83.
- Lusvardi, G., Malavasi, G., Menabue, L., Aina, V., & Morterra, C. (2009). Fluoride-containing bioactive glasses: surface reactivity in simulated body fluids solutions. *Acta Biomaterialia*, 5(9), 3548-3562.
- Lutz, F., & Phillips, R. W. (1983). A classification and evaluation of composite resin systems. *The Journal of Prosthetic Dentistry*, 50(4), 480-488.
- Lyman, C. E., Newbury, D. E., Goldstein, J., Williams, D. B., Romig Jr, A. D., Armstrong, J., and Peters, K. R. (2012). *Scanning electron microscopy, X-ray microanalysis, and analytical electron microscopy: a laboratory workbook*. Springer Science & Business Media.
- Lynch, R. J. M., & Ten Cate, J. M. (2006). The effect of lesion characteristics at baseline on subsequent de-and remineralisation behaviour. *Caries Research*, 40(6), 530-535.

References

- Lynch, R. J. M., Mony, U., & Ten Cate, J. M. (2007). Effect of lesion characteristics and mineralising solution type on enamel remineralisation in vitro. *Caries Research*, 41(4), 257-262.
- Lynch, E., Brauer, D. S., Karpukhina, N., Gillam, D. G., & Hill, R. G. (2012). Multi-component bioactive glasses of varying fluoride content for treating dentine hypersensitivity. *Dental Materials*, 28(2), 168-178.
- MacColl, G. A., Rossouw, P. E., Titley, K. C., & Yamin, C. (1998). The relationship between bond strength and orthodontic bracket base surface area with conventional and microetched foil-mesh bases. *American Journal of Orthodontics and Dentofacial Orthopedics*, 113(3), 276-281.
- Magalhães, A. C., Moron, B. M., Comar, L. P., Wiegand, A., Buchalla, W., & Buzalaf, M. A. R. (2009). Comparison of cross-sectional hardness and transverse microradiography of artificial carious enamel lesions induced by different demineralising solutions and gels. *Caries Research*, 43(6), 474-483.
- Mahajan, M., Singla, A., & Saini, S. S. (2015). Comparative evaluation of different prophylaxis pastes on shear bond strength of orthodontic brackets bonded with Self Etch Primer: An in-vitro study. *Journal of Indian Orthodontic Society*, 49(1), 32-36.
- Mahoney, E., Beattie, J., Swain, M., & Kilpatrick, N. (2003). Preliminary in vitro assessment of erosive potential using the ultra-micro-indentation system. *Caries Research*, 37(3), 218-224.
- Main, C., Thomson, J. L., Cummings, A., Field, D., Stephen, K. W., & Gillespie, F. C. (1983). Surface treatment studies aimed at streamlining fissure sealant application. *Journal of Oral Rehabilitation*, 10(4), 307-317.
- Mandurah, M. M., Sadr, A., Shimada, Y., Kitasako, Y., Nakashima, S., Bakhsh, T. A., Sumi, Y. (2013). Monitoring remineralization of enamel subsurface lesions by optical coherence tomography. *Journal of Biomedical Optics*, 18(4), 046006-046006.
- Manfred, L., Covell, D. A., Crowe, J. J., Tufekci, E., & Mitchell, J. C. (2012). A novel biomimetic orthodontic bonding agent helps prevent white spot lesions adjacent to brackets. *The Angle Orthodontist*, 83(1), 97-103.

References

- Manning, N., Chadwick, S. M., Plunkett, D., & Macfarlane, T. V. (2006). A randomized clinical trial comparing 'one-step' and 'two-step' orthodontic bonding systems. *Journal of Orthodontics*, 33(4), 276-283.
- Marcusson, A., Norevall, L. I., & Persson, M. (1997). White spot reduction when using glass ionomer cement for bonding in orthodontics: a longitudinal and comparative study. *European Journal of Orthodontics*, 19(3), 233-242.
- Margolis, H. C., & Moreno, E. C. (1990). Physicochemical perspectives on the cariostatic mechanisms of systemic and topical fluorides. *Journal of Dental Research*, 69(2), 606-613.
- Marinho, V. C., Higgins, J. P., Sheiham, A., & Logan, S. (2004). Combinations of topical fluoride (toothpastes, mouthrinses, gels, varnishes) versus single topical fluoride for preventing dental caries in children and adolescents. *Cochrane Database Syst Rev*, 1-11.
- Marković, E., Glišić, B., Šćepan, I., Marković, D., & Jokanovic, V. (2008). Bond strength of orthodontic adhesives. *Metallurgija-Journal of Metallurgy*, 14(2), 79-88.
- Marks, L. A. M., Weerheijm, K. L., Van Amerongen, W. E., Groen, H. J., & Martens, L. C. (1999). Dyract versus Tytin Class II restorations in primary molars: 36 months evaluation. *Caries Research*, 33(5), 387-392.
- Mattick, C. R., Mitchell, L., Chadwick, S. M., & Wright, J. (2001). Fluoride-releasing elastomeric modules reduce decalcification: a randomized controlled trial. *Journal of Orthodontics*, 28(3), 217-220.
- Mattousch, T. J. H., Van der Veen, M. H., & Zentner, A. (2007). Caries lesions after orthodontic treatment followed by quantitative light-induced fluorescence: a 2-year follow-up. *The European Journal of Orthodontics*, 29(3), 294-298.
- Mayne, R. J., Cochrane, N. J., Cai, F., Woods, M. G., & Reynolds, E. C. (2011). In-vitro study of the effect of casein phosphopeptide amorphous calcium fluoride phosphate on iatrogenic damage to enamel during orthodontic adhesive removal. *American Journal of Orthodontics and Dentofacial Orthopedics*, 139(6), e543-e551.

References

- McDermott, A. E., & Polenova, T. (Eds.). (2012). Solid State NMR Studies of Biopolymers. John Wiley & Sons.
- Meehan, M. P., Foley, T.F., & Mamandras, A.H. (1999). A comparison of the shear bond strengths of two glass ionomer cements. *American Journal of Orthodontics and Dentofacial Orthopedics*, 115(2), 125-132.
- Mehta, A. B., Veena Kumari, R. J., Izadikhah, V. (2014). Remineralization potential of bioactive glass and casein phosphopeptide-amorphous calcium phosphate on initial carious lesion: An in-vitro pH-cycling study. *Journal of Conservative Dentistry: JCD*, 17(1), 3-7.
- Meireles, S.S., Andre Dde, A., Leida, F.L., Bocangel, J.S., & Demarco, F.F. (2009). Surface roughness and enamel loss with two microabrasion techniques. *J Contemp Dent Pract*, 10(1), 58-65.
- Mellberg, J.R. (1992). Hard-tissue substrates for evaluation of cariogenic and anti-cariogenic activity in situ. *Journal of Dental Research*, 71, 913-919.
- Melrose, C. A., Appleton, J., & Lovius, B. B. (1996). A scanning electron microscopic study of early enamel caries formed in vivo beneath orthodontic bands. *British Journal of Orthodontics*, 23(1), 43-47.
- Meredith, N., Sherriff, M., Setchell, D. J., & Swanson, S. A. V. (1996). Measurement of the microhardness and Young's modulus of human enamel and dentine using an indentation technique. *Archives of Oral Biology*, 41(6), 539-545.
- Mhatre, A. C., Tandur, A. P., Reddy, S. S., Karunakara, B. C., & Baswaraj, H. (2015). Enamel Surface Evaluation after Removal of Orthodontic Composite Remnants by Intraoral Sandblasting Technique and Carbide Bur Technique: A Three-Dimensional Surface Profilometry and Scanning Electron Microscopic Study. *Journal of International Oral Health*, 7(2), 34-39.
- Mickenautsch, S., Yengopal, V., & Banerjee, A. (2012). Retention of orthodontic brackets bonded with resin-modified GIC versus composite resin adhesives—a quantitative systematic review of clinical trials. *Clinical Oral Investigations*, 16(1), 1-14.

References

- Miller, J. R., Mancl, L., Arbuckle, G., Baldwin, J., & Phillips, R. W. (1996). A three-year clinical trial using a glass ionomer cement for the bonding of orthodontic brackets. *The Angle Orthodontist*, 66(4), 309-312.
- Millett, D. T., Hallgren, A., Cattanach, D., McFadzean, R., Pattison, J., Robertson, M., & Love, J. (1998). A 5-year clinical review of bond failure with a light-cured resin adhesive. *The Angle Orthodontist*, 68(4), 351-356.
- Millett, D. T., Hallgren, A., & Robertson, M. (1999a). Bonded molar tubes: a retrospective evaluation of clinical performance. *American Journal of Orthodontics and Dentofacial Orthopedics*, 115(6), 667-674.
- Millett, D. T., Cattanach, D., McFadzean, R., Pattison, J., & McColl, J. (1999b). Laboratory evaluation of a compomer and a resin-modified glass ionomer cement for orthodontic bonding. *The Angle Orthodontist*, 69(1), 58-64.
- Millett, D. T., Nunn, J. H., Welbury, R. R., & Gordon, P. H. (1999c). Decalcification in relation to brackets bonded with glass ionomer cement or a resin adhesive. *The Angle Orthodontist*, 69(1), 65-70.
- Millett, D. T., McCluskey, L. A., McAuley, F., Creanor, S. L., Newell, J., & Love, J. (2000). A comparative clinical trial of a compomer and a resin adhesive for orthodontic bonding. *The Angle Orthodontist*, 70(3), 233-240.
- Milly, H., Andiappan, M., Thompson, I., & Banerjee, A. (2014a). Bio-active glass air-abrasion has the potential to remove resin composite restorative material selectively. *Applied Surface Science*, 303, 272-276.
- Milly, H., Festy, F., Watson, T. F., Thompson, I., Banerjee, A. (2014b). Enamel white spot lesions can remineralise using bio-active glass and polyacrylic acid-modified bio-active glass powders. *Journal of Dentistry*, 42(2), 158-166.
- Milly, H., Festy, F., Andiappan, M., Watson, T. F., Thompson, I., & Banerjee, A. (2015). Surface pre-conditioning with bioactive glass air-abrasion can enhance enamel white spot lesion remineralization. *Dental Materials*, 31(5), 522-533.
- Mirzakouchaki, B., Shirazi, S., Sharghi, R., Shirazi, S., Moghimi, M., & Shahrabaf, S. (2016). Shear bond strength and debonding characteristics of metal and ceramic

References

brackets bonded with conventional acid-etch and self-etch primer systems: An in-vivo study. *Journal of Clinical and Experimental Dentistry*, 8(1), e38-e43.

Mitchell, L. (2007). *An introduction to orthodontics*. Oxford University Press.

Mitchell, L. (1992a). An investigation into the effect of a fluoride releasing adhesive on the prevalence of enamel surface changes associated with directly bonded orthodontic attachments. *British Journal of Orthodontics*, 19, 207-214.

Mitchell, L. (1992b). Decalcification during orthodontic treatment with fixed appliances--an overview. *British Journal of Orthodontics*, 19, 199-205.

Miura, F., Nakagawa, K., & Masuhara, E. (1971). New direct bonding system for plastic brackets. *American journal of orthodontics*, 59(4), 350-361. Cited by: Pickett, K. L., Lionel Sadowsky, P., Jacobson, A., & Lacefield, W. (2001). Orthodontic in vivo bond strength: comparison with in vitro results. *The Angle Orthodontist*, 71(2), 141-148.

Miura, F., Nakagawa, K., & Ishizaki, A. (1973). Scanning electron microscopic studies on the direct bonding system. *The Bulletin of Tokyo Medical and Dental University*, 20(3), 245.

Mizrahi, E. (1983). Surface distribution of enamel opacities following orthodontic treatment. *American Journal of Orthodontics*, 84(4), 323-331.

Mneimne, M., Hill, R. G., Bushby, A. J., & Brauer, D. S. (2011). High phosphate content significantly increases apatite formation of fluoride-containing bioactive glasses. *Acta Biomaterialia*, 7(4), 1827-1834.

Mneimne, M (2014). *Development of Bioactive Glasses For Dental Treatment* (Doctoral dissertation).

Mohammed, N. R., Kent, N. W., Lynch, R. J. M., Karpukhina, N., Hill, R., & Anderson, P. (2013). Effects of Fluoride on in vitro Enamel Demineralization Analyzed by 19F MAS-NMR. *Caries Research*, 47(5), 421-428.

Mohebi, S., Shafiee, H. A., & Ameli, N. (2017). Evaluation of enamel surface roughness after orthodontic bracket debonding with atomic force microscopy. *American Journal of Orthodontics and Dentofacial Orthopedics*, 151(3), 521-527.

References

- Moher D., Liberati A., Tetzlaff J., Altman D.G. (2009). PRISMA Group Preferred reporting items for systematic reviews and meta-analyses: the PRISMA Statement. *BMJ*, 339 (b2535),1-8.
- Moore, D. M., Reynolds, R. C. (1989). *X-ray Diffraction and the Identification and Analysis of Clay Minerals* (Vol. 332). New York: Oxford university press.
- Motisuki, C., Lima, L. M., Bronzi, E. S., Spolidório, D. M. P., & Santos-Pinto, L. (2006). The effectiveness of alumina powder on carious dentine removal. *Operative Dentistry*, 31(3), 371-376.
- Movahhed, H. Z., Øgaard, B., & Syverud, M. (2005). An in vitro comparison of the shear bond strength of a resin-reinforced glass ionomer cement and a composite adhesive for bonding orthodontic brackets. *The European Journal of Orthodontics*, 27(5), 477-483.
- Murphy, T. C., Willmot, D. R., & Rodd, H. D. (2007). Management of postorthodontic demineralized white lesions with microabrasion: a quantitative assessment. *American Journal of Orthodontics and Dentofacial Orthopedics*, 131(1), 27-33.
- Myers, G. 1954. The air abrasive technique: a report. *British Dental Journal*, 7, 291-295. Cited by: Milly, H., Andiappan, M., Thompson, I., & Banerjee, A. (2014). Bio-active glass air-abrasion has the potential to remove resin composite restorative material selectively. *Applied Surface Science*, 303, 272-276.
- Nanci, A. (2007). *Ten cate's oral histology-page burst on vital source: development, structure, and function*. Elsevier Health Sciences.
- Narayana, S. S., Deepa, V. K., Ahamed, S., Sathish, E. S., Meyappan, R., Kumar, K. S. (2014). Remineralization efficiency of bioactive glass on artificially induced carious lesion an in-vitro study. *Journal of Indian Society of Pedodontics and Preventive Dentistry*, 32(1), 19-25.
- Naumova, E. A., Niemann, N., Aretz, L., & Arnold, W. H. (2012). Effects of different amine fluoride concentrations on enamel remineralization. *Journal of Dentistry*, 40(9), 750-755.

References

- Nazari, A., Sadr, A., Campillo-Funollet, M., Nakashima, S., Shimada, Y., Tagami, J., & Sumi, Y. (2013). Effect of hydration on assessment of early enamel lesion using swept-source optical coherence tomography. *Journal of Biophotonics*, 6(2), 171-177.
- Newman, G. V. (1969). Adhesion and orthodontic plastic attachments. *American Journal of Orthodontics*, 56(6), 573-588.
- Nordenvall, K. J., Brännström, M., & Malmgren, O. (1980). Etching of deciduous teeth and young and old permanent teeth: a comparison between 15 and 60 seconds of etching. *American Journal of Orthodontics*, 78(1), 99-108.
- Norevall, L. I., Marcusson, A., & Persson, M. (1996). A clinical evaluation of a glass ionomer cement as an orthodontic bonding adhesive compared with an acrylic resin. *The European Journal of Orthodontics*, 18(4), 373-384.
- Øgaard, B., Gjermo, P., & Rølla, G. (1980). Plaque-inhibiting effect in orthodontic patients of a dentifrice containing stannous fluoride. *American Journal of Orthodontics*, 78(3), 266-272.
- Øgaard, B., & Ten Bosch, J. J. (1994). Regression of white spot enamel lesions. A new optical method for quantitative longitudinal evaluation in vivo. *American Journal of Orthodontics and Dentofacial Orthopedics*, 106(3), 238-242.
- Øgaard, B. (1998). The cariostatic mechanism of fluoride. *Compendium of Continuing Education in Dentistry*, 20(1), 10-7.
- Øgaard, B. (2001). Oral microbiological changes, long-term enamel alterations due to decalcification, and caries prophylactic aspects. *Orthodontic materials. Scientific and Clinical Aspects. Stuttgart: Thieme*, 123-42.
- Øgaard, B., Larsson, E., Henriksson, T., Birkhed, D., & Bishara, S. E. (2001). Effects of combined application of antimicrobial and fluoride varnishes in orthodontic patients. *American Journal of Orthodontics and Dentofacial Orthopedics*, 120(1), 28-35.
- Øgaard, B., Bishara, S. E., & Duschner, H. (2004). Enamel effects during bonding-debonding and treatment with fixed appliances. *Risk management in orthodontics: experts' guide to malpractice. Chicago: Quintessence*, 19-46.

References

- Øgaard, B., Alm, A. A., Larsson, E., & Adolfsson, U. (2006). A prospective, randomized clinical study on the effects of an amine fluoride/stannous fluoride toothpaste/mouthrinse on plaque, gingivitis and initial caries lesion development in orthodontic patients. *The European Journal of Orthodontics*, 28(1), 8-12.
- O'Donnell, M. D., Watts, S. J., Law, R. V., & Hill, R. G. (2008a). Effect of P₂O₅ content in two series of soda lime phosphosilicate glasses on structure and properties—Part I: NMR. *Journal of Non-Crystalline Solids*, 354(30), 3554-3560.
- O'Donnell, M. D., Watts, S. J., Law, R. V., & Hill, R. G. (2008b). Effect of P₂O₅ content in two series of soda lime phosphosilicate glasses on structure and properties—Part II: Physical properties. *Journal of Non-Crystalline Solids*, 354(30), 3561-3566.
- O'Donnell, M. D., Watts, S. J., Hill, R. G., & Law, R. V. (2009). The effect of phosphate content on the bioactivity of soda-lime-phosphosilicate glasses. *Journal of Materials Science: Materials in Medicine*, 20(8), 1611-1618.
- O'Donnell, M. D. (2011). Predicting bioactive glass properties from the molecular chemical composition: Glass transition temperature. *Acta Biomaterialia*, 7(5), 2264-2269.
- Oho, T., & Morioka, T. (1990). A possible mechanism of acquired acid resistance of human dental enamel by laser irradiation. *Caries Research*, 24(2), 86-92.
- Okazaki, M., & Sato, M. (1990). Computer graphics of hydroxyapatite and β -tricalcium phosphate. *Biomaterials*, 11(8), 573-578.
- Olsen, M. E., Bishara, S. E., & Jakobsen, J. R. (1997). Evaluation of the shear bond strength of different ceramic bracket base designs. *The Angle Orthodontist*, 67(3), 179-182.
- O'Reilly, M. M., & Featherstone, J. D. B. (1987). Demineralization and remineralization around orthodontic appliances: an in vivo study. *American Journal of Orthodontics and Dentofacial Orthopedics*, 92(1), 33-40.
- OSHA regulations (Standards—29 CFR) 2007. U.S. Department of Labour, Occupational Safety and Health Administration. Apr 18, Available from: http://www.osha-slc.gov/OshStd_data/1910_1000_TABLE_Z-1.html

References

- Owens Jr, S. E., & Miller, B. H. (2000). A comparison of shear bond strengths of three visible light-cured orthodontic adhesives. *The Angle Orthodontist*, 70(5), 352-356.
- Özer, T., Başaran, G., & Kama, J. D. (2010). Surface roughness of the restored enamel after orthodontic treatment. *American Journal of Orthodontics and Dentofacial Orthopedics*, 137(3), 368-374.
- Oztoprak, M. O., Nalbantgil, D., Erdem, A. S., Tozlu, M., & Arun, T. (2010). Debonding of ceramic brackets by a new scanning laser method. *American Journal of Orthodontics and Dentofacial Orthopedics*, 138(2), 195-200.
- Palaniswamy, U. K., Prashar, N., Kaushik, M., Lakkam, S. R., Arya, S., Pebbeti, S. (2016). A comparative evaluation of remineralizing ability of bioactive glass and amorphous calcium phosphate casein phosphopeptide on early enamel lesion. *Dental Research Journal*, 13(4), 297-302.
- Paolinelis, G., Watson, T. F., & Banerjee, A. (2006). Microhardness as a predictor of sound and carious dentine removal using alumina air abrasion. *Caries Research*, 40(4), 292-295.
- Paolinelis, G., Banerjee, A., & Watson, T. F. (2008). An in vitro investigation of the effect and retention of bioactive glass air-abrasive on sound and carious dentine. *Journal of Dentistry*, 36(3), 214-218.
- Paolinelis, G., Banerjee, A., & Watson, T. F. (2009). An in-vitro investigation of the effects of variable operating parameters on alumina air-abrasion cutting characteristics. *Operative Dentistry*, 34(1), 87-92.
- Park, Y. S., Bae, K. H., Chang, J., & Shon, W. J. (2011). Theory of X-ray microcomputed tomography in dental research: application for the caries research. *Journal of Korean Academy of Conservative Dentistry*, 36(2), 98-107.
- Paul, A. (1989). *Chemistry of glasses*. Springer Science & Business Media.
- Peitl Filho, O., Latorre, G. P., & Hench, L. L. (1996). Effect of crystallization on apatite-layer formation of bioactive glass 45%. *J Biomed Mater Res*, 30, 509-514.

References

- Peltola, M., Aitasalo, K., Suonpää, J., Varpula, M., & Yli-Urpo, A. (2006). Bioactive glass S53P4 in frontal sinus obliteration: A long-term clinical experience. *Head & Neck*, 28(9), 834-841.
- Peruchi, C., Santos-Pinto, L., Santos-Pinto, A., & Barbosa e Silva, E. (2002). Evaluation of cutting patterns produced in primary teeth by an air-abrasion system. *Quintessence International*, 33(4).
- Petersson, L. G., Magnusson, K., Andersson, H., Almquist, B., & Twetmana, S. (2000). Effect of Quarterly Treatments with a Chlorhexidine and a Fluoride Varnish on Approximal Caries in Caries-Susceptible Teenagers: A 3-Year Clinical Study. *Caries Research*, 34(2), 140-143.
- Phantumvanit, P., Feagin, F. F., & Koulourides, T. (1977). Strong and weak acid sampling for fluoride of enamel remineralised in sodium fluoride solutions. *Caries Research*, 11(1), 52-61.
- Phulari, B. S. (2013). *History of Orthodontics*. JP Medical Ltd.
- Pickett, K. L., Lionel Sadowsky, P., Jacobson, A., & Lacefield, W. (2001). Orthodontic in vivo bond strength: comparison with in vitro results. *The Angle Orthodontist*, 71(2), 141-148.
- Pignatta, L. M. B., Duarte Júnior, S., & Santos, E. C. A. (2012). Evaluation of enamel surface after bracket debonding and polishing. *Dental Press Journal of Orthodontics*, 17(4), 77-84.
- Pithon, M. M., Oliveira, M. V. D., Ruellas, A. C. D. O., Bolognese, A. M., & Romano, F. L. (2007). Shear bond strength of orthodontic brackets to enamel under different surface treatment conditions. *Journal of Applied Oral Science*, 15(2), 127-130.
- Pithon, M. M., Santos, M. D. J., Souza, C. A. D., Leão Filho, J. C. B., Braz, A. K. S., Araujo, R. E. D., & Oliveira, D. D. (2015). Effectiveness of fluoride sealant in the prevention of carious lesions around orthodontic brackets: an OCT evaluation. *Dental Press Journal of Orthodontics*, 20(6), 37-42
- Pretty, I. A., Pender, N., Edgar, W. M., & Higham, S. M. (2003). The in vitro detection of early enamel de-and re-mineralization adjacent to bonded orthodontic cleats using

References

quantitative light-induced fluorescence. *The European Journal of Orthodontics*, 25(3), 217-223.

Pseiner, B. C., Freudenthaler, J., Jonke, E., & Bantleon, H. P. (2010). Shear bond strength of fluoride-releasing orthodontic bonding and composite materials. *The European Journal of Orthodontics*, 32(3), 268-273.

Polenova, T., Gupta, R., & Goldbourt, A. (2015). Magic angle spinning NMR spectroscopy: a versatile technique for structural and dynamic analysis of solid-phase systems. *Analytical Chemistry*, 87(11):5458-5469.

Pont, H. B., Özcan, M., Bagis, B., & Ren, Y. (2010). Loss of surface enamel after bracket debonding: an in-vivo and ex-vivo evaluation. *American Journal of Orthodontics and Dentofacial Orthopedics*, 138(4), 387-388.

Pulido, R., Perdomo, B. J., Pérez, J. P., Ramírez, R. A. (2012). Potencial de remineralización ultraestructural del vidrio bioactivo versus fluoruro estañoso. *Acta Odontol.*, 50(4),4-8.

Pus, M. D., & Way, D. C. (1980). Enamel loss due to orthodontic bonding with filled and unfilled resins using various clean-up techniques. *American Journal of Orthodontics*, 77(3), 269-283.

Rafique, S., Fiske, J., & Banerjee, A. (2003). Clinical trial of an air-abrasion/chemomechanical operative procedure for the restorative treatment of dental patients. *Caries Research*, 37(5), 360-364.

Rawls, H. R., & Owen, W. D. (1978). Demonstration of dye-uptake as a potential aid in early diagnosis of incipient caries. *Caries Research*, 12(2), 69-75.

Reema, S. D., Lahiri, P. K., & Roy, S. S. (2014). Review of casein phosphopeptides-amorphous calcium phosphate. *Chin J Dent Res*, 17(1), 7-14.

Redford, D. A., Clarkson, B. H., & Jensen, M. (1986). The effect of different etching times on the sealant bond strength, etch depth, and pattern in primary teeth. *Pediatr Dent*, 8(1), 11-15.

References

- Regalla, R. R., Jadav, C., Babu, D. A., Sriram, R. R. S., Sriram, S. K., & Kattimani, V. S. (2014). Evaluation and Comparison of Quantity and Pattern of Fluoride release from Orthodontic Adhesives: An in vitro Study. *The Journal of Contemporary Dental Practice*, 15(1), 99-102.
- Rekha, C. V., & Varma, B. (2012). Comparative evaluation of tensile bond strength and microleakage of conventional glass ionomer cement, resin modified glass ionomer cement and compomer: An in vitro study. *Contemporary Clinical Dentistry*, 3(3), 282-287.
- Retief, D. H. (1974). A comparative study of three etching solutions. *Journal of Oral Rehabilitation*, 1(4), 381-390.
- Reynolds, I. R. (1975). A review of direct orthodontic bonding. *British Journal of Orthodontics*, 2(3), 171-178.
- Richter, A. E., Arruda, A. O., Peters, M. C., & Sohn, W. (2011). Incidence of caries lesions among patients treated with comprehensive orthodontics. *American Journal of Orthodontics and Dentofacial Orthopedics*, 139(5), 657-664.
- Robertson, K.J, Toumba, A.J (1999). Cross-polarized photography in the study of enamel defects in dental paediatrics. *Journal of Audiovisual Media in Medicine*, 22(2), 63-70.
- Robinson, C., Shore, R. C., Brookes, S. J., Strafford, S., Wood, S. R., & Kirkham, J. (2000). The chemistry of enamel caries. *Critical Reviews in Oral Biology & Medicine*, 11(4), 481-495.
- Robinson, P. (2013). Clinical applications of bioactive glasses: Periodental repair. *An Introduction to Bioceramics*, 1(4), 125-135.
- Rock, W. P., & Abdullah, M. S. B. (1997). Shear bond strengths produced by composite and compomer light cured orthodontic adhesives. *Journal of Dentistry*, 25(3), 243-249.
- Roush, E. L., Marshall, S. D., Forbes, D. P., & Perry, F. U. (1997). In vitro study assessing enamel surface roughness subsequent to various final finishing procedures after debonding. *Northwestern Dental Research*, 7(2), 2-6.

References

- Rueggeberg, F. A., & Lockwood, P. (1990). Thermal debracketing of orthodontic resins. *American Journal of Orthodontics and Dentofacial Orthopedics*, 98(1), 56-65.
- Russell, A. L. (1961). The differential diagnosis of fluoride and non-fluoride enamel opacities. *Journal of Public Health Dentistry*, 21(4), 143-146.
- Saito, A., Namura, Y., Isokawa, K., & Shimizu, N. (2015). CO2 laser debonding of a ceramic bracket bonded with orthodontic adhesive containing thermal expansion microcapsules. *Lasers in Medical Science*, 30(2), 869-874.
- Sambashiva, R. P., Pratap, K. M., Nanda, K. K., & Sandya, P. S. (2011). "Drill-less" dentistry-the new air abrasion technology. *Indian Journal of Dental Advancements*, 3(3), 598-602.
- Sangamesh, B., & Kallury, A. (2011). Iatrogenic effects of Orthodontic treatment—Review on white spot lesions. *Int J Sci Eng Res*, 2(5), 2-16.
- Santos-Pinto, L., Peruchi, C., Marker, V. A., & Cordeiro, R. (2001). Evaluation of cutting patterns produced with air-abrasion systems using different tip designs. *Operative Dentistry*, 26(3), 308-312.
- Sarkis-Onofre, R., Skupien, J. A., Cenci, M. S., Moraes, R. R., Pereira-Cenci, T. (2014). The role of resin cement on bond strength of glass-fiber posts luted into root canals: a systematic review and meta-analysis of in vitro studies. *Operative Dentistry*, 39(1), E31-E44.
- Sarp, A. S. K., & Gülsoy, M. (2011). Ceramic bracket debonding with ytterbium fiber laser. *Lasers in Medical Science*, 26(5), 577-584.
- Sauro, S., Osorio, R., Watson, T. F. & Toledano, M. (2012). Therapeutic effects of novel resin bonding systems containing bioactive glasses on mineral depleted areas within the bonded-dentine interface. *Journal of Materials Science: Materials in Medicine*, 23, 1521-1532.
- Scheie, A. A., Arneberg, P., & Krogstad, O. (1984). Effect of orthodontic treatment on prevalence of *Streptococcus mutans* in plaque and saliva. *European Journal of Oral Sciences*, 92(3), 211-217.

References

- Schlüter, N., Hara, A., Shellis, R. P., & Ganss, C. (2011). Methods for the measurement and characterization of erosion in enamel and dentine. *Caries Research*, 45(1), 13-23.
- Scholze, H. (2012). *Glass: nature, structure, and properties*. Springer Science & Business Media.
- Scougall-Vilchis, R. J., Ohashi, S., & Yamamoto, K. (2009). Effects of 6 self-etching primers on shear bond strength of orthodontic brackets. *American Journal of Orthodontics and Dentofacial Orthopedics*, 135(4), 424-425.
- Sengun, A., Sari, Z., Ramoglu, S. I., Malkoç, S., & Duran, I. (2004). Evaluation of the dental plaque pH recovery effect of a xylitol lozenge on patients with fixed orthodontic appliances. *The Angle Orthodontist*, 74(2), 240-244.
- Sfondrini, M. F., Cacciafesta, V., Pistorio, A., & Sfondrini, G. (2001). Effects of conventional and high-intensity light-curing on enamel shear bond strength of composite resin and resin-modified glass-ionomer. *American Journal of Orthodontics and Dentofacial Orthopedics*, 119(1), 30-35.
- Sharma-Sayal, S. K., Rossouw, P. E., Kulkarni, G. V., & Titley, K. C. (2003). The influence of orthodontic bracket base design on shear bond strength. *American Journal of Orthodontics and dentofacial orthopedics*, 124(1), 74-82.
- Shelby, J. E. (2005). *Introduction to glass science and technology*. Royal Society of Chemistry.
- Sheridan, J. J., Brawley, G., & Hastings, J. (1986). Electrothermal debracketing Part I. An in vitro study. *American Journal of Orthodontics*, 89(1), 21-27.
- Shrestha, B. M. (1980). Use of ultraviolet light in early detection of smooth surface carious lesions in rats. *Caries Research*, 14(6), 448-451.
- Shungin, D., Olsson, A. I., & Persson, M. (2010). Orthodontic treatment-related white spot lesions: a 14-year prospective quantitative follow-up, including bonding material assessment. *American Journal of Orthodontics and Dentofacial Orthopedics*, 138(2), 136-137.
- Silverstone, L. M. (1974). Fissure sealants. *Caries Research*, 8(1), 2-26.

References

- Silverstone, L. M., Saxton, C. A., Dogon, I. L., & Fejerskov, O. (1975). Variation in the pattern of acid etching of human dental enamel examined by scanning electron microscopy. *Caries Research*, 9(5), 373-387.
- Silverstone, L. M., Wefel, J. S., Zimmerman, B. F., Clarkson, B. H., & Featherstone, M. J. (1981). Remineralization of Natural and Artificial Lesions in Human Dental Enamel in vitro. *Caries Research*, 15(2), 138-157.
- Singh, G. (2008). *Textbook of orthodontics*. Jaypee Brothers Publishers.
- Sirdeshmukh, D. B., Sirdeshmukh, L., & Subhadra, K. G. (2006). *Micro-and Macro-properties of Solids*. Berlin: Springer.
- Smith N.R., Reynolds I.R. (1991). A comparison of three bracket bases: an in vitro study. *Br J Orthod.*, 18,29–35.
- Soliman, M. M., Bishara, S. E., Wefel, J., Heilman, J., & Warren, J. J. (2006). Fluoride release rate from an orthodontic sealant and its clinical implications. *The Angle Orthodontist*, 76(2), 282-288.
- Sorel, O., El Alam, R., Chagneau, F., & Cathelineau, G. (2002). Comparison of bond strength between simple foil mesh and laser-structured base retention brackets. *American Journal of Orthodontics and Dentofacial Orthopedics*, 122(3), 260-266.
- Srivastava, K., Tikku, T., Khanna, R., & Sachan, K. (2013). Risk factors and management of white spot lesions in orthodontics. *Journal of Orthodontic Science*, 2(2), 43-49.
- Stadtländer, C. T. K. H. (2007). Scanning electron microscopy and transmission electron microscopy of mollicutes: challenges and opportunities. *Modern Research and Educational Topics in Microscopy*, 1, 122-131.
- Stavrianos, C., Papadopoulos, C., Vasiliadis, L., Dagkalis, P., Stavrianou, I., & Petalotis, N. (2010). Enamel structure and forensic use. *Res. J. Biol. Sc*, 5, 650-655.
- Stecksén-Blicks, C., Renfors, G., Oscarson, N. D., Bergstrand, F., & Twetman, S. (2007). Caries-preventive effectiveness of a fluoride varnish: a randomized controlled trial in adolescents with fixed orthodontic appliances. *Caries Research*, 41(6), 455-459.

References

- Sumali, C., Hidayat, A., Kusnoto, J., & Sudhana, W. (2013). Effect of One-Step and Multi-Steps Polishing System on Enamel Roughness. *Journal of Dentistry Indonesia*, 19(3), 65-69.
- Summers, A., Kao, E., Gilmore, J., Gunel, E., & Ngan, P. (2004). Comparison of bond strength between a conventional resin adhesive and a resin-modified glass ionomer adhesive: an in vitro and in vivo study. *American Journal of Orthodontics and Dentofacial Orthopedics*, 126(2), 200-206.
- Sundararaj, D., Venkatachalapathy, S., Tandon, A., & Pereira, A. (2015). Critical evaluation of incidence and prevalence of white spot lesions during fixed orthodontic appliance treatment: A meta-analysis. *Journal of International Society of Preventive & Community Dentistry*, 5(6), 433-439.
- Swift, E. J. (2002). Dentine/enamel adhesives: review of the literature. *Pediatric Dentistry*, 24(5), 456-461.
- Tai, B. J., Bian, Z., Jiang, H., Greenspan, D. C., Zhong, J., Clark, A. E., & Du, M. Q. (2006). Anti-gingivitis effect of a dentifrice containing bioactive glass (NovaMin®) particulate. *Journal of Clinical Periodontology*, 33(2), 86-91.
- Tatsi, C. (2014). *Slow release fluoride glass devices in the prevention of enamel demineralisation during fixed appliance orthodontic treatment* (Doctoral dissertation, University of Leeds).
- Taylor, A. M., Satterthwaite, J. D., Ellwood, R. P., & Pretty, I. A. (2010). An automated assessment algorithm for micro-CT images of occlusal caries. *The Surgeon*, 8(6), 334-340.
- Ten Bosch, J. J., Borsboom, P. C. F., & ten Cate, J. M. (1980). A nondestructive method for monitoring de-and remineralization of enamel. *Caries Research*, 14(2), 90-95.
- Ten Cate, J. M., & Duijsters, P. P. E. (1982). Alternating demineralization and remineralization of artificial enamel lesions. *Caries Research*, 16(3), 201-210.

References

- Ten Cate, J. M., & Featherstone, J. D. B. (1991). Mechanistic aspects of the interactions between fluoride and dental enamel. *Critical Reviews in Oral Biology & Medicine*, 2(3), 283-296.
- ten Cate J. M., Dundon, K. A., Vernon, P. G., Damato, F. A., Huntington, E., Exterkate, R. A. M., Wefel, J. S., & Roberts, A. J. (1996). Preparation and measurement of artificial enamel lesions, a four-laboratory ring test. *Caries Research*, 30(6), 400-407.
- Ten Cate, J. M., Exterkate, R. A. M., & Buijs, M. J. (2006). The relative efficacy of fluoride toothpastes assessed with pH cycling. *Caries Research*, 40(2), 136-141.
- Ten Cate, J. M., Buijs, M. J., Miller, C. C., & Exterkate, R. A. M. (2008). Elevated fluoride products enhance remineralization of advanced enamel lesions. *Journal of Dental Research*, 87(10), 943-947.
- Tehranchi, A., Fekrazad, R., Zafar, M., Eslami, B., Kalhori, K. A., & Gutknecht, N. (2011). Evaluation of the effects of CO2 laser on debonding of orthodontics porcelain brackets vs. the conventional method. *Lasers in Medical Science*, 26(5), 563-567.
- Theocharopoulos, A., Zou, L., Hill, R., & Cattell, M. (2010). Wear quantification of human enamel and dental glass–ceramics using white light profilometry. *Wear*, 269(11), 930-936.
- Tilocca, A., Cormack, A. N., & de Leeuw, N. H. (2007a). The structure of bioactive silicate glasses: new insight from molecular dynamics simulations. *Chemistry of Materials*, 19(1), 95-103.
- Tilocca, A., & Cormack, A. N. (2007b). Structural effects of phosphorus inclusion in bioactive silicate glasses. *The Journal of Physical Chemistry B*, 111(51), 14256-14264.
- Todd, M. A., Staley, R. N., Kanellis, M. J., Donly, K. J., & Wefel, J. S. (1999). Effect of a fluoride varnish on demineralization adjacent to orthodontic brackets. *American Journal of Orthodontics and Dentofacial Orthopedics*, 116(2), 159-167.
- Toledano, M., Osorio, E., Osorio, R., & García-Godoy, F. (1999). Microleakage of Class V resin-modified glass ionomer and compomer restorations. *The Journal of Prosthetic Dentistry*, 81(5), 610-615.

References

- Trimpeneers, L. M., & Dermaut, L. R. (1996). A clinical evaluation of the effectiveness of a fluoride-releasing visible light-activated bonding system to reduce demineralization around orthodontic brackets. *American Journal of Orthodontics and Dentofacial Orthopedics*, 110(2), 218-222.
- Tsichlaki, A., Chin, S. Y., Pandis, N., Fleming, P. S. (2016). How long does treatment with fixed orthodontic appliances last? A systematic review. *American Journal of Orthodontics and Dentofacial Orthopedics*, 149(3), 308-318.
- Turner, P. J. (1993). The clinical evaluation of a fluoride-containing orthodontic bonding material. *British Journal of Orthodontics*, 20, 307-13.
- Twetman, S., McWilliam, J. S., Hallgren, A., & Oliveby, A. (1996). Cariostatic effect of glass ionomer retained orthodontic appliances. An in vivo study. *Swedish Dental Journal*, 21(5), 169-175.
- Ulusoy C. (2009). Comparison of finishing and polishing systems for residual resin removal after debonding. *J Appl Oral Sci*, 17, 209-215.
- Van der Veen, M. H., Attin, R., Schwestka-Polly, R., & Wiechmann, D. (2010). Caries outcomes after orthodontic treatment with fixed appliances: do lingual brackets make a difference? *European Journal of Oral Sciences*, 118(3), 298-303.
- Van Dijk, J. W. E., Borggreven, J. M. P. M., & Driessens, F. C. M. (1979). Chemical and mathematical simulation of caries. *Caries Research*, 13(3), 169-180.
- Van Meerbeek, B., De Munck, J., Yoshida, Y., Inoue, S., Vargas, M., Vijay, P., & Vanherle, G. (2003). Adhesion to enamel and dentine: current status and future challenges. *OPERATIVE DENTISTRY-UNIVERSITY OF WASHINGTON*-, 28(3), 215-235.
- Van Meerbeek, B. (2008). Mechanisms of resin adhesion: dentine & enamel bonding. *Journal of Esthetic and Restorative Dentistry*, 2(1), 2-8.
- Viazis, A. D., Cavanaugh, G., & Bevis, R. R. (1990). Bond strength of ceramic brackets under shear stress: an in vitro report. *American Journal of Orthodontics and Dentofacial Orthopedics*, 98(3), 214-221.

References

- Vieira, A. C., Pinto, R. A., Chevitarese, O., & Almeida, M. A. (1993). Polishing after debracketing: its influence upon enamel surface. *The Journal of Clinical Pediatric Dentistry*, 18(1), 7-11.
- Voss, A., Hickel, R., & Mölkner, S. (1993). In vivo bonding of orthodontic brackets with glass ionomer cement. *The Angle Orthodontist*, 63(2), 149-153.
- Wahl, N. (2005). Orthodontics in 3 millennia. Chapter 6: More early 20th-century appliances and the extraction controversy. *American Journal of Orthodontics and Dentofacial Orthopedics*, 128(6), 795-800.
- Wallace, K. E., Hill, R. G., Pembroke, J. T., Brown, C. J., & Hatton, P. V. (1999). Influence of sodium oxide content on bioactive glass properties. *Journal of Materials Science: Materials in Medicine*, 10(12), 697-701.
- Walther, D. P. (1994). *Walther and Houston's orthodontic notes*. 5th ed. Wright.
- Wang, W. N., Meng, C. L., & Tarng, T. H. (1997). Bond strength: a comparison between chemical coated and mechanical interlock bases of ceramic and metal brackets. *American journal of orthodontics and dentofacial orthopedics*, 111(4), 374-381.
- Welbury, R. R., & Carter, N. E. (1993). The hydrochloric acid-pumice microabrasion technique in the treatment of post-orthodontic decalcification. *British Journal of Orthodontics*, 20(3), 181-185.
- Wen, H. B., Moradian-Oldak, J., & Fincham, A. G. (1999). Modulation of apatite crystal growth on Bioglass® by recombinant amelogenin. *Biomaterials*, 20(18), 1717-1725.
- White, D. J. (1987). Use of synthetic polymer gels for artificial carious lesion preparation. *Caries Research*, 21(3), 228-242.
- White, J. M., & Eakle, W. S. (2000). Rationale and treatment approach in minimally invasive dentistry. *The Journal of the American Dental Association*, 131, 13S-19S.
- Willmot, D. R. (2004). White lesions after orthodontic treatment: does low fluoride make a difference? *Journal of Orthodontics*, 31(3), 235-242.

References

- Willmot, D. (2008). White spot lesions after orthodontic treatment. In *Seminars in Orthodontics* 14(3), 209-219.
- Wilson, R. M., & Donly, K. J. (2000). Demineralization around orthodontic brackets bonded with resin-modified glass ionomer cement and fluoride-releasing resin composite. *Pediatric Dentistry*, 23(3), 255-259.
- Yassen, G. H., Platt, J. A., & Hara, A. T. (2011). Bovine teeth as substitute for human teeth in dental research: a review of literature. *Journal of Oral Science*, 53(3), 273-282.
- Yoshida, Y., Van Meerbeek, B., Nakayama, Y., Snauwaert, J., Hellemans, L., Lambrechts, P., Wakasa, K. (2000). Evidence of chemical bonding at biomaterial-hard tissue interfaces. *Journal of Dental Research*, 79(2), 709-714.
- Zaghrisson, B. U., Zachrisson, S. (1971). Caries incidence and oral hygiene during orthodontic treatment. *European Journal of Oral Sciences*, 79(4), 394-401.
- Zero, D. T. (1995). In situ caries models. *Advances in Dental Research*, 9(3), 214-230.
- Zhang, Y., Franklin, N. W., Chen, R. J., & Dai, H. (2000). Metal coating on suspended carbon nanotubes and its implication to metal-tube interaction. *Chemical Physics Letters*, 331(1), 35-41.
- Zhong, J. P., Greenspan, D. C., & Feng, J. W. (2002). A microstructural examination of apatite induced by Bioglass® in vitro. *Journal of Materials Science: Materials in Medicine*, 13(3), 321-326.
- Zimmer, B. W., & Rottwinkel, Y. (2004). Assessing patient-specific decalcification risk in fixed orthodontic treatment and its impact on prophylactic procedures. *American Journal of Orthodontics and Dentofacial Orthopedics*, 126(3), 318-324.

APPENDICES

Appendix 1. A copy of published research paper based on this project

ARTICLE IN PRESS

Journal of Dentistry xxx (xxxx) xxx–xxx




ELSEVIER

Contents lists available at ScienceDirect

Journal of Dentistry

journal homepage: www.elsevier.com/locate/jdent



Review article

The effect of bioactive glasses on enamel remineralization: A systematic review

Ayam A. Taha^{a,b}, Mangala P. Patel^a, Robert G. Hill^a, Padhraig S. Fleming^{c,*}

^a Dental Physical Sciences, Barts and the London School of Medicine and Dentistry, Institute of Dentistry, Queen Mary University of London, Mile End Road, London, E1 4NS, UK

^b Department of Paediatric, Orthodontic and Preventive Dentistry, College of Dentistry, Al-Mustansiriyah University, Iraq

^c Department of Orthodontics, Barts and the London School of Medicine and Dentistry, Institute of Dentistry, Queen Mary University of London, Turner St., London, E1 2AD, UK

ARTICLE INFO

Keywords:
Bioactive glasses
Enamel remineralization
Systematic review

ABSTRACT

Introduction/Objectives: To evaluate the effectiveness of bioactive glasses in promoting enamel remineralization.

Data: An electronic search with a complementary gray literature search for in vivo and in vitro research. No language restrictions were applied.

Sources: MEDLINE and EMBASE via OVID, the Cochrane Oral Health Group's Trials Register, CENTRAL and LILACS

Study selection: One hundred and sixteen studies were identified, of which, eleven met the inclusion criteria and formed the basis of this systematic review. Methodological quality was assessed independently by two reviewers. Factors investigated in the selected articles included the objective and subjective measures of enamel remineralisation; harms, including evidence of damage to the enamel surface; patient satisfaction; and in vitro evidence of enamel remineralisation, using recognized laboratory techniques.

Results: A total of 11 laboratory-based studies were included in this review. The methodological quality was deemed to be high in four, and medium in the remaining studies. Based on the in vitro studies, enamel remineralization improved with bioactive glasses, irrespective of the method of application. Ex vivo signs of remineralization such as increase in enamel hardness, the formation of an enamel-protective layer and reduced intensity of light backscattering were less evident with alternatives including fluoride, and casein phosphopeptide-amorphous calcium phosphate (CPP-ACP).

Conclusions: Based on in vitro findings only, bioactive glasses may be capable of enhancing enamel remineralization in various formulations, compared with other topical remineralizing materials including fluoride, and CPP-ACP. However, clinical research to confirm their effectiveness is now overdue.

Clinical significance: Bioactive glasses have potential utility in promoting enamel remineralization; however, clinical research exploring their clinical effectiveness is required.

1. Introduction

Enamel demineralization is a reversible precursor of overt dental caries and is highly prevalent both among orthodontic and non-orthodontic populations. White spot lesions (WSLs), for example, are a common complication associated with fixed orthodontic treatment, particularly in the presence of poor oral hygiene [1]. Fixed appliances offer retentive areas for accumulation of bacterial plaque. The acidic by-products of cariogenic bacteria are responsible for the subsequent enamel demineralisation and formation of WSLs, which are reported in up to 96% of orthodontic patients [2]. This is further aggravated by the fact that most orthodontic patients are adolescents, who are at

increased risk due to the susceptibility of newly-erupting teeth to acid attack [3].

A number of topical remineralizing agents have been used to inhibit and remineralize enamel and WSLs, in particular [4]. Fluoride has formed the mainstay of enamel remineralization for many decades. It is known to control caries predominantly through its topical effect inhibiting demineralization by forming fluorapatite on the enamel surface. Fluorapatite is less soluble, therefore increasing the resistance of enamel to dissolution relative to hydroxyapatite during acid attack [5]. Various modes and formulations have been used to deliver fluoride such as varnishes, toothpastes, mouth-rinses, solutions, gels and orthodontic adhesives incorporating a source of fluoride.

* Corresponding author.
E-mail address: padhraig.fleming@gmail.com (P.S. Fleming).

<http://dx.doi.org/10.1016/j.jdent.2017.09.007>

Received 12 July 2017; Received in revised form 14 August 2017; Accepted 18 September 2017

0300-5712/ © 2017 Elsevier Ltd. All rights reserved.

Please cite this article as: Taha, A.A., Journal of Dentistry (2017), <http://dx.doi.org/10.1016/j.jdent.2017.09.007>

Appendix 2. A copy of published research paper based on this project in Clinical Oral Investigations Journal

Development of a novel bioactive glass for air-abrasion to selectively remove orthodontic adhesives: An *in vitro* study

Ayam A. Taha^{a,b*}, Robert G. Hill^a, Padhraig S. Fleming^c and Mangala P. Patel^a

^a Dental Physical Sciences, Barts and the London School of Medicine and Dentistry, Institute of Dentistry, Queen Mary University of London, Mile End Road, London, E1 4NS, UK

^b Department of Paedodontic, Orthodontic and Preventive Dentistry, College of Dentistry, Al-Mustansiriyah University, Iraq

^c Department of Orthodontics, Barts and the London School of Medicine and Dentistry, Institute of Dentistry, Queen Mary University of London, Turner St., London E1 2 AD, UK

*Corresponding author: Dental Physical Sciences, Dental Institute, Barts and the London, Queen Mary University of London, Mile End Road, London, E1 4NS, UK. Tel.: +4474 59882829;

E-mail: a.a.h.taha@qmul.ac.uk

Abstract

Objectives: To develop a novel, bioactive glass for removing residual orthodontic adhesive via air-abrasion, following bracket debonding, and to evaluate its effectiveness against a proprietary bioactive glass 45S5(SylcTM)-air-abrasion, and a slow-speed tungsten carbide (TC) bur.

Materials and Methods: Three glasses were prepared and their bioactivity was proved. One novel glass (QMAT3) was selected due to its appropriate hardness, lower than that of enamel 45S5(SylcTM). Sixty extracted human premolars were randomly assigned to adhesive removal using: (a) QMAT3-air-abrasion, (b) 45S5(SylcTM)-air-abrasion, and (c) TC bur, which were further subdivided (n=10) based on the adhesive used (Transbond XTTM or Fuji Ortho LCTM). Enamel roughness was assessed using Scanning Electron Microscopy (SEM) and non-contact profilometry before bracket bonding, after removing residual adhesive following bracket debonding and after polishing.

Results: QMAT3 formed apatite faster (6 hours) than 45S5(SylcTM) (24 hours) in Tris solution. QMAT3-air-abrasion gave the lowest enamel roughness (Ra) after removing the adhesives. SEM images showed a pitted, roughened enamel surface in the TC bur group and to a lesser extent with 45S5(SylcTM), while a virtually smooth surface without any damage was observed in the QMAT3-air-abrasion group. The time taken for adhesive removal with QMAT3 was comparable to 45S5(SylcTM) but was twice as long with the TC bur.

Conclusions: QMAT3-air-abrasion is a promising technique for selective removal of adhesives without inducing tangible enamel damage.

Clinical relevance: A novel bioactive glass has been developed as an alternative to the use of TC burs for orthodontic adhesive removal.

Keywords: Orthodontic adhesive removal; Bioactive glass; Air-abrasion

Introduction

Several factors may predispose to or directly induce enamel damage during, or after, fixed orthodontic treatment. The post clean-up procedure after removal of attachments is regarded as the most significant cause of enamel damage [1,2]. Therefore, various methods have been proposed for clean-up of residual orthodontic adhesives from the enamel surface, such as: hand instruments, stones (Arkansas stone, green stone), wheels and discs, scalers, dental burs (typically tungsten carbide burs), lasers and pumice or zirconium paste [3]. Currently, no technique has proven capable of complete and efficient removal of residual adhesives, without inducing even a minor amount of enamel damage [4]. These surface changes reduce the resistance of enamel to bacterial/organic acid attacks therefore increasing its susceptibility to demineralization and dental caries.

The critical threshold value of enamel surface roughness for bacterial adhesion has been established at $0.2\mu\text{m}$ by Bollen et al. [5]. A number of studies have shown that conventional methods of adhesive removal, including scalers and dental burs, may lead to visible surface roughness with gouges ranging from $10\mu\text{m}$ - $20\mu\text{m}$ deep, and loss of up to $100\mu\text{m}$ thickness of enamel [6]. Thus, maintaining the integrity of the enamel surface during the removal of residual adhesives is a key consideration during the removal of orthodontic appliances.

In recent years, air-abrasion has shown promise as a method for removing residual adhesives [7]. Banerjee and his co-workers, in an in vitro air-abrasion study, reported that the bioactive glass powder 45S5 produced less enamel damage compared with alumina air-abrasion and tungsten carbide burs [7]. However, there still remains a need to improve the properties of bioactive glasses to facilitate the safe removal of residual adhesives, with minimal/no enamel damage, following bracket debonding.

The aims of the present study were therefore:

- to develop a novel fluoride-containing bioactive glass with a hardness lower than that of the bioactive glass 45S5 (SylcTM) and that of sound enamel surface, and
- to study the effectiveness of the novel glass in the removal of residual orthodontic adhesives from the enamel surface, when propelled via an air-abrasion hand-piece, in comparison with a TC bur and 45S5 (SylcTM)-air-abrasion.

Material and Methods

Glass design and synthesis

A series of three novel glasses incorporating SiO_2 - P_2O_5 - CaO - Na_2O - CaF_2 , based on the molar composition of a commercially-used bioactive glass 45S5 (SylcTM, Denfotex Research Ltd., London, UK) were synthesized using a melt quench route (Table 1). The Na_2O content was systematically increased (in exchange for CaO) up to 30mol%. High phosphate content (6.1mol% P_2O_5) was also used. In addition, a constant ratio of calcium fluoride (3mol% CaF_2) was added. The network connectivity value was kept constant (2.08) for all the experimental glasses. Each glass (batch size 200g) was prepared by melting SiO_2 (analytical grade; Prince Minerals Ltd, Stoke-on-Trent, UK), Na_2CO_3 , CaO , P_2O_5 , and CaF_2 (Sigma-Aldrich, Gillingham, UK) in a platinum-rhodium crucible, in an electrical furnace (EHF 17/3, Lenton, UK) for 60 minutes between 1420°C to 1450°C (Table 1). The resulting molten glass was rapidly quenched in deionized water (DW) to obtain glass frits, which were collected into a sieve and kept in a vacuum oven (Harvard LTE, UK) to dry at 80°C overnight.

Table 1 Nominal glass composition (in Mol %) and melting temperature (T_m)

Glasses	Mol %					T_m
	SiO_2	Na_2O	CaO	P_2O_5	CaF_2	
45S5 (Sylc TM)	46.1	24.4	26.9	2.6		1450
QMAT1	37	20	33.9	6.1	3	1440
QMAT2	37	25	28.9	6.1	3	1430
QMAT3	37	30	23.9	6.1	3	1420

After drying, 100 grams of each glass frit was ground using a vibratory mill (Gy-Ro mill, Glen Creston, London UK) for one minute to form glass powders, which were then sieved for 10 minutes ($38\mu\text{m}$ and $90\mu\text{m}$ mesh analytical

sieves; Endecotts, Ltd, London, UK), to obtain glass particle size fractions between 38µm and 90µm. Each glass powder was stored in dry re-sealable plastic bags until further use. Glass particles of <38µm size were used for bioactivity tests to assess apatite formation (in Tris buffer solution), whereas glass particles between 38µm and 90µm were used for propulsion via the air-abrasion hand-piece. This range of particle size allowed escape of the glass powder through the hand-piece nozzle tip without agglomeration. Bioactive glass 45S5(Sylc™) was used as a reference with a particle size less than 38µm for bioactivity tests and between 38µm and 90µm for air-abrasion studies.

Glass characterization

X-ray diffraction (XRD; X'Pert PRO MPD, PANalytical, Cambridge, UK; 40 kV/40 mA, Cu Kα, data collected at room temperature; results not shown) was used to determine the amorphous state of the glass. The glass transition temperature (T_g) was determined for each glass composition using Differential Scanning Calorimetry (DSC; Stanton Redcroft DSC1500, Rheometric Scientific, Epsom, UK). 50mg (± 0.1 mg) of glass powder (<38µm) was placed in a DSC platinum crucible and run against alumina powder (analytical grade) as a reference, at a heating rate 20°C per minute in flowing Nitrogen gas (flow rate of 60ml/min), from 25°C to 1000°C.

Glass Vickers hardness measurements

For hardness measurements, a glass rod (20mm in diameter) was prepared from each glass batch, by re-melting approximately 100g of glass frit, pouring into a graphite mould, and annealed for 1 hour in a preheated furnace, at the T_g determined in 2.2. Thereafter, the casting glass was slowly cooled to room temperature overnight in the furnace, which was switched off. The rod from each glass batch was sectioned into approximately 1mm thick discs using a diamond cutter machine (Accutom-5, Struers A/S, Ballerup, Denmark). These discs were subsequently polished with silicon carbide paper (P1000 in roughness) wet with acetone (instead of water), to avoid the glass reacting with water during polishing. The hardness of the discs was measured using a Vickers diamond pyramid indenter (Zwick/Roell, ZHU 187.5) with an applied load of 29.4N for 10 seconds. The Vickers Hardness Number (VHN) of each glass composition was taken 10 times. The VHN values (displayed on the LCD) were averaged and presented as mean \pm standard deviation (SD). QMAT3 experimental glass was selected for air-abrasion tests on the basis of its lower hardness compared to that of enamel and bioactive glass 45S5(Sylc™).

Glass particle size and shape

Particle size analysis was performed on glass powders using a Malvern/E Mastersizer (Malvern instruments, UK), since air abrasion technique utilizes kinetic energy, which depends on the mass (size) and the velocity of the propelled glass powder particles. Approximately 30mg of the glass powder was dispersed in DW until the ideal laser absorbance level was achieved. Two measurements were recorded and the average of these measurements was taken to produce a more reliable value. For glass particle shape, a scanning electron microscope (SEM-FEI Inspect F, Oxford instruments, UK) with an accelerating voltage of 20kV and a working distance of 10mm was used after mounting the glass particles on stubs, and sputter-coated with gold using an automatic sputter coater (SC7620, Quorum Technologies, UK).

Apatite formation in Tris buffer

Tris buffer solution was prepared (15.09g Tris (hydroxymethyl) aminomethane powder, 800ml of DW and 44.2ml of 1M hydrochloric acid - Sigma Aldrich), and shaken (orbital shaker; IKA® KS 4000i control, Germany) at 37°C overnight. The pH of the solution was measured using a pH meter (Oakton Instruments), and adjusted to ~7.25 -7.4 (with 1 M hydrochloric acid); the volume of Tris buffer solution was increased to 2 litres by adding DW and stored in an incubator at 37°C. In order to observe apatite formation of each glass powder, the latter was dispersed (75mg; with a particle size < 38µm) into 50ml of Tris buffer solution in a polyethylene bottle (150ml). These bottles were

then kept in a shaking incubator at 37°C, with a rotation rate of 60 rpm, for the following time intervals: 1, 3, 6, 9 and 24 hours.

After the designated time intervals, the glass powders immersed in Tris buffer solution were filtered (through filter paper; Fisher brand® qualitative filter paper). The glass powder within the filter paper was then placed in an oven at 37°C for 24 hours to be dried. The dried powders were subsequently analysed using Fourier Transform Infrared Spectroscopy (FTIR; ~5mg of each glass powder; < 38µm) and X-ray Diffraction (XRD; 1 to 20mg of each glass powder, with a particle size <38µm). The FTIR (Spectrum GX, Perkin-Elmer, Waltham, USA) data was collected between from 500-1800cm⁻¹, absorbance mode. The XRD (X'Pert PRO MPD, PANalytical, Cambridge, UK; 40kV/40mA, Cu Kα) data was collected at room temperature in the 2θ range of 10° to 70° degrees.

Glass particle size and shape

Particle size analysis was performed on glass powders using a Malvern/E Mastersizer (Malvern instruments, UK), since air abrasion technique utilizes kinetic energy, which depends on the mass (size) and the velocity of the propelled glass powder particles. Approximately 30mg of the glass powder was dispersed in DW until the ideal laser absorbance level was achieved. Two measurements were recorded and the average of these measurements was taken to produce a more reliable value. For glass particle shape, a scanning electron microscope (SEM-FEI Inspect F, Oxford instruments, UK) with an accelerating voltage of 20kV and a working distance of 10mm was used after mounting the glass particles on stubs, and sputter-coated with gold using an automatic sputter coater (SC7620, Quorum Technologies, UK).

Tooth Sample preparation

Sixty human premolars, extracted for orthodontic purposes, were used (with approval from Queen Mary Research Ethics Committee QMREC 2011/99). These teeth were selected on the basis of visual observation using an optical stereo-microscope at 4.5x magnification (VWR International Microscope). The inclusion criteria were: no carious lesions, cracks or any other defects on the buccal surfaces. The selected teeth were cleaned and stored in DW in a refrigerator at 4°C until required. Prior to the start of the experiment, these teeth were washed with DW, air-dried, and embedded into plastic moulds filled with cold cure acrylic resin (Orthocryl™, UK), leaving the buccal surfaces exposed. The buccal surface of each tooth sample was polished with non-fluoridated pumice paste (20 seconds), rinsed with water and air-dried. Thereafter, a polyvinyl chloride tape was placed on the buccal surface of each tooth sample, excluding a 4mm x 4mm window at the centre for bonding of orthodontic brackets to the exposed enamel. The covered area was used as a reference for later visual comparison between the treated and untreated surfaces. Finally, these prepared teeth samples were stored in an incubator at 37°C until the brackets were bonded.

Orthodontic adhesive removal

Following the manufacturer's instructions, two light-cured orthodontic adhesive systems: resin composite; Transbond XT™ (3M Unitek, Monrovia, CA, USA), and resin modified glass ionomer cement; Fuji Ortho LC™ (GC corporation, Tokyo, Japan) were used to bond 60 premolar metal brackets (MiniSprint®, Forestadent, Pforzheim, Germany) to the prepared teeth samples (30 premolar teeth per each orthodontic adhesive system group). Enamel etching with 37% phosphoric acid was undertaken for 30 seconds prior to application of Transbond XT™. When the brackets were placed, each bracket was subjected to a 300g compressive force using a force gauge (Correx Co, Berna, Switzerland) for 5 seconds, to ensure a uniform thickness of the adhesive [8]. After bonding, the teeth with the attached brackets were stored in DW for one week at 37°C. Thereafter, the plastic moulds (with the extracted teeth mounted) were held by a special holding device (Instron® machine, UK), to remove the attached brackets from the buccal surfaces using a debonding plier (Exion™, DB Orthodontics) by one operator. Three different clean-up methods (slow-speed tungsten carbide bur (TC), 45SS (Sylc™)-air-abrasion, and the selected experimental glass (QMAT3)-air-abrasion were used for removal of the residual of the aforementioned two orthodontic adhesive systems following bracket debonding. The teeth samples of each orthodontic adhesive system group were randomly assigned to three groups (10 teeth for each post clean-up method). Both the commercially-available bioactive glass 45SS (Sylc™) and QMAT3 glass were propelled via an air-abrasion hand-piece (BA Ultimate air polisher) connected to a dental chair unit. The operating parameters were: air-pressure 60psi, nozzle angle 75°, and nozzle tip-enamel surface distance of 5mm. Complete removal of the adhesive remnants was assessed

by visual inspection under a dental operating light, and later verified by an optical stereo-microscope at 4.5x magnification (VWR International Microscope). A non-contact white light profilometry (Proscan®2000, Scantron, Taunton, UK) was used to measure the enamel surface roughness for all prepared teeth samples before bracket bonding, after post clean-up method, and after polishing (using rubber cup and non-fluoridated pumice for 20 seconds). In addition, Scanning Electron Microscopy (SEM-FEI Inspect F, Oxford instruments, UK) was used to examine the enamel surface damage following the aforementioned post clean-up methods and the time required to remove adhesive remnants was also assessed.

Statistical analysis

Statistical analysis was performed with the SPSS software package (Version 24; SPSS Inc., New York, NY, USA). Two-way analysis of variance (ANOVA) and Tukey's HSD post-hoc test were used to test significant differences in enamel surface roughness under three different conditions (before bracket bonding, after post clean-up methods following bracket debonding, and after polishing). The level of significance was pre-specified at $\alpha=0.05$.

Results

Glass characterization and Vickers hardness measurements

The glass transition temperature (T_g) of both 45S5(Sylc™) and experimental glasses are shown in Table 2. The T_g was 530°C for 45S5(Sylc™) with sodium and phosphate contents of 24.4mol % and 2.6mol %, respectively. The T_g of QMAT3 reduced to 355°C as the sodium and phosphate increased to 30mol% and 6.1mol%, respectively. This was also associated with the addition of a constant ratio of fluoride (3mol%). Furthermore, the Vickers hardness number (VHN) decreased dramatically (Table 2) from 472.8 ± 2.28 VHN (~ 4.63 GPa) for 45S5(Sylc™) to 350.4 ± 1.14 VHN (~ 3.43 GPa) for QMAT3. The experimentally determined VHN were converted to GPa units using the equation: $\text{GPa} = \text{VHN} \times 0.009807$.

Table 2 Glass transition temperature (T_g), and Vickers hardness number (VHN) of 45S5(Sylc™) and experimental glasses

Bioactive Glasses	T_g (°C)	Vickers hardness (VHN) Mean \pm SD	Hardness (GPa)
45S5(Sylc™)	530	472.8 ± 2.28	4.63
QMAT1	524	458.6 ± 2.50	4.49
QMAT2	450	433.6 ± 1.94	4.25
QMAT3	355	350.4 ± 1.14	3.43

Glass particle size and shape

The particle size distribution (in micrometres; μm) of 45S5(Sylc™) glass and experimental glasses are given in Table 3, where D10 represents 10% of the glass particle size, indicating the fine particles within the distribution D50 represents 50% of the glass particle size, giving a measure of the mean particle size within the distribution and D90 represents 90% of the glass particle size, reflecting larger particle sizes.

Table 3 Particle size distribution of 45S5(Sylc™) and experimental glasses

Bioactive glasses	Particle size (μm)		
	D10	D50	D90
45S5(Sylc™)	34.1	63.5	76.8
QMAT1	38.6	65.5	77.2
QMAT2	38.9	65.5	77.2
QMAT3	33.8	62.7	76.7

SEM images of 45S5(Sylc™) and experimental glasses are presented in Fig.1. All glasses show similar morphology, represented as sharp, angular irregular particles of variable sizes (in micrometres).

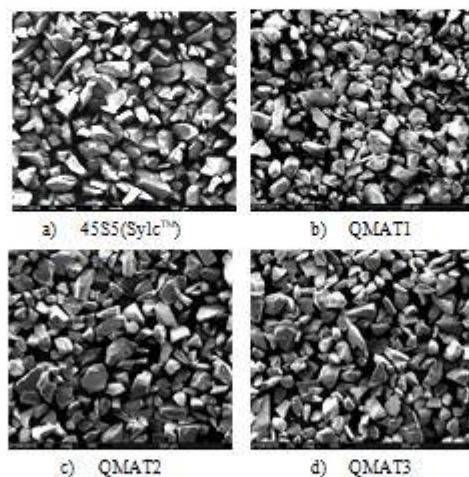


Fig. 1 SEM images of 45S5(Sylc™) and experimental glasses at 250x magnification.

Apatite formation in Tris buffer

After immersion in Tris buffer solution for 1, 3, 6, 9 and 24 hours, the FTIR spectra for all experimental glasses showed dramatic changes compared to their respective untreated (not immersed) versions. The latter were characterized by the presence of two main bands at 910cm^{-1} and 1040cm^{-1} , indicating non-bridging oxygen ($\text{Si}^+-\text{O}-\text{M}^+$, where M^+ is an alkali metal modifier element) and vibrational stretching of $\text{Si}-\text{O}-\text{Si}$, respectively [9,10]. After immersion, the non-bridging oxygen ($\text{Si}^+-\text{O}-\text{M}^+$) band at 910cm^{-1} disappeared, and a single P-O vibration band at

560 cm^{-1} appeared after 3 hours, which is an indicator for the presence of apatite precursors [9]. At 6 hours, the latter band split into prominent twin bands at 560 cm^{-1} and 600 cm^{-1} , which became well-defined with longer immersion times. These twin bands indicate the presence of apatitic PO_4^{3-} groups, the main characteristic feature of apatite, including hydroxyapatite, fluorapatite and carbonated hydroxyapatite [11,12]. The formation of apatite was confirmed by the presence of a sharp phosphate band (PO_4^{3-}) at 1040 cm^{-1} after 6 hours, 9 hours and 24 hours of immersion [9]. Conversely, 45S5(SylcTM) did not show any bands at 560 cm^{-1} and 600 cm^{-1} , with the absence of the sharp phosphate band at 1040 cm^{-1} at 6 hours. Apatite formation features of 45S5(SylcTM) appeared at 24 hours but these were still less prominent compared to those obtained for all experimental glasses (Fig. 2).

With regard to XRD patterns, all the experimental glasses showed a small peak at 26° and a broad peak from 32° to $34^\circ 2\theta$ after 6 hours of immersion in Tris buffer solution, superimposing the amorphous broad peak of untreated glass and those that were immersed for 1 hour and 3 hours (Fig. 3). These two peaks, indicating the presence of apatite, became more pronounced as the immersion time increased. However, all these peaks were absent in 45S5(SylcTM) until 24 hours, when much smaller peaks indicative of apatite appeared [13].

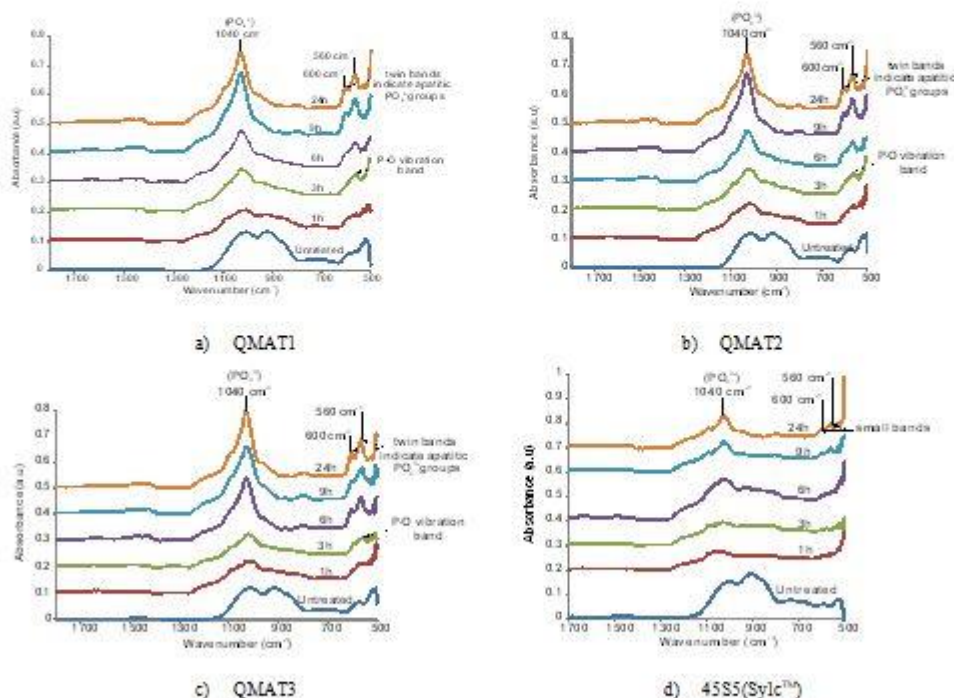


Fig. 2 FTIR spectra for experimental glasses and 45S5(SylcTM) after immersion in Tris buffer solution

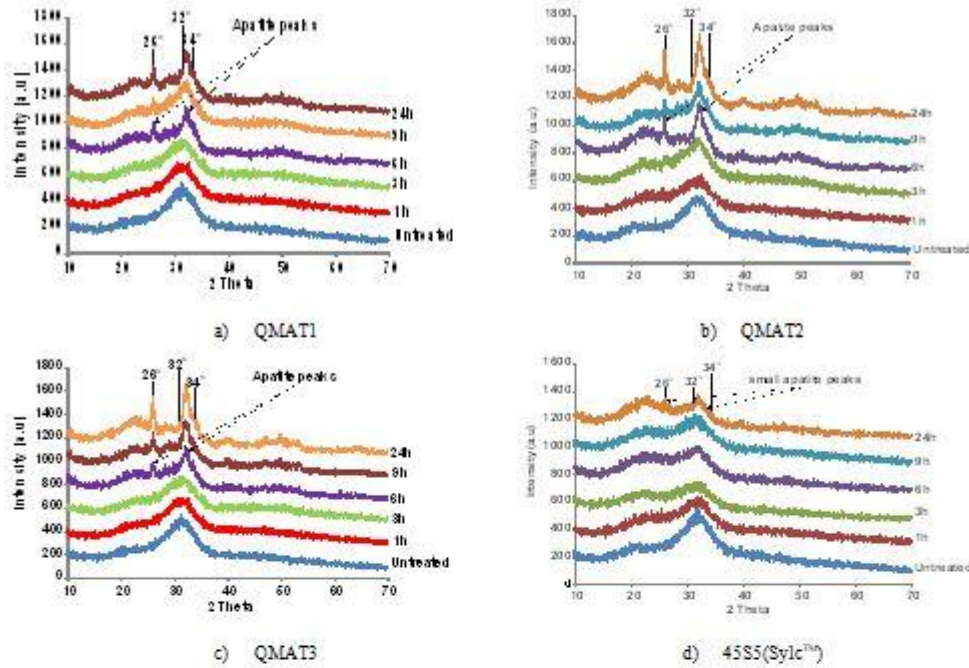


Fig. 3 XRD data for experimental glasses and 45S5(Sylc™) after immersion in Tris buffer solution

Orthodontic adhesive removal

The profilometry analysis was carried out on three experimental groups (TC group, 45S5(Sylc™)-air-abrasion, and QMAT3-air-abrasion) for each orthodontic adhesive. The means and standard errors (SE) of the average enamel surface roughness (Ra) in micrometers, under three different conditions, are presented in Table 4. No statistically significant differences were observed in the enamel roughness measurements among the six experimental study groups before bracket bonding (baseline measurements). For Transbond XT™ resin groups, the enamel roughness significantly increased after post clean-up with TC bur ($2.93 \pm 0.06 \mu\text{m}$), and 45S5(Sylc™) ($1.89 \pm 0.04 \mu\text{m}$) compared with their corresponding baseline measurements ($p < 0.001$), while QMAT3-air-abrasion group did not exhibit any significant difference in enamel roughness ($p = 0.927$). In addition, enamel roughness values after polishing were significantly higher for both the TC and 45S5(Sylc™)-air-abrasion groups ($2.73 \pm 0.77 \mu\text{m}$ and $1.81 \pm 0.05 \mu\text{m}$, respectively), than their corresponding baseline measurements ($p < 0.001$). However, no significant difference was shown following clean-up with QMAT3-air-abrasion and subsequent polishing and baseline values ($p = 0.983$). Furthermore, enamel roughness measurements did not appear to be affected by polishing subsequent to clean-up in each group ($p = 0.104$ to 1.000) compared to those after clean-up.

With Fuji Ortho™ resin modified glass ionomer cement, similar patterns were observed for enamel roughness measurements. They were significantly higher after post clean-up in the TC ($2.57 \pm 0.05 \mu\text{m}$) and 45S5(Sylc™)-air-abrasion groups ($1.59 \pm 0.02 \mu\text{m}$) compared to baseline measurements ($p < 0.001$), but the QMAT3-air-abrasion group ($0.51 \pm 0.04 \mu\text{m}$) did not show any significant difference with their corresponding baseline measurements. In addition, significantly higher enamel roughness values were shown in TC and 45S5(Sylc™)-air-abrasion groups ($2.63 \pm 0.06 \mu\text{m}$ and $1.74 \pm 0.04 \mu\text{m}$, respectively) after polishing than their corresponding baseline measurements (p

Appendices

<0.001), but no significant difference was shown between those of QMAT3-air-abrasion and their corresponding baseline measurements ($p=1.000$).

Table 4 Enamel surface roughness (Ra) in micrometers (Mean \pm SE) for each experimental group under three different conditions

Group (n=10)	Experimental group based on : orthodontic adhesive + post clean-up method used	Before bracket bonding (Baseline)	After post clean-up method	After polishing
1	Transbond XT TM + TC	0.49 \pm 0.27	2.93 \pm 0.06	2.73 \pm 0.77
2	Transbond XT TM + 45SS(Sylc TM)-air-abrasion	0.51 \pm 0.03	1.89 \pm 0.04	1.81 \pm 0.05
3	Transbond XT TM + QMAT3-air-abrasion	0.49 \pm 0.04	0.58 \pm 0.02	0.56 \pm 0.03
4	Fuji Ortho LC TM + TC	0.54 \pm 0.02	2.57 \pm 0.05	2.63 \pm 0.06
5	Fuji Ortho LC TM + 45SS(Sylc TM)-air-abrasion	0.46 \pm 0.04	1.59 \pm 0.02	1.74 \pm 0.04
6	Fuji Ortho LC TM + QMAT3-air-abrasion	0.36 \pm 0.02	0.51 \pm 0.04	0.45 \pm 0.01

The time required to remove the orthodontic adhesives was recorded for three post clean-up methods: TC bur, SylcTM-air-abrasion, and QMAT3-air-abrasion (Table 5). Differences between QMAT3 glass (42.51 \pm 1.11 seconds) and SylcTM (40.72 \pm 0.92 seconds) were not statistically significant ($p=0.913$) in the Transbond XTTM groups. However, both took longer ($p<0.001$) to remove excess Transbond XTTM resin compared to the TC bur (23.2 \pm 1.58 seconds). A similar pattern was observed in the Fuji Ortho LCTM groups with no significant differences ($p=0.893$) found between the time required to remove Fuji Ortho LCTM by both QMAT3 and SylcTM glasses, while both glasses took significantly longer than the TC bur ($p<0.001$).

Table 5 Means \pm SE of the time (seconds) required to remove two residual orthodontic adhesives after bracket debonding

Group (n=10)	Experimental study group based on : orthodontic adhesive + post clean-up method used	Time (Sec.)
1	Transbond XT TM + TC	23.20 \pm 4.99
2	Transbond XT TM + 45SS(Sylc TM)-air-abrasion	40.71 \pm 2.89
3	Transbond XT TM + QMAT3-air-abrasion	42.51 \pm 3.51
4	Fuji Ortho LC TM + TC	22.90 \pm 4.41
5	Fuji Ortho LC TM + 45SS(Sylc TM)-air-abrasion	38.42 \pm 4.29
6	Fuji Ortho LC TM + QMAT3-air-abrasion	40.32 \pm 3.36

Representative SEM images (at 250x magnification) are shown in Fig.4 prior to bracket bonding and after the three post clean-up methods (TC bur, 45SS(SylcTM)-air-abrasion, and QMAT3-air-abrasion). The sound enamel surface appeared smooth before bracket bonding (Fig.4a), whilst it became roughened and pitted surface after the use of a slow-speed TC bur (Fig.4b). In addition, the enamel surface, following 45SS(SylcTM)-air-abrasion is seen to have microscopic roughness in some areas (Fig.4c), while a uniformly smooth surface was obtained after using QMAT3-air-abrasion (Fig.4d).

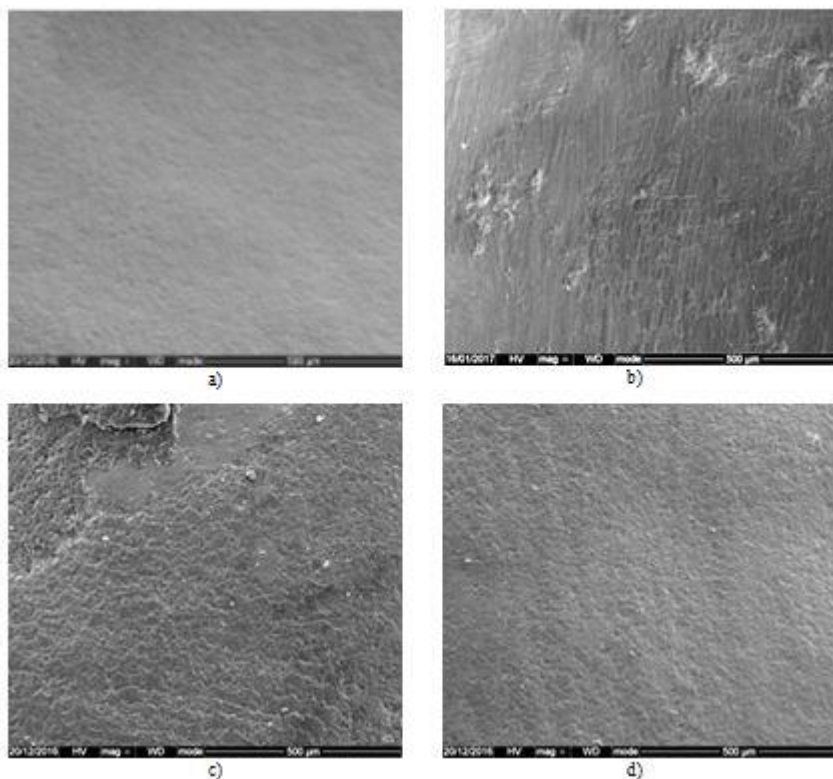


Fig.4 Representative SEM images (250x magnification) of the enamel surface: a) before bracket bonding; b) after clean-up using the TC bur; c) after clean-up using 45S5(Sylc[™])-air-abrasion; d) after clean-up using QMAT3-air-abrasion

Discussion

Glass characteristics

Bioactive glass, 45S5, has been used in a number of commercial products such as NovaBone[™] (orthopaedic application), Perioglass[™] (periodontal application), Sylc[™] and NovaMin[™] (dental application) [14]. Furthermore, preliminary in vitro research has been undertaken on its use via propulsion using air-abrasion, in order to cut sound and carious enamel and dentine [15,16], remove residual orthodontic adhesive following bracket de-bonding from enamel surfaces [7], and potentially to re-mineralize white spot lesions [17]. However, this glass has higher hardness than that of sound enamel (~3.5GPa) [20] with reported values varying between 4.5GPa [18] and 5.75GPa [19], thus risking roughening of the enamel surface. Therefore, it is desirable to develop glasses which have similar or lower hardness than that of enamel.

It has been reported that increasing Na₂O content (in exchange for CaO), across a series of bioactive glasses, with a constant network connectivity value close to two, resulted in a linear decrease in T_g and density of the glass [21,22]. This was attributed to the substitution of CaO for Na₂O producing a more disrupted silicate glass network, since one

Ca^{2+} was replaced by two Na^+ ions. This resulted in the loss of the ionic bridges that Ca^{2+} ions provided between two adjacent non-bridging oxygens, contributing to a decrease in the packing density of the glass. Therefore, less rigid glasses were formed with a lower glass transition temperature (T_g) to transform them from a molten liquid to a glassy state.

Additionally, it has also been reported that a reduction in silica content, characteristic of all experimental glasses tested compared to the proprietary bioactive glass 45S5(SylcTM), resulted in a decrease in T_g [23]. In the latter study, a reduction in silica content was accompanied by an increase in phosphate content. Similarly, a range of studies [13,14,25] have reported a decrease in T_g related to a reduction in silica content accompanied by an increase in phosphate content and the addition of fluoride. Moreover, the addition of fluoride to bioactive glasses has also been reported to lower the T_g as well as to promote fluorapatite formation, which is more stable and resistant to acid attack, compared with hydroxyapatite [26,27].

Fluoride, in the form of CaF_2 , was incorporated in the composition of all experimental glasses in this study. The amount of CaF_2 was kept constant (3mol %) to enhance fluorapatite formation and prevent fluorite development (as a result of excessive fluoride; $\geq 5\text{mol } \%$) [13,27,28]. The formation of fluorite indicates crystallization of the glass, resulting in inhibition of its bioactive properties; the presence of crystalline phases gives rise to increased resistance to ion exchange reactions between the glass surface and physiological solution, which in turn affect apatite formation. Furthermore, the phosphate content in this study was also increased from 2.6mol% in the reference glass 45S5(SylcTM) to 6.1mol % in all experimental glasses. This formulation was informed by two recent studies [13,24] indicating that increasing the phosphate content to approximately 6mol % in fluoride-containing glasses resulted in an increase in the degradation of the glass, leading to a rapid release of calcium (Ca^{2+}) and orthophosphate (PO_4^{3-}) ions to the surrounding solution, thus forming fluorapatite within 6 hours after immersion in Tris buffer solution. The results of this study regarding apatite formation are consistent with these findings.

Interestingly, it was also evident that increasing the Na_2O content in the present study, resulted in a decrease in hardness values for all experimental glasses to (3.43GPa for QMAT3) compared with the reference 45S5(SylcTM; 4.63 GP). Hence, QMAT3 conserved the enamel surface while removing the residual adhesives, without inducing undesirable surface enamel changes. It should be noted that the available information on the hardness values of bioactive glasses is limited due to the relatively small number of studies investigating this property. Reported values vary significantly from one study to another; for example, the hardness for bioactive glass, 45S5 reported by Lopez-Esteban et al. [19] and Farooq et al. [24] were 5.75GPa and 5.84GPa, respectively. This variation might be due to the differences in the methodology used to prepare these glasses, and the indenter load used to measure the hardness, although all studies used a Vickers's instrument. Moreover, in the current study the indenter load was 2.9 kg while the indenter loads used by Lopez-Esteban et al. [19] and Farooq et al. [24] were 0.5-1.2kg, and 0.01kg, respectively. Ninety per cent of each experimental glass (QMAT1, QMAT2, and QMAT3) had a particle size of 77.2 μm , 77.2 μm , and 76.7 μm , respectively. These values were close to those for 45S5(SylcTM; 76.8 μm). The larger mass (particle size) leads to higher kinetic energy since the latter relates to the mass (particle size) and velocity. In addition, the presence of large particles and the absence of fine particles prevented agglomeration of the glass powder, since fine particles can result in clumping and stagnation of the glass powder within the nozzle tip of the air abrasion hand-pieces, thus potentially hindering the air-abrasion process.

With regard to the morphology of the commercially-available 45S5(SylcTM) glass and experimental glasses, the SEM images revealed a very similar appearance characterized by sharp, angular and irregular particles, thus aiding in removing the residual of orthodontic adhesives.

The FTIR spectra and XRD patterns of 45S5(SylcTM) and all experimental glasses showed dramatic changes after immersion in Tris buffer solution for periods of 1, 3, 6, 9 and 24 hours. These changes related to ion exchange between the glass powder and the Tris buffer solution forming a silica-gel surface layer- $\text{Si}(\text{OH})_4$ on the glass surface after breaking of the Si-O-Si bonds. This was followed by leaching of calcium, phosphate and fluoride from the glass into the solution to form apatite. These findings were in agreement with the mechanism of apatite formation proposed by Hanch [29,30]. Furthermore, the ability of experimental glasses to form apatite in 6 hours, compared with 24 hours for the commercially-available 45S5(SylcTM), after immersion in Tris buffer solution, were consistent with previous findings of Farooq et al. [24] and Mneimne et al. [13].

Orthodontic adhesive removal

It has previously been reported that TC bur increased enamel roughness compared to composite burs [31], white stone [32], stainburster bur [33] and adhesive residue remover [34]. These studies compared results with atomic force microscopy, profilometry, and 3D scanning in blue-light technology. In the present study, the profilometry data revealed that the use of the TC bur in removing residual orthodontic adhesive increased enamel surface roughness regardless of the type of adhesive used. 45S5(SylcTM)-air-abrasion also produced an increase in the enamel roughness to some extent. These findings are in agreement with Banerjee et al. [7], who demonstrated that removal of residual adhesive resin (UniteTM) using alumina air-abrasion caused more enamel loss (0.0386 mm³), followed by the TC bur (0.285 mm³) and finally 45S5 air-abrasion (0.135 mm³). In the present study, the novel experimental glass (QMAT3) induced less enamel roughness compared with the TC bur and 45S5(SylcTM)-air-abrasion, irrespective of the adhesive material used, a finding which was corroborated using SEM imaging. This finding relates to the lower hardness value of QMAT3 which approximates but does not exceed that of the enamel surface. Therefore, propelling this glass powder was less likely to roughen the enamel surface, mitigating the associated risk of plaque accumulation and caries formation. Furthermore, the handling technique used in this study was similar to that used by Paolinelis et al. [16], who confirmed that using the aforementioned operating parameters increased the cutting efficiency of the air-abrasion technique. Consequently, using accepted clinical handling parameters it appears that this novel glass powder may be capable of selective removal of orthodontic adhesives without inducing deleterious abrasion of the enamel surface, although quantification of the volume of loss was not undertaken.

Further laboratory research in relation to the cutting efficiency of this approach is required prior to clinical application, although preliminary data suggests comparable levels of efficiency to other bioactive glass formulations. Adhesive removal took approximately half the time with the TC bur. This discrepancy might relate to the aggressive cutting associated with sharp cutting blades of TC bur while bioactive glass propulsion works by means of abrasion. Similar conclusions were reached by both Karam et al.[31] and Mohebi et al.[32], who reported that TC burs removed adhesive remnants faster than composite bur and white stone, respectively. Moreover, polishing with non-fluoridated pumice for 20 seconds has little effect on enamel surface roughness values. These findings mirror analogous studies involving use of non-fluoridated pumice for 10 to 30 seconds [35-37] suggesting that polishing does not affect either the grooves or pits induced by enamel clean-up methods.

The ability of QMAT3 glass to form apatite earlier than 45S5(SylcTM) offers further promise to induce enamel remineralization; this potential may lead to application in the management of both pit and fissure, and smooth surface enamel caries. Notwithstanding this, it is important to emphasize that the present research is limited by its *ex vivo* nature; as such, replication within an *in vivo* situation is required. Moreover, blinding of the investigator was not performed, risking the introduction of assessor bias. In addition, teeth were stored in deionized water rather than undergoing a simulated artificial aging process involving thermomechanical cycling, the latter approach may have been more clinically representative, although use of water storage remains an accepted approach [38]. However, in view of the promising physical and handling properties highlighted in the present study, the remineralization potential of QMAT3 for orthodontically-induced white spot lesions will be explored in ongoing laboratory research.

Conclusions

A novel bioactive glass (QMAT3) with a lower hardness than 45S5(SylcTM) and enamel has been developed. Its bioactivity was proved by early apatite formation compared with a proprietary agent. QMAT3 was capable of selective removal of residual orthodontic adhesive without inducing enamel damage. It, therefore, shows promise as a viable alternative to adhesive removal with a TC bur.

Compliance with Ethical Standards

Conflicts of interest: One of the four authors is an inventor on the patented bioactive glass: WO 2011/161422.

Funding: This study is a part of a PhD that is being funded by the Iraqi Ministry of Higher Education and Scientific Research.

Ethical approval: This article does not contain any studies with human participants or animals performed by any of the authors.

Informed consent: For this type of study, formal consent is not required.

References


- Knösel M, Martysek S, Jung K, Sadat-Khonsari R, Kubein M, Meerschburg D, Baus O, Ziebold D (2010) Impulse debonding compared to conventional debonding: Extent of enamel damage, adhesive residues and the need for post processing. *Angle Orthod* 80(6): 1036-1044.
- Pont HB, Özcan M, Bagis B, Ren Y (2010) Loss of surface enamel after bracket debonding: an in-vivo and ex-vivo evaluation. *Am J Orthod Dentofacial Orthop* 138(4): 387.e1-387.e9.
- Bonatti GA, Zanarini M, Paranti SI, Lamuca M, Marchionni S, Gatto MR (2011) Evaluation of enamel surfaces after bracket debonding: an in-vivo study with scanning electron microscopy. *Am J Orthod Dentofacial Orthop* 140(5): 696-702.
- Janiszewska-Olszowska J, Szafkiewicz T, Tomkowski R, Tandedka K, Grochowski K (2014) Effect of orthodontic debonding and adhesive removal on the enamel—current knowledge and future perspectives—a systematic review. *Med Sci Monit Basic Res* 20: 1991-2001.
- Bollen M, Lambrechts P, Quirynen M (1997) Comparison of surface roughness of oral hard materials to the threshold surface roughness for bacterial plaque retention: a review of the literature. *Dent Mater* 13(4): 258-269.
- Dumora T, Fried D (2000) Selective ablation of orthodontic composite by using sub-microsecond IR laser pulses with optical feedback. *Lasers Surg Med* 27: 103-10.
- Banerjee A, Paolinis G, Sodder M, McDonald F, Watson TF (2008) An in vitro investigation of the effectiveness of bioactive glass air-abrasion in the 'selective' removal of orthodontic resin adhesive. *Eur J Oral Sci* 116(5): 488-492.
- Eliades T, Bramley WA (2000) The inappropriateness of conventional orthodontic bond strength assessment protocols. *Eur J Orthod* 22(1): 13-23.
- Jones JR, Sepulveda P, Hench LL (2001) Dose-dependent behaviour of bioactive glass dissolution. *J Biomed Mater Res* 58(6): 720-726.
- Aina V, Malavasi G, Pia AF, Munaron L, Montera C (2009) Zinc-containing bioactive glasses: surface reactivity and behaviour towards endothelial cells. *Acta Biomater* 5(4): 1211-1222.
- Kim CY, Clark AE, Hench LL (1989) Early stages of calcium-phosphate layer formation in bioglasses. *J Non-Cryst Solids* 113(2-3): 195-202.
- Peirl Filho O, Latorre GP, Hench LL (1996) Effect of crystallization on apatite-layer formation of bioactive glass 45%. *J Biomed Mater Res* 30: 509-514.
- Mneimne M, Hill RG, Bushby AJ, Brauer DS (2011) High phosphate content significantly increases apatite formation of fluoride-containing bioactive glasses. *Acta Biomater* 7(4): 1827-1834.
- Hench LL (2006) The story of Bioglass®. *J Mater Sci: Mater Med* 17(11): 967-978.
- Banerjee A, Thompson ID, Watson TF (2011) Minimally invasive caries removal using bio-active glass air-abrasion. *J Dent* 39(1): 2-7.
- Paolinis G, Banerjee A, & Watson TF (2009) An in-vitro investigation of the effects of variable operating parameters on alumina air-abrasion cutting characteristics. *Oper Dent* 34(1): 87-92.
- Milly H, Fasty F, Andiappan M, Watson TF, Thompson I, Banerjee A (2015) Surface pre-conditioning with bioactive glass air-abrasion can enhance enamel white spot lesion remineralisation. *Dent Mater* 31(5): 522-533.
- Cook RJ, Watson TF, Hench LL, Thompson ID (2008) U.S. Patent No. 7,329,126. Washington, DC: U.S. Patent and Trademark Office.
- Lopez-Esteban S, Saiz E, Fujino S, Oku T, Suganuma K, Tomsia AP (2003) Bioactive glass coatings for orthopedic metallic implants. *J Eur Ceram Soc* 23(15): 2921-2930.
- O'Donnell MD (2011) Predicting bioactive glass properties from the molecular chemical composition: Glass transition temperature. *Acta Biomater* 7(5): 2264-2269.
- Wallace KE, Hill RG, Pembroke JT, Brown CJ, Hanton PV (1999) Influence of sodium oxide content on bioactive glass properties. *J Mater Sci: Mater Med* 10(12): 697-701.
- Lockyer MW, Holland D, Dupree R (1995) NMR investigation of the structure of some bioactive and related glasses. *J Non-Cryst Solids* 188(3): 207-219.

23. O'Donnell MD, Watts SJ, Hill RG, Law RV (2009) The effect of phosphate content on the bioactivity of soda-lime-phosphosilicate glasses. *J Mater Sci: Mater Med* 20(8): 1611-1618.
24. Farooq I, Tytkowski M, Müller S, Janicki T, Brauer DS, Hill RG (2009) Influence of sodium content on the properties of bioactive glasses for use in air abrasion. *Biomed Mater* 8(6): 065008.
25. Brauer DS, Kapukhina N, Law RV, Hill RG (2009) Structure of fluoride-containing bioactive glasses. *J Mater Chem* 19(31): 5629-5636.
26. Hill RG, Brauer DS (2011) Predicting the bioactivity of glasses using the network connectivity or split network models. *J Non-Cryst Solids* 357(24): 3884-3887.
27. Brauer DS, Kapukhina N, O'Donnell MD, Law RV, Hill RG (2010) Fluoride-containing bioactive glasses: effect of glass design and structure on degradation, pH and apatite formation in simulated body fluid. *Acta Biomater* 6(8): 3275-3282.
28. Luvardi G, Malavasi G, Menabue L, Aina V, Morterra C (2009) Fluoride-containing bioactive glasses: surface reactivity in simulated body fluids solutions. *Acta Biomater* 5(9): 3548-3562.
29. Hench LL (1991) Bioceramics: from concept to clinic. *J Am Ceram Soc* 74(7): 1487-1510.
30. Jones J, Clare A (2012) Bio-glasses: an introduction. John Wiley and Sons.
31. Karan S, Kircelli BH, Tasdelen B (2010) Enamel surface roughness after debonding: comparison of two different bus Angle. *Orthod* 80(6): 1081-1088.
32. Mohebi S, Shafiee HA, Ameli N (2017) Evaluation of enamel surface roughness after orthodontic bracket debonding with atomic force microscopy. *Am J Orthod Dentofacial Orthop* 151(3): 521-527.
33. Esdir EA, Akop M, Cime L, Ileri Z (2016) Evaluation of Enamel Surface Roughness after Various Finishing Techniques for Debonding of Orthodontic Brackets. *Turkish J Orthod* 29(1): 1-5.
34. Janiszewska-Olszowska J, Tandacka K, Szadkiewicz T, Stępień P, Sporniak-Turak K, Grocholewicz K (2015) Three-dimensional analysis of enamel surface alteration resulting from orthodontic clean-up—comparison of three different tools. *BMC Oral Health* 15(1): 146-153.
35. Gwinnett AJ, Gorelick L (1977) Microscopic evaluation of enamel after debonding: clinical application. *Am J Orthod* 71(6): 651-665.
36. Vieira AC, Pinto RA, Chevitarese O, Almeida MA (1993) Polishing after debracketing: its influence upon enamel surface. *J Clin Pediatr Dent* 18(1): 7-11.
37. Ahrani F, Akbari M, Akbari J, Dabin G (2013) Enamel surface roughness after debonding of orthodontic brackets and various clean-up techniques. *J Dent (Tehran)*, 10(1), 82-93.
38. Amoral FL, Colucci V, Palma-Dioh RG, Corona SA (2007) Assessment of in vitro methods used to promote adhesive interface degradation: a critical review. *J Esthetic Rest Dent* 19(6): 340-53.

Appendix 3. BSODR Poster (Cardiff, 2015)



Appendix 4. IADR Poster (San Francisco, 2017)



Queen Mary
University of London

#3105

A Novel Bioactive Glass for Remineralization of White Spot Lesions

Ayam A. Taha, Padhraig S. Fleming, Robert Hill and Mangala P. Patel

Dental Physical Sciences, Oral Growth and Development, Barts and the London School of Medicine and Dentistry,
Queen Mary University of London, United Kingdom

Aim

To design a novel fluoride-containing bioactive glass powder and verify its capacity to remineralize white spot lesions (WSLs).

Introduction

WSLs are common and significantly associated with fixed orthodontic treatment [1]. Although attempts have been made to remineralize these lesions, a material/technique that entirely cures them does not exist. In recent years, a 45S5 glass powder, propelled via air abrasion, was used in an *in vitro* study to promote remineralization of WSLs [2]. This glass powder improved their appearance, but increased the surface roughness of enamel. Hence there remains a need to improve the properties of this glass powder to promote remineralization of WSLs without inducing enamel damage.

Materials & Methods

An experimental bioactive glass (Exp. glass) with hardness (3.4GPa) lower than that of enamel (~3.5GPa) was prepared (melt quench route), with a similar composition to 45S5 (hardness 4.6GPa), but with high sodium and phosphate content and a constant ratio of fluoride. Artificial WSLs were induced on 30 healthy extracted human premolar teeth (demineralization protocol: 8% methylocellulose gel buffered/lactic acid 0.1mol/L; pH 4.6; 14 days, 37°C). 20 teeth (treated) were propelled with either Exp. glass or 45S5 (n=10), via an air-abrasion hand-piece (BA Ultimate Air Polisher; at 5 bar for 20 secs; 5mm distance; 90° angle). Treated and untreated teeth (controls; n=10) were immersed in artificial saliva (AS, 24hrs, 37°C to induce remineralization), rinsed with deionized water (DW) and left to dry (2 days at room temperature), before scanning with Scanning Electron Microscope (SEM) and Energy Dispersive X-ray spectroscopy (EDX).

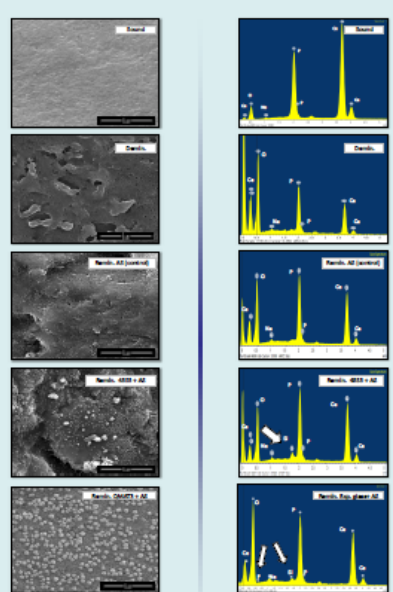


Figure 1: SEM images of enamel surface - different conditions (20,000x magnification)

Figure 2: EDX spectra of enamel surface - different conditions

Results & Discussion

The SEM images (Figure 1) showed no mineral precipitation on the control group, while smaller quantities of minerals were found on a rough enamel surface with 45S5 glass. A distinctive morphology with fluorapatite-like structures covered a smooth enamel surface that was remineralized by the Exp. glass. This newly-formed mineral layer was resistant to rinsing with DW. In addition, the EDX spectra (Figure 2) confirmed the observations of SEM showing differences in the intensity of Ca, P, F, Si peaks of natural, demineralized, and remineralized enamel surfaces. An additional peak for Si occurred with 45S5 (remin.), which indicates embedding of 45S5 particles into the enamel surface. Two additional peaks, for Si and F, occurred with Exp. glass (remin.) confirming its presence on the enamel surface.


Conclusion & Future Plan

A novel bioactive glass with appropriate hardness has been developed to promote remineralization of WSLs. Further development and refinement is necessary to assess its potential clinical utility.


References:

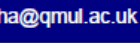
- Phuan, B. S. (2013). History of Orthodontics. JP Medical Ltd.
- Milly, H., Festy, F., Andlappan, M., Watson, T. F., Thompson, I. & Banerjee, A. 2015. Surface preconditioning with bioactive glass air-abrasion can enhance enamel WSL remineralisation. Dental Materials, 31, 522-533.

Acknowledgment: The Iraqi Ministry of Higher Education and Scientific Research



a.a.h.taha@qmul.ac.uk





Appendices

Appendix 5.

	Record Number	Sample Name	Dx (10) (μm)	Dx (50) (μm)	Dx (90) (μm)
	31	Sylc 38-90	31.1	57.3	97.0
	32	Sylc 38-90	31.2	57.5	97.3
	33	Sylc 38-90	31.1	57.3	96.9
	34	Sylc 38-90	31.1	57.4	97.1
	35	Sylc 38-90	31.1	57.4	97.1
Mean			31.1	57.4	97.1
1xStd Dev			0.0234	0.0690	0.136
1xRSD (%)			0.0750	0.120	0.140

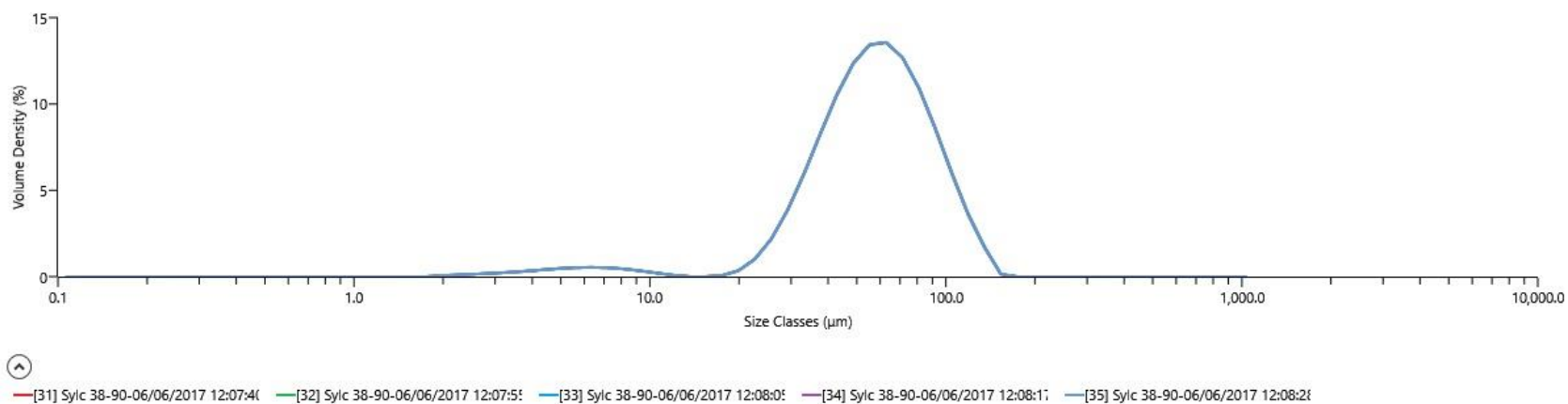


Figure 10.1. The frequency distribution curve for Sylc™ batch of particle size ranging between ranging between 38μm-90μm

Appendices

	Record Number	Sample Name	Dx (10) (μm)	Dx (50) (μm)	Dx (90) (μm)
	41	qmat 3 38-90	34.5	58.2	94.1
	42	qmat 3 38-90	34.5	58.2	94.2
	43	qmat 3 38-90	34.0	58.1	94.9
	44	qmat 3 38-90	34.0	58.1	94.9
	45	qmat 3 38-90	34.0	58.1	94.9
Mean			34.2	58.1	94.6
1xStd Dev			0.283	0.0526	0.403
1xRSD (%)			0.827	0.0904	0.426

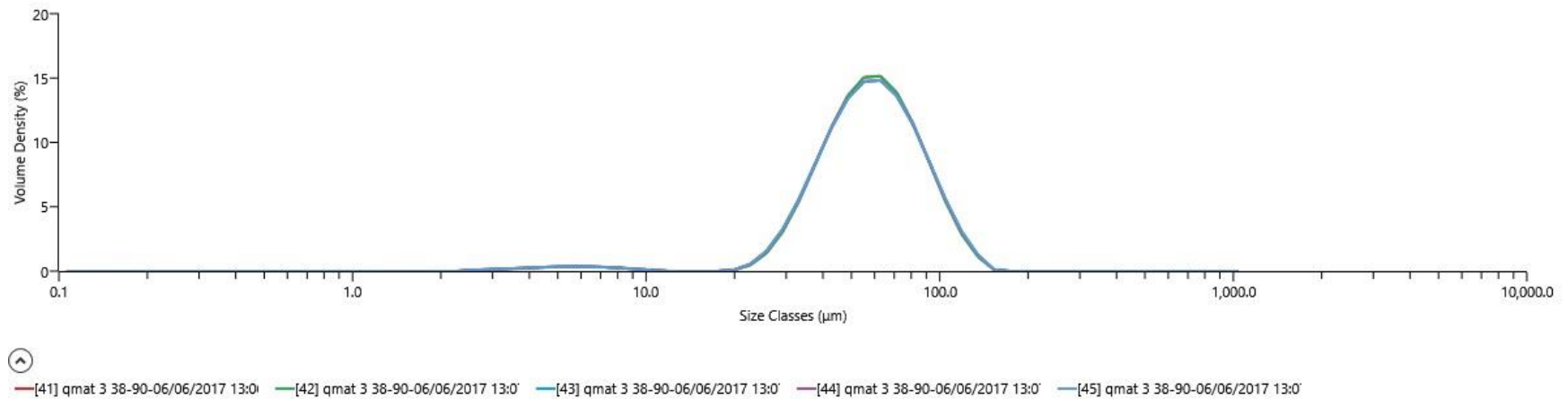
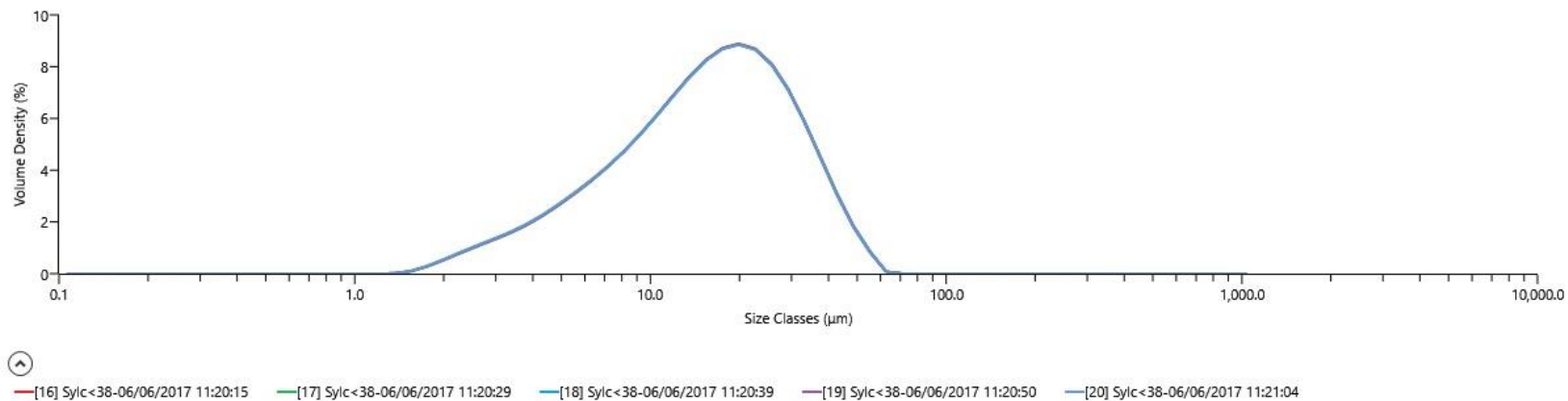


Figure 10.2. The frequency distribution curve for QMAT3 batch of particle size ranging between 38μm-90μm.

Appendices

	Record Number	Sample Name	Dx (10) (μm)	Dx (50) (μm)	Dx (90) (μm)
	16	Sylc<38	5.14	15.9	34.0
	17	Sylc<38	5.11	15.9	34.0
	18	Sylc<38	5.09	15.8	33.9
	19	Sylc<38	5.08	15.8	33.9
	20	Sylc<38	5.06	15.8	33.9
Mean			5.09	15.8	33.9
1xStd Dev			0.0288	0.0328	0.0481
1xRSD (%)			0.566	0.207	0.142



90μm

Figure 10.3. The frequency distribution curve for Sylc™ batch of particle size <38μm

Appendices

	Record Number	Sample Name	Dx (10) (μm)	Dx (50) (μm)	Dx (90) (μm)
	6	qmat3<38	5.23	15.7	34.3
	7	qmat3<38	5.22	15.7	34.3
	8	qmat3<38	5.21	15.7	34.1
	9	qmat3<38	5.20	15.7	34.1
	10	qmat3<38	5.16	15.5	33.1
Mean			5.20	15.7	34.0
1xStd Dev			0.0283	0.0953	0.520
1xRSD (%)			0.544	0.609	1.53

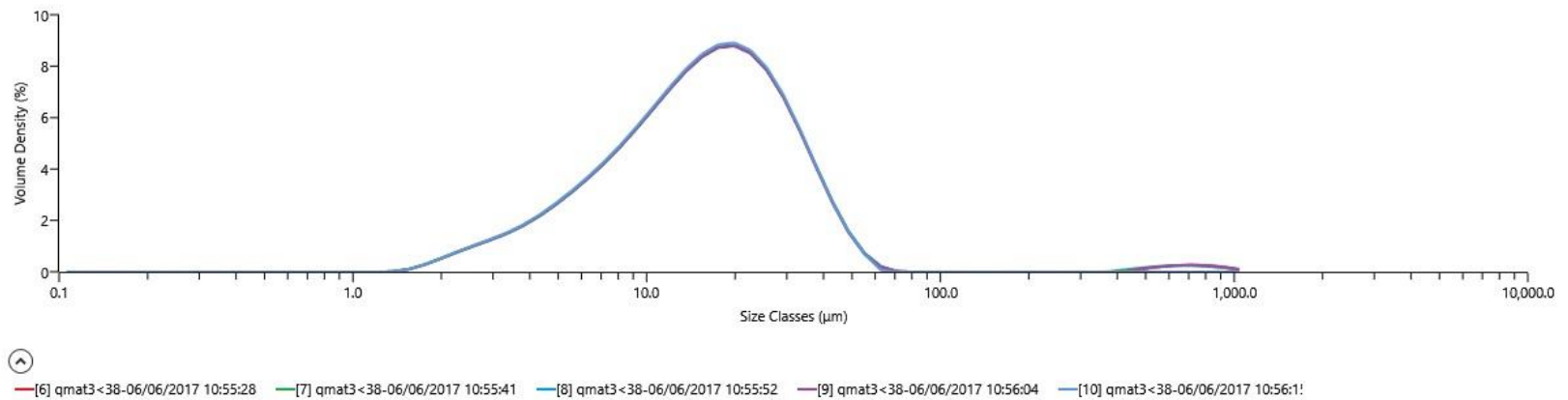


Figure 10.4. The frequency distribution curve for QMAT3 batch of particle size <38μm